UNIVERSITY OF CALIFORNIA,
IRVINE

Synthesis, Characterization and Reactivity of Organometallic Complexes of Uranium and Plutonium in the +2 and +3 Oxidation States

DISSERTATION

submitted in partial satisfaction of the requirements
for the degree of

DOCTOR OF PHILOSOPHY

in Chemistry

by

Cory J. Windorff

Dissertation Committee:
Professor William J. Evans, Chair
Professor Andrew S. Borovik
Professor Jenny Y. Yang

2017

DEDICATION

To my parents, wife and family.

"You have to let go of your desires and just let the chemistry be what it is
– only then will you achieve chemical enlightenment."
–Andrew J. Gaunt

TABLE OF CONTENTS

LIST OF FIGURES

LIST OF TABLES

LIST OF COMPLEXES

Molecular Formula	Number
$(C_5Me_4SiMe_3)_2UCl_2$	**1**
$(C_5Me_4SiMe_3)_2UMe_2$	**2**
$(C_5Me_4SiMe_3)_2UMeCl$	**3**
$(\eta^5:\eta^1\text{-}C_5Me_4SiMe_2CH_2)_2U$	**4**
$(C_5Me_4SiMe_3)_2UMe_2K(THF)_x$	**5**
$[(C_5Me_4SiMe_3)_2U][(\mu\text{-}Ph_2)BPh_2]$	**6**
$(C_5Me_4SiMe_3)_3U$	**7**
Cp'_3U $[Cp' = C_5H_4SiMe_3]$	**8-U**
$Cp'_3U(THF)$	**8-U(THF)**
Cp'_3Ln	**8-Ln**
Cp'_3Ce	**8-Ce**
Cp'_3Pr	**8-Pr**
Cp'_3Nd	**8-Nd**
$[K(crypt)][Cp'_3UH]$ [crypt = 2.2.2-Cryptand]	**9**
$[(C_5Me_5)_2U][(\mu\text{-}Ph_2)BPh_2]$	**10**
$(C_5Me_5)_2U[N(SiMe_3)_2]$	**11**
$U[N(SiMe_3)_2]_4$	**12**
$U[N(SiMe_3)_2]_2(\kappa^2\text{-}CH_2SiMe_2NSiMe_3)$	**13**
$[K(THF)_x]\{U[N(SiMe_3)_2]_4\}$	**14**
$U[N(SiMe_3)_2]_3$	**15-U**
$Ln[N(SiMe_3)_2]_3$	**15-Ln**

$La[N(SiMe_3)_2]_3$	**15-La**
$Ce[N(SiMe_3)_2]_3$	**15-Ce**
$Nd[N(SiMe_3)_2]_3$	**15-Nd**
UI_3	**16**
$(C_5Me_5)_2U[CH(SiMe_3)_2]$	**17**
$(C_5Me_4SiMe_3)_2U[CH(SiMe_3)_2]$	**18**
$(C_5Me_4SiMe_3)_2U[N(SiMe_3)_2]$	**19**
Cp''_3U $[Cp'' = C_5H_3(SiMe_3)–1,3]$	**20-U**
Cp''_3M	**20-M**
Cp''_3Th	**20-Th**
Cp''_3Pu	**20-Pu**
Cp''_3La	**20-La**
Cp''_3Ce	**20-Ce**
Cp''_3Nd	**20-Nd**
$[K(crypt)][Cp'_3U]$	**21-U**
$[K(crypt)][Cp'_3U]$•THF	**21•THF**
$[K(crypt)][Cp'_3Ln]$	**21-Ln**
$[K(crypt)][Cp'_3Ce]$	**21-Ce**
$[K(crypt)][Cp'_3Pr]$	**21-Pr**
$[K(crypt)][Cp'_3Nd]$	**21-Nd**
$[K(crypt)][Cp''_3U]$	**22-U**
$[K(crypt)][Cp''_3Th]$	**22-Th**
$[K(crypt)][Cp''_3Pu]$	**22-Pu**

[K(crypt)][Cp″$_3$M]	**22-M**
[K(crypt)][Cp″$_3$La]	**22-La**
[K(crypt)][Cp″$_3$Ce]	**22-Ce**
[K(crypt)][Cp″$_3$Pr]	**22-Pr**
[K(crypt)][Cp″$_3$Nd]	**22-Nd**
[K(18-crown-6)(THF)$_2$][Cp″$_3$U]	**23-U**
[K(18-crown-6)(THF)$_2$][Cp″$_3$Th]	**23-Th**
[Na(18-crown-6)(THF)$_2$][Cp″$_3$U]	**24-U**
[Na(12-crown-4)$_2$][Cp″$_3$U]	**25-U**
[K(18-crown-6)(THF)$_2$][Cp″$_3$UH]	**26**
[K(18-crown-6)(THF)$_2$][Cp″$_3$UD]	**26-D**
[K(crypt)][Cp″$_3$UH]	**27-U**
[K(crypt)][Cp″$_3$PuH]	**27-Pu**
[K(crypt)][Cp′$_4$U]	**28-U**
[K(crypt)][Cp′$_4$Y]	**28-Y**
[K(18-crown-6)(OEt$_2$)][(Cp′$_3$U)$_2$(μ−H)]	**29**
Cp′$_2$Pb	**30**
Cp$_3$U(THF) [Cp = C$_5$H$_5$]	**31-U(THF)**
(C$_5$Me$_4$H)$_3$U(THF)	**32-U(THF)**
(C$_5$Me$_4$H)$_3$U	**32-U**
(C$_5$Me$_4$H)$_3$La	**32-La**
(C$_5$Me$_4$H)$_3$Ce	**32-Ce**
(C$_5$Me$_4$H)$_3$Nd	**32-Nd**

Cp'_3UCl	**33-U**
Cp'_3ThCl	**33-Th**
Cp'_3UI	**34**
Cp'_3UMe	**35**
Cp'_3UMe/Cl mixture	**35/33**
$[Cp'_3U(THF)][BPh_4]$	**36**
Cp'_4U	**37-U**
Cp'_4Th	**37-Th**
Cp'_3ThBr	**38**
$LnI_3(OEt_2)_x$	**39-Ln**
$LaI_3(OEt_2)_x$	**39-La**
$CeI_3(OEt_2)_x$	**39-Ce**
$NdI_3(OEt_2)_x$	**39-Nd**
$PuI_3(OEt_2)_x$	**39-Pu**
$LnI_3(py)_4$ [py = pyridine, NC_5H_5]	**40-Ln**
$UI_3(py)_4$	**40-U**
$LaI_3(py)_4$	**40-La**
$CeI_3(py)_4$	**40-Ce**
$NdI_3(py)_4$	**40-Nd**
$PuI_3(py)_4$	**40-Pu**
$UI_3(THF)_4$	**41-U**
$LnI_3(THF)_4$	**41-Ln**
$LaI_3(THF)_4$	**41-La**

$CeI_3(THF)_4$	**41-Ce**
$NdI_3(THF)_4$	**41-Nd**
$[LaI_2(THF)_5][LaI_4(THF)_2]$	**41-La′**
$\{(THF)[(SiMe_3)_2N]_2La\}_2(\mu\text{–}O)$	**42**

ACKNOWLEDGMENTS

There are too many people to thank for this body of work. The first person would be my graduate advisor William J. Evans. I was overjoyed when I was allowed to join your lab. I was attracted to UCI in part because of your interest in the *f*-block, a largely ignored part of chemistry in the undergraduate curriculum. Your undying thirst for knowledge inspired me to keep trying no matter what. Your constant support, positive attitude and concern for my well being got me through the difficult times when I was not sure I could make it. I felt truly fortunate to have an advisor who was concerned not only with how my development as a scientist was, but as a person as well.

I would also like to the members of my thesis committee, Professor Jenny Yang and Professor Andrew Borovik. I am grateful to the research labs of my committee getting the opportunity to interact with their groups gave me a different perspective that I carried throughout graduate school. My committee challenged me scholastically and forced me to think about chemistry from a different angle, thank you for letting me discuss ideas with you at any time.

This research would not be possible without excellent facilities managers and collaborators, particularly Katie Meihaus for the magenetometry in Chapter 2 and Guo Chen for the theoretical calculations in Chapter 5. None of the NMR described, particularly Chapter 1, would be possible without Dr. Phil Denison, who helped me run any hair brained experiment I could think of with a smile on his face and a depth of knowledge about NMR spectroscopy I could only begin to understand.

A special thanks to the crystallographers who helped with this work. In particular, Dr. Joe Ziller, who always managed to find the little gem of a crystal that I could not seem to find. Joe and his assistants (Dr, Jordan Crobey, Jason Jones and Mikey Wojinar) mentored me in crystallographic collection and refinement, and didn't get too mad when I did things like close BIS. I have really enjoyed learning about crystallography. Two other crystallographers have made this possible as well, Dr. Brian Scott at LANL, who let me just start solving crystals to learn (and Dr. Douglas Kindra for growing the crystals), and Dr. Justin Cross, who taught me to just sit down and do it, "Is fine, we solves."

The people that I have worked with on the day to day have made it all worthwhile, seeing me through the good and bad times. At LANL I had the opportunity to have the deepest discussions I've ever had about organoactinide chemistry with Prof. Pete La Pierre. Discussed spectroscopy with Dr. Ben Stein "it is what it is" and laughed harder than I can remember with Dr. Marilyn Ferrier. Sam Schrell was always willing to get "pyrophoric" reagents for me from the glovebox. Again to Dr. Justin Cross for guiding me into the worlds of crystallography and trans-uranic chemistry, "it's the best".

In Bill's lab I got to work with some top notch people, too many to adequately thank here, so sorry for the brief nature. A heartfelt thanks to Dr. Megan Fieser who was always willing to help and make suggestions, she taught me a lot about being a good graduate student and I like to think that some of it rubbed off. Dr. Ryan Langeslay went down the road of grad school with me, and I really enjoyed that, working on Th and U chemistry side by side comparing and contrasting the intricacies and nuances of each element's chemistry. Though I didn't get to work in lab with him, Dr Nate Siladke left me a project that I turned into a thing and a paper. Dr. Matt Macdonald taught me how to be careful in my chemistry while working with highly reactive complexes. I've gotten some advice from Prof. Joy Farnaby, that put me in touch with a wider community outside the Evans lab. Dr. Douglas Kindra reminded me that bismuth is, and will always be, the best. There are too many others to thank, Dr. ShanShan Liu, Dr. Conrad Goodwin, Dr. Jordan Corbey, Dr. Chris Kotyk and Dr. Chris Webster as well as current graduate students David Woen, Chad Palumbo, Sam Moering, Megan Dumas, Austin Ryan, Dan Huh, Tenner Jenkins, and Monica Boshart, who didn't tire of me telling her how great uranium chemistry was, much to her chagrin. A special thanks to undergraduate Mary Angodal, who was brave enough to work with me at the end of my graduate career.

A special thanks to Dr. Andrew Gaunt, who taught me about air free plutonium chemistry, and letting me burden him for almost a year. I really enjoyed it and learned a lot. I look forward to being able to would with you more in the future. None of the work at LANL would be possible without Dr. Stosh Kozimor. He taught me about handling actinides, working at LANL, how to think outside the box, and for supporting me through some very tough times. I put him through more hell than I know, and I deeply appreciate it. I hope to be half the scientist he is.

"It's gonna be great!"

I am grateful to my professors at my undergraduate university, UW-River Falls, specifically Prof. Magdalena Pala and Prof. K. W. McLaughlin, as well as Prof. James Mayer and Prof Caroline Saouma from my undergraduate internship. A personal thank you to all of my friends in and outside of science that saw me through the last five years, particularly Joe, Todd, Eve, Thom, Glen, even Corey and many more. They may not have understood it but they were there for me when I needed it.

I of course could not forget my loving parents, Ed and Kathy and my sister Ashley. They didn't understand what I was doing, but they have supported me every step of the way, thank you doesn't begin to describe my gratitude.

Last, but certainly not least, my loving wife Kelsey. You have always been there for me, and I'm so glad I've gotten to go down this road with you. A special thank you for letting me type this document on your computer when all of mine broke down. You've supported me in ways I can't express. I love you.

CURRICULUM VITAE
Cory J. Windorff

7617 Palo Verde rd
Irvine, CA 92617
Mobile: 414.940.4154
cwindorf@uci.edu
Born: October 26, 1986
Place: Brookfield, WI

EDUCATION

Doctor of Philosophy, July 2017
University of California–Irvine
Advised by Professor William J. Evans
Thesis title "*Synthesis, Characterization and Reactivity of Organometallic Complexes of Uranium and Plutonium in the +2 and +3 Oxidation States*"

Bachelor of Science, May 2012
University of Wisconsin–River Falls
GPA: 3.5 on 4.0 scale
Major: ACS Polymer Chemistry
Major: Modern Languages–German
Minor: Mathematics

Fellowships, Grants and Scholarships Received

Graduate School:

Department of Energy (DOE) Office of Science Graduate Student Research Fellow (2015 – 2016)
UCI Department of Physical Sciences Dissertation Fellowship (Winter 2017)
La Verne Noyes Fellowship (Spring 2014, 2017)

Undergraduate School:

National Science Foundation (NSF) Center for Enabling New Technology through Catalysis (CENTC) summer internship (Summer 2011)
Federal Pell Grant (2010 – 2012)
Federal SMART Grant (2010 – 2011)
Wisconsin Higher Education Grant (2010 – 2012)
UW–RF Chemistry Department Scholarships (2009 – 2012)

Honors – Undergraduate

Ronald E. McNair Post-Baccalaureate Achievement Program (2010 – 2012)
2012 Recipient of the *Outstanding Senior Award* in the Department of Chemistry, UW–RF
2011 Recipient of the *ACS Award for Outstanding Inorganic Achievement*

Honors Program (2008 – 2012)
Dean's List: Fall 2007, Spring 2008, and Spring 2011

Professional Affiliations, Identifiers and Memberships

American Chemical Society – Inorganic Division (November 2010)
ORCiD: 0000-0002-5208-9129
University of WI–River Falls

- Chemistry Club and Chemistry Demonstrators (Member 2007 – 2012, secretary 2008 – 2010)
- German Club (Member 2009 – 2011)

Instrumentation and Technique Proficiencies

Positive and negative pressure inert atmosphere glovebox techniques
Schlenk and high vacuum line techniques
Handling radioactive nuclei
Handling small quantities of material (<5 mg material)
Variable temperature nuclear magnetic resonance spectroscopy (VT–NMR) ^{1}H, ^{2}H, ^{11}B, ^{13}C, ^{29}Si, ^{77}Se and ^{209}Pb.
X–ray crystallographic collection and refinement
Ultraviolet-visible-near infrared spectroscopy (UV/vis/NIR)
Fourier transform infrared spectrometry (FTIR)
Elemental analysis (EA)
Differential scanning calorimetry (DSC)
Thermogravimetric analysis (TGA)
Cyclic voltammetry (CV)
High pressure liquid chromatography (HPLC)
Gas chromatography and mass spectrometry (GC–MS)

Research Experience

Graduate School:

Synthesis, Characterization and Reactivity of Organometallic Complexes of Uranium and Plutonium in the +2 and +3 Oxidation States
December 2012 – July 2017
Research Advisor: Professor William J. Evans.

Synthesized highly air/water sensitive organometallic plutonium, uranium and thorium compounds in the +2, +3 and +4 oxidation states and examined their reactivity using Schlenk line, vacuum line and glovebox techniques. Characterized compounds using X-ray crystallography, multi-nuclear ^{1}H, ^{13}C and ^{29}Si NMR, UV/vis/NIR, and IR spectroscopy.
Through a DOE fellowship, performed one year of research at Los Alamos National Laboratory (LANL) with Dr. Stosh A. Kozimor and Dr. Andrew J. Gaunt on the isolation of Pu^{2+}.

Undergraduate School:

Investigating Iron-Sulfur Clusters
University of Washington, Chemistry Department
June 2011 to August 2011
Research Advisor: Professor James Mayer

Awarded a scholarship through National Science Foundation (NSF) Center for Enabling New Technologies through Catalysis (CENTC) to study in Professor Mayer's Lab. Synthesized and characterized bio-mimetic complexes of the Rieske [2Fe-2S] metalloproteins to examine the kinetics of electron transfer. Used Schlenk line and glovebox techniques, characterized by variable temperature ^{1}H NMR spectroscopy.

Polyvinyl alcohol: Pre-Gel Viscous Fluid or Covalently Cross-Linked Network?
University of Wisconsin–River Falls, Chemistry Department
August to December 2011
Research Advisor: Professor Kevin McLaughlin

Prepared high molecular weight borate crosslinked polyvinyl alcohol polymers and determined the gel point. Examined the importance of NaOH concentration to push the $B(OH)_3 + (OH)^- \rightleftharpoons B(OH)_4^-$ equilibrium to the right.

Teaching Organic First
University of Wisconsin – River Falls, Chemistry Department
January – December 2010
Research Advisor: Professor Jamie Schneider

Analyzed and organized student data to determine if an undergraduate curriculum of Organic Chemistry First causes a higher STEM student retention. Analyzed data using Excel and SPSS programs.

Relevant Work and Teaching Experiences

Graduate School:

Graduate Classes: Mentoring fellow graduate students and an undergraduate student in air free laboratory techniques for synthesis and characterization. Teaching Assistant for introductory chemistry, upper level undergraduate and graduate courses, leading discussion sections, preparing students for exams and grading, in addition to leading laboratory sections.
Undergraduate Classes: Teaching Assistant: Led exam reviews, assisted professors during laboratory sections, and tutored students in lower level chemistry courses. Organized and performed lab experiments to introduce the inorganic laboratory to students ranging from inner city elementary schools to honors non-science college students.

Undergraduate School:

REU intern at the NSF Center for Enabling New Technologies in Catalysis (summer 2011)
Chemistry Help Room at University of WI – River Falls (2008 – 2012)
Private Tutor in General, Organic and Analytical Chemistry (2008 – 2012)
General Chemistry Lab Assistant (September 2008 – 2012)
Exam Study Session Leader, Chem 230, Survey of Organic Chemistry (2010 – 2011)
General Chemistry II Online Teachers Assistant (spring 2009)
Perform chemical experiments for students, families and the community as part of the "Chem Demons" student group (2007 – 2012)

Publications

Published

5. "Covalency in Americium(III) Hexachloride" Cross, J. N.; Su, J.; Batista, E. R.; Cary, S. K.; Evans, W. J.; Kozimor, S. A.; Mocko, V.; Scott, B. L.; Stein, B. S.; Windorff, C. J.; Yang, P. *Journal of the American Chemical Society*, **2017**, *139*, 8667–8677. DOI: 10.1021/jacs.7b03755

4. "Identification of the Formal +2 Oxidation State of Plutonium: Synthesis and Characterization of $\{Pu(II)[C_5H_3(SiMe_3)_2]_3\}^-$" Windorff, C. J.; Chen, G. P.; Cross, J. N.; Evans, W. J.; Furche, F.; Gaunt, A. J.; Janicke, M. T.; Kozimor, S. A.; Scott, B. L. *Journal of the American Chemical Society*, **2017**, *139*, 3970–3973. DOI: 10.1021/jacs.7b00706

   Highlighted by:
   Eureka Alert! By AAAS: "Unexpected oxidation state for molecular plutonium discovered" March 9, 2017 https://www.eurekalert.org/pub_releases/2017-03/danl-uos030917.php
   Chemistry World: "Plutonium gets another oxidation state added to its arsenal" March 17, 2017 https://www.chemistryworld.com/news/plutonium-gets-another-oxidation-state-added-to-its-arsenal/3006982.article
   C&EN: "Actinide chemistry expands to new oxidation states" March 21, 2017 http://cen.acs.org/articles/95/web/2017/03/Actinide-chemistry-expands-new-oxidation.html

3. "Synthesis, Structure and Reactivity of the Sterically Crowded Th^{3+} Complex $(C_5Me_5)_3Th$ Including Formation of the Thorium Carbonyl, $[(C_5Me_5)_3Th(CO)][BPh_4]$" Langeslay, R. R.; Chen, G. P.; Windorff, C. J.; Chan, A. K.; Ziller, J. W.; Furche, F.; Evans, W. J. *Journal of the American Chemical Society*, **2017**, *139*, 3387–3398. DOI: 10.1021/jacs.6b10826

2. "Expanding the Chemistry of Molecular U^{2+} Complexes: Synthesis, Characterization, and Reactivity of the $\{[C_5H_3(SiMe_3)_2]U\}^{1-}$ Anion" Windorff, C. J; MacDonald, M. R.; Meihaus, K. R.; Ziller, J. W.; Long, J. R.; Evans, W. J. *Chemistry – A European Journal*, **2016**, *22*, 772–782. DOI: 10.1002/chem.201503583

1. "^{29}Si NMR Spectra of Silicon-Containing Uranium Complexes" Windorff, C. J.; Evans, W. J. *Organometallics*, **2014**, *33*, 3786–3791. DOI: 10.1021/om500512q

Manuscripts Prepared for Submission

"Small-Scale Metal-Based Syntheses of Lanthanide Iodide, Amide, and Cyclopentadienyl Complexes as Surrogates for Transuranic Reactions" Windorff, C. J.; Dumas, M. T.; Ziller, J. W.; Evans, W. J. *Target Journal: Inorganic Chemistry.*

"Synthesis and Characterization of the Linear Thorium Metallocenes, $[(C_5Me_5)_2Th(NCR)_5][BPh_4]_2$" Langeslay, R. R.; Windorff, C. J.; Ziller, J. W.; Evans, W. J. *Target Journal: Organometallics.*

"Tetrakis(trimethylsilylcyclopentadienyl) An^{4+} Chemistry: Synthesis of Cp'_4An ($Cp' = C_5H_4SiMe_3$, An = Th, U)" Windorff, C. J; MacDonald, M. Ziller, J. W.; Evans, W. J. *Target Journal: Journal of Organometallic Chemistry.*

Manuscripts in Preparation

"XAS Spectroscopy of Lanthanide Thiocyanates" Windorff, C. J.; Batista, E. R.; Cross, J. N.; Evans, W. J.; Kozimor, S. A.; Scott, B. L.; Yang, P. *Target Journal: Inorganic Chemistry.*

"Synthesis and Characterization of Homoleptic Metal Selenocyanates" Windorff, C. J.; Cross, J. N.; Evans, W. J.; Kozimor, S. A.; Scott, B. L.; Ziller, J. W. *Target journal: Inorganic Chemistry.*

"Synthesis and Characterization of $U(C_5H_4SiMe_3)_3(BH_4)$" Windorff, C. J.; Evans, W. J.; Kozimor, S. A.; Scott, B. L. *Target Journal: Polyhedron.*

Graduate School Presentations

"Synthesis and X-ray Crystallogrphic Characterization of Low Valent Organoplutonium Complexes: Identification of Plutonium in +2 Oxidation State" Windorff C. J.; Chen, G.; Gaunt, A. J.; Janicke, M. H.; Kozimor, S. A.; Scott, B. L.; Fuche, F.; Evans, W. J. Oral Presentation at the 253rd National Meeting of the American Chemical Society, Invited award session talk in honor of David L. Clark, San Francisco, CA, April 4th 2017.

"Exploration of Low Valent Organoplutonium Chemistry: Identification of Pu^{2+} in $\{Pu[C_5H_3(SiMe_3)_2]_3\}^{1-}$" Windorff C. J.; Chen, G.; Gaunt, A. J.; Janicke, M. H.; Kozimor, S. A.; Scott, B. L.; Fuche, F.; Evans, W. J. Oral Presentation at Southern California Organometallics Meeting, University of California–Los Angeles, Los Angeles, CA, December 4th, 2016.

"Synthesis of $(C_5H_4SiMe_3)_4U$ reveals that a $(C_5H_4SiMe_3)_3UCl/(C_5H_4SiMe_3)_3UMe$ mixture of is more crystalline than the pure compounds" Windorff, C. J.; MacDonald, M. R.; Ziller, J. W.; Evans, W. J. Oral Presentation at the 251st ACS Meeting, San Diego, CA, March 15, 2016.

"Synthesis, Characterization, and Reactivity of U^{2+} in the $\{[C_5H_3(SiMe_3)_2]_3U\}^{1-}$ Anion" Windorff, C. J.; MacDonald, M. R.; Ziller, J. W.; Evans, W. J. Oral Presentation at the 249th ACS Meeting, Denver, CO, March 26, 2015.

"^{29}Si NMR Spectra of Silicon-Containing Uranium Complexes" Windorff, C. J.; Evans, W. J. Oral Presentation at the 248th ACS Meeting, San Francisco, CA, August 14, 2014.

Volunteer Activities

Chemical Demonstrations (2009 – 2016)

Perform, organize and explain laboratory experiments for a wide range of audiences ranging from low-income middle school children to non-science major college students.

Restorative Justice–River Falls, WI (2009 & 2011)

Mentored juveniles in their community service to facilitate restorative justice.

References

Professor William J. Evans
Department of Chemistry, University of California-Irvine
2046B Fredrick Reines Hall, Irvine, CA 92697
(949) 824-5174, wevans@uci.edu

Dr. Stosh A. Kozimor
Inorganic, Isotope, and Actinide Chemistry
PO 1663, MS J975; Los Alamos, NM 87545, USA
(505) 695-4713, stosh@lanl.gov

Dr. Andrew J. Gaunt
Inorganic, Isotope, and Actinide Chemistry
PO 1663, MS J514; Los Alamos, NM 87545, USA
(505) 667-3395, gaunt@lanl.gov

Professor Jenny Y. Yang
Department of Chemistry, University of California-Irvine
3038D Fredrick Reines Hall, Irvine CA 92698
(949) 824-1533, j.yang@uci.edu

Professor A.S. Borovik
Department of Chemistry, University of California-Irvine
4138 Natural Sciences 1, Irvine, CA 92697
(949) 824-1510, aborovik@uci.edu

ABSTRACT OF THE DISSERTATION

Synthesis, Characterization and Reactivity of Organometallic Complexes of Uranium and Plutonium in the +2 and +3 Oxidation States

By

Cory J. Windorff

Doctor of Philosophy in Chemistry

University of California, Irvine, 2017

Professor William J. Evans, Chair

This dissertation focuses on the synthesis, characterization, and reactivity of unique organometallic complexes of uranium, plutonium, and the lanthanides in efforts to expand the limits of known redox chemistry of these elements. The results in this dissertation extend investigations of previously established reduction reactions involving these metal ions to extend them to more challenging systems. These reactions utilized the tri(cyclopentadienide) coordination environment examining the differences in the substitution pattern on the cyclopentadienide rings, particularly the Cp″ ligand [Cp″ = $C_5H_3(SiMe_3)$–1,3]. In the course of these studies, the +2 oxidation state for plutonium was confirmed, and the most stable form of U^{II} to date was isolated. To accomplish the plutonium chemistry, several surrogate syntheses were performed using lanthanides of similar size and reactivity to that of plutonium, namely cerium and neodymium. These experiments examined the electronic structure to compare and contrast the +2 oxidation state across the actinide series.

In Chapter 1 ^{29}Si NMR spectra were recorded for a series of uranium complexes containing silicon and the data have been combined with results in the literature to determine if

any trends exist between chemical shift and structure, ligand type, or oxidation state. Data on 48 paramagnetic inorganic and organometallic uranium complexes are presented. The survey reveals that although there is some overlap in the range of shifts of U^{IV} complexes versus U^{III} complexes. In general U^{III} species have more negative shifts than their U^{IV} analogs. The single U^{II} example has the most negative shift of all at −322 ppm at 170 K. With only a few exceptions, U^{IV} complexes have shifts between 0 and −150 ppm (vs. $SiMe_4$) whereas U^{III} complexes resonate between −120 and −250 ppm. The small data set on U^{V} species exhibits a broad 250 ppm range centered near 40 ppm. The data also show that aromatic ligands such as cyclopentadienide, cyclooctatetraenide, and the pentalene dianion, exhibit less negative chemical shifts than other types of ligands.

Chapter 2 describes the synthesis of new molecular complexes of U^{II} that were pursued to make comparisons in structure, physical properties, and reactivity with the first U^{II} complex, [K(crypt)][Cp′$_3$U], **21-U** (Cp′ = $C_5H_4SiMe_3$, crypt = 2.2.2-Cryptand). Reduction of Cp″$_3$U, **20-U**, [Cp″ = $C_5H_3(SiMe_3)_2$–1,3] with KC_8 in the presence of crypt or 18-crown-6 generates [K(crypt)][Cp″$_3$U], **22-U,** or [K(18-crown-6)(THF)$_2$][Cp″$_3$U], **23-U**, respectively. The UV/vis spectra of **22-U** and **21-U** are similar, and they are much more intense than those of U^{III} analogs. Variable temperature magnetic susceptibility data for **21-U** and **22-U** reveal a lower room temperature $\chi_M T$ value relative to the experimental value for the $5f^3$ U^{III} precursors. Stability studies monitored by UV/vis spectroscopy show that **22-U** and **23-U** have $t_{1/2}$ values of 20 and 15 h at room temperature, respectively, vs 1.5 h for **21-U**. Complex **23-U** reacts with H_2 or $PhSiH_3$ to form the uranium hydride, [K(18-crown-6)(THF)$_2$][Cp″$_3$UH], **26.** **21-U** and **23-U**

both reduce cyclooctatetraene to form uranocene, $(C_8H_8)_2U$, as well as the U^{III} byproducts [K(crypt)][Cp′$_4$U], **28-U**, and Cp″$_3$U, **20**-U, respectively.

In Chapter 3 Cp′$_4$U, **37-U**, was synthesized from (a) KCp′ and [Cp′$_3$U(THF)][BPh$_4$], **36**, (b) Cp′$_3$U, **8-U**, and Cp′$_2$Pb,**30**, and (c) [K(crypt)][Cp′$_4$U], **28-U**, and AgBPh$_4$ and identified by X-ray crystallography as a rare example of a structurally-characterized tetrakis(cyclopentadienyl)U^{IV} complex. The corresponding Th complex, Cp′$_4$Th, **37-Th**, was obtained from the direct combination of ThBr$_4$(THF)$_4$ with excess KCp′ in low yield. During the preparation of Cp′$_3$UMe, **35**, the precursor of the [Cp′$_3$U(THF)][BPh$_4$], **36**, reagent used above, it was discovered that the reaction of Cp′$_3$UCl, **33-U**, and MeLi gives a mixture of Cp′$_3$UMe, **35** and **33-U** that can co-crystallize better than **35** in pure form. Although **35** typically is an oil, a mixture of **35** and **33-U** forms single crystals that are suitable for X-ray crystallography and contain a 4:1 ratio of the compounds. Hence, forming a mixture provided a new way to get structural data on the oil, **35**. **33-U** and Cp′$_3$UI, **34**, were also crystallographically characterized for comparison with the Cp′$_3$UMe/Cp′$_3$UCl, **35/33** crystals.

Chapter 4 examines the optimization of reaction conditions for milligram scale plutonium reactions. Starting from the metal, small-scale reactions of the Pu surrogates, La, Ce, and Nd, were explored. Oxidation of these lanthanide metals with iodine in ether or pyridine was studied and it was found that LnI$_3$(Et$_2$O)$_x$, **39-Ln** (x = 1.5–1.8), and LnI$_3$(py)$_4$, **40-Ln** (py = pyridine, NC$_5$H$_5$), can be synthesized on scales ranging from 15 mg to 2 g. The THF adducts LnI$_3$(THF)$_4$, **41-Ln**, were synthesized by dissolving **39-Ln** in THF which was found to be preferable to synthesis from the metal in THF on this small scale. The viability of these small scale samples

as starting materials for amide and cyclopentadienyl *f*–element complexes was tested by reacting *in situ* generated **39-Ln** with $KN(SiMe_3)_2$, KCp′, Cp″, and KC_5Me_4H. This produced $Ln[N(SiMe_3)_2]_3$, **15-Ln**, Cp'_3Ln, **8-Ln**, Cp''_3Ln, **20-Ln**, and $(C_5Me_4H)_3Ln$, **32-Ln**. Small scale samples of Cp'_3Ce, **8-Ce**, and Cp'_3Nd, **8-Nd**, were reduced with potassium graphite (KC_8) in the presence of crypt to check the viability for generation of crystallographically-characterizable Ln^{II} complexes, [K(crypt)][Cp'_3Ln], **21-Ln** (Ln = Ce, Nd). Similar reactions of Cp''_3Nd, **20-Nd**, with KC_8 in the presence of crypt gave [K(crypt)][Cp''_3Nd], **22-Nd**, as a crystallographically characterizable complex.

Chapter 5 combines and extends the chemistry described in Chapters 2 and 4 to plutonium. Over seventy years of chemical investigations have shown plutonium exhibits some of the most complicated chemistry in the periodic table. Six Pu oxidation states have been unambiguously confirmed (0, +3 to +7) and five different oxidation states can exist simultaneously in solution. The synthesis and characterization of a new formal oxidation state for plutonium, namely Pu^{II} in [K(crypt)][Cp''_3Pu], **22-Pu**, is examined. The synthetic precursor, Cp''_3Pu, **20-Pu**, is also synthesized and discussed, comprising the first structural characterization of a Pu–C bond. Absorption spectroscopy and DFT calculations indicate that the Pu^{II} ion has predominantly a $5f^6$ electron configuration with some 6*d*-mixing. Reactivity studies show that **22-Pu** reacts with $AgBPh_4$ to reform **20-Pu** in high yield.

INTRODUCTION

The actinide elements (An), those spanning actinium (89) to lawrencium (103), are a unique set of elements that represent the heaviest elements on which routine chemistry can be performed. Their applications include nuclear energy and weapons and oil and gas exploration and are proposed for targeted α-therapy.[1-4] To fully utilize these elements, their chemistry must be understood. The electronic structure of the actinides are different to that of other metals as well. Whereas transition metal n*d* orbitals show significant radial extension outside the noble gas core, lanthanides (Ln) have contracted 4*f* orbitals inside the [Xe] core, and the actinide 5*f* orbitals have a small radial extent outside the [Rn] core, Figure 0.1.[5-7] This difference in radial extent about the noble gas core gives rise to the highly covalent interactions often exhibited by transition metals, while the lanthanides show primarily ionic interactions. The small radial extent outside of the [Xe] core in the actinide 5*f* orbitals gives intermediate properties where small amounts of covalency are observed. This covalency is most pronounced in the early actinides (Ac – Np), with the later actinides (Am – Lr) showing "lanthanide like behavior," Figure 0.2, [14, 15] though this is a contested topic still under debate.[8-10] Additionally, the role and extent to which 6*d* orbitals participate in bonding is still being examined.[11-13]

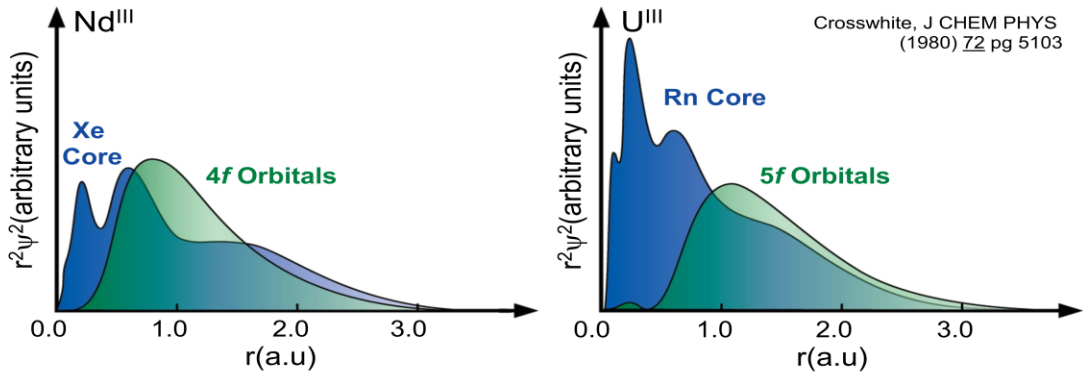

Figure 0.1. Probability distribution as a function of radial extension of 4*f* orbitals in Nd^{III} and 5*f* orbitals in U^{III}.

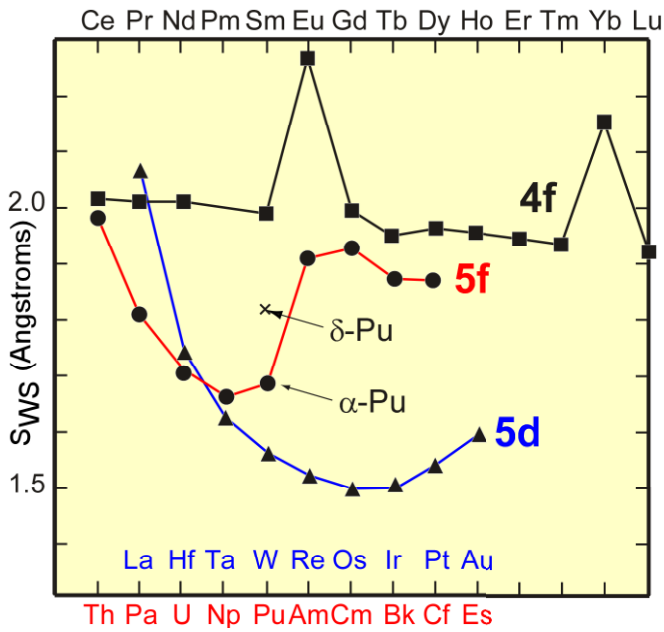

Figure 0.2. Wigner–Seitz radii (S_{WS}) for the actinides (red trace), lanthanides (black trace), and 5*d* transition metals (blue trace) across the series.[1]

In addition to small amounts of covalency, the early actinides show a wide variety of available oxidation states, with plutonium showing the largest number of available oxidation sates (+2 to +7 with the +8 oxidation state claimed but not substantiated), Table 0.1.[1] The availability of oxidation states in the lanthanides is a different story where for many years the +3

Table 0.1. Available Oxidation States for the Actinide Elements, **Most Stable**, (Unstable), ? = Claimed But Not Substantiated.

Ac	Th	Pa	U	Np	Pu	Am	Cm	Bk	Cf	Es	Fm	Md	No	Lr
												1?		
	2		2	2?	2	(2)			(2)	(2)	2	2	**2**	
3	3	(3)	3	3	3	**3**	**3**	**3**	**3**	**3**	**3**	**3**	3	**3**
	4	4	4	4	**4**	4	4	4	4	4?				
		5	5	**5**	5	5	5?		5?					
			6	6	6	6	6?							
				7	7	7?								
					8?									

oxidation state dominated with the exception of accessible +2 oxidation states for Sm, Eu and Yb, and the +4 oxidation state for Ce. During a five year span from 1997–2001, compounds of Nd, Dy and Tm in the +2 oxidation state were isolated and characterized. These six elements, Nd, Sm, Eu, Dy, Tm, and Yb, comprised the so called "six traditional divalent lanthanides" as it was thought other Ln^{II} ions would be too unstable in common solvent to isolate.[16] However some solid state experimental evidence suggested that many of the *f* elements (La – Lu; U – No) possess a $M^{II/III}$ couple no more negative than −2.94±0.08 V (vs. SHE) for lanthanum.[17] In 2008, Lappert successfully characterized the first molecular La^{2+} complex through the reduction of Cp''_3La^{III} [Cp″ = $C_5H_3(SiMe_3)_2$–1,3] along with encapsulation of the K^+ ion inside 2.2.2-cryptand (crypt), to form $[K(crypt)][Cp''_3La^{II}]$[18] eq 0.1. Further work from 2012–2015 utilized the tris(mono-silyl cyclopentadienide) ligand environment, Cp'_3Ln^{III} (Cp′ = $C_5H_4SiMe_3$) to isolate all of the available lanthanides as $[K(crypt)][Cp'_3Ln^{II}]$, eq. 0.1.[19-22]

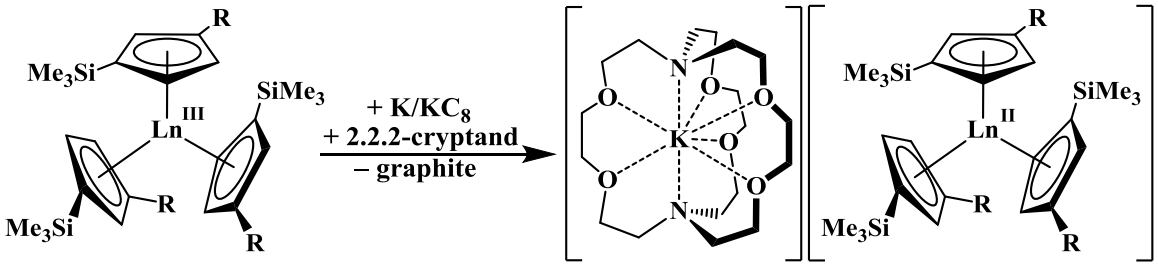

(0.1)

R = $SiMe_3$; M = La

R = H; M = Y, La, Ce, Pr, Nd, Sm, Gd, Tb, Dy, Ho, Er, Tm, Lu

Efforts to synthesize U^{II} have appeared since the 1980's, but only U^{III} products have been isolated.[23-25] There have also been numerous examples of low-valent uranium with reduced ligands, typically arenes, i.e. $[(anion)_2U](C_6H_5R)$ (R = H, Me).[26-29] The successful isolation of U^{II} was achieved by reduction of Cp'_3U^{III} to isolate $[K(crypt)][Cp'_3U^{II}]$,[30] Figure 0.3. Later it was reported that a tris-aryloxide arene environment could also stabilize the U^{II} ion as $[K(crypt)]\{[(^{Ad,Me}ArO)_3mes]U^{II}\}$,[31] Figure 0.3.

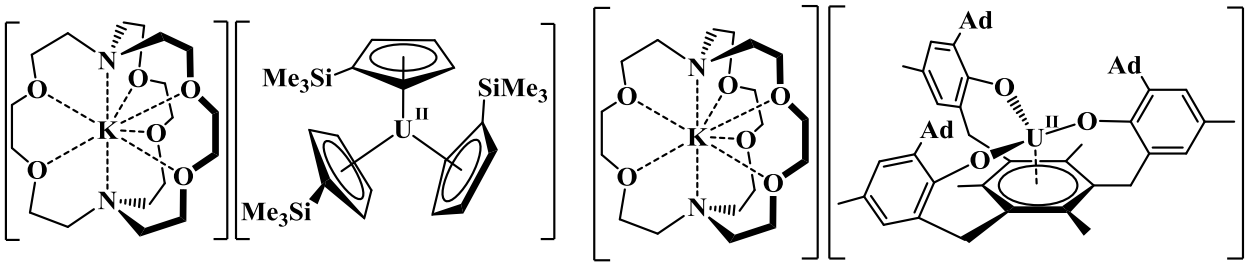

Figure 0.3. Crystallographically characterized U^{II} complexes, [K(crypt)][Cp'_3U^{II}] (left) and [K(crypt)]{[(^{Ad,Me}ArO)$_3$mes]U^{II}} (right).

These results spurred extension of +2 chemistry to other actinide elements, with the isolation of [K(crypt)][Cp''_3Th^{II}],[32] the first Th^{II} complex, which was quite unexpected considering the +3 oxidation state is unusual and difficult to isolate for thorium.[33]

The chemistry of the actinides is dominated by uranium and thorium due to their low radioactivity and high natural abundance. The chemistry of the trans-uranium (TRU) elements is significantly underdeveloped, particularly in terms of air-free chemistry. The majority of the air-free complexes of TRU elements have focused on the cyclopentadienide (Cp, C_5H_5) and cyclooctatetraenide dianion ($C_8H_8^{2-}$), primarily through the success of ferrocene, and the isolation of uranocene, $(C_8H_8)_2U$.[34] These ligands have proven very successful as they have high coordination numbers and low charge, ideally suited for the large trivalent actinides cations, Figure 0.4. Although several Cp_3An complexes (An = Np, Pu, Cm, Bk, Cf)[35-38] have been crystallographically characterized, the organometallic chemistry remains limited.[39-40]

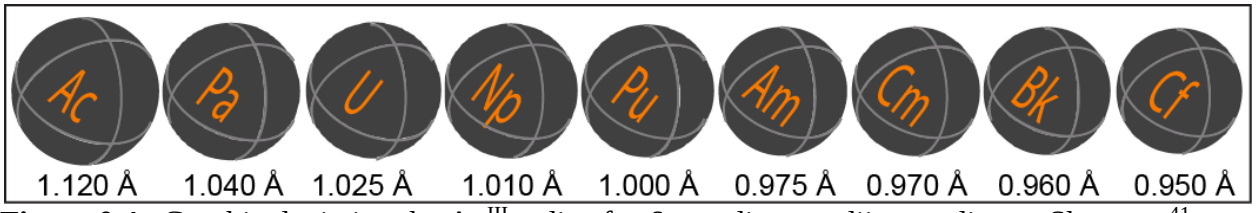

Figure 0.4. Graphic depicting the An^{III} radius for 6 coordinate radii according to Shannon.[41]

The results discussed in this thesis expand and characterize the nature of low valent organoactinide complexes, primarily those of uranium and plutonium, in the +2 and +3 oxidation states. Due to the difficulty in working with plutonium, lanthanides, cerium and neodymium in particular, are used as surrogates. These results show that the structure of the ligands is important for stabilizing (or destabilizing) the +2 oxidation state. The di-silylcyclopentadienide, Cp″ ligand provides significantly increased stabilization of An^{II} (An = U, Pu) complexes over those of Cp′. These synthetic results were examined by single crystal X-ray crystallography, multi-nuclear variable-temperature NMR spectroscopy, and UV/vis/NIR spectroscopy.

REFERENCES

(1) Morss, L. R.; Edelstein, N. M.; Fuger, J., *The Chemistry of the Actinide and Transactinide Elements*. 4th ed.; Springer: Dordrecht, The Netherlands, 2010; Vol. 1-6.

(2) Clark, D. L.; Hobart, D. E.; Neu, M. P., *Chem. Rev.* **1995,** *95*, 25-48.

(3) Sykora, R. E.; Assefa, Z.; Haire, R. G.; Albrecht-Schmitt, T. E., *Inorg. Chem.* **2006,** *45*, 475-477.

(4) Ferrier, M. G.; Stein, B. W.; Batista, E. R.; Berg, J. M.; Birnbaum, E. R.; Engle, J. W.; John, K. D.; Kozimor, S. A.; Lezama Pacheco, J. S.; Redman, L. N., *ACS Cent. Sci.* **2017,** *3*, 176-185.

(5) Crosswhite, H. M.; Crosswhite, H.; Carnall, W. T.; Paszek, A. P., *J. Chem. Phys.* **1980,** *72*, 5103-5117.

(6) Neidig, M. L.; Clark, D. L.; Martin, R. L., *Coord. Chem. Rev.* **2013,** *257*, 394-406.

(7) Minasian, S. G.; Keith, J. M.; Batista, E. R.; Boland, K. S.; Clark, D. L.; Kozimor, S. A.; Martin, R. L.; Shuh, D. K.; Tyliszczak, T., *Chem. Sci.* **2014,** *5*, 351-359.

(8) Cary, S. K.; Silver, M. A.; Liu, G.; Wang, J. C.; Bogart, J. A.; Stritzinger, J. T.; Arico, A. A.; Hanson, K.; Schelter, E. J.; Albrecht-Schmitt, T. E., *Inorg. Chem.* **2015,** *54*, 11399-11404.

(9) Cary, S. K.; Vasiliu, M.; Baumbach, R. E.; Stritzinger, J. T.; Green, T. D.; Diefenbach, K.; Cross, J. N.; Knappenberger, K. L.; Liu, G.; Silver, M. A.; DePrince, A. E.; Polinski, M. J.; Van Cleve, S. M.; House, J. H.; Kikugawa, N.; Gallagher, A.; Arico, A. A.; Dixon, D. A.; Albrecht-Schmitt, T. E., *Nat. Commun.* **2015,** *6*, 6827.

(10) Cross, J. N.; Su, J.; Batista, E. R.; Cary, S. K.; Evans, W. J.; Kozimor, S. A.; Mocko, V.; Scott, B. L.; Stein, B. W.; Windorff, C. J.; Yang, P., *J. Am. Chem. Soc.* **2017,** *139*, 8667-8677.

(11) Minasian, S. G.; Boland, K. S.; Feller, R. K.; Gaunt, A. J.; Kozimor, S. A.; May, I.; Reilly, S. D.; Scott, B. L.; Shuh, D. K., *Inorg. Chem.* **2012,** *51*, 5728-5736.

(12) Minasian, S. G.; Keith, J. M.; Batista, E. R.; Boland, K. S.; Kozimor, S. A.; Martin, R. L.; Shuh, D. K.; Tyliszczak, T.; Vernon, L. J., *J. Am. Chem. Soc.* **2013,** *135*, 14731-14740.

(13) Ferrier, M. G.; Batista, E. R.; Berg, J. M.; Birnbaum, E. R.; Cross, J. N.; Engle, J. W.; La Pierre, H. S.; Kozimor, S. A.; Lezama Pacheco, J. S.; Stein, B. W.; Stieber, S. C.; Wilson, J. J., *Nat. Commun.* **2016,** *7*, 12312.

(14) Yasuoka, H.; Koutroulakis, G.; Chudo, H.; Richmond, S.; Veirs, D. K.; Smith, A. I.; Bauer, E. D.; Thompson, J. D.; Jarvinen, G. D.; Clark, D. L., *Science* **2012,** *336*, 901-904.

(15) Los Alamos Science, 2006, *Plutonium: An Element at Odds With Itself*.

(16) Evans, W. J., *Inorg. Chem.* **2007,** *46*, 3435-3449.

(17) Mikheev, N. B.; Kamenskaya, A. N., *Coord. Chem. Rev.* **1991,** *109*, 1-59.

(18) Hitchcock, P. B.; Lappert, M. F.; Maron, L.; Protchenko, A. V., *Angew. Chem., Int. Ed.*, ***20*08,** *47*, 1488-1491.

(19) MacDonald, M. R.; Ziller, J. W.; Evans, W. J., *J. Am. Chem. Soc.* **2011,** *133*, 15914-15917.

(20) MacDonald, M. R.; Bates, J. E.; Fieser, M. E.; Ziller, J. W.; Furche, F.; Evans, W. J., *J. Am. Chem. Soc.* **2012,** *134*, 8420-8423.

(21) MacDonald, M. R.; Bates, J. E.; Ziller, J. W.; Furche, F.; Evans, W. J., *J. Am. Chem. Soc.* **2013,** *135*, 9857-9868.

(22) Fieser, M. E.; MacDonald, M. R.; Krull, B. T.; Bates, J. E.; Ziller, J. W.; Furche, F.; Evans, W. J., *J. Am. Chem. Soc.* **2015,** *137*, 369-382.

(23) McLaren, A. B.; Kanellakopulos, B.; Dornberger, E., *Inorg. Nucl. Chem. Lett.* **1980,** *16*, 223-225.

(24) Fagan, P. J.; Manriquez, J. M.; Marks, T. J.; Day, C. S.; Vollmer, S. H.; Day, V. W., *Organometallics* **1982,** *1*, 170-180.

(25) Warner, B. P.; Scott, B. L.; Burns, C. J., *Angew. Chem., Int. Ed.*, **1998,** *37*, 959-960.

(26) Diaconescu, P. L.; Arnold, P. L.; Baker, T. A.; Mindiola, D. J.; Cummins, C. C., *J. Am. Chem. Soc.* **2000,** *122*, 6108-6109.

(27) Evans, W. J.; Kozimor, S. A.; Ziller, J. W.; Kaltsoyannis, N., *J. Am. Chem. Soc.* **2004,** *126*, 14533-14547.

(28) Vlaisavljevich, B.; Diaconescu, P. L.; Lukens, W. L.; Gagliardi, L.; Cummins, C. C., *Organometallics* **2013,** *32*, 1341-1352.

(29) Liddle, S. T., *Coord. Chem. Rev.* **2015,** *293–294*, 211-227.

(30) MacDonald, M. R.; Fieser, M. E.; Bates, J. E.; Ziller, J. W.; Furche, F.; Evans, W. J., *J. Am. Chem. Soc.* **2013,** *135*, 13310-13313.

(31) LaPierre, H. S.; Scheurer, A.; Heinemann, F. W.; Hieringer, W.; Meyer, K., *Angew. Chem., Int. Ed.*, **2014,** *53*, 7158-7162.

(32) Langeslay, R. R.; Fieser, M. E.; Ziller, J. W.; Furche, F.; Evans, W. J., *Chem. Sci.* **2015,** *6*, 517-521.

(33) Ortu, F.; Formanuik, A.; Innes, J. R.; Mills, D. P., *Dalton Trans.* **2016,** *45*, 7537-7549.

(34) Seyferth, D., *Organometallics* **2004,** *23*, 3562-3583.

(35) Dutkiewicz, M. S.; Apostolidis, C.; Walter, O.; Arnold, P. L., *Chem. Sci.* **2017,** *8*, 2553-2561.

(36) Laubereau, P. G.; Burns, J. H., *Inorg. Nucl. Chem. Lett.* **1970,** *6*, 59-63.

(37) Laubereau, P. G.; Burns, J. H., *Inorg. Chem.* **1970,** *9*, 1091-1095.

(38) Walter, O., *Private Communication.*

(39) Gaunt, A. J.; Neu, M. P., *C. R. Chimie* **2010,** *13*, 821-831.

(40) Jones, M. B.; Gaunt, A. J., *Chem. Rev.* **2013,** *113*, 1137-1198.

(41) Shannon, R., *Acta Crystallogr., Sect. A.* **1976,** *32*, 751-767.

CHAPTER 1

^{29}Si NMR SPECTRA OF SILICON-CONTAINING URANIUM COMPLEXES

INTRODUCTION[†]

^{29}Si NMR spectroscopy has been used extensively to characterize many types of silicon-containing molecules and materials.[1-7] Correlations of ^{29}Si NMR chemical shifts with charge, substitution pattern, ring size, coordination number, and π interactions have been made.[2-6] Typically, the range of shifts for a given structural type is large and the ranges overlap as the structural type is varied, but trends can be discerned when comparing mean chemical shifts for each structural type. This has provided an additional analytical criterion for examining new silicon-containing compounds.

One area of chemistry for which few ^{29}Si NMR data have been reported is that of silicon-containing complexes of uranium. It is understandable that only a few reports of ^{29}Si NMR spectra of uranium compounds are in the literature[8-23] since complexes of uranium in the +2, +3, +4, and +5 oxidation states are paramagnetic. To date, these data serve only as a fingerprint of a specialized type for these compounds.

Since several series of silicon-containing uranium complexes were known that could provide the opportunity to collect a substantial amount of ^{29}Si NMR data on closely related complexes,[24-29] it was of interest to determine if the ^{29}Si NMR spectra would reveal any correlations between the chemical shift and any aspect of the composition, structure, or oxidation state of the uranium complexes. Of particular interest were correlations with oxidation state since the 3.62 μ_B and 3.58 μ_B calculated free ion magnetic moments for U^{III} and U^{IV},

[†]Portions of this chapter have been published: Windorff, C. J.; Evans, W. J. *Organometallics*, **2014**, *33*, 3786–3791. DOI: 10.1021/om500512q.

respectively, are too close to be distinguished by room temperature magnetic susceptibility measurements.[30] Moreover, in practice, the room temperature magnetic moments of complexes of U^{III} and U^{IV} exhibit broad ranges that overlap considerably and variable temperature SQUID analysis is necessary to accurately assess oxidation state.[30-39]

To explore the utility of ^{29}Si NMR spectroscopy in uranium chemistry, NMR data was collected on previously reported inorganic and organometallic uranium complexes with silicon-containing ligands were synthesized as well as new examples and their ^{29}Si NMR spectra were obtained. The literature was scanned to find ^{29}Si NMR data already reported on uranium complexes.[8-23] The data obtained show interesting preliminary trends. This information was originally assembled to encourage a broader collection of data of this type to determine how powerful this method of analysis could become in the area of uranium chemistry.

EXPERIMENTAL

All manipulations and syntheses described below were conducted with the rigorous exclusion of air and water using standard Schlenk line and glovebox techniques under an argon or dinitrogen atmosphere. Solvents were sparged with UHP argon and dried by passage through columns containing Q-5 and molecular sieves prior to use. Deuterated NMR solvents were dried over sodium benzophenone ketyl or sodium/potassium alloy, degassed by three freeze-pump-thaw cycles, and vacuum transferred before use. 2.2.2-cryptand (crypt, 4,7,13,16,21,24-hexaoxa-1,10-diazabicyclo[8.8.8]hexacosane, Aldrich) was placed under vacuum (10^{-3} Torr) for 12 h before use. $KN(SiMe_3)_2$ was dissolved in toluene, centrifuged, and dried *in vacuo* before use. ^{1}H, ^{13}C{^{1}H} and ^{29}Si{^{1}H} NMR spectra were recorded on a Bruker GN500 MHz spectrometer operating at 499.3, 125.6 and 99.2 MHz, respectively, at 298 K unless otherwise stated. ^{1}H

NMR spectra were referenced internally to residual protio-solvent resonances; $^{13}C\{^{1}H\}$ NMR spectra were referenced internally to solvent and $^{29}Si\{^{1}H\}$ NMR spectra were referenced externally to $SiMe_4$. The following compounds were prepared following literature procedures with changes noted: $LiCH(SiMe_3)_2$,[40] $C_5Me_4SiMe_3MgCl(THF)$,[24] $(C_5Me_4SiMe_3)_2UCl_2$,[24] **1**, was recrystallized from toluene at −35 °C after filtration $(C_5Me_4SiMe_3)_2UMe_2$, **2**,[24] $(C_5Me_4SiMe_3)_2UMeCl$, **3**, was made analogously to $(C_5Me_4H)UMeCl$,[41] (η^5:η^1-$C_5Me_4SiMe_2CH_2)_2U$, **4**,[24] $(C_5Me_4SiMe_3)_2UMe_2K(THF)_x$, **5**,[25] $[(C_5Me_4SiMe_3)_2U][(\mu\text{-}Ph_2)BPh_2]$, **6**,[25] was washed with methylcyclohexane and hexane then extracted in benzene, $(C_5Me_4SiMe_3)_3U$, **7**,[25] Cp'_3U, (Cp′ = $C_5H_4SiMe_3$), **8-U**,[29] [K(crypt)][Cp'_3UH], **9**,[29] $[(C_5Me_5)_2U][(\mu\text{-}Ph_2)BPh_2]$, **10**,[42] $(C_5Me_5)_2U[N(SiMe_3)_2]$, **11**,[43] $U[N(SiMe_3)_2]_4$, **12**,[39] $U[N(SiMe_3)_2]_2(\kappa^2\text{-}CH_2SiMe_2NSiMe_3)$, **13**,[39] $[K(THF)_x]\{U[N(SiMe_3)_2]_4\}$, **14**,[39] $U[N(SiMe_3)_2]_3$, **15-U**,[44] was sublimed under vacuum at 10^{-7} torr at 80 °C for 6 h before use, and UI_3, **16**.[45]

$C_5Me_4SiMe_3H$.[46] As a variation from the literature methods,[46-49] Me_3SiCl (0.83 g, 7.6 mmol) in toluene (10 mL) was added dropwise over 5 minutes to a stirred suspension of KC_5Me_4H (1.23 g, 7.67 mmol). The solution was stirred for 48 h and the solvent was removed under reduced pressure. Hexane (60 mL) was added to the reaction which was then filtered on a 60 mL medium porosity frit and washed with hexane (2 × 10 mL). The hexane was removed under reduced pressure to yield $C_5Me_4SiMe_3H$ as a colorless liquid (0.850 g, 57%). ^{1}H NMR[46, 49] (C_6D_6): δ 2.67 (s, 1H, $C_5Me_4SiMe_3\mathit{H}$), 1.90 (s, 6H, $C_5\mathit{Me}_4SiMe_3H$), 1.79 (s, 6H, $C_5\mathit{Me}_4SiMe_3H$), −0.04 (s, 9H, $C_5Me_4Si\mathit{Me}_3H$). $^{13}C\{^{1}H\}$ NMR (C_6D_6): δ 135.4 ($\mathit{C}_5Me_4SiMe_3$), 133.0 ($\mathit{C}_5Me_4SiMe_3$), 55.3 (i-$C_5\mathit{Me}_4SiMe_3$), 11.3 ($C_5\mathit{Me}_4SiMe_3$), −1.6 ($C_5Me_4\mathit{SiMe}_3$). $^{29}Si\{^{1}H\}$ NMR (C_6D_6): δ 1.29 ($C_5Me_4\mathit{Si}Me_3$).

$(C_5Me_5)_2U[CH(SiMe_3)_2]$, 17.[50] This complex was prepared following the method of $(C_5Me_5)U[N(SiMe_3)_2]$, **11**,[43] rather than the literature synthesis. $LiCH(SiMe_3)_2$ (37 mg, 0.22 mmol) was added to a stirred slurry of $[(C_5Me_5)_2U][(\mu\text{-}Ph_2)BPh_2]$, **10**, (170 mg, 0.206 mmol) in benzene (5 mL). After 20 h, an aliquot was drawn for NMR spectroscopy to ensure the reaction had gone to completion, following which white solids (presumably $LiBPh_4$) were removed by centrifugation and the solvent was removed under reduced pressure to yield $(C_5Me_5)_2U[CH(SiMe_3)_2]$, **17** as a dark brown solid (104 mg, 75%). The product was confirmed by ^1H NMR spectroscopy.[50] $^{29}Si\{^1H\}$ NMR (C_6D_6): δ −158 ($CH(\textit{Si}Me_3)_2$).

$(C_5Me_4SiMe_3)_2U[CH(SiMe_3)_2]$, 18. The synthesis is analogous to that of **11**.[43] $LiCH(SiMe_3)_2$ (11 mg, 0.065 mmol) was added to a stirred slurry of $[(C_5Me_4SiMe_3)_2U][(\mu\text{-}Ph_2)BPh_2]$, **6**,[25] (61 mg, 0.065 mmol) in benzene (3 mL). After 4 h, white solids (presumably $LiBPh_4$) were precipitated by the addition of 5 mL hexane and removed by centrifugation. The solvent was removed under reduced pressure to yield $(C_5Me_4SiMe_3)_2U[CH(SiMe_3)_2]$, **18**, as a brown oil (42 mg, 82 %). ^1H NMR (C_6D_6): δ 46.30 (1H, $CH(SiMe_3)_2$), 5.06 (6H, $C_5\textit{Me}_4SiMe_3$), 4.94 (6H, $C_5\textit{Me}_4SiMe_3$), −7.12 (9H, $CH(Si\textit{Me}_3)_2$), −8.96 (9H, $CH(Si\textit{Me}_3)_2$), −9.37 (6H, $C_5\textit{Me}_4SiMe_3$), −14.48 (6H, $C_5\textit{Me}_4SiMe_3$), −21.67 (18H, $C_5Me_4Si\textit{Me}_3$). $^{29}Si\{^1H\}$ (C_6D_6): δ −137 ($C_5Me_4\textit{Si}Me_3$), −181 ($CH(\textit{Si}Me_3)_2$), −198 ($CH(\textit{Si}Me_3)_2$).

$(C_5Me_4SiMe_3)_2U[N(SiMe_3)_2]$, 19. The synthesis of this complex is analogous to that of $(C_5Me_5)_2U[N(SiMe_3)_2]$.[43] $KN(SiMe_3)_2$ (8 mg, 0.04 mmol) was added to a stirred slurry of $[(C_5Me_4SiMe_3)_2U][(\mu\text{-}Ph_2)BPh_2]$[25] (34 mg, 0.036 mmol) in benzene (7 mL) and the mixture was stirred for 16 h. The solution was filtered and the volatiles were removed under reduced pressure to yield **(**$C_5Me_4SiMe_3)_2U[N(SiMe_3)_2]$ as a dark blue tacky solid (28 mg, 96%). ^1H NMR (C_6D_6):

δ 6.47 (12H, $C_5\mathit{Me}_4SiMe_3$), −8.99 (18H, $Si\mathit{Me}_3$), −9.08 (12H, $C_5\mathit{Me}_4SiMe_3$), −23.69 (18H, $Si\mathit{Me}_3$). $^{29}Si\{^1H\}$ (C_6D_6): δ −206 ($C_5Me_4\mathit{Si}Me_3$), −231 ($N(\mathit{Si}Me_3)_2$).

Cp″$_3$U, 20-U.[51] This is an alternative synthesis to the one given in the literature. Solid KCp″ [Cp″ = $C_5H_3(SiMe_3)_2$–1,3] (321 mg, 1.29 mmol) was added to a stirred slurry of UI_3, (264 mg, 0.427 mmol) in Et_2O (10 mL). An immediate color change from purple to green was observed, and the volume was increased to 20 mL. After 1 h, white solids (presumably KI) were removed by centrifugation and the solvent was removed under reduced pressure. The product was dissolved in 15 mL of hexane and stirred 4 h. More white solids (presumably excess KCp″) were removed by centrifugation and the solvent was removed under reduced pressure to give Cp″$_3$U, **20-U**, as a green solid **(**262 mg, 70%). The product was confirmed by ^1H NMR spectroscopy.[51] $^{29}Si\{^1H\}$ NMR (C_6D_6): δ −162 ($C_5H_3(\mathit{Si}Me_3)_2$).

Small Scale Synthesis of [K(crypt)][Cp′$_3$U], 21-U, for Low Temperature NMR Studies. Cp′$_3$U, **8-U**, (85 mg, 0.13 mmol) and crypt (59 mg, 0.16 mmol) were dissolved in 1 mL of d_8-THF to form a red/brown solution and placed into a −35 °C freezer for 2 h along with a pipette packed with ~45 mg KC_8, an NMR tube, and a scintillation vial filled with hexane. Once removed from the freezer the NMR tube was placed in the hexane bath and the KC_8 column was placed above the NMR tube. The red/brown solution was quickly added to the column and pushed through to yield a very dark green solution. The NMR tube was capped, removed from the glovebox, sealed with parafilm, frozen in liquid nitrogen and taken to the NMR facility. The NMR spectrometer was locked and shimmed using pure d_8-THF at low temperature. The sample was thawed in water and placed into the pre-cooled probe. ^1H and ^{29}Si NMR spectra were recorded at 170 K and spectra were then taken from 183 to 233 K in 10 degree increments.

U···Si Distance vs. Chemical Shift Correlations. The U···Si distances were measured using data from the CDCC (ver. 2014) in the Mercury program. All U···Si distances were measured and averaged for consideration. Only compounds with room temperature (293 – 303 K) or calculated room temperature chemical shifts, in the case of the U^{II} compound, [K(2.2.2-crypt)][$(C_5H_4SiMe_3)_3U$], **21-U** were included. Only compounds with unambiguously identifiable distance-shift pairs were included.

RESULTS AND DISCUSSION

Data Collection. ^{29}Si NMR spectroscopy is typically more challenging than ^{1}H or ^{13}C NMR because of low natural abundance (4.67%), a low negative gyromagnetic ratio (−5.3146 10^7 rad T^{-1} s^{-1}), low sensitivity (4 x10^{-4} relative to ^{1}H, about half that of ^{13}C), and long relaxation times.[1-6] There is also an inherent resonance from the glass in the NMR tube and probe that extends from −80 to −130 ppm and has the potential to obstruct signals. Due to these considerations, concentrated samples were needed (≥ 20 mg/ 0.5 mL). Initially the data were collected with an acquisition time of 0.5 s and a t_1 of ≥ 2 s. It was subsequently found, however, that spectra with acceptable signal to noise ratios could be obtained with this shorter t_1 of 1 sec. The "INEPT" pulse sequence can also be used and this eliminates the glass peak entirely. Initial experiments were conducted with a large window, from 200 to −400 ppm, since it was uncertain how much the paramagnetic uranium would shift the signal. Each experiment was followed by a second experiment with a smaller window, typically 250 ppm. Data collection required 1 – 3 h per sample with the 2 s t_1. Typical examples of spectra are given in Figure 1.1.

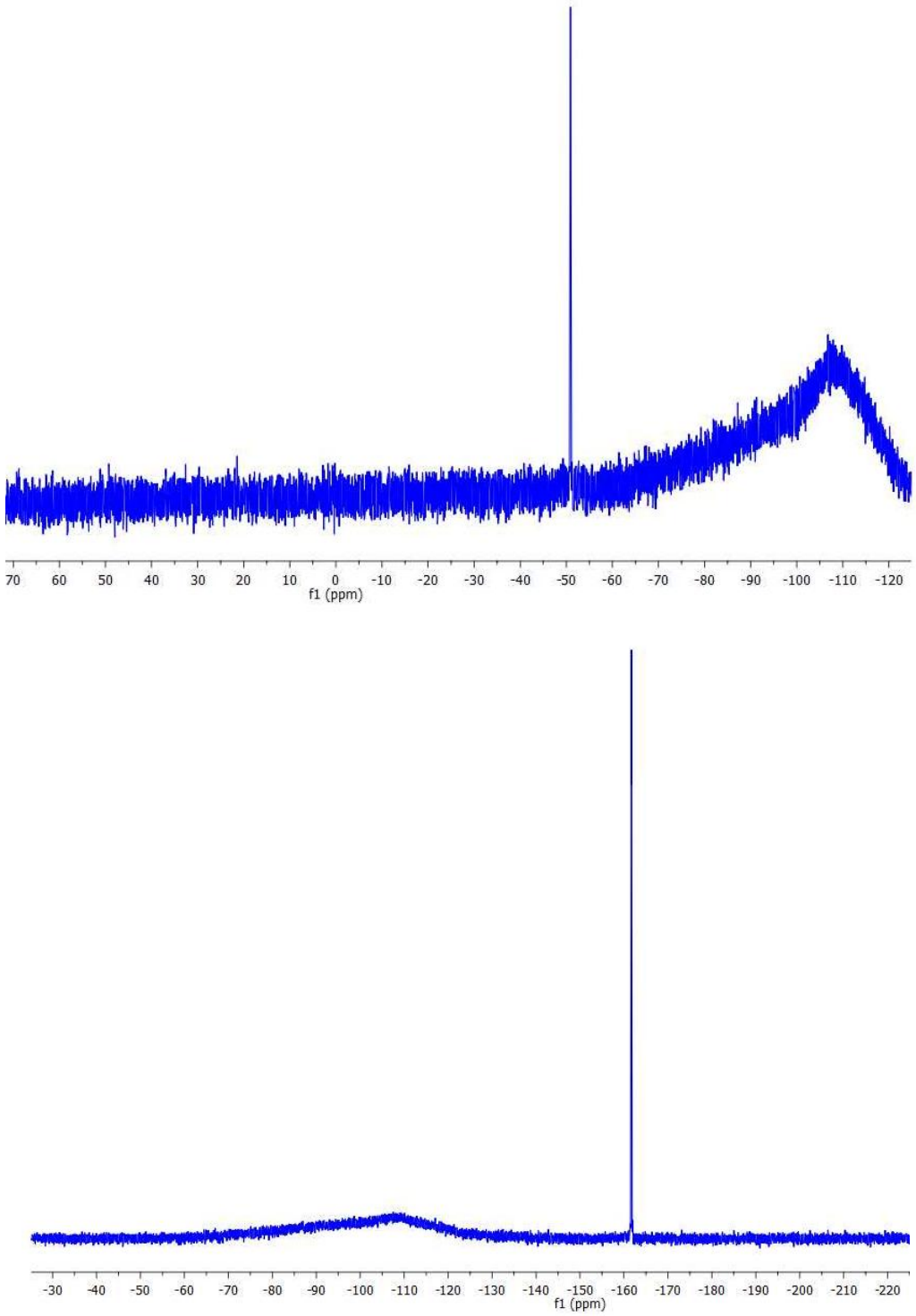

Figure 1.1. Representative ^{29}Si NMR spectra of $(C_5Me_4SiMe_3)_2UCl_2$, **1**, (top, δ −51 ppm) and Cp''_3U, **20-U**, (bottom, δ −162 ppm) in C_6D_6 at 298 K.

All samples in this study used C_6D_6 as the solvent except $(C_5Me_4SiMe_3)MgCl(THF)$, $[K(THF)_x][(C_5Me_4SiMe_3)_2UMe_2]$, **5**, $[K(crypt)][Cp'_3UH]$, **9** ($Cp' = C_5H_4SiMe_3$), and $[K(crypt)][Cp'_3U]$, **21-U**, which are insoluble in C_6D_6 and were measured in either C_4H_8O or C_4D_8O. Previous studies have shown that solvent does not have a large effect on ^{29}Si NMR shifts.[2, 4] Several samples were examined in both C_6D_6 and C_4H_8O (THF) to test this generalization with uranium-containing species and a similarly small solvent effect was again observed: complex (shift in C_6D_6, shift in C_4H_8O in ppm) $(C_5Me_4SiMe_3)_2UCl_2$, **1** (−51, −50); $(C_5Me_4SiMe_3)_2UMeCl$, **3** (−67, −66); $(C_5Me_4SiMe_3)_2UMe_2$, **2** (−84, −84); and Cp''_3U, **20-U** (−162, −163) [$Cp'' = C_5H_3(SiMe_3)$–1.3]. Exceptions to this solvent independence were observed in the case of a solvated cation such as $[K(THF)_6]\{U[N(SiMe_3)_2]_4\}$, **14**, which has chemical shifts of −192 and −142 ppm in C_6D_6 and C_4H_8O, respectively.

All newly reported data were collected at room temperature except for the U^{II} complex, $[K(crypt)][Cp'_3U]$, **21-U**,[23] that has limited stability in solution at room temperature. To obtain ^{29}Si NMR data on this complex, it was synthesized at low temperature in an NMR tube. The chemical shift of this complex as a function of 1/T is plotted in Figure 1.2. The data follow a typical Curie-Weiss dependence on temperature.

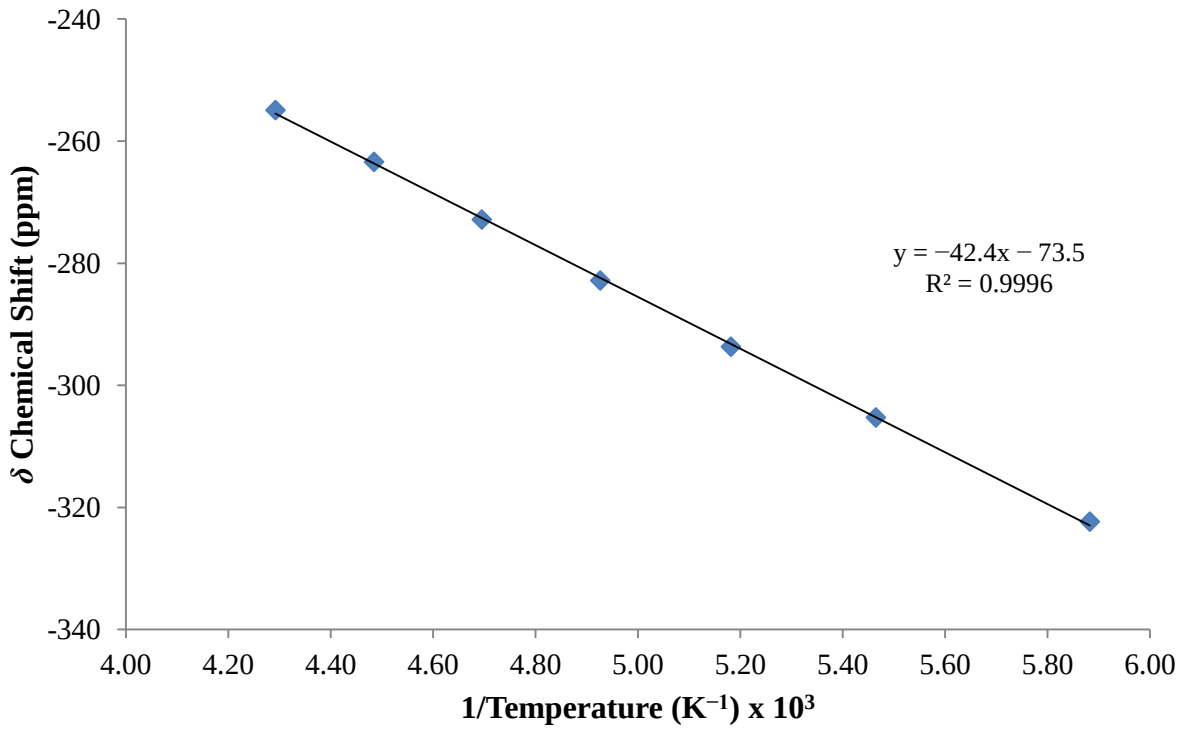

Figure 1.2. Plot of chemical shift (δ) vs T^{-1} for [K(crypt)][Cp′$_3$U], **21-U**.

The ^{29}Si NMR Data. The most common types of silicon-containing ligands in the uranium complexes are the bulky trimethylsilyl-substituted amide and alkyl ligands, $[N(SiMe_3)_2]^{1-}$ and $[CH(SiMe_3)_2]^{1-}$, and trimethylsilyl-substituted cyclopentadienyl groups, $(C_5Me_4SiMe_3)^{1-}$, Cp′$^{1-}$, and Cp′′$^{1-}$. The prevalence of the trimethylsilyl substituent in this study provides some uniformity in the immediate environment of the silicon.

Table 1.1 shows ^{29}Si NMR data collected in this study on inorganic and organometallic U^{III} and U^{IV} complexes with silicon-containing ligands, along with other data found in the literature. A single example of U^{II} is also in Table 1.1. Data on U^{V} and U^{VI} complexes are in Table 1.2. For reference, data on free ligands and derivatives are shown in Table 1.3. The data are arranged according to decreasing chemical shift in C_6D_6 at 293 – 303 K, except where noted. For convenience, the data are presented as a graph of the ^{29}Si resonances in Figure 1.3.

Table 1.1. ^{29}Si NMR Chemical Shifts (δ, ppm), of U^{n+} Complexes (n = 2, 3, 4) at 298 K, Except Where Noted.

Compound	**n**	**^{29}Si Chemical Shift δ[a]**	**Reference**
$\{U[OSi(Mes)_3]_3\}_2(\mu\text{-}\eta^2\text{:}\eta^2\text{-}N_2)$	4	64[b]	23
$[(Tren^{TIPS})U(THF)][BPh_4]$	4	36	20
$(Tren^{TIPS})U(PH_2)$	4	21	20
$(Tren^{TIPS})UCl$	4	13	17
$[\kappa^2\text{-}C_5H_4N(2\text{-}NR)]_3UI$	4	−11	14
$(Tren^{TIPS})UN_3$	4	−11	19
$[\kappa^2\text{-}C_5H_4N(2\text{-}NR)]_3UCl$	4	−41	14
$(C_5Me_4R)_2UCl_2$, **1**	4	−51	this work
$(C_5Me_4R)_2UMeCl$, **3**	4	−67	this work
$[\kappa^5\text{-}(NHCMe_2Si^iPr_2NCH_2CH_2)N(CH_2CH_2NR')_2]U$	4	5; −74	19
$(C_5Me_4R)_2UMe_2$, **2**	4	−84	this work
$U(NR_2)_2(\kappa^2\text{-}CH_2SiMe_2NR)$, **13**	4	−74; −83; −152	this work
$(Tren^{TIPS})UNH_2$	4	−90	19
$(Tren^{TIPS})UF$	4	−97	19
$(C_8H_4R'_2)_2U$	4	−101; −134[b]	8
$[(C_8H_4R'_2)(C_5Me_5)U]_2(\mu\text{-}\eta^2\text{:}\eta^2\text{-}N_2)$	4	−108; −185	9
$[(C_8H_6R_2)(C_5Me_4R)U]_2(\mu\text{-}\eta^1\text{:}\eta^1\text{-}^{13}C_2O_2)$	4	−108; −143[b]	12
$[(C_8H_6R'_2)(C_5Me_4Et)U]_2(\mu\text{-}\eta^1\text{:}\eta^1\text{-}^{13}C_2O_2)$	4	−113[b]	12
$[(C_8H_6R'_2)(C_5Me_5)U]_2(\mu\text{-}\eta^1\text{:}\eta^1\text{-}^{13}C_2O_2)$	4	−115[b]	10
$(C_8H_6R'_2)\ U(\kappa^3\text{-}Tp^{Me2})$	3	−116[b†]	11
$[K(crypt)][(Tren^{TIPS})U(PH)]$	4	−121	20
$(C_8H_6R'_2)(C_5Me_4R)U$	3	−124 $(C_8H_6R'_2)$[b]	12
$U(NR_2)_4$, **12**	4	−127	this work
$(C_8H_6R'_2)(C_5Me_4{}^iPr)U$	3	−133[b]	12
$(C_8H_6R'_2)(C_5Me_4Et)U$	3	−137[b]	12
$(C_8H_6R_2)(C_5Me_5)U$	3	−145[c]	12

$[(Tren^{DMSB})U]_2(\mu\text{-}\eta^1\text{:}\eta^1\text{-}C_2O_2)$	4	−149	16
[K(crypt)][$(C_5H_4R)_3UH$], **9**	3	−154[d]	this work
$(C_8H_6R_2)(C_5Me_4R)U$	3	−154[b]	12
$(C_5Me_4R)_3U$, **7**	3	−155	this work
$(C_5Me_5)_2U(CHR_2)$, **17**	3	−158	this work
$(C_8H_4R'_2)U(\kappa^3\text{-}Tp^{Me2})$	3	−159[b]	11
$(C_5H_3R_2)_3U$, **20-U**	3	−162	this work
$(C_5H_4R)_3U$, **8-U**	3	−165 (−158[d])	this work
$(C_8H_4R'_2)(C_5Me_5)U$	3	−173 (−295[b‡])	9,13
$(C_8H_6R_2)(C_5Me_5)U(THF)$	3	−176[b]	12
$(Tren^{TIPS})U$	3	−178	17
$(C_5Me_4R)_2U(CHR_2)$, **18**	3	−137; −181; −198	this work
$[K(THF)_6][U(NR_2)_4]$, **14**	3	−192 (−142[d])	this work
$(C_5Me_4R)_2U(NR_2)$, **19**	3	−206; −231	this work
$U(NR_2)_3$, **15-U**	3	−219	this work
$[K(THF)_x][(C_5Me_4R)_2UMe_2]$, **5**	3	−237[b]	this work
$(C_5Me_5)_2U(NR_2)$, **11**	3	−247	this work
$[(\eta^5\text{:}\eta^1\text{-}C_5Me_4SiMe_2CH_2)_2U]$, **4**	4	−255	this work
[K(crypt)][$(C_5H_4R)_3U$], **21-U**	2	−322[e‡‡]	this work

[a] C_6D_6 [b] C_7D_8 [c] C_6D_{12} [d] C_4H_8O [e] C_4D_8O

†at 328 K ‡at 201 K ‡‡at 170 K

R = $SiMe_3$, R′ = Si^iPr_3, $Tren^{TIPS}$ = $N(CH_2CH_2NSi^iPr_3)_3$, $Tren^{DMSB}$ = $N(CH_2CH_2NSiMe_2{}^tBu)_3$, Tp^{Me2} = hydridotris(3,5-dimethylpyrazolyl)borate

Table 1.2. ^{29}Si NMR Chemical Shifts (δ, ppm) of U^{n+} Complexes (n = 5, 6) at 298 K, Except Where Noted.

Compound	**n**	**^{29}Si Chemical Shift δ[a]**	**Reference**
$(ROUO)_2(L)$	5	160	[22]
$(PhMe_2SiOUO)_2(L)$	5	152	[22]
$(BIPM)UOCl_2$	6	−0.69	[15]
$(BIPM)U(NMes)(O)(DMAP)_2$	6	−8.28	[21]
$(Tren^{TIPS})U(\mu\text{-}N)[\mu\text{-}Na(15\text{-crown-}5)]$	5	−13	[19]
$(Tren^{TIPS})UN$	6	−21.70	[19]
$(Tren^{TIPS})UNAd$	5	−37	[19]
$(Tren^{TIPS})UNR$	5	−58	[17, 19]
$(Tren^{TIPS})UO$	5	−71	[18]
$[(C_8H_6R_2)(C_5Me_5)U]_2(\mu\text{-}\eta^2\text{:}\eta^2\text{-}C_4O_4)$	5	−90[b]	[12]

[a] C_6D_6 [b] C_7D_8

R = $SiMe_3$, R′ = Si^iPr_3, L = Pacman-like binucleating Schiff-base calixpyrrole macrocycle, BIPM = bis(iminophosphorano)methanediide = $C(PPh_2NSiMe_3)_2$, Mes = mesityl, DMAP = 4-dimethylaminopyridine, $Tren^{TIPS}$ = $N(CH_2CH_2NSi^iPr_3)_3$, Ad = adamantyl

Table 1.3. ^{29}Si NMR Chemical Shifts (δ, ppm) of Diamagnetic Derivatives of Ligands at 298 K, Except Where Noted.

Compound	**^{29}Si Chemical Shift δ[a]**	**Reference**
RCl	30.11	2, this work
R_2CHCl	4.40/3.43	2, this work
$K_2[C_8H_4R'_2]$	4.19	8
$Li_3(Tren^{TIPS})$	2.60	17
HNR_2	1.95-2.22[b]	2, this work
C_5Me_4RH	1.32	this work
CH_2R_2	0.50/−0.12	2, this work
$HC[SiMe_2N(Li)Ar]_3$	−0.56	52
$HC[SiMe_2N(Li)Ar']_3(OEt_2)_2$	−4.01	52
$HC[SiMe_2N(Li)Ar]_3(OEt_2)$	−6.06	52
$K[C_5H_4N(2\text{-}NR)](THF)_{0.25}$	−8.52	14
$Li[C_5H_4N(2\text{-}NR)](THF)_2$	−8.55	14
$C_8H_6(SiPh_3)_2$	−9.9[c]	28
$(C_5Me_4R)MgCl(THF)$	−11.75[d]	this work
$(RNPPh_2)_2C{=}C(H)Ph$	−12.02; −12.51	15
$(RNPPh_2)_2C{=}C(H)R''$	−12.47; −13.36	53
$K(C_5H_4R)$	−14.43	this work
$K(C_5H_3R_2)$	−14.59	this work
$(RNPPh_2)_2C{=}CPh_2$	−17.22	54
KNR_2	−20.49	this work
Bis(trimethylsiloxy)furanone	−21.82	16
Bis(dimethylphenylsiloxy)furanone	−21.94	16

[a] C_6D_6 [b] C_6H_6 [c] $CDCl_3$ [d] C_4H_8O

R = $SiMe_3$, R′ = Si^iPr_3, R″ = anthracene, $C_{14}H_9$, $Tren^{TIPS}$ = $N(CH_2CH_2NSi^iPr_3)_3$, Ar = 3,5-$Me_2C_6H_3$, Ar′ = 4-MeC_6H_4

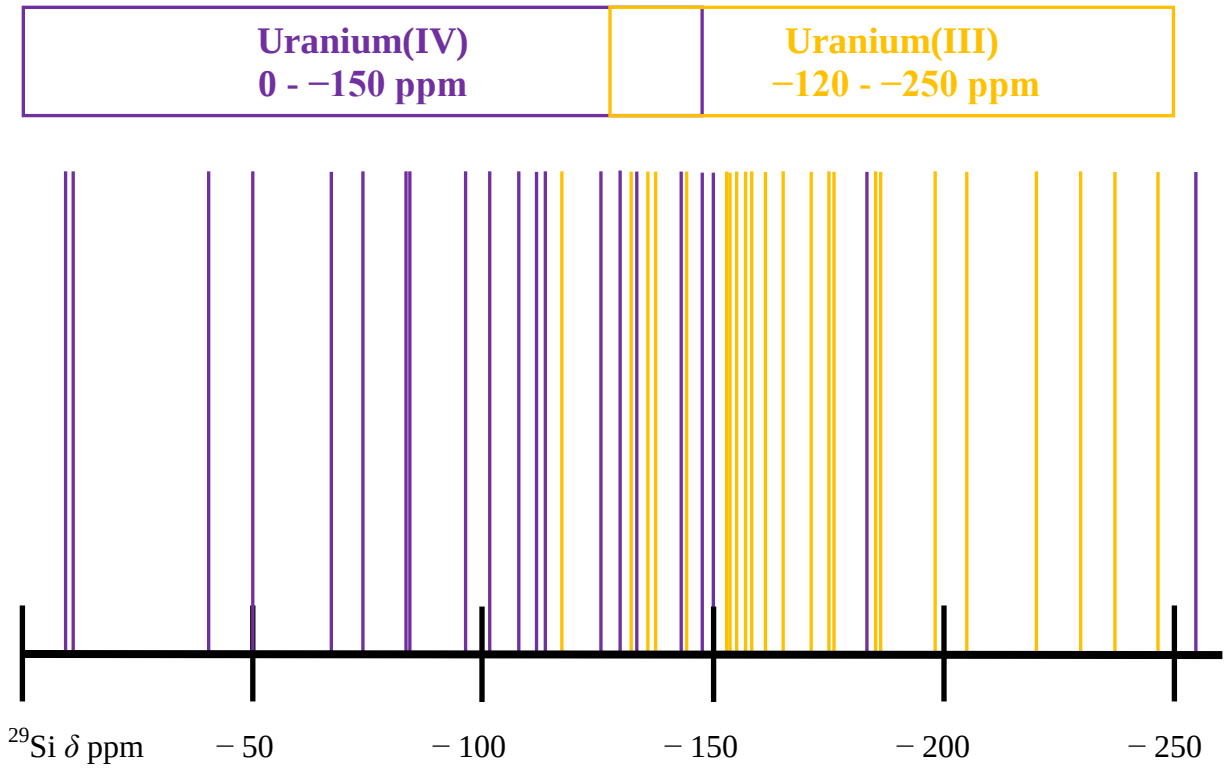

Figure 1.3. Graphical representation of the $U^{IV/III}$ data where purple lines represent the shift of a U^{IV} complex and yellow lines represent U^{III} complexes. Not shown are the resonances at positive chemical shifts for $\{U[OSi(Mes)_3]_3\}_2(\mu\text{-}\eta^2\text{:}\eta^2\text{-}N_2)$ at 64 ppm,[23] $[Tren^{TIPS}U(THF)][BPh_4]$ at 36 ppm,[20] $(Tren^{TIPS})U(PH_2)$ at 21 ppm, [20] $(Tren^{TIPS})UCl$ at 13 ppm,[17] and one of the resonances for $[\kappa^5\text{-}(NHCMe_2Si^iPr_2NCH_2CH_2)N(CH_2CH_2NR')_2]U$ at 5 ppm, R′ = Si^iPR_3.[19]

Correlations of chemical shift and the distance of silicon from uranium in the solid state X-ray crystal structures were also examined and show no consistent correlations (Figure 1.4 – 1.10). For example, for U^{IV} complexes, a scatter plot is observed, Figure 1.5. For U^{III} complexes, Figure 1.6, four compounds with close U···Si distances have larger shifts than thirteen compounds with longer U···Si distances, but within these two groups there is no correlation of shift and the U···Si distance in the solid state structure, Figure 1.6. Correlations

were also examined within a ligand set, Figure 1.7 – 1.10. Three U^{III} complexes of $[N(SiMe_3)_2]^{1-}$ show a correlation, Figure 1.9 as do four U^{V} complexes of Tren ligands, Figure 1.10, but two pairs of U^{IV} complexes with similar U···Si distances have shifts that vary 100 ppm, Figure 1.7. A correlation for four U^{IV} complexes of cyclopentadienyl, cyclooctatetraenyl, and pentalenyl ligands looks better than that for eleven U^{III} complexes of the same types of ligands, Figure 1.8, but over-interpretation of these correlations should not be made with so few data. A summary of the U···Si distance vs. chemical shift data is summarized in Table 1.4. The difficulty of finding correlations in the NMR shifts of paramagnetic species has been pointed out.[3] Competing factors can affect the shift (e.g. contact and pseudo-contact effects) and distances and geometries in solution may not reflect data obtained in the solid state.

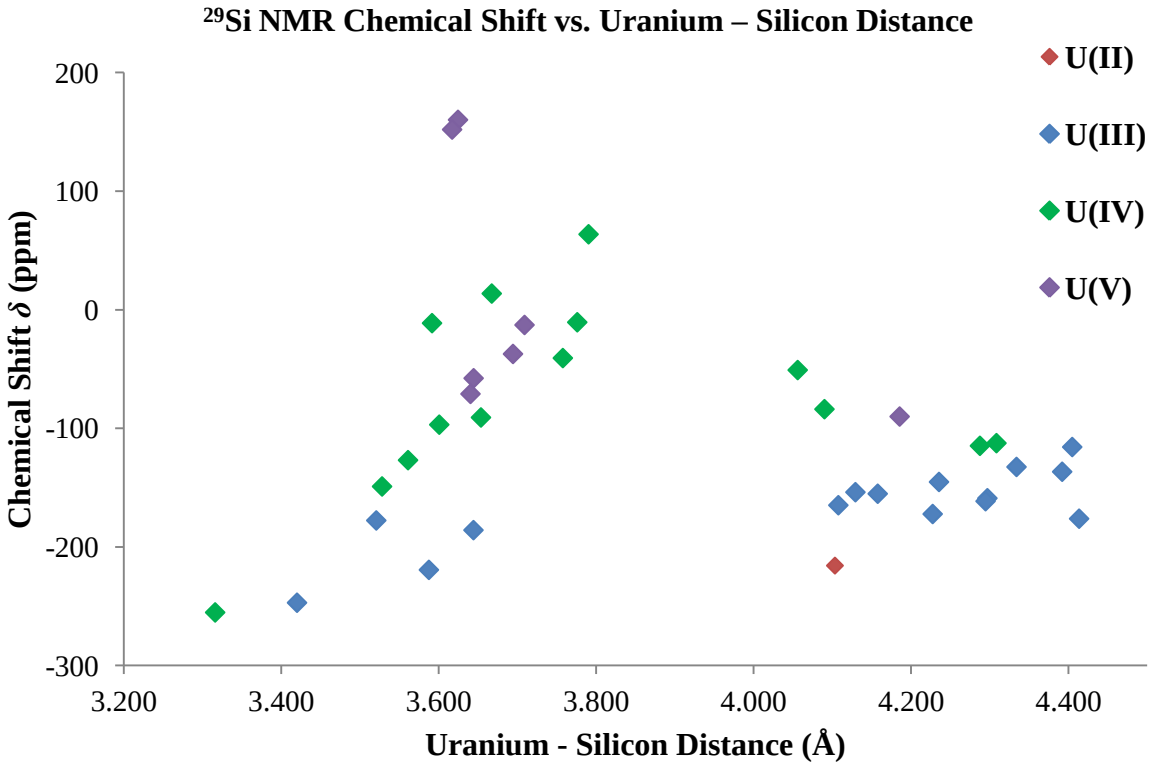

Figure 1.4: Graph of ^{29}Si NMR shifts vs. uranium – silicon distances as measured from the solid state crystal structures. Only peaks that could unambiguously identified were included.

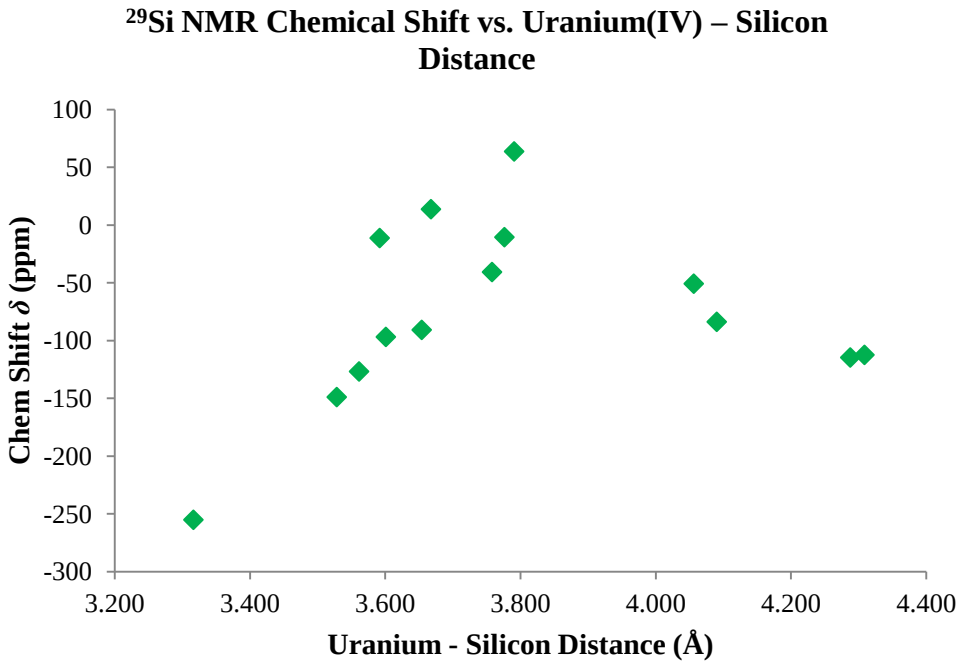

Figure 1.5. Graph of ^{29}Si NMR chemical shift vs. uranium(IV) – silicon distances, as measured in the solid state structure.

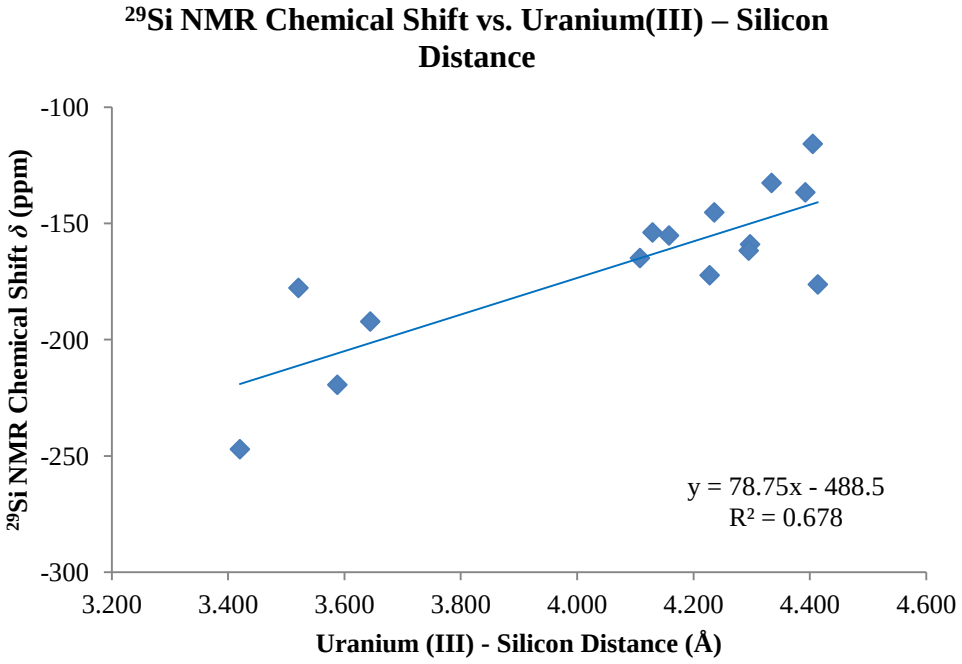

Figure 1.6: Graph of ^{29}Si NMR chemical shift vs. uranium(III) – silicon distances, as measured in the solid state structure.

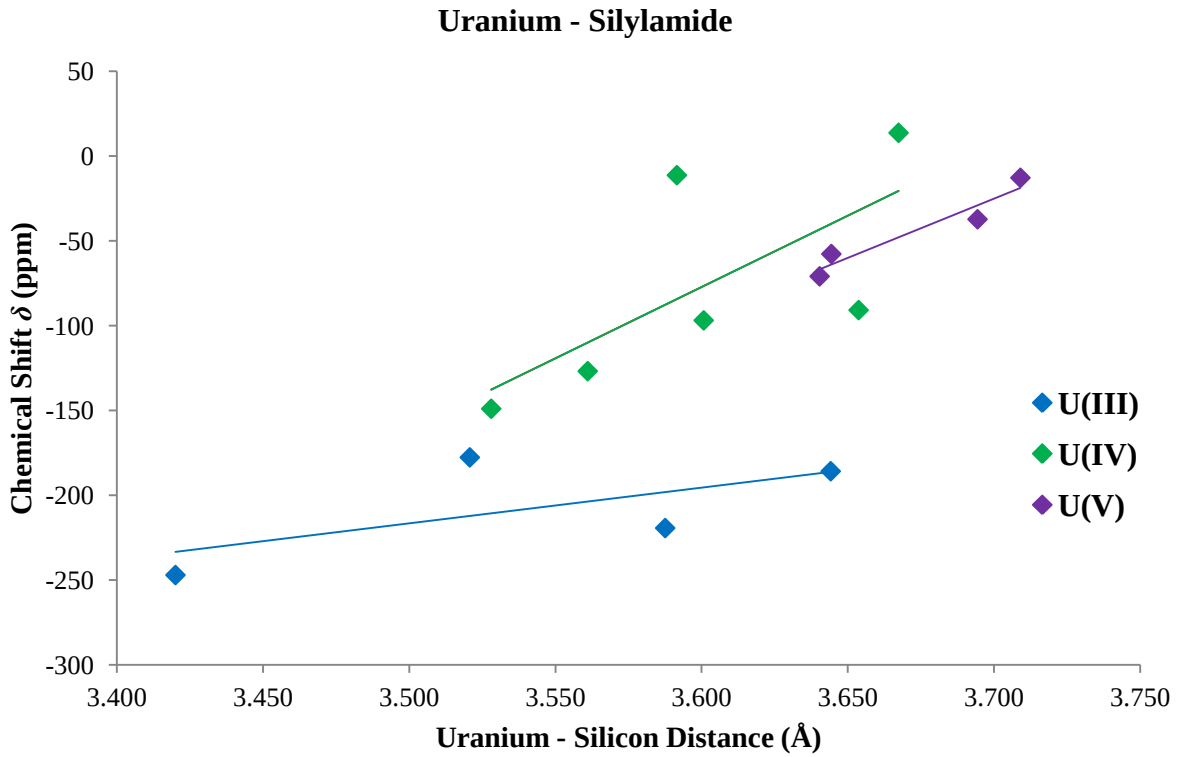

Figure 1.7: Graph displaying ^{29}Si NMR chemical shift vs. uranium – silicon distances for complexes containing silylamide functionalities [U-N(R)-SiR$^{(\prime)}_3$], R= $SiMe_3$, R′ = Si^iPr_3. The data are fit for the three different uranium oxidation states with R^2 correlation values for $U^{III/IV/V}$ of 0.403, 0.481, and 0.917, respectively.

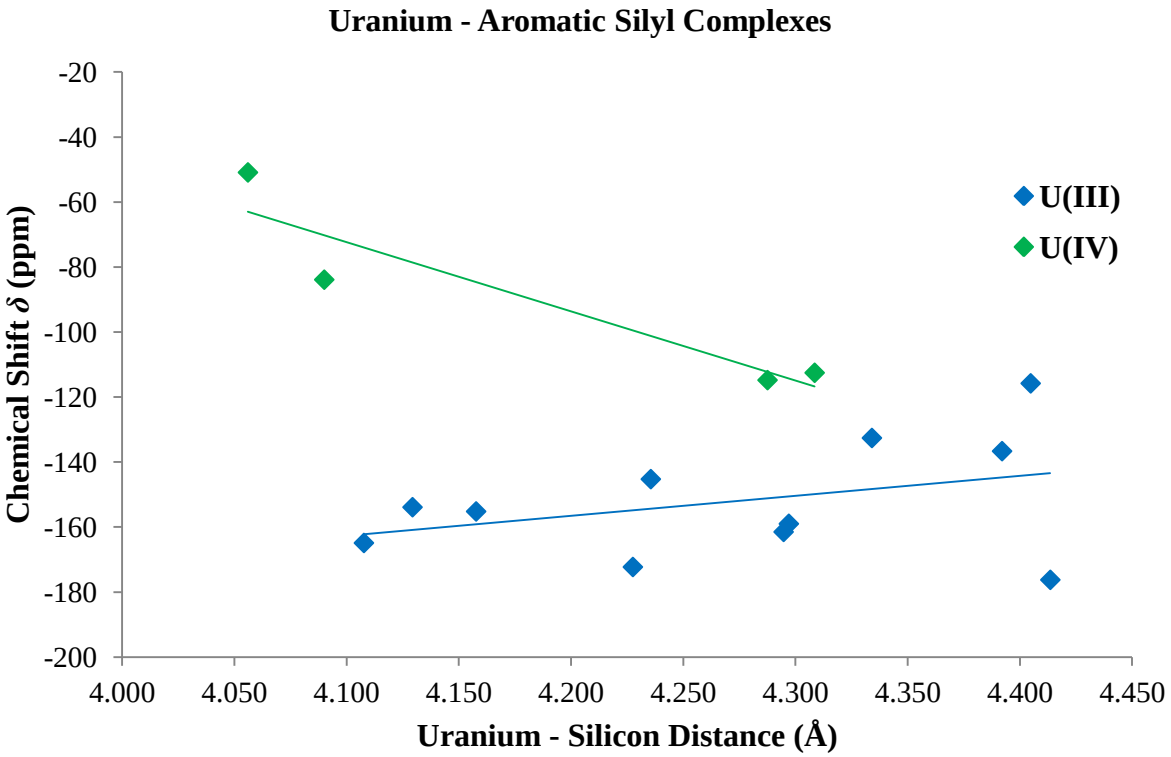

Figure 1.8: Graph of ^{29}Si NMR chemical shift vs. uranium – silicon distances for aromatic silyl complexes where aromatic silyl ligands are either $C_5R_{4-x}(SiMe_3)_x^-$ (R = Me, H), $C_8H_6(SiR'_3)_2^{2-}$ (R′ = Me, ^{i}Pr) or $C_8H_4(Si^iPr_3)_2^{2-}$. Correlation R^2 values for $U^{III/IV}$ are 0.139 and 0.867, respectively.

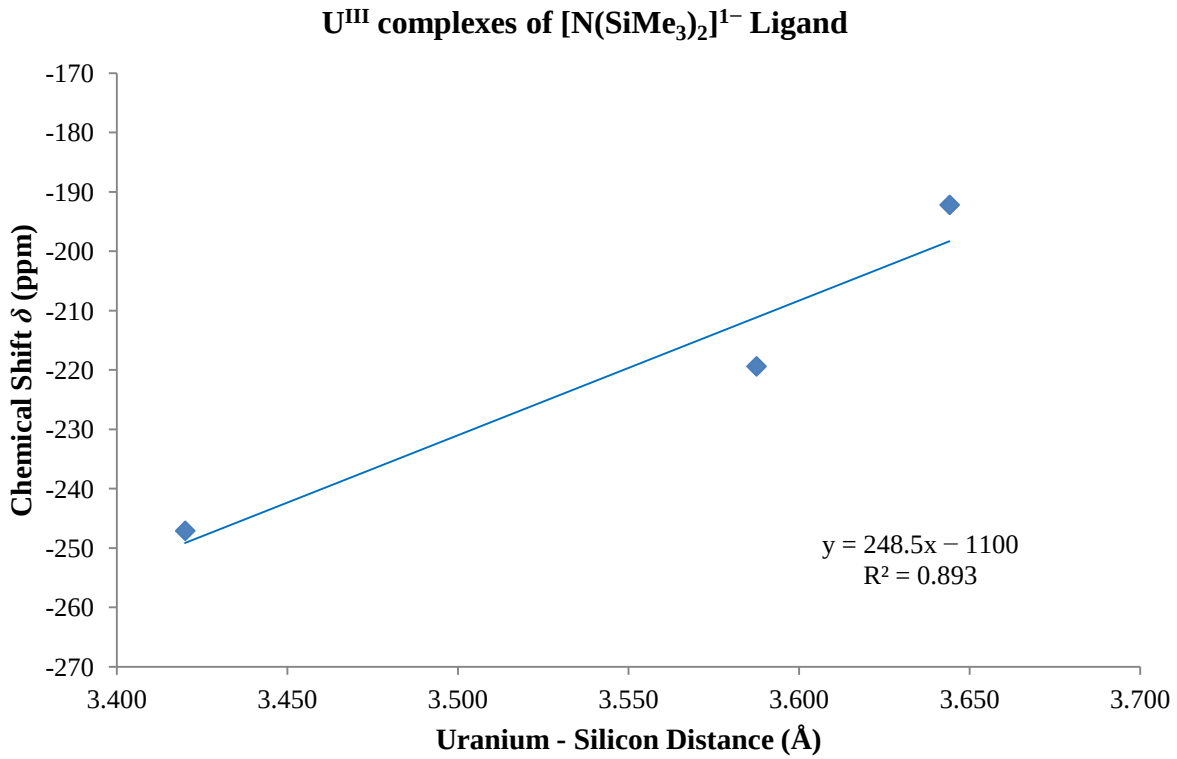

Figure 1.9: Graph displaying ^{29}Si NMR chemical shift vs. uranium(III) – silicon distances for U^{III} complexes of $[N(SiMe_3)_2]^{1-}$ ligands: $(C_5Me_5)_2UN(SiMe_3)$, **11**, $[K(THF)_6]\{U[N(SiMe_3)_2]_4\}$, **14**, $U[N(SiMe_3)_2]_3$, **15-U**, and. The distances are measured from the solid state crystal structure.

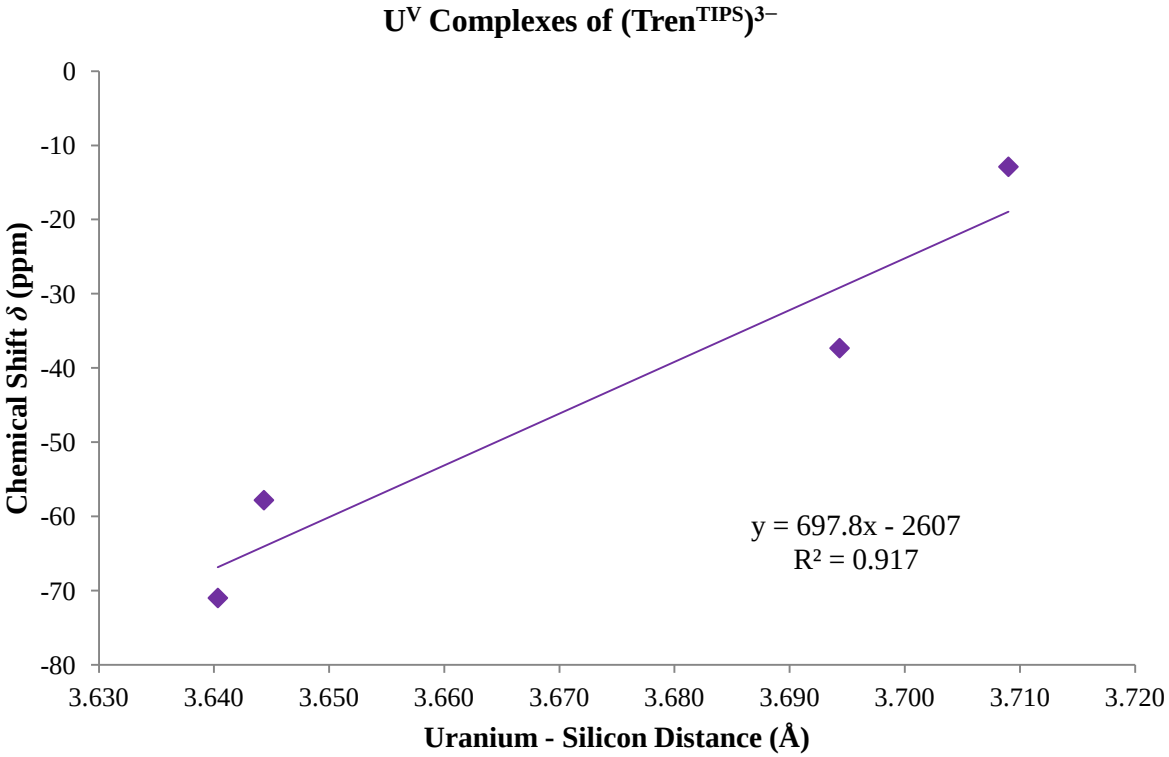

Figure 1.10: Graph displaying ^{29}Si NMR chemical shift vs. uranium(V) – silicon distances, for the ligand $[N(CH_2CH_2NSi^iPr_3)_3]^{3-}$ ($Tren^{TIPS}$) for the complexes $Tren^{TIPS}UX$, X = O, $NSiMe_3$, N(adamantyl), and N-μ-Na(15-crown-5).

Table 1.4: U···Si Average Distances and ^{29}Si NMR Chemical Shift (δ, ppm) for U^{n+} Complexes (n = 2, 3, 4, 5, 6).

Compound	**n**	**^{29}Si δ (ppm)**[a]	**Average U···Si (Å)**
[K(crypt)][$(C_5H_4R)_3U$], **21-U**	2	−216[b‡‡]	4.103
$(C_5Me_5)_2U(NR_2)$, **11**	3	−247	3.420
$U(NR_2)_3$, **15-U**	3	−219	3.588
[$K(THF)_6$][$(C_5Me_4R)_2UMe_2$], **5**	3	−192	3.644
$(Tren^{TIPS})U$	3	−173	3.521
$(C_8H_6R_2)(C_5Me_5)U(THF)$	3	−176[c]	4.414
$(C_8H_4R'_2)(C_5Me_5)U$	3	−172	4.228
$(C_5H_4R)_3U$, **8-U**	3	−165	4.108
$(C_5H_3R_2)_3U$, **20-U**	3	−162	4.295
$(C_8H_4R'_2)U(\kappa^3\text{-}Tp^{Me2})$	3	−159[c]	4.297
$(C_5Me_4R)_3U$, **7**	3	−155	4.158
[K(crypt)][$(C_5H_4R)_3UH$], **9**	3	−154[d]	4.129
$(C_8H_6R_2)(C_5Me_5)U$	3	−145[e]	4.236
$(C_8H_6R'_2)(C_5Me_4Et)U$	3	−137[c]	4.392
$(C_8H_6R'_2)(C_5Me_4{}^{i}Pr)U$	3	−133[c]	4.334
$[(\eta^5\text{:}\eta^1\text{-}C_5Me_4SiMe_2CH_2)_2U]$, **4**	4	−255	3.316
$[(Tren^{DMSB})U]_2(\mu\text{-}\eta^1\text{:}\eta^1\text{-}C_2O_2)$	4	−149	3.528
$U(NR_2)_4$, **12**	4	−127	3.561
$[(C_8H_6R'_2)(C_5Me_5)U]_2(\mu\text{-}\eta^1\text{:}\eta^1\text{-}{}^{13}C_2O_2)$	4	−115[c]	4.288
$[(C_8H_6R'_2)(C_5Me_4Et)U]_2(\mu\text{-}\eta^1\text{:}\eta^1\text{-}{}^{13}C_2O_2)$	4	−113[c]	4.309
$(Tren^{TIPS})UF$	4	−97	3.601
$(Tren^{TIPS})UNH_2$	4	−90	3.654
$(C_5Me_4R)_2UMe_2$, **2**	4	−84	4.090
$(C_5Me_4R)_2UCl_2$, **1**	4	−51	4.056
$[\kappa^2\text{-}C_5H_4N(2\text{-}NR)]_3UCl$	4	−41	3.758
$(Tren^{TIPS})UN_3$	4	−11	3.592
$[\kappa^2\text{-}C_5H_4N(2\text{-}NR)]_3UI$	4	−11	3.776
$(Tren^{TIPS})UCl$	4	13	3.667
$\{U[OSi(Mes)_3]_3\}_2(\mu\text{-}\eta^2\text{:}\eta^2\text{-}N_2)$	4	64[c]	3.790

$[(C_8H_6R_2)(C_5Me_5)U]_2(\mu\text{-}\eta^2\text{:}\eta^2\text{-}C_4O_4)$	5	−90[c]	4.186
$(Tren^{TIPS})UO$	5	−71	3.640
$(Tren^{TIPS})UNR$	5	−58	3.644
$(Tren^{TIPS})UNAd$	5	−37	3.694
$(Tren^{TIPS})U(\mu\text{-}N)[\mu\text{-}Na(15\text{-crown-}5)]$	5	−13	3.709
$(PhMe_2SiOUO)_2(L)$	5	152	3.617
$(ROUO)_2(L)$	5	160	3.625
$(Tren^{TIPS})UN$	6	−21.70	3.592
$(BIPM)UOCl_2$	6	−0.69	3.713

[a] C_6D_6 [b] C_4D_8O [c] C_7D_8 [d] C_4H_8O [e] C_6D_{12}

‡‡Extrapolated to 298 K from variable temperature data

R = $SiMe_3$, R′ = Si^iPr_3, $Tren^{TIPS}$ = $N(CH_2CH_2NSi^iPr_3)_3$, $Tren^{DMSB}$ = $N(CH_2CH_2NSiMe_2{}^tBu)_3$, Tp^{Me2} = hydridotris(3,5-dimethylpyrazolyl)borate, Ad = adamantyl, L = Pacman-like binucleating Schiff-base calixpyrrole macrocycle, BIPM = bis(iminophosphorano)methanediide = $C(PPh_2NR)_2$,

Ligand Effects. A ligand-based trend discernible from the data in Table 1.1 is that uranium complexes with ligands such as the triamidoamine (Tren), and alkyl exhibit more negative chemical shifts than those with aromatic ligands such as cyclopentadienide, cyclooctatetraenide, and the pentalene dianion. This is exemplified by the U^{III} complexes $[C_8H_6(SiMe_3)_2]U(C_5Me_5)$, and **20-U**, which resonate at −145 and −162 ppm, respectively,[12] whereas $(Tren^{TIPS})U$ and **15-U** resonate at −178, and −219 ppm, respectively.[17] Comparison of the −247 ppm shift for **11** versus the −158 ppm shift of **17** shows the amide to resonate at a more negative shift than the corresponding alkyl. The order of the resonances in these two complexes is reversed from what is observed in the free ligands. For example, $CH_2(SiMe_3)_2$, resonates at −0.12 ppm, whereas $HN(SiMe_3)_2$ resonates at 1.95 ppm.

The data show that cyclopentadienide ligands resonate at less negative shifts than cyclooctatetraenyl ligands $(C_8H_6R_2–1,4)^{2–}$ (R = $SiMe_3$, Si^iPr_3,). For example, three of the U^{III} complexes containing the $U[C_8H_6R_2–(1,4–R)](C_5Me_4R')U$ (R = Si^iPr_3, R′ = ^{i}Pr, Et; R = $SiMe_3$, R′ = Me) structure resonate at −133, −137, and −145 ppm, respectively,[12] whereas the tris-cyclopentadienyl complexes, **7**, **20-U** and **8-U**, resonate at −155, −162, and −165 ppm, respectively.

Oxidation State Analysis. As can be seen in Table 1.1 and Figure 1.2, there is a general trend of U^{III} complexes occurring at more negative values than U^{IV} complexes. The range of most of the U^{IV} complexes in Table 1.1 is between 0 and −150 ppm. In contrast, most of the U^{III} complexes have resonances between −120 and −250 ppm. The low temperature spectrum of the U^{II} example had the most negative chemical shift of all, −322 ppm at 170 K, but extrapolation of the data in Figure 1.1 gives an estimated shift of −216 ppm at 298 K, at the low end of the U^{III} range. This calculated room temperature shift is significantly shifted from the neutral $(C_5H_4SiMe_3)_3U(THF)$, **8-U(THF)**, compound (at −159 ppm) and more negative that most cyclopentadienyl complexes. All of these shifts are substantially more negative than the 30 to −25 ppm range found for the ligands in diamagnetic compounds such as $C_5Me_4SiMe_3H$, KCp″, and $KN(SiMe_3)_2$ and the two examples of U^{VI} compounds in Tables 1.2 and 1.3. The U^{V} compounds, on the other hand, exhibit the widest range of shifts: 160 to −90 ppm. However, at the time of the compilation, only seven examples of ^{29}Si NMR data on U^{V} compounds had been reported.[12, 17-19, 22]

The ranges for most U^{IV} and U^{III} complexes do not overlap, but there are some exceptions. The two U^{IV} complexes that have resonances more negative than the other examples each contain cyclometalated silicon-containing ligands. In the U^{IV} complex, (η^5:η^1-

$C_5Me_4SiMe_2CH_2)_2U$, **4**, in which the only silicon is in the ring of a cyclometalated ligand, a chemical shift at −255 ppm is observed. $U[N(SiMe_3)_2]_2(\kappa^2\text{-}CH_2SiMe_2NSiMe_3)$, **13**, has three observable resonances at −74, −83, and −152 ppm. The latter resonance is outside the normal range and is attributed to the silicon in the cyclometalated ring. ^{29}Si NMR shifts in cyclic silanes are known to be sensitive to ring size and ring strain,[1-7] so there is precedence for these silicon resonances to be shifted outside the expected range.

CONCLUSION

^{29}Si NMR spectra on uranium complexes containing silicon and a review of the known literature have revealed some general trends between chemical shift, composition, and oxidation states that should prove to be useful for further studies. These trends should not be considered definitive at this stage since ^{29}Si NMR shifts are often variable and data on only 52 paramagnetic uranium complexes were collected in this survey. Therefore, the following correlations should be further examined when more data are available. Complexes containing non-aromatic ligands resonate at lower shifts than those with aromatic ligands. Complexes containing ligands with silicon bound to nitrogen resonate at more negative values than those with silicon bound to carbon. Silicon in cyclic ligands tends to exhibit more negative shifts. The lower the oxidation state of the uranium in the series +4, +3, +2, the lower the ^{29}Si NMR chemical shift.

REFERENCES

(1) Iggo, J. A., *NMR Spectroscopy in Inorganic Chemistry*. Oxford University Press Inc: New York, 1999; Vol. 83, p 87.

(2) Marsmann, H., *NMR 17: Basic Principles and Progress*. Springer-Verlag: New York, 1981; Vol. 17, p 235.

(3) Harris, R. K.; Mann, B. E., *NMR and the Periodic Table*. Academic Press: San Francisco, 1978; p 459.

(4) Schraml, J., *The Chemistry of Organic Silicon Compounds*. John Wiley & Sons, LTD: New York, 2001; Vol. 3, p 1148.

(5) Coleman, B., *Chemically and Biochemically Important Elements*. Academic Press Inc: New York, 1983; Vol. 2, p 436.

(6) Kennedy, J. D.; McFarlane, W., *Multinuclear NMR*. Plenum Publishing Corp: New York, 1987; p 639.

(7) Kupce, E.; Wrackmeyer, B., *Advanced Application of NMR to Organometallic Chemistry*. John Wiley & Sons: New York, 1996; p 376.

(8) Cloke, F. G. N.; Green, J. C.; Jardine, C. N., *Organometallics* **1999,** *18*, 1080-1086.

(9) Cloke, F. G. N.; Hitchcock, P. B., *J. Am. Chem. Soc.* **2002,** *124*, 9352-9353.

(10) Frey, A. S.; Cloke, F. G. N.; Hitchcock, P. B.; Day, I. J.; Green, J. C.; Aitken, G., *J. Am. Chem. Soc.* **2008,** *130*, 13816-13817.

(11) Farnaby, J. H.; Cloke, F. G. N.; Coles, M. P.; Green, J. C.; Aitken, G., *C. R. Chim.* **2010,** *13*, 812-820.

(12) Tsoureas, N.; Summerscales, O. T.; Cloke, F. G. N.; Roe, S. M., *Organometallics* **2013,** *32*, 1353-1362.

(13) Tsoureas, N.; Kilpatrick, A. F. R.; Summerscales, O. T.; Nixon, J. F.; Cloke, F. G. N.; Hitchcock, P. B., *Eur. J. Inorg. Chem.* **2013,** *2013*, 4085-4089.

(14) King, D. M.; Lewis, W.; Liddle, S. T., *Inorg. Chim. Acta* **2012,** *380*, 167-173.

(15) Mills, D. P.; Cooper, O. J.; Tuna, F.; McInnes, E. J. L.; Davies, E. S.; McMaster, J.; Moro, F.; Lewis, W.; Blake, A. J.; Liddle, S. T., *J. Am. Chem. Soc.* **2012,** *134*, 10047-10054.

(16) Gardner, B. M.; Stewart, J. C.; Davis, A. L.; McMaster, J.; Lewis, W.; Blake, A. J.; Liddle, S. T., *Proc. Natl. Acad. Sci. U. S. A.* **2012,** *109*, 9265-9270.

(17) King, D. M.; Tuna, F.; McInnes, E. J.; McMaster, J.; Lewis, W.; Blake, A. J.; Liddle, S. T., *Science* **2012,** *337*, 717-720.

(18) King, D. M.; Tuna, F.; McMaster, J.; Lewis, W.; Blake, A. J.; McInnes, E. J. L.; Liddle, S. T., *Angew. Chem., Int. Ed.* **2013,** *52*, 4921-4924.

(19) King, D. M.; Tuna, F.; McInnes, E. J.; McMaster, J.; Lewis, W.; Blake, A. J.; Liddle, S. T., *Nat. Chem.* **2013,** *5*, 482-488.

(20) Gardner, B. M.; Balázs, G.; Scheer, M.; Tuna, F.; McInnes, E. J. L.; McMaster, J.; Lewis, W.; Blake, A. J.; Liddle, S. T., *Angew. Chem., Int. Ed.* **2014,** *53*, 4484-4488.

(21) Lu, E.; Cooper, O. J.; McMaster, J.; Tuna, F.; McInnes, E. J. L.; Lewis, W.; Blake, A. J.; Liddle, S. T., *Angew. Chem., Int. Ed.* **2014,** *53*, 6696-6700.

(22) Arnold, P. L.; Jones, G. M.; Odoh, S. O.; Schreckenbach, G.; Magnani, N.; Love, J. B., *Nat. Chem.* **2012,** *4*, 221-227.

(23) Mansell, S. M.; Farnaby, J. H.; Germeroth, A. I.; Arnold, P. L., *Organometallics* **2013,** *32*, 4214-4222.

(24) Evans, W. J.; Siladke, N. A.; Ziller, J. W., *Chem. Eur. J.* **2010,** *16*, 796-800.

(25) Siladke, N. A.; Ziller, J. W.; Evans, W. J., *Z. Anorg. Allg. Chem.* **2010,** *636*, 2347-2351.

(26) Evans, W. J.; Siladke, N. A.; Ziller, J. W., *C. R. Chimie* **2010,** *13*, 775-780.

(27) Siladke, N. A.; Ziller, J. W.; Evans, W. J., *J. Am. Chem. Soc.* **2011,** *133*, 3507-3516.

(28) Lorenz, V.; Schmiege, B. M.; Hrib, C. G.; Ziller, J. W.; Edelmann, A.; Blaurock, S.; Evans, W. J.; Edelmann, F. T., *J. Am. Chem. Soc.* **2011,** *133*, 1257-1259.

(29) MacDonald, M. R.; Fieser, M. E.; Bates, J. E.; Ziller, J. W.; Furche, F.; Evans, W. J., *J. Am. Chem. Soc.* **2013,** *135*, 13310-13313.

(30) Kindra, D. R.; Evans, W. J., *Chem. Rev.* **2014,** *114*, 8865-8882.

(31) Castro-Rodriguez, I.; Nakai, H.; Zakharov, L. N.; Rheingold, A. L.; Meyer, K., *Science* **2004,** *305*, 1757-9.

(32) Castro-Rodriguez, I.; Meyer, K., *Chem Commun.* **2006**, 1353-1368.

(33) Lam, O. P.; Anthon, C.; Heinemann, F. W.; O'Connor, J. M.; Meyer, K., *J. Am. Chem. Soc.* **2008,** *130*, 6567-6576.

(34) Graves, C. R.; Vaughn, A. E.; Schelter, E. J.; Scott, B. L.; Thompson, J. D.; Morris, D. E.; Kiplinger, J. L., *Inorg. Chem.* **2008,** *47*, 11879-11891.

(35) Graves, C. R.; Yang, P.; Kozimor, S. A.; Vaughn, A. E.; Clark, D. L.; Conradson, S. D.; Schelter, E. J.; Scott, B. L.; Thompson, J. D.; Hay, P. J.; Morris, D. E.; Kiplinger, J. L., *J. Am. Chem. Soc.* **2008,** *130*, 5272-5285.

(36) Kraft, S. J.; Fanwick, P. E.; Bart, S. C., *Inorg. Chem.* **2010,** *49*, 1103-1110.

(37) Matson, E. M.; Forrest, W. P.; Fanwick, P. E.; Bart, S. C., *Organometallics* **2012,** *31*, 4467-4473.

(38) Fortier, S.; Brown, J. L.; Kaltsoyannis, N.; Wu, G.; Hayton, T. W., *Inorg. Chem.* **2012,** *51*, 1625-1633.

(39) Lewis, A. J.; Williams, U. J.; Carroll, P. J.; Schelter, E. J., *Inorg. Chem.* **2013,** *52*, 7326-7328.

(40) Davidson, P. J.; Harris, D. H.; Lappert, M. F., *J. Chem. Soc., Dalton Trans.* **1976**, 2268-2274.

(41) Evans, W. J.; Kozimor, S. A.; Hillman, W. R.; Ziller, J. W., *Organometallics* **2005,** *24*, 4676-4683.

(42) Evans, W. J.; Nyce, G. W.; Forrestal, K. J.; Ziller, J. W., *Organometallics* **2002,** *21*, 1050-1055.

(43) Evans, W. J.; Kozimor, S. A.; Ziller, J. W.; Kaltsoyannis, N., *J. Am. Chem. Soc.* **2004,** *126*, 14533-14547.

(44) Andersen, R. A., *Inorg. Chem.* **1979,** *18*, 1507-1509.

(45) Carmichael, C. D.; Jones, N. A.; Arnold, P. L., *Inorg. Chem.* **2008,** *47*, 8577-8579.

(46) Horacek, M.; Gyepes, R.; Cisarova, I.; Polasek, M.; Varga, V.; Mach, K., *Collect. Czech. Chem. Commun.* **1996,** *61*, 1307-1320.

(47) Kucht, A.; Kucht, H.; Barry, S.; Chien, J. C. W.; Rausch, M. D., *Organometallics* **1993,** *12*, 3075-3078.

(48) Kasi, R. M.; Coughlin, E. B., *Organometallics* **2003,** *22*, 1534-1539.

(49) Krut'ko, D. P.; Borzov, M. V.; Veksler, E. N., *Russ. Chem. Bull.* **2004,** *53*, 2182-2186.

(50) Fagan, P. J.; Manriquez, J. M.; Marks, T. J.; Day, C. S.; Vollmer, S. H.; Day, V. W., *Organometallics* **1982,** *1*, 170-180.

(51) del Mar Conejo, M.; Parry, J. S.; Carmona, E.; Schultz, M.; Brennann, J. G.; Beshouri, S. M.; Andersen, R. A.; Rogers, R. D.; Coles, S.; Hursthouse, M. B., *Chem. Eur. J.* **1999,** *5*, 3000-3009.

(52) Patel, D.; Lewis, W.; Blake, A. J.; Liddle, S. T., *Dalton Trans.* **2010,** *39*, 6638-6647.

(53) Cooper, O. J.; Mills, D. P.; McMaster, J.; Moro, F.; Davies, E. S.; Lewis, W.; Blake, A. J.; Liddle, S. T., *Angew. Chem.* **2011,** *123*, 2431-2434.

(54) Cooper, O. J.; Mills, D. P.; Lewis, W.; Blake, A. J.; Liddle, S. T., *Dalton Trans.* **2014,** *43*, 14275-14283.

CHAPTER 2

EXPANDING THE CHEMISTRY OF MOLECULAR U^{II} COMPLEXES: SYNTHESIS, CHARACTERIZATION, AND REACTIVITY OF THE $\{[C_5H_3(SiMe_3)_2]U^{II}\}^{1-}$ ANION

INTRODUCTION[†]

A critical aspect for understanding the chemistry of an element and the reactivity of its molecules is the range of available oxidation states. Accordingly, extensive studies have been made to establish the limits of oxidation states for all the elements in the periodic table. Although uranium has received extra scrutiny because of its applications in nuclear energy, the number of oxidation states found in isolable molecular species was limited to +3 through +6 for many years.

However, the organometallic chemistry of uranium has revealed that the +2 oxidation state is accessible for uranium in the proper ligand environment. As described in the introduction, the first example of a crystallographically characterized, molecular, U^{II} complex, [K(crypt)][Cp′$_3$U], **21-U**, (Cp′ = $C_5H_4SiMe_3$, crypt = 2.2.2-cryptand), was obtained by reduction of Cp′$_3$U, **8-U**, with potassium-graphite (KC_8) in the presence of crypt at −35 °C, eq 2.1.[1]

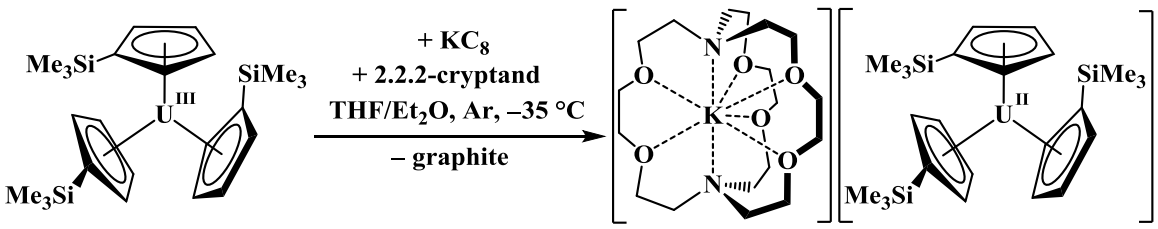

8-U **21-U** **(2.1)**

[†]Portions of this chapter have been published: Windorff, C. J; MacDonald, M. R.; Meihaus, K. R.; Ziller, J. W.; Long, J. R.; Evans, W. J. *Chemistry – A European Journal*, **2016**, *22*, 772–782. DOI: 10.1002/chem.201503583

Subsequently, a second example was obtained by Meyer and co-workers in a tris(aryloxide) arene ligand environment by potassium reduction of [(^{Ad,Me}ArO)$_3$mes]U, eq 2.2.[2] These

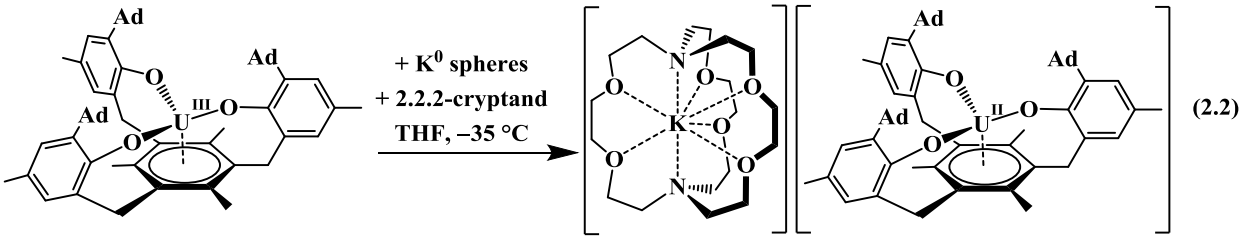

(2.2)

reactions are variations of reductions examined with Cp″$_3$M [Cp″ = $C_5H_3(SiMe_3)_2$–1,3; M = La, **20-La**,[3] and Th, **20-Th**[4]), and with Cp′$_3$Ln, **8-Ln**,[5-8] to make +2 ions of the rare earth metals and thorium, eq 2.3.

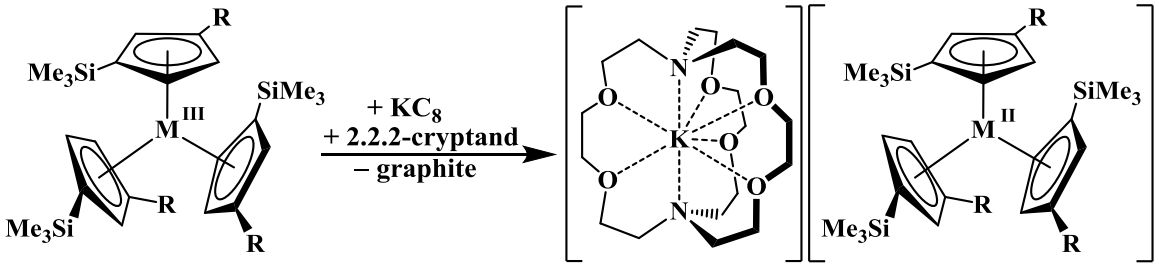

(2.3)

R = SiMe$_3$; M = La, Th

R = H; M = Y, La, Ce, Pr, Nd, Sm, Gd, Tb, Dy, Ho, Er, Tm, Lu, U

The existence of the [K(crypt)][Cp″$_3$M], **22-M**, for M = La, **22-La**, and Th, **22-Th**, eq 2.3, and of [K(crypt)][Cp′$_3$U], **21-U**, eq 2.1, suggested that the analogous Cp″ complex of U^{II}, namely [K(crypt)][Cp″$_3$U], **22-U**, was a reasonable synthetic target.[9] The reactivity/stability of **22-U** is of particular interest since **21-U** is so reactive that it is difficult to characterize its physical properties. Described here is the reduction chemistry of Cp″$_3$U, **20-U**, which leads to more examples of U^{II} complexes. The spectroscopic and magnetic properties of these additional U^{II} complexes are described and compared to those of **21-U** and reactivity studies on both **21-U** and **22-U** are presented to allow further elaboration of the chemistry of U^{II}.

EXPERIMENTAL SECTION

All manipulations and syntheses described below were conducted with the rigorous exclusion of air and water using standard Schlenk line and glovebox techniques under an argon or dinitrogen atmosphere. Solvents were sparged with UHP argon and dried by passage through columns containing Q-5 and molecular sieves prior to use. Deuterated NMR solvents were dried over sodium benzophenone ketyl or sodium/potassium alloy, degassed by three freeze-pump-thaw cycles, and vacuum transferred before use. ^{1}H, ^{2}H, ^{13}C, ^{29}Si and ^{207}Pb NMR spectra were recorded on a Bruker GN500 or CRYO500 MHz spectrometer operating at 499.3, 76.8, 125.6, 99.2 and 103.3 MHz, respectively, at 298 K unless otherwise stated. ^{1}H, ^{2}H and ^{13}C NMR spectra were referenced internally to solvent resonances. ^{29}Si and ^{207}Pb NMR spectra were referenced externally to $SiMe_4$ and $Pb(NO_3)_2$, respectively. Elemental analyses were performed on a Perkin-Elmer 2400 Series II CHNS elemental analyzer. IR spectra were recorded as KBr pellets on a JASCO 4700 FTIR. UV/visible spectra were collected in THF or hexane at 298 K using a Varian Cary 50 Scan UV/visible spectrophotometer in a 1 mm cuvette. Near IR (NIR) spectra were collected in THF or hexane at 298 K using a Perkin Elmer Lambda 900 UV/vis/NIR spectrometer in a 1 cm cuvette. All optical spectra were recorded as 1.5 – 2 mM solutions except NIR of U^{III} compounds which were recorded in 3 mM solutions. Samples for magnetic susceptibility measurements were prepared by adding the powdered crystalline compound to a 5 mm inner diameter quartz tube with a quartz platform ¾ down the length of the tube. Solid eicosane was then added to prevent crystallite torqueing and provide good thermal contact between the sample and the bath. The tubes were fitted with Teflon sealable adapters, evacuated using a glove box vacuum pump, and flame sealed under static vacuum. Following flame sealing, the solid eicosane was melted in a water bath held at 40 °C. Magnetic susceptibility

measurements were performed using a Quantum Design MPMS2 SQUID magnetometer. DC susceptibility data were collected at temperatures ranging from 1.8 to 300 K, using applied fields of 1.0, 0.5, and 0.1 T. All data were corrected for diamagnetic contributions from the core diamagnetism estimated using Pascal's constants.[10,11] Evans method[12-14] samples were weighed directly into a tared NMR tube, and charged with THF and a flame sealed capillary tube containing a sample of neat THF. The NMR sample was removed from the glovebox and recorded on a Bruker GN500 NMR at room temperature (298 K).

H_2 (99.99%, Praxair) and D_2 (99.98%, Cambridge Isotope Laboratories) gases were used as received. KH (30% wt dispersion in mineral oil, Aldrich) was washed several times with hexane, filtered, and dried under vacuum before use. Potassium and sodium metals (Aldrich) were washed with hexane and scraped to provide fresh surfaces before use. 12-Crown-4 (Aldrich) was dried over activated molecular sieves and degassed by three freeze-pump-thaw cycles before use. PbI_2 (Aldrich), 18-crown-6 (Aldrich), and 2.2.2-cryptand (crypt, 4,7,13,16,21,24-hexaoxa-1,10-diazabicyclo[8.8.8]hexacosane, Aldrich) were placed under vacuum (10^{-3} Torr) for 12 h before use. $KN(SiMe_3)_2$ was dissolved in toluene, centrifuged, and dried *in vacuo* before use. C_8H_8 was distilled, dried over 4 Å activated molecular sieves, and degassed by three freeze-pump-thaw cycles. The following compounds were prepared following literature procedures: KCp′,[15] UI_3, **16**,[16] Cp'_3U, **8-U**,[1] Cp''_3U, **20-U**,[17] [K(crypt)][Cp'_3U]•THF, **21•THF**,[1] and KC_8.[18] KCp″ was made analogously to KCp′ .[15]

[K(crypt)][Cp''_3U], 22-U. In a glovebox, addition of solid KC_8 (47 mg, 0.35 mmol) to a 2:1 Et_2O/THF (3 ml) solution of Cp''_3U, **20-U** (210 mg, 0.243 mmol) and crypt (93 mg, 0.25 mmol) caused the mixture to immediately turn black. After stirring 4 min, the reaction was filtered and the solvent was removed under reduced pressure. The black solid was triturated with

hexane to yield **22-U** as a black powder (270 mg, 87%). ^{1}H NMR (THF-d_8): δ 11.14 (s, $C_5H_3(SiMe_3)_2$, 3H), 3.71 (s, OCH_2CH_2O, 12H), 3.65 (t, $^{3}J_{HH}$ = 4.5 Hz, NCH_2CH_2O, 12H), 2.62 (t, $^{3}J_{HH}$ = 4.5 Hz, NCH_2CH_2O, 12H), −4.38 (s, $C_5H_3(SiMe_3)_2$, 54H), −12.35 (s, $C_5H_3(SiMe_3)_2$, 6H). ^{29}Si NMR (THF-d_8): δ −329.5 (br, $\nu_{1/2}$ = 120 Hz, $C_5H_3(SiMe_3)_2$). Evans method (THF, 298 K): 2.4 μ_B. UV/vis/NIR (THF) λ_{max} nm (ε, $M^{-1}cm^{-1}$) 315 (7500), 470 (6000), 605 (3200 shoulder), 1086 (300), 1382 (100 shoulder). FTIR (ν, cm^{-1}): 2949s, 2887s, 2815m, 1738s, 1447w, 1446m, 1355s, 1297w, 1234s, 1201m, 1134m, 1106vs, 1078s, 951s, 921s, 829vs, 748m, 663w, 632w. Anal. Calcd for $C_{51}H_{99}N_2O_6Si_6KU$: C, 47.78; H, 7.78; N, 2.19. Found: C, 47.25; H, 7.86; N, 2.22.

[K(18-crown-6)(THF)$_2$][Cp′′$_3$U], 23-U. In a glovebox, addition of solid KC_8 (70 mg, 0.50 mmol) to a vigorously stirred green solution of **20-U** (204 mg, 0.236 mmol) and 18-crown-6 (68 mg, 0.26 mmol) in THF (3 mL) caused the mixture to immediately turn black. After stirring 4 min, the reaction was filtered to remove black solids and the solvent was removed under reduced pressure. The black solids were washed with hexane and crystallized from THF layered with hexane at −30 °C (310 mg, 90%). X-ray quality crystals were grown from a 1:1 THF/Et_2O solution at −30 °C. ^{1}H NMR (THF-d_8): δ 11.16 (s, $C_5H_3(SiMe_3)_2$, 3H), 3.78 (s, $C_{12}H_{24}O_6$, 24H), −4.46 (s, $C_5H_3(SiMe_3)_2$, 54H), −12.30 (s, $C_5H_3(SiMe_3)_2$, 6H). ^{29}Si NMR (THF-d_8): δ −327.3 (br, $\nu_{1/2}$ = 150 Hz, $C_5H_3(SiMe_3)_2$). Evans method (THF, 298 K): 2.9 μ_B. UV/vis/NIR (THF) λ_{max} nm (ε, $M^{-1}cm^{-1}$): 315 (7500), 470 (6000), 605 (3200 shoulder), 926 (400), 982 (400), 1075 (300, shoulder), 1382 (100, shoulder). FTIR (ν, cm^{-1}): 3043w, 2948s, 2892s, 1472m, 1454m, 1434m, 1396w, 1351m, 1314w, 1283w, 1244s, 1201m, 1110vs, 1077s, 962s, 921s, 830vs, 749s, 681m, 635m. Anal. Calcd for $C_{53}H_{103}O_8Si_6KU$: C, 48.44; H, 7.90. Found: C, 48.13; H, 7.88.

[Na(18-crown-6)(THF)$_2$][Cp′′$_3$U], 24-U. In a glovebox, solid (290 mg, 0.335 mmol) was added to a stirred solution of 18-crown-6 (100 mg, 0.371 mmol) in THF (5 mL) in a scintillation vial with sodium metal (50 mg, 2.0 mmol) smeared on the walls. The green solution quickly turned black and was stirred for 30 min. The solution was filtered and the solvent was removed under reduced pressure. The resulting black solids were washed with hexane and dried under reduced pressure to yield **24-U** (365 mg, 84%). X-ray quality crystals were grown from a 1:1 THF/Et_2O solution at −30 °C. ^{1}H NMR (THF-d_8): δ 11.33 (s, $C_5H_3(SiMe_3)_2$, 3H), 3.73 (s, $C_{12}H_{24}O_6$, 24H), −4.49 (s, $C_5H_3(SiMe_3)_2$, 54H), −12.39 (s, $C_5H_3(SiMe_3)_2$, 6H). ^{29}Si NMR (THF-d_8): δ −328.6 (br, $\nu_{1/2}$ = 120 Hz, $C_5H_3(SiMe_3)_2$). Evans method (THF, 298 K): 2.9 μ_B. UV/vis/NIR (THF) λ_{max} nm (ε, $M^{-1}cm^{-1}$): 315 (6000), 470 (5000), 605 (2500 shoulder), 978 (300), 1082 (300), 1382 (100 shoulder). FTIR (ν, cm^{-1}): 2953s, 2898s, 1558w, 1451m, 1456m, 1353s, 1270w, 1249s, 1114vs, 1076m, 965m, 923s, 832vs, 753m. Anal. Calcd for $C_{53}H_{103}O_8Si_6NaU$: C, 49.05; H, 8.00. Found: C, 49.45; H, 8.11.

[Na(12-crown-4)$_2$][Cp′′$_3$U], 25-U. In a glovebox, solid **20-U** (114 mg, 0.132 mmol) was added to a stirred solution of 12-crown-4 (80 μL, 0.49 mmol) in THF (5 mL) in a scintillation vial with sodium metal (70 mg, 3.0 mmol) smeared on the walls. The green solution quickly turned black and was stirred for 30 min. The solution was filtered and the solvent was removed under reduced pressure. The resulting black solids were washed with hexane and dried under reduced pressure to yield **25-U** (155 mg, 95%). ^{1}H NMR (THF-d_8): δ 11.09 (s, $C_5H_3(SiMe_3)_2$, 3H), 3.70 (s, $C_8H_{16}O_4$, 32H), −4.39 (s, $C_5H_3(SiMe_3)_2$, 54H), −12.23 (s, $C_5H_3(SiMe_3)_2$, 6H). ^{13}C NMR (THF-d_8): δ 195.4 ($C_5H_3(SiMe_3)_2$), 194.3 ($C_5H_3(SiMe_3)_2$), 76.7 ($C_5H_3(SiMe_3)_2$), 67.4 ($C_8H_{16}O_4$), −111.0 ($C_5H_3(SiMe_3)_2$). ^{29}Si NMR (THF-d_8): δ −329.9 (br, $\nu_{1/2}$ = 120 Hz, $C_5H_3(SiMe_3)_2$). Evans method (THF, 298 K): 2.6 μ_B. UV/vis/NIR (THF) λ_{max} nm (ε, $M^{-1}cm^{-1}$):

315 (6000), 470 (4500), 605 (2300 shoulder) 1086 (300), 1382 (100 shoulder). FTIR (ν, cm^{-1}): 2951s, 2909s, 2871s, 1471m, 1454m, 1446m, 1391w, 1365m, 1286w, 1291m, 1239s, 1137s, 1098vs, 1023s, 958w, 919vs, 833vs, 748s, 687w, 634w. Anal. Calcd for $C_{49}H_{95}O_8Si_6NaU$: C, 47.39; H, 7.71. Found: C, 47.17; H, 7.93.

[K(18-crown-6)(THF)$_2$][Cp′′$_3$UH], 26, From 23-U and H$_2$. A 30 mL Schlenk flask fitted with a high vacuum greaseless stopcock was charged with a solution of **23-U** (184 mg, 0.140 mmol) in THF (5 mL), sealed, removed from the glovebox, and placed in a 0 °C ice bath. The flask was attached to a high vacuum line and briefly degassed three times to the solvent pressure. The flask was charged with H_2 (1 atm), sealed, and allowed to warm to 25 °C. After stirring overnight, the dark red solution was dried under reduced pressure, the flask was brought into the glovebox, and the solids were washed with hexane. The product was crystalized from a THF solution layered with hexane at −30 °C and isolated as a dark red crystalline solid (175 mg, 95%). ^{1}H NMR (THF-d_8): δ 601 (s, br, $\nu_{1/2}$ = 250 Hz, U*H*, 1H), 7.54 (s, $C_5H_3(SiMe_3)_2$, 3H), 3.84 (s, $C_{12}H_{24}O_6$, 24H), −3.92 (s, $C_5H_3(SiMe_3)_2$, 54H). ^{13}C NMR (THF-d_8): δ 274.7 ($C_5H_3(SiMe_3)_2$), 249.8 ($C_5H_3(SiMe_3)_2$), 71.3 ($C_{12}H_{24}O_8$), −9.7 ($C_5H_3(SiMe_3)_2$). No ^{29}Si NMR resonance was observed. Evans method (THF, 298 K): 3.3 μ_B. UV/vis/NIR (THF) λ_{max} nm (ε, $M^{-1}cm^{-1}$): 504 (1000), 561 (700 shoulder), 686 (300), 932 (200 shoulder), 976 (300), 1026 (200 shoulder), 1072 (200), 1230 (100), 1290 (100), 1380 (100). FTIR (ν, cm^{-1}): 2043w, 2950s, 2894s, 2822m, 1451m, 1454m, 1435m, 1395w, 1352s, 1267w, 1248s, 1160w, 1115vs, 1077s, 1033w, 964s, 930m, 924s, 830vs, 750s, 688w, 636w. Anal. Calcd for $C_{53}H_{104}O_8Si_6KU$: C, 48.41; H, 7.97. Found: C, 47.30; H, 7.96. The low carbon content is sometimes observed in complexes with high silicon content.[3]

[K(18-crown-6)(THF)$_2$][Cp′′$_3$UD], 26-D, from 23-U and D_2. The deuterium analog of **26** was prepared in 79% yield as described above but using D_2 instead of H_2. ^{1}H NMR (THF-d_8): δ 7.54 (s, $C_5H_3(SiMe_3)_2$, 3H), 3.84 (s, $C_{12}H_{24}O_6$, 24H), −3.92 (s, $C_5H_3(SiMe_3)_2$, 54H). ^{2}H NMR (THF-d_8): δ 601 (s, br, $\nu_{1/2}$ = 250 Hz, U*H*, 1H). No H/D exchange was observed on the NMR timescale.

[K(18-crown-6)(THF)$_2$][Cp′′$_3$UH], 26, from 23-U and $PhSiH_3$. In a glovebox, addition of solid KC_8 (50 mg, 0.37 mmol) to a vigorously stirred green solution of **20-U** (194 mg, 0.224 mmol) and 18-crown-6 (60 mg, 0.23 mmol) in THF (4 mL) caused the mixture to immediately turn black. After stirring 4 min, the reaction was filtered into a colorless stirred solution of $PhSiH_3$ (30 mg, 0.290 mmol) in THF (2 mL). The mixture turned red over the next 30 min and was stirred overnight. The volatiles were removed under reduced pressure and the product was washed with hexane leaving **26** as a dark red powder (232 mg, 79%, based on **20-U**) identified by ^{1}H NMR spectroscopy. Complex **26** can also be made from isolated **23-U** (17 mg, 0.013 mmol) in (THF-d_8) and 1 drop of $PhSiH_3$. The NMR tubed was briefly vortexed and taken to the NMR spectrometer. ^{1}H NMR analysis showed full conversion to **26** within 30 min.

[K(18-crown-6)(THF)$_2$][Cp′′$_3$UH], 26, from 20-U and KH. Solid KH (20 mg, 0.50 mmol) was added to a solution of **20-U** (99 mg, 0.11 mmol) and 18-crown-6 (32 mg, 0.12 mmol) in THF (4 mL). After stirring for 6 h, the solvent was removed under reduced pressure. The solids were washed with hexane and extracted with Et_2O. The solvent was removed under reduced pressure yielding **26** as a dark red powder (115 mg, 77%), identified by ^{1}H NMR spectroscopy.

[K(crypt)][Cp′′$_3$UH], 27-U, from 20-U and KH. In a glovebox KH (14 mg, 0.35 mmol) was added to a green solution of **20-U** (50 mg, 0.060 mmol) and crypt (25 mg, 0.066

mmol) in THF (5 ml). After stirring overnight, the mixture was filtered and the volatiles were removed under reduced pressure to give [K(crypt)][Cp″$_3$UH], **27-U** (70 mg, 94 %), as a dark red oil that did not give a solid product upon trituration. FTIR (ν, cm^{-1}): 1299(s), 1260(s), 1238(s), 1135(m), 1106(s), 1079(s), 952(m), 925(m), 833(vs), 747(s), 722(sh), 688(w), 636(w).

[K(crypt)][Cp′$_3$UH], 9, from 21•THF and PhSiH$_3$. In the glovebox, solid [K(crypt)][Cp′$_3$U]·THF, **21•THF**, (41 mg, 0.036 mmol) was tapped into a stirred solution of PhSiH$_3$ (47 mg, 0.43 mmol) in THF (3 mL), the reaction quickly turned dark red. After 3 h the mixture was filtered and the volatiles were removed under reduced pressure to produce a red oil. The oil was dissolved in minimal 1:1 THF/Et$_2$O and an additional 5 mL of Et$_2$O was added and the solution was cooled to −35 °C and layered with hexane. Dark red solids deposited (30 mg, 79%) and were identified as **9** by ^{1}H NMR spectroscopy.[1]

Reaction of [K(crypt)][Cp′$_3$U]•THF, 21-U•THF, with Cyclooctatetraene. In a glovebox, a solution of cyclooctatetraene (73 mg, 0.70 mmol) in THF (2 mL) was quickly added to a cold stirred solution of **21-U•THF**, (90 mg, 0.085 mmol) in THF (5 mL, −35 °C). The mixture was stirred for 1 h as it warmed to room temperature. The resulting brown-red/green solution was concentrated to 4 mL, layered with Et$_2$O, and stored at −35 °C overnight. The dark amber red mother liquor was decanted and the resulting green crystalline solids were dried under reduced pressure and identified as (C$_8$H$_8$)$_2$U, by ^{1}H NMR spectroscopy[19-20] and single crystal X-ray diffraction[21] (7 mg, 30%). The solvent was removed from the mother liquor until a dark red-brown oil remained. The oil was dissolved in Et$_2$O (5 mL), layered with hexane (5 mL), and stored at −35 °C for 2 d to yield a mixture of colorless and dark red crystals that were determined by X-ray diffraction and ^{1}H NMR spectroscopy to be [K(crypt)][Cp′][22] and [K(crypt)][Cp′$_4$U], **28-U**, respectively in a 1:5 ratio by ^{1}H NMR analysis (see below).

Independent Synthesis of [K(crypt)][Cp′$_4$U], 28-U, from 8-U. In a glovebox, a solution of KCp′ (35 mg, 0.20 mmol) and crypt (75 mg, 0.20 mmol) in THF (2 mL) was added to a stirred solution of **8-U** (130 mg, 0.200 mmol) in THF (2 mL). After 10 min, the solvent was removed from the dark red solution under vacuum until a dark red oily residue formed. The oil was dissolved in Et_2O (6 mL) and stored at −35 °C for 2 d to produce dark red crystals suitable for X-ray diffraction. The mother liquor was decanted and the crystals were dried under vacuum to yield **28-U** as a dark red crystalline solid (204 mg, 85%). ^{1}H NMR (THF-d_8, 298 K): δ 3.08 (s, OCH_2CH_2O, 12H), 3.04 (t, $^3J_{HH}$ = 4.5 Hz, NCH$_2$CH_2O, 12H), 2.07 (t, $^3J_{HH}$ = 4.5 Hz, NCH_2CH$_2$O, 12H), −2.42 (br s, C$_5$H$_4$SiMe_3, 36H), −9.69 (br s, C$_5H_4$SiMe$_3$, 8H), −25.50 (br s, C$_5H_4$SiMe$_3$, 6H). ^{1}H NMR (THF-d_8, 238 K): δ 2.87 (s, OCH_2CH_2O + NCH$_2$CH_2O, 24H), 2.07 (s, NCH_2CH$_2$O, 12H), −3.15 (br s, C$_5$H$_4$SiMe_3, 36H), −13.82 (br s, C$_5H_4$SiMe$_3$, 8H), −32.94 (br s, C$_5H_4$SiMe$_3$, 6H). ^{1}H NMR (THF-d_8, 183 K): δ 2.69 (s, br, C$_{18}H_{36}$N$_2$O$_6$, 6H), 2.53 (s, br, C$_{18}H_{36}$N$_2$O$_6$, 6H), 2.14 (s, br, C$_{18}H_{36}$N$_2$O$_6$, 12H), 2.05 (s, br, C$_{18}H_{36}$N$_2$O$_6$, 6H), 0.90 (s, br, C$_{18}H_{36}$N$_2$O$_6$, 6H), −4.38 (br s, C$_5$H$_4$SiMe_3, 36H), −20.93 (br s, C$_5H_4$SiMe$_3$, 8H), −43.70 (br s, C$_5H_4$SiMe$_3$, 6H). ^{29}Si NMR (THF-d_8, 298 K): δ −121.8 (C$_5$H$_4$$SiMe_3$). Evans method (THF, 298 K): 3.0 μ_B. UV/vis/NIR (THF) λ_{max} nm (ε, M^{-1}cm^{-1}): 370 (1500), 470 (1300), 580 (600), 656 (300), 740 (300), 940 (200), 1000 (200), 1096 (100), 1202 (100), 1426 (100). FTIR (ν, cm^{-1}): 3083w, 3033w, 2951m, 2888m, 2818m, 2763w, 2732w, 2362w, 1927w, 1480m, 1444m, 1400w, 1356m, 1301m, 1260m, 1246s, 1177m, 1134m, 1105s, 1082m, 1037m, 949s, 933m, 903m, 831s, 778m, 748s, 699m, 683m, 637m, 628m, 605m, 571w cm^{-1}. Anal. Calcd for C$_{50}$H$_{88}$N$_2$O$_6$Si$_4$KU: C, 49.93; H, 7.37; N, 2.33. Found: C, 49.69; H, 7.46; N, 2.25.

Synthesis of [K(crypt)][Cp′$_4$U], 28-U, from 21•THF, and Cp′$_2$Pb. In a glovebox, a cold yellow solution of Cp′$_2$Pb, **30**, (11 mg, 0.023 mmol) in THF (2 mL, −35 °C) was added to a

stirred cold solution of **21-U•THF**, (49 mg, 0.043 mmol) in THF (5 mL, −35 °C). As the stirred solution warmed to room temperature over 15 min, the color changed from black-green to red-brown. The solvent was removed under reduced pressure and the resulting tacky red-brown residue was dissolved in Et_2O (3 mL) and stored at −35 °C for 4 h. The mother liquor was decanted and the resulting dark red crystals were rinsed with cold Et_2O (1 mL, −35 °C) and dried under vacuum to yield **28-U** as a red crystalline solid (33 mg, 64%) as identified by ^{1}H NMR spectroscopy.

Reaction of [K(18-crown-6)(THF)$_2$][Cp″$_3$U], 23-U, with Cyclooctatetraene. In a glovebox, **23-U** (21 mg, 0.016 mmol) was added as a solid to a solution of C_8H_8 (14 mg, 0.93 mmol) in THF (4 mL). After stirring 3 h, the volatiles were removed under reduced pressure. The solids were washed with hexane and extracted with THF. Solvent was removed to give a green powder identified as a mixture of $(C_8H_8)_2U$ and K(18-crown-6)Cp″ (7 mg) by NMR spectroscopy.[19-20] Under reduced pressure, the solvent was removed from the hexane washes to yield green-brown **20-U** (12 mg) as determined by ^{1}H NMR spectroscopy.[23]

Cp′$_3$U(THF), 8-U(THF). **8-U** (97 mg. 0.15 mmol) was stirred in Et_2O (4 mL) and then THF (0.5 mL) was added. The color immediately turned red. After 2 min, the volatiles were removed under reduced pressure to give a quantitate yield of dark red Cp′$_3$U(THF), identified by ^{1}H NMR spectroscopy.[24] X-ray quality crystals were obtained from Et_2O at – 35 °C. Evans Method (THF, 298 K): 3.10 μ_B.

Attempted Synthesis of "[K(18-crown-6)(THF)$_2$][Cp′$_3$U]," Leading to Isolation of [K(18-crown-6)(OEt$_2$)][(Cp′$_3$U)$_2$(μ–H)], 29. In a glovebox, a vial with KC_8 (70 mg, 0.52 mmol) and a separate vial containing **8-U** (190 mg, 0.292 mol) and 18-crown-6 (85 mg, 0.32 mmol) in a 2:1:1 hexane:THF:Et_2O solvent mixture (3 mL) was chilled to –30 °C for 1 h, along

with an empty vial, a vial with a 1:1 hexane:THF solvent mixture, several pipettes and one pipette with a piece of kimwipe packed inside for filtration. The vials and pipettes were removed from the freezer and the KC_8 was tapped into the **8-U**/18-crown-6 mixture causing an immediate change from red to black/green. After 1 min, the solution had become dark red, and black solids (presumably graphite) were removed by filtration, the solids were washed with the cold 1:1 hexane:THF mixture until the filtrate was colorless. The filtrates were combined and returned to the –30 °C freezer. After 3 d dark red X-ray quality crystals of **29** formed.

Cp′$_2$Pb, 30. In a variation of the literature preparation,[25] in a glovebox, a solution of KCp′ (500 mg, 2.83 mmol) in THF (10 mL) was added to a stirred yellow slurry of PbI_2 (638 mg, 1.38 mmol) in THF (10 mL). Within 1 min, the mixture became bright yellow. After stirring overnight in the dark, the bright yellow mixture was centrifuged to remove white solids, presumably KI, and the solvent was removed under reduced pressure. The bright yellow residue was dissolved in hexane (20 mL), stirred for 2 h, and filtered to remove more white precipitate. Removal of solvent from the filtrate yielded **30** as a bright microcrystalline solid (572 mg, 86%). ^{1}H NMR (C_6D_6): δ 6.05 (m, $C_5\mathit{H}_4SiMe_3$, 4H), 5.98 (m, $C_5\mathit{H}_4SiMe_3$, 4H), 0.24 (s, $C_5H_4Si\mathit{Me}_3$, 18H). ^{13}C NMR (C_6D_6): δ 122.6 ($\mathit{C}_5H_4SiMe_3$), 118.2 ($\mathit{C}_5H_4SiMe_3$), 115.2 ($\mathit{C}_5H_4SiMe_3$), 1.33 ($C_5H_4Si\mathit{Me}_3$). ^{29}Si NMR (C_6D_6): δ −11.27 ($C_5H_4\mathit{Si}Me_3$). ^{207}Pb NMR (C_6D_6): δ −4970. FTIR: 3075w, 2951m, 2890w, 2361w, 1436w, 1400w, 1349w, 1301w, 1241s, 1195w, 1172m, 1035m, 900s, 834s, 766s, 750s, 688m, 622s, 593w, 539s cm^{-1}. Anal. Calcd for $C_{16}H_{26}Si_2Pb$: C, 39.89; H, 5.44. Found: C, 39.62; H, 5.41. Bright yellow, needle-like crystals of Cp′$_2$Pb suitable for X-ray diffraction were grown from a pentane solution at −35 °C.

Decomposition studies. In a glovebox, compounds were weighed into a scintillation vial then washed into a 10 mL volumetric flask and diluted to the mark with THF to form a 1.5 mM

solution. The solution was added to a 1 mm cuvette fitted with a high vacuum greaseless stopcock. The sample was sealed and taken from the glovebox to the UV/vis spectrometer. Spectra were recorded in 15 min intervals over the course of 17 h. A_∞ was measured after 1 month on a sample that remained in the UV/vis cell with periodic recording of spectra until the spectrum no longer changed.

X-ray Crystallographic Data. Crystallographic details for complexes $Cp'_3U(THF)$, **8-U(THF)**, [K(crypt)][Cp'_4U], **28-U**, [K(18-crown-6)(OEt_2)][($Cp'_3U)_2(\mu$-H)], **29** and Cp'_2Pb, **30** are summarized in the text below and in Table 2.1.

X-ray Data Collection, Structure Solution and Refinement for 8-U(THF). A brown crystal of approximate dimensions 0.133 x 0.152 x 0.241 mm was mounted on a glass fiber and transferred to a Bruker SMART APEX II diffractometer. The APEX2[26] program package was used to determine the unit-cell parameters and for data collection (30 sec/frame scan time for a sphere of diffraction data). The raw frame data was processed using SAINT[27] and SADABS[28] to yield the reflection data file. Subsequent calculations were carried out using the SHELXTL[29] program. The diffraction symmetry was *mmm* and the systematic absences were consistent with the orthorhombic space groups *Pnma* and *Pna*2_1. It was later determined that space group *Pna*2_1 was correct.

The structure was solved by direct methods and refined on F^2 by full-matrix least-squares techniques. The analytical scattering factors[30] for neutral atoms were used throughout the analysis. Hydrogen atoms were located from a difference-Fourier map and refined (x,y,z and U_{iso}). At convergence, wR2 = 0.0295 and Goof = 0.81 for 486 variables refined against 7315 data (0.74Å), R1 = 0.0142 for those 6833 data with $I > 2.0\sigma(I)$. The absolute structure was assigned by refinement of the Flack parameter.[31]

X-ray Data Collection, Structure Solution and Refinement for 28-U. A red crystal of approximate dimensions 0.277 x 0.453 x 0.455 mm was mounted on a glass fiber and transferred to a Bruker SMART APEX II diffractometer. The APEX2[32] program package was used to determine the unit-cell parameters and for data collection (10 sec/frame scan time for a sphere of diffraction data). The raw frame data was processed using SAINT[33] and SADABS[34] to yield the reflection data file. Subsequent calculations were carried out using the SHELXTL[35] program. There were no systematic absences nor any diffraction symmetry other than the Friedel condition. The centrosymmetric triclinic space group $P\bar{1}$ was assigned and later determined to be correct.

The structure was solved by direct methods and refined on F^2 by full-matrix least-squares techniques.[36] The analytical scattering factors[37] for neutral atoms were used throughout the analysis. Hydrogen atoms were included using a riding model. There was one-half molecule of diethylether solvent present per formula-unit. The solvent molecule was disordered about an inversion center and included with site-occupancy-factors of 0.50 for all atoms. At convergence, wR2 = 0.0423 and Goof = 1.029 for 636 variables refined against 14529 data (0.74Å), R1 = 0.0166 for those 13928 data with $I > 2.0\sigma(I)$.

X-ray Data Collection, Structure Solution and Refinement for 29. A red crystal of approximate dimensions 0.261 x 0.353 x 0.396 mm was mounted on a glass fiber and transferred to a Bruker SMART APEX II diffractometer. The APEX2[38] program package was used to determine the unit-cell parameters and for data collection (20 sec/frame scan time for a sphere of diffraction data). The raw frame data was processed using SAINT[39] and SADABS[40] to yield the reflection data file. Subsequent calculations were carried out using the SHELXTL[41] program. There were no systematic absences nor any diffraction symmetry other than the Friedel

condition. The centrosymmetric triclinic space group $P\bar{1}$ was assigned and later determined to be correct.

The structure was solved by direct methods and refined on F^2 by full-matrix least-squares techniques. The analytical scattering factors[42] for neutral atoms were used throughout the analysis. Hydride atoms H(1) and H(2) were located from a difference-Fourier map and refined (x,y,z and U_{iso}). Hydrogen atoms were included using a riding model. There were two molecules of the formula-unit present, each was located on an inversion center at the hydride positions. There was one molecule of diethylether present. C(48) was disordered and included using multiple components with partial site-occupancy-factors. At convergence, wR2 = 0.0529 and Goof = 1.019 for 790 variables refined against 19335 data (0.74Å), R1 = 0.0229 for those 16608 data with $I > 2.0\sigma(I)$.

X-ray Data Collection, Structure Solution and Refinement for 30. A yellow crystal of approximate dimensions 0.079 x 0.138 x 0.293 mm was mounted on a glass fiber and transferred to a Bruker SMART APEX II diffractometer. The APEX2[43] program package was used to determine the unit-cell parameters and for data collection (30 sec/frame scan time for a sphere of diffraction data). The raw frame data was processed using SAINT[44] and SADABS[45] to yield the reflection data file. Subsequent calculations were carried out using the SHELXTL[46] program. The diffraction symmetry was 2/*m* and the systematic absences were consistent with the monoclinic space group $P2_1/c$ that was later determined to be correct.

The structure was solved by direct methods and refined on F^2 by full-matrix least-squares techniques. The analytical scattering factors[47] for neutral atoms were used throughout the analysis. Hydrogen atoms were included using a riding model. The molecule was polymeric repeating through the ring defined by atoms C(9)-C(13). At convergence, wR2 = 0.0702 and

Goof = 1.210 for 178 variables refined against 3604 data (0.82Å), R1 = 0.0278 for those 3262 data with I > 2.0σ(I).

Table 2.1. X-ray Data and Collection Parameters for $Cp'_3U(THF)$, **8-U(THF)**, [K(crypt)][Cp'_4U], **28-U**, [K(18-crown-6)(OEt_2)][($Cp'_3U)_2(\mu$-H)], **29** and Cp'_2Pb, **30**

Compound	**8-U(THF)**	**28-U**	**29**	**30**
Empirical Formula	$C_{28}H_{47}OSi_3U$	$C_{50}H_{88}KN_2O_6Si_4U$ • ½($C_4H_{10}O$)	$C_{68}H_{123}KO_8Si_6U_2$	$[C_{16}H_{26}PbSi_2]_\infty$
Temperature (K)	133(2)	88(2)	133(2)	143(2)
Crystal System	Orthorhombic	Triclinic	Triclinic	Monoclinic
Space Group	$Pna2_1$	$P\bar{1}$	$P\bar{1}$	$P2_1/c$
***a* (Å)**	13.1677(7)	13.9525(5)	11.4055(8)	8.9298(8)
***b* (Å)**	17.2087(9)	14.8015(6)	15.5800(10)	9.0844(8)
***c* (Å)**	13.4591(7)	17.2291(7)	24.5647(16)	23.550(2)
α (deg)	90	73.3154(4)	74.3416(8)	90
β (deg)	90	77.5696(4)	81.9956(8)	96.7424(11)
γ (deg)	90	63.1158(4)	77.7729(8)	90
Volume (Å^3)	3049.8(3)	3024.7(2)	4092.1(5)	1897.2(3)
Z	4	2	2	4
ρ_{calcd} (Mg/m^3)	1.572	1.361	1.422	1.687
μ (mm^{-1})	5.458	2.876	4.136	9.007
R1[a] ($I > 2.0\sigma$(I))	0.0142	0.0166	0.0229	0.0278
wR2 (all data)	0.0295	0.0419	0.0529	0.0702

[a]Definitions: $R1 = \Sigma||F_o| - |F_c||/\Sigma|F_o|$, $wR2 = [\Sigma w(F_o^2 - F_c^2)^2/\Sigma w(F_o^2)^2]^{1/2}$.

Goof = $S = [\Sigma[w(F_o^2-F_c^2)^2] / (n-p)]^{1/2}$ where n is the number of reflections and p is the total number of parameters refined.

RESULTS

New U^{II} Complexes. Synthesis of [M(chelate)][Cp′′$_3$U] (M = K, Na), 22-U to **25-U.** Addition of KC_8 under an atmosphere of argon or dinitrogen to a stirred dark green/brown THF solution of Cp′′$_3$U, **20-U**, and crypt at room temperature caused an immediate color change to black. After the reaction mixture was stirred for 4 min, solids were removed by filtration. The solvent was removed under reduced pressure to give a black oil that was triturated with hexane to give a black powder characterizd as [K(crypt)][Cp′′$_3$U], **22-U**. Despite numerous attempts, X-ray quality single crystals were not obtained. Repitition of the procudure using 18-crown-6 as a chelate gave a black powder after work up and was crystallized from THF/hexane. Black crystals of [K(18-crown-6)(THF)$_2$][Cp′′$_3$U], **23-U**, were isolated in 90% yield and crystallographically characterized, Figure 2.1.

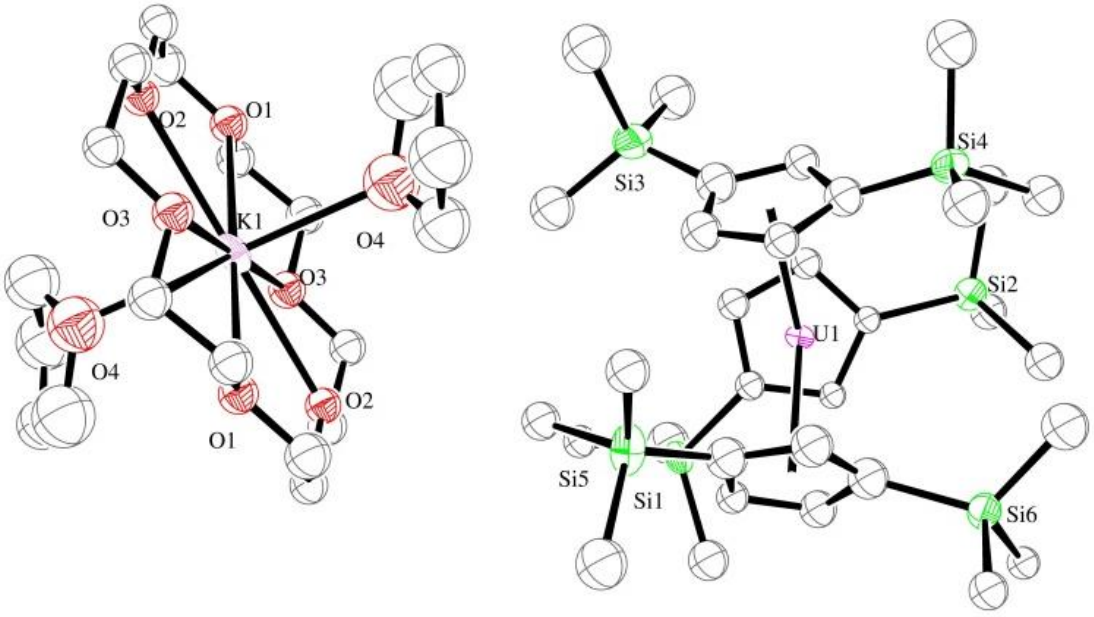

Figure 2.1. Connectivity structure of [K(18-crown-6)(THF)$_2$][Cp′′$_3$U], **23-U**, drawn at the 30% probability level with hydrogen atoms omitted for clarity.

Since the quality of the crystal structure of **23-U** did not allow a discussion of metrical parameters, the synthesis of a variant was pursued. Addition of solid **20-U** to a THF solution of 18-crown-6 stirred over a smear of sodium metal at room temperature also quickly generated a black solution. After 30 min, work-up of the reaction mixture provided black crystals of [Na(18-crown-6)$(THF)_2$][Cp''_3U], **24-U**, Figure 2.2. Unfortunately, crystallographic characterization of **24-U** showed high disorder in the Cp″ rings and, like **23-U**, detailed metrical data cannot be discussed. Sodium reduction of Cp''_3U in the presence of 12-crown-4 was also conducted and solids with properties consistent with [Na(12-crown-4)$_2$][Cp''_3U], **25-U**, were isolated, but provided no better crystallographic data. The reactions are summarized in Figure 2.3.

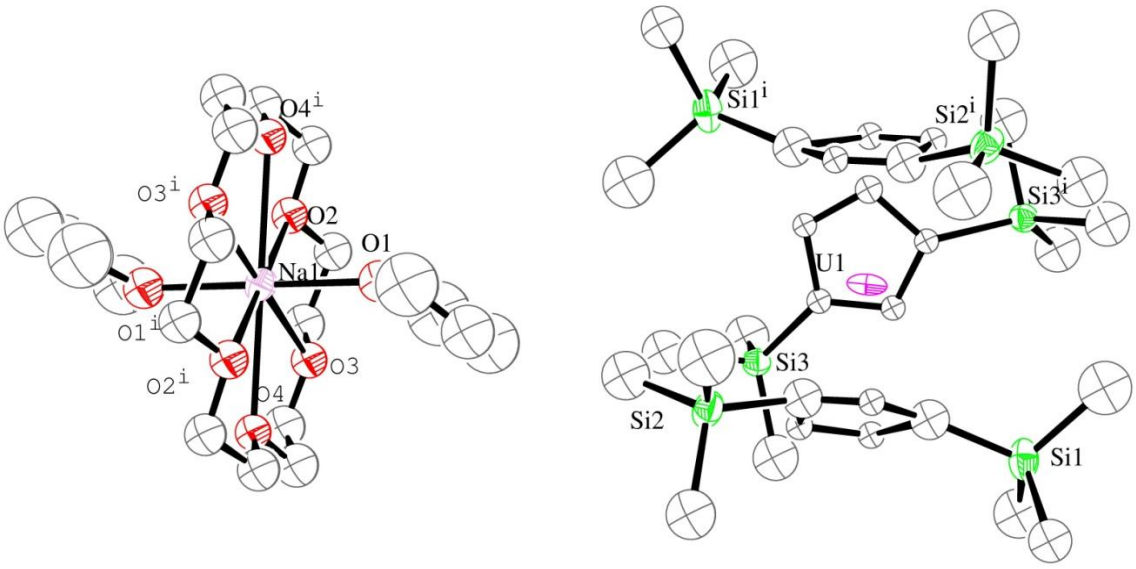

Figure 2.2. Connectivity structure of [Na(18-crown-6)$(THF)_2$][Cp''_3U], **24-U**, drawn at the 30% probability level. There is disorder that gives two sets of $(Cp''_3)^{3-}$ rings, one set of $(Cp''_3)^{3-}$ rings and hydrogen atoms have been omitted for clarity.

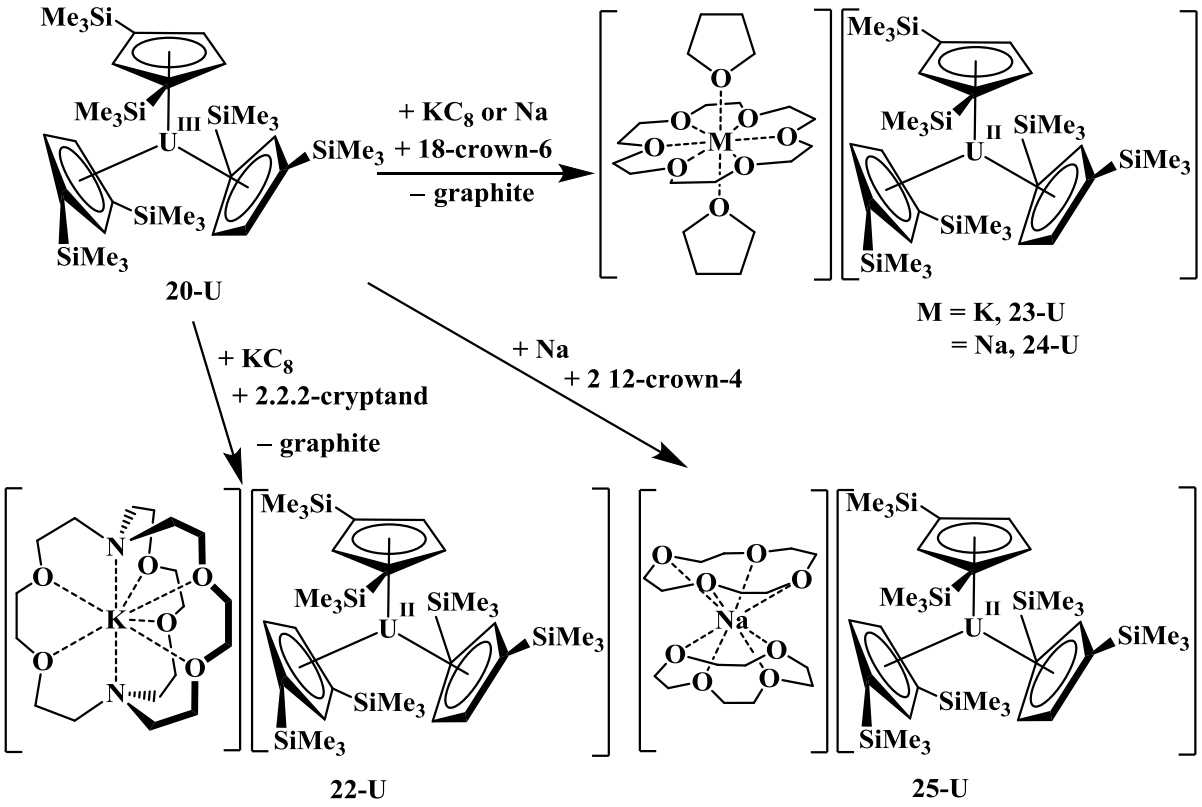

Figure 2.3. Summary for multiple syntheses of $(Cp''_3U)^-$, [K(crypt)][Cp''_3U], **22-U**, [M(18-crown-6)$(THF)_2$][Cp''_3U], (M = K, **23-U**; Na = **24-U**), and [Na(12-crown-$4)_2$][Cp''_3U], **25-U**.

Structural Data. The crystallographic data on **23-U** and **24-U** showed, in each case, a trigonal planar arrangement of the Cp″ ring centroids about the uranium center. The structure of **23-U** is not isomorphous with the thorium complex of the same formula, [K(18-crown-6)$(THF)_2$][Cp''_3Th], **23-Th**.[4] The $[K(18\text{-crown-6})(THF)_2]^+$ and $[Na(18\text{-crown-6})(THF)_2]^+$ cations in **23-U** and **24-U** are well-separated from the anion, showing no cation-Cp″ interaction, which contrasts with the rare earth complexes, [K(18-crown-6)][Cp'_3Ln] (Ln = Y, Ho, Er), in which the $[K(18\text{-crown-6})]^+$ cation is located next to one of the Cp′ rings.[5-6] Unfortunately, the crystal data were not of high enough quality for any additional analyses.

NMR Data. The ^{1}H NMR spectra of **22-U**, **23-U**, **24-U**, and **25-U** in THF-d_8 are nearly identical and show paramagnetically broadened resonances around δ −4 ppm for the $C_5H_3(SiMe_3)_2$ protons, and around 11 and −12 ppm for the $C_5H_3(SiMe_3)_2$ protons in a 1:2 ratio, respectively. There is less than 0.25 ppm difference in resonance shifts among the four complexes Figure 2.4. All of these resonances are shifted compared to the U^{III} precursor, **20-U**, in THF-d_8, which has the trimethylsilyl protons at δ −9 and the cyclopentadienyl protons at 20 and −6 ppm Figure 2.4.

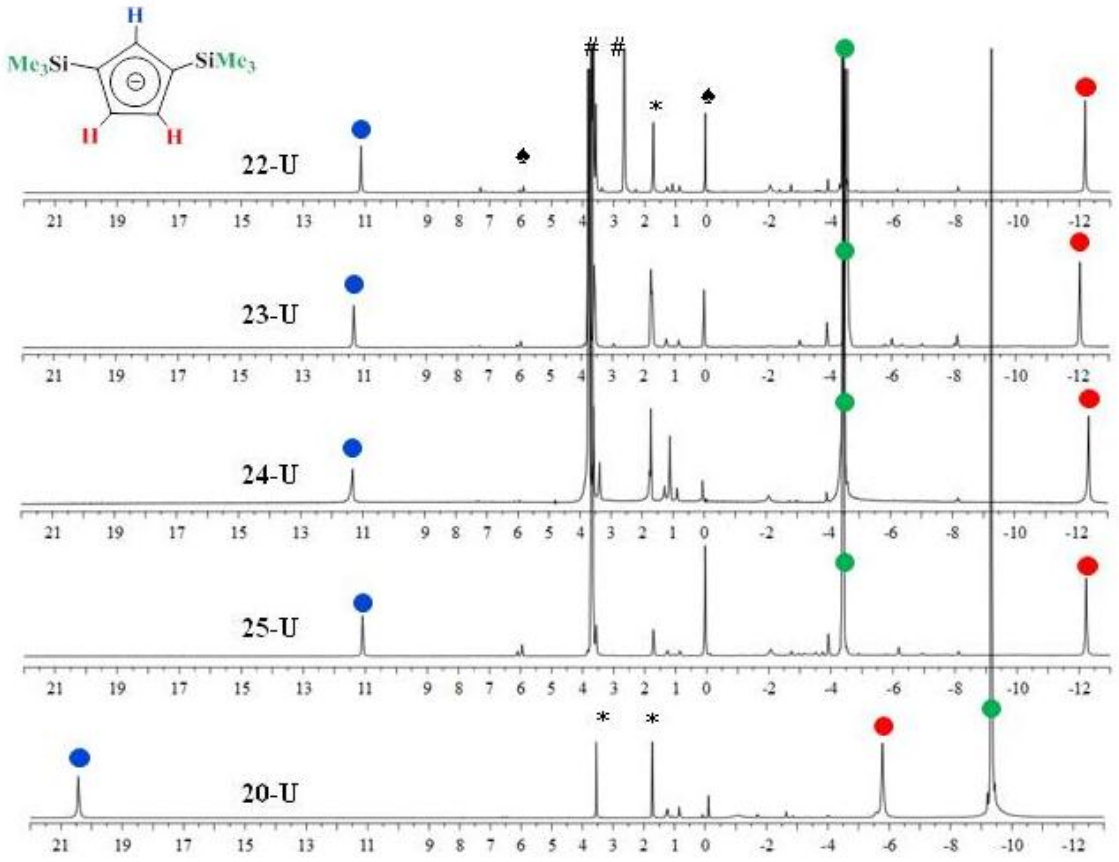

Figure 2.4. ^{1}H NMR spectra of **22-U**, **23-U**, **24-U**, **25-U**, and **20-U** in THF-d_8 at 298 K. The labeling scheme for the ligand is noted in the upper left corner, and the characters denote the following: # = chelate (18-crown-6, 12-crown-4 or 2.2.2-cryptand), * = residual protio solvent and ♠ = residual [M(chelate)][Cp″] ligand.

The greater thermal stability of the new U^{II} complexes allowed ^{29}Si NMR spectroscopy at room temperature for the first time on this new oxidation state. Previously, complex **21-U** was found to have a ^{29}Si resonance at δ −322.4 ppm at 170 K. The low temperature of this NMR experiment was necessary due to the limited thermal stability of **21-U**. The ^{29}Si NMR spectra of **22-U**, **23-U**, **24-U**, and **25-U** at room temperature contained broad ($\nu_{1/2} \geq 120$ Hz) resonances at δ −329.5; −327.3, −328.6 and −329.9 ppm, respectively. These are significantly shifted upfield from those of **20-U** in THF at δ −162.9 ppm[17] and are the most negative shifts ever observed for uranium complexes containing silicon.

When **23-U** and **20-U** were mixed together in an approximately 1:1 ratio, a single set of ^{1}H NMR resonances was observed with shifts intermediate between the resonances for the two isolated complexes. This suggests that on the NMR time scale there is electron exchange between the complexes of the U^{II} and U^{III} ions. Exchange of this type has been observed in non-aqueous systems with $U^{III/IV}$ cation/neutral and neutral/anion pairs[48-49] and has been examined for $U^{III/IV/V/VI}$ ions in aqueous solution.[50-52] The principal resonance assigned to the $SiMe_3$ units remains sharp at room temperature, but it becomes broad below −50 °C and becomes too broad to be unambiguously identified at −100 °C. Separate resonances were not observed at low temperature.

Optical Spectra. The UV/visible spectra of **20-U**, **21-U** and **22-U** in THF are shown in Figure 2.5. Due to the highly absorbing nature of compounds **21-U** and **22-U** to **25-U**, UV/vis samples were recorded as 1.5 mM solutions in 1 mm cuvettes. The spectra of **23-U**, **24-U** and **25-U** are nearly identical to that of **22-U**, Figure 2.6, and all of these are similar to that of **21-U**. The spectrum of **20-U** in THF is similar to those of **20-U** and **8-U** in hexane, but differs from that of **8-U** in THF because the latter compound forms a THF adduct, **8-U(THF)**, as confirmed by X-ray crystallography, see Figure 2.11, Tables 2.2 and 2.3 for structural details and Figures 2.12 and 2.13 for optical spectra on **8-U(THF)**.

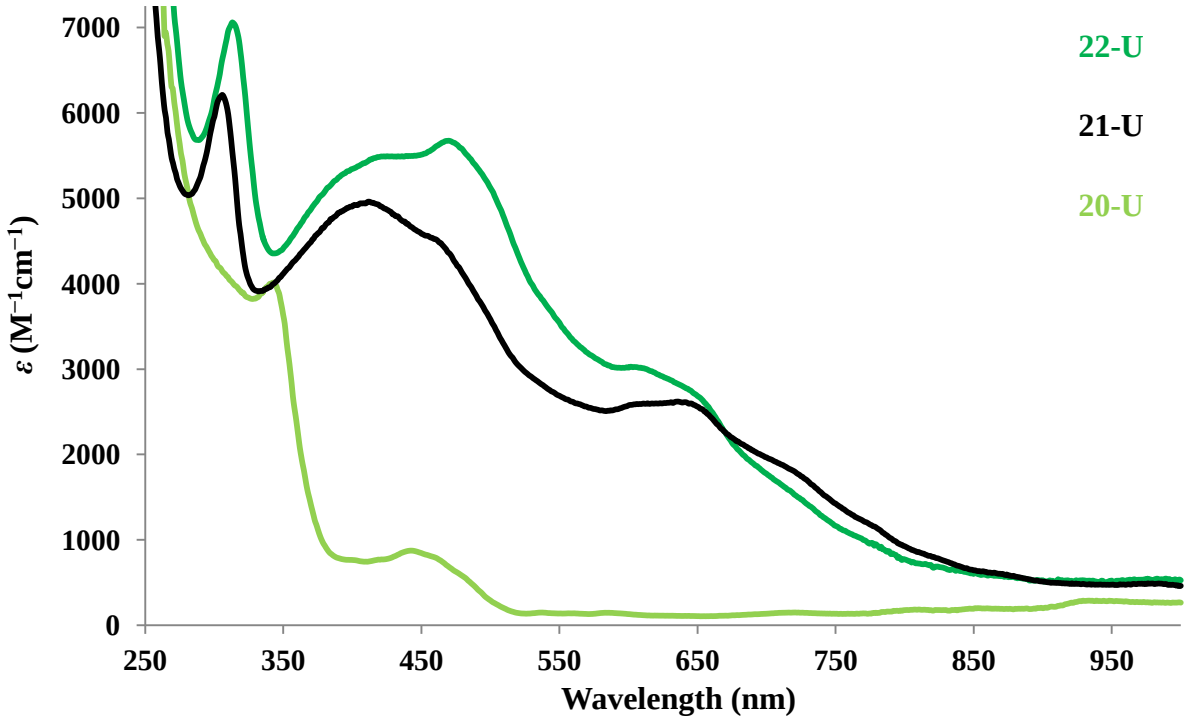

Figure 2.5. Experimental UV/vis spectra of [K(crypt)][Cp″$_3$U], **22-U** (dark green trace), [K(crypt)][Cp′$_3$U], **21-U** (black trace), and Cp″$_3$U, **20-U** (light green trace) in THF at 298 K.

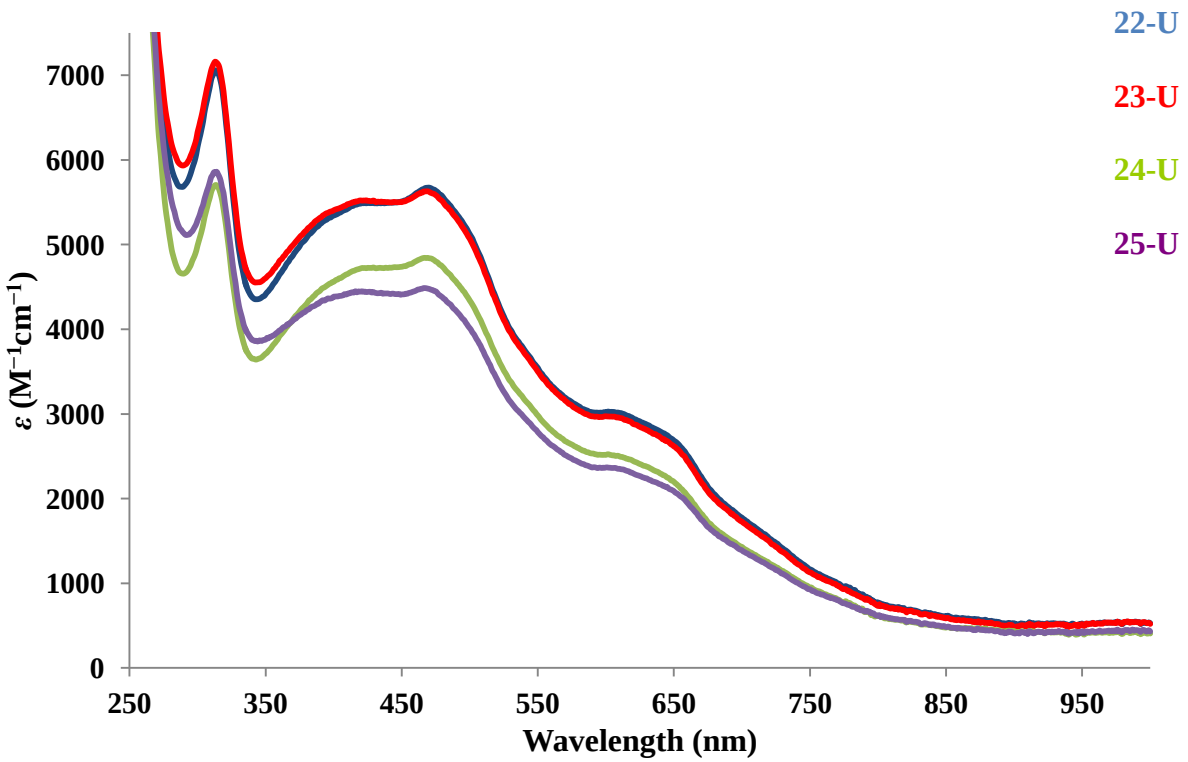

Figure 2.6. Experimental UV/vis spectra of **22-U** (blue trace), **23-U** (red trace), **24-U** (green trace) and **25-U** (purple trace) in THF at 298 K.

The 3000 to 7500 M^{-1} cm^{-1} extinction coefficients of the U^{II} complexes are much larger than those of the U^{III} compounds. This difference is similar to the larger intensities observed for other Ln^{II} and An^{II} complexes, [K(crypt)][Cp′$_3$Ln], **21-Ln** [Ln = Y, La, Ce, Pr, Nd, Gd, Tb, Dy, Ho, Er, Lu],[5-8] [K(crypt)][Cp″$_3$M] [M = La, **22-La**; Th, **22-Th**],[3-4] and **21-U**,[1] compared to their +3 analogs, Cp′$_3$Ln, **8-Ln**, Cp″$_3$La, **20-La**, Cp″$_3$Th, **20-Th**, and Cp′$_3$U, **8-U**, respectively.

Near infrared (NIR) spectra were also obtained on **21-U**, **22-U** and **20-U**, Figure 2.7 and Figure 2.8. NIR spectra were recorded in 1 cm cuvettes at 2-3 mM concentration for U^{II} and U^{III} complexes. Numerous absorptions were observed in the 900 – 1600 nm range which was limited by the highly absorbing nature of THF.[53] See Figure 2.8 for NIR spectra of **22-U**, **23-U**, and **24-U**.

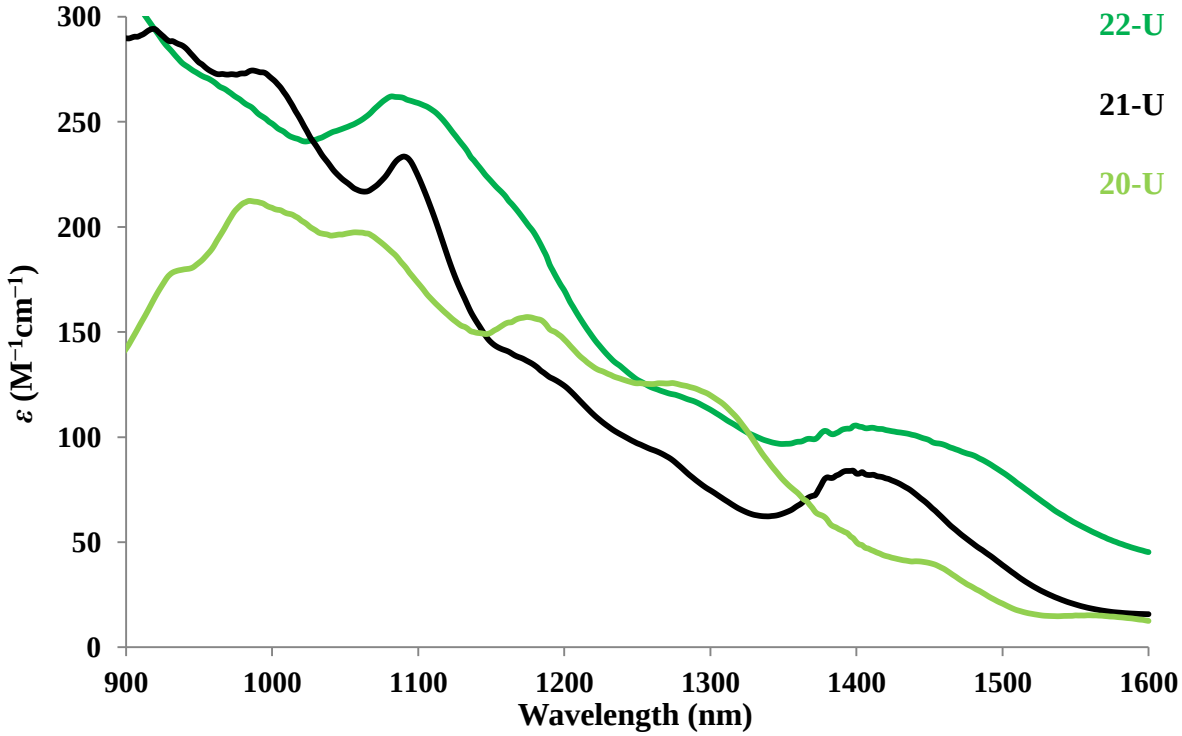

Figure 2.7. Experimental NIR spectra of [K(crypt)][Cp″$_3$U], **22-U** (dark green trace), [K(crypt)][Cp′$_3$U], **21-U** (black trace), and Cp″$_3$U, **20-U** (light green trace) in THF at 298 K.

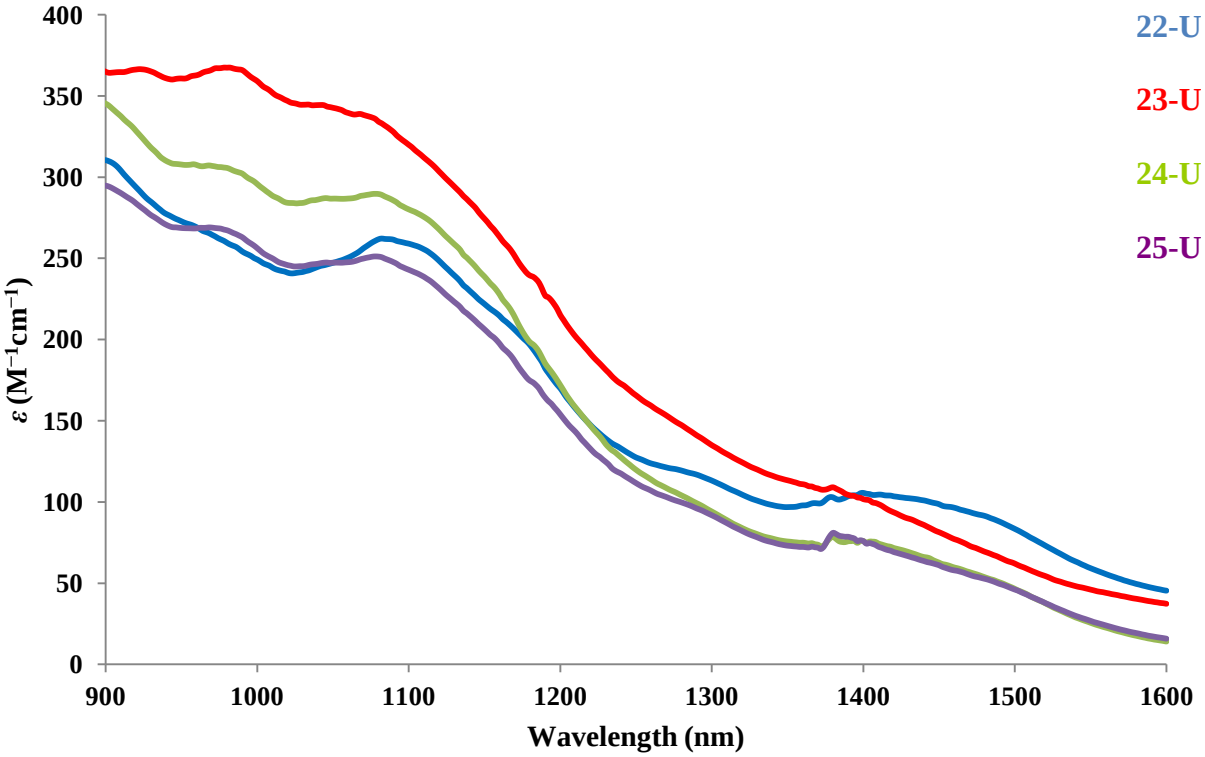

Figure 2.8. Experimental NIR spectra of **22-U** (blue trace), **23-U** (red trace), **24-U** (green trace) and **25-U** (purple trace) in THF at 298 K.

Magnetic Susceptibility. DC magnetic susceptibility data were collected at the University of California, Berkeley, by Katie R. Meihaus and Jeffrey R. Long for **20-U**, **21-U** and **22-U** over the temperature range 1.8 to 300 K under an applied field of 1000 Oe, Figure 2.9. At 300 K, the values of the molar magnetic susceptibility times temperature, $\chi_M T$, for **21-U** and **22-U** are 0.98 and 0.64 emu·K/mol, respectively. These are considerably lower than the room temperature $\chi_M T$ value of 1.33 emu·K/mol observed for the representative U^{III} complex, **8-U**, which is consistent with different oxidation states for **21-U** and **22-U**.[54] The data on **8-U** are similar to those on **20-U**: $\chi_M T$ = 1.38 emu·K/mol at 300 K and 0.51 emu·K/mol at 5 K.[55-57] Field-dependent $\chi_M T$ data for **21-U** (Figure 2.10, top) suggest that the larger moment is likely due to a temperature-independent paramagnetic contribution which is not exhibited by **22-U** (Figure 2.10, bottom). With decreasing temperature, $\chi_M T$ declines gradually for **21-U** and **22-U** and reaches values of 0.12 and 0.04 emu·K/mol, respectively, at 1.8 K.

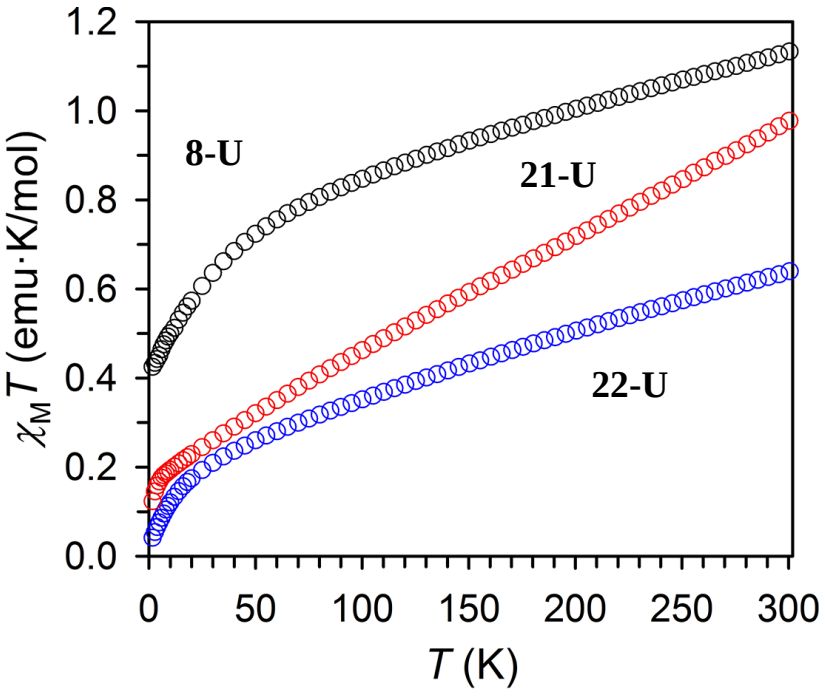

Figure 2.9. Experimental plot of the static molar magnetic susceptibility times temperature ($\chi_M T$) versus T collected at 0.1 T for **8-U** (black trace), **21-U** (red trace), and **22-U** (blue trace)

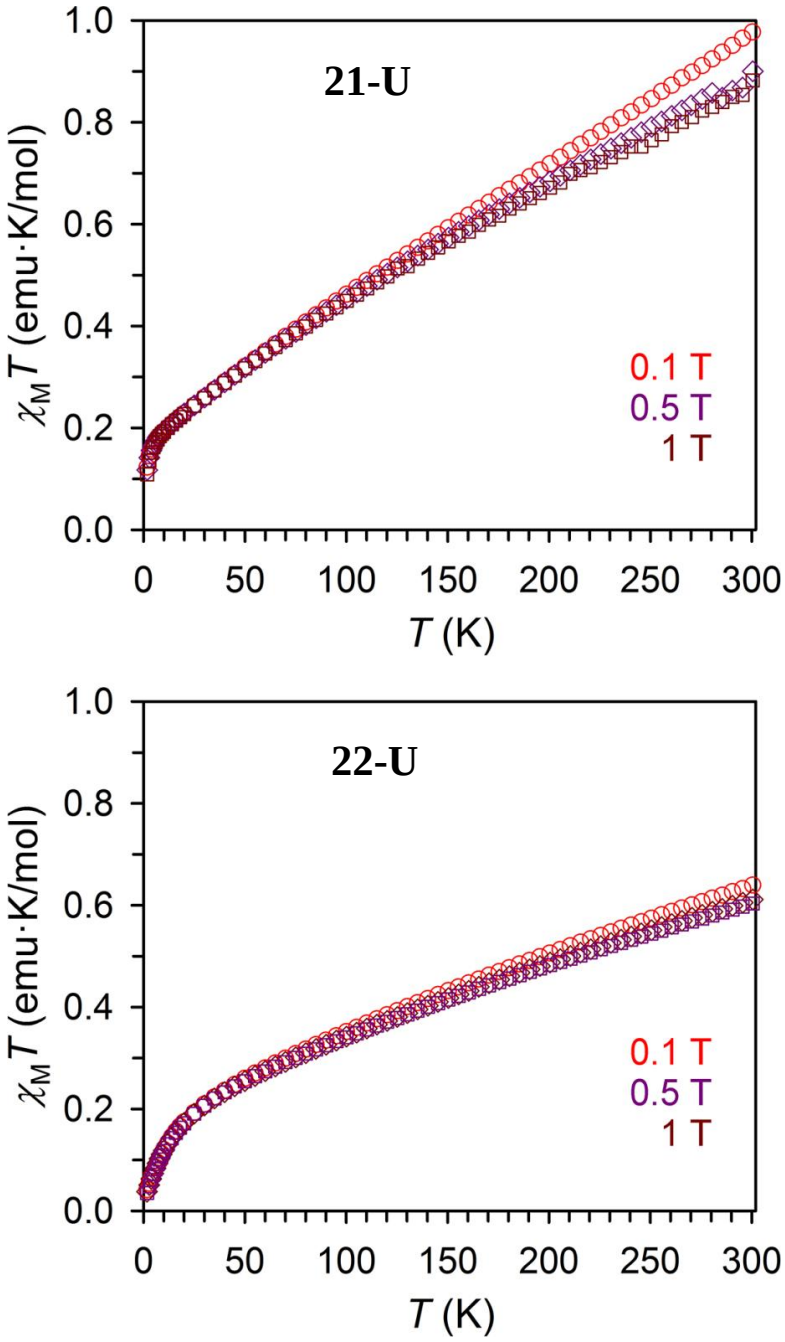

Figure 2.10. Experimental plot of the magnetic susceptibility times temperature ($\chi_M T$) versus temperature for **21-U** (top) **22-U** (bottom) collected at fields of 0.1 T (red circles), 0.5 T (purple diamonds), and 1 T (dark red squares). The pronounced linearity for **21-U** and greater field-dependence of $\chi_M T$ is suggestive of a more substantial temperature-independent paramagnetic contribution than for **22-U**.

Crystal Structure and Optical Spectroscopy of $Cp'_3U(THF)$, 8-U(THF). Addition of excess THF (0.5 mL) to a green Et_2O solution of **8-U** causes an immediate color change to dark red. Removal of volatiles and crystallization from Et_2O at –30 °C gives crystals of $Cp'_3U(THF)$, **8-U(THF)**, Figure 2.11.

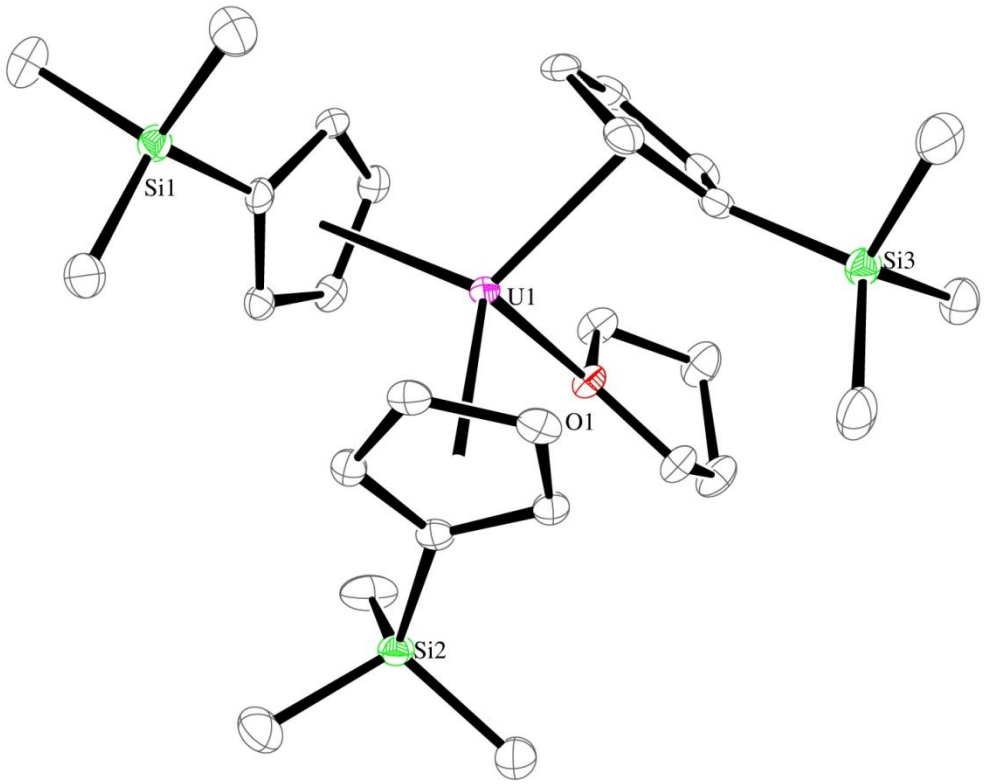

Figure 2.11. Thermal ellipsoid plot of $Cp'_3U(THF)$, **8-U(THF)**, drawn at the 50% probability level with hydrogen atoms omitted for clarity.

The structure of **8-U(THF)** shows an average U–(Cp′, centroid) distance of 2.544(8) Å, an U–O distance of 2.529(2) Å, and an average (Cp′, cent)–U–(Cp′, cent) angle of 117.3°. These values are comparable to $Cp_3U(THF)$, **31-U(THF)**, (Cp = C_5H_5)[58] and $(C_5Me_4H)_3U(THF)$, **32-U(THF)**,[59] Table 2.2. The U–O distance in $(C_5Me_4H)_3U(THF)$ is longer, but makes sense given the higher steric hindrance on $(C_5Me_4H)^-$. Other Cp'_3UL complexes have been reported, e.g. L

= CNEt,[60] pyridine,[61] lutidine,[61] pyrimidine[61] and dimethylpyrazine,[61] and these complexes display similar U–(cent) distances and (cent)–U–(cent) angles. However, the U–L distances range from 2.646(4)–2.688(7) Å, although the U–C distance in $Cp'_3U(CNEt)$ is comparable at 2.57(3) Å,[60] Table 2.3.

Table 2.2. Metrical Parameter Comparisons of $Cp'_3U(THF)$, **8-U(THF)**, With Other $(C_5R_5)_3U(THF)$ Complexes (cent = C_5R_5 Ring Centroid).

	U–(cent) avg(Å)	U–O (Å)	(cent)–U–(cent) avg (°)
8-U(THF)	2.544(8)	2.529(2)	117.3
31-U(THF)[58]	2.523	2.55(1)	117.6
32-U(THF)[59]	2.597	2.605(6)	116.8

Table 2.3. Metrical Parameter Comparisons of $Cp'_3U(THF)$, **8-U(THF)**, With Other $Cp'_3U–L$ Complexes (cent = Cp′ Ring Centroid).

L in $Cp'_3U–L$	U–L (Å)	U–(cent) avg(Å)	(cent)–U–L range (°)	(cent)–U–(cent) range (°)
THF**, 8-U(THF)**	2.529(2)	2.544(8)	96.3–102.6	115.7–118.2
CNEt[60]	2.57(3)	2.53	94.7–99.5	114.4–121.2
Pyridine[61]	2.683(8)	2.55(2)	96.4–100.9	114.5–118.9
Lutidine[61]	2.646(4)	2.55(2)	96.0–103.8	117.2–117.5
Pyrimidine[61]	2.688(7)	2.540(8)	94.9–102.9	115.6–119.0
dimethylpyrazine[61]	2.656(6)	2.54(2)	96.2–103.2	117.4–117.6

The ^1H and ^{29}Si NMR data on **8-U(THF)** have already been discussed in Chapter 1 and elsewhere.[17, 24] The UV/vis spectra of **8-U** and **20-U** in hexane show little difference, Figure 2.12. However the UV/vis spectra of **8-U(THF)** and **20-U in THF** show the changes in

absorptions upon coordination of a THF ligand to uranium, along with the noted color change. These changes in spectral features are also observed upon the same comparisons of the NIR spectra of **8-U** and **20-U** in hexane compared to **8-U(THF)** in THF, Figure 2.13. This suggests **20-U** does not coordinate THF, and is supported by the lack of change in ^{1}H and ^{29}Si NMR chemical shifts, Figure 2.4 and Chapter 1.[9, 17]

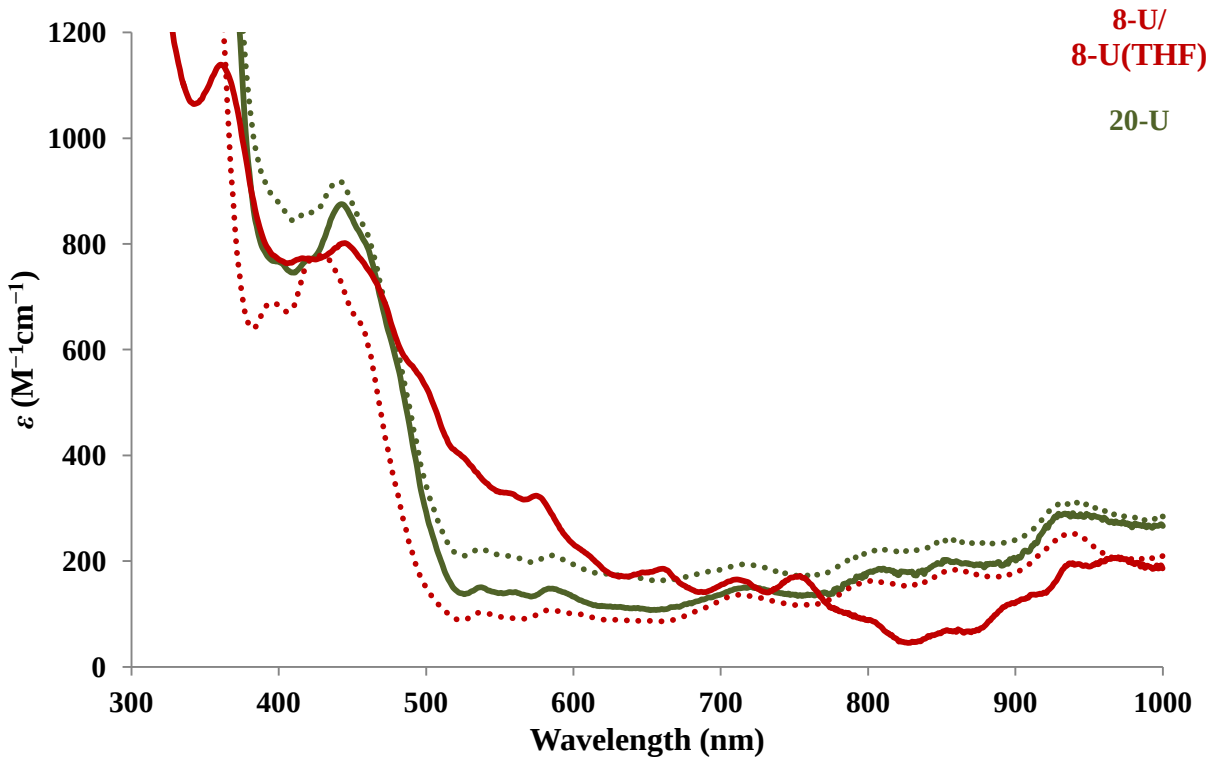

Figure 2.12. Experimental UV/vis spectra of **8-U/8-U(THF)** (red traces) and **20-U** (green traces) in THF (solid traces) and hexane (dotted traces) at 298 K.

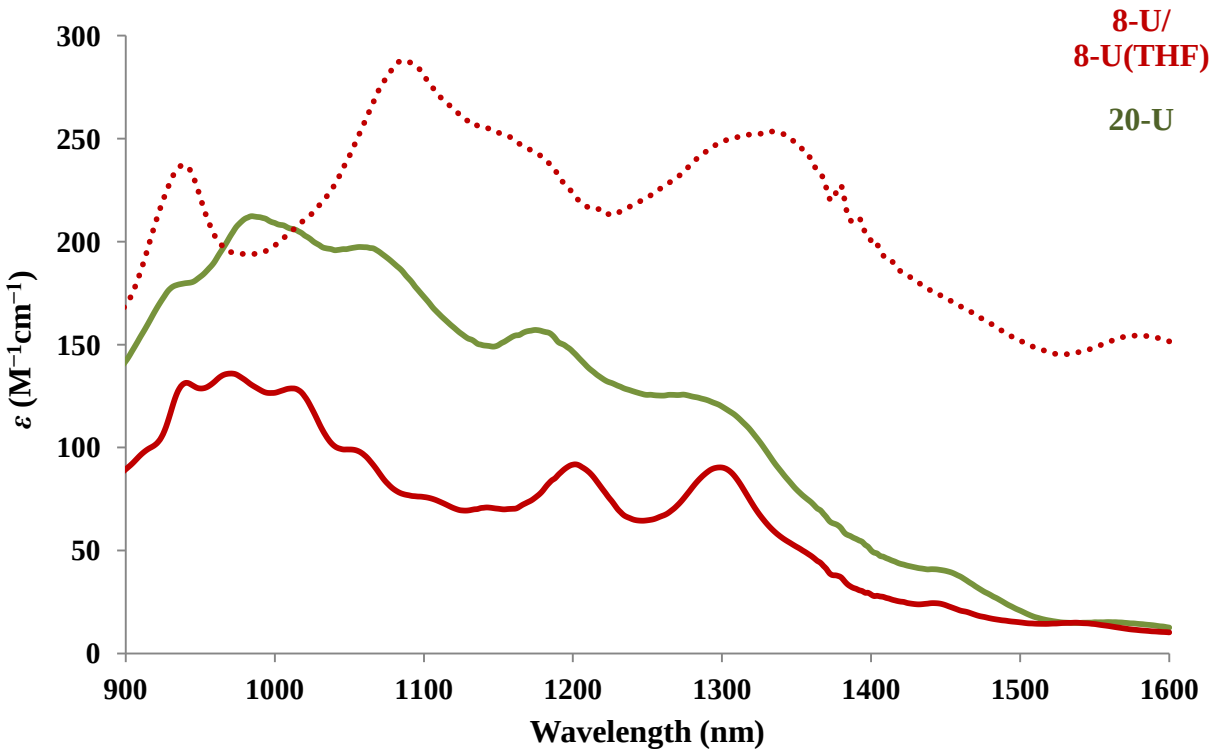

Figure 2.13. Experimental NIR spectra of **8-U/8-U(THF)** (red traces) and **20-U** (green trace) in THF (solid traces) and hexane (dotted trace) at 298 K, **20-U** in hexane overlays with **20-U** in THF and has been omitted for clarity.

Reactivity. Formation of a U^{III} Hydride Complex from 23-U. To make the claim that **21-U**, was the first unequivocal example of a U^{II} complex, it was necessary to characterize the corresponding U^{III} hydride, [K(crypt)][Cp′$_3$UH], **9**, to demonstrate that **21-U** did not contain a crystallographically undetected hydride.[1] This hydride was made in two ways: by adding KH to **8-U** in the presence of crypt and by reacting **21-U** with H_2.[1] When similar experiments were attempted with **22-U**, an analogous compound, [K(crypt)][Cp″$_3$UH], **27-U**, was formed, but it was isolated as a red oil. The analogous 18-crown-6 compound, [K(18-crown-6)(THF)$_2$][Cp″$_3$UH], **26**, was synthesized from **23-U** and isolated as a dark red solid.

Complex **26** can be generated in several ways, Figure 2.14. Addition of KH and 18-crown-6 to a solution of **20-U** in THF quickly forms a dark red solution from which **26** could be isolated as a dark red powder. The compound has a UV/vis spectrum in THF at 298 K that is nearly identical to that of [K(crypt)][Cp′$_3$UH], **9**,[1] Figure 2.15. Complex **26** can also be synthesized from the reaction of **23-U** with H_2 (1 atm) or with $PhSiH_3$, Scheme 2. Both methods are preferable to the KH reaction which requires crystallization to obtain pure product. The H_2 reaction works best for large scale preparations and the $PhSiH_3$ reaction is most convenient for smaller reactions. After it was determined that **23-U** reacts with $PhSiH_3$, the analogous reaction with **21-U** was conducted to show that it reacts similarly to form compound **9**,[1] eq 2.4.

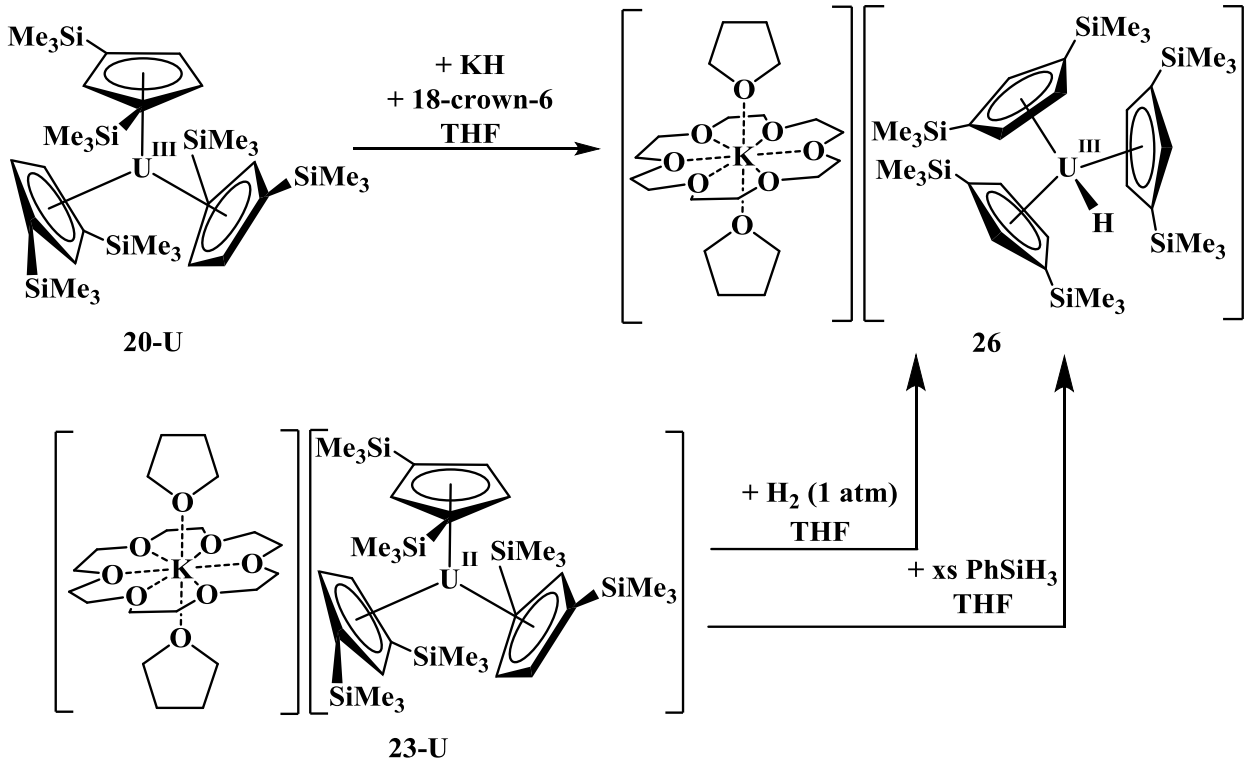

Figure 2.14. Multiple syntheses of [K(18-crown-6)(THF)$_2$][Cp″$_3$UH], **26**.

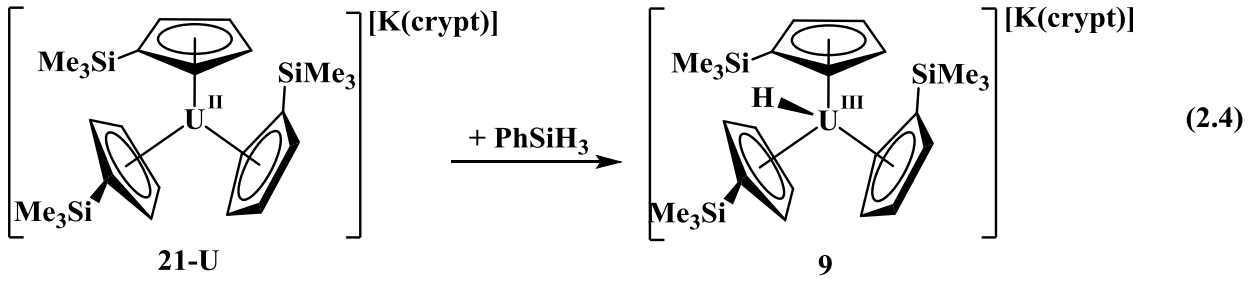

The ^{1}H and ^{13}C NMR spectra of **3** show paramagnetically broadened peaks ranging from 8 to −4 ppm in the ^{1}H NMR spectrum, which is consistent with two of the three resonances expected for the $[C_5H_3(SiMe_3)_2]^{1-}$ ligand. In addition, there is a broad resonance in the ^{1}H NMR spectrum at δ 601 ppm ($\nu_{1/2}$ = 250 Hz), which is consistent with other monomeric anionic U^{III} hydride compounds (δ U–H, $\nu_{1/2}$), **9** (560, 175 Hz),[1] [Na(18-crown-6)(THF)$_2$][Cp′$_3$UH] (547, 220 Hz),[49, 62] [Na(18-crown-6)(THF)$_2$][(C$_5$H$_4$^{t}Bu)$_3$UH] (521, 160 Hz).[62] When the reaction of

22-U with H_2 was repeated with D_2, the product had an identical ^{1}H NMR spectrum except the resonance at 601 ppm was no longer present. The ^{2}H NMR spectrum contained only one resonance at 601 ppm. No H/D exchange was observed on the NMR time scale.

Cyclooctatetraene Reactions. Reactions of the U^{II} complexes **21-U** and **23-U** with 1,3,5,7-cyclooctatetraene, C_8H_8, were conducted to determine if they could function as two electron reductants and generate a $(C_8H_8)^{2-}$ product as was found for Th^{II}, eq 2.5.[4] A cold THF

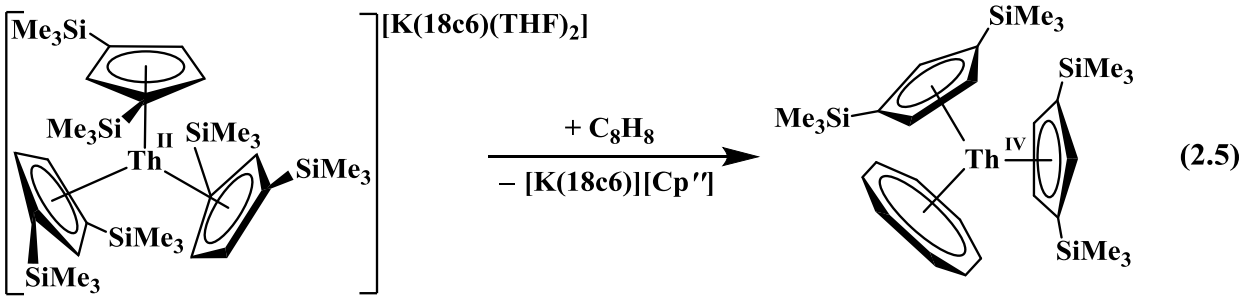

23-Th

solution of **21-U** reacted with C_8H_8 over one hour and crystallization of the crude mixture yielded $(C_8H_8)_2U$ by ^{1}H NMR analysis[19] and unit cell determination.[21] The brown-red mother liquor was reduced in volume and crystallization from THF/Et_2O yielded a mixture of [K(crypt)][Cp′] and [K(crypt)][Cp′$_4$U], **28-U**, both of which were identified by X-ray crystallography and NMR spectroscopy,[22] eq 2.6, Figure 2.15. This result contrasts with the reaction of **8-U** with C_8H_8 which forms Cp′$_2$U(C_8H_8).[63]

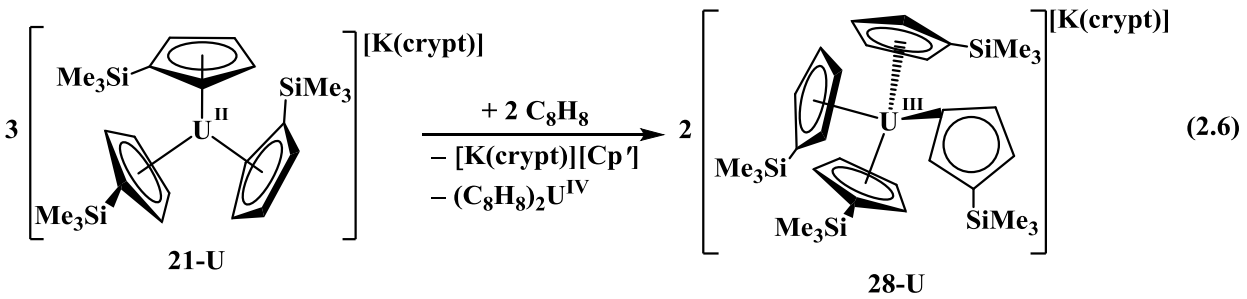

21-U **28-U**

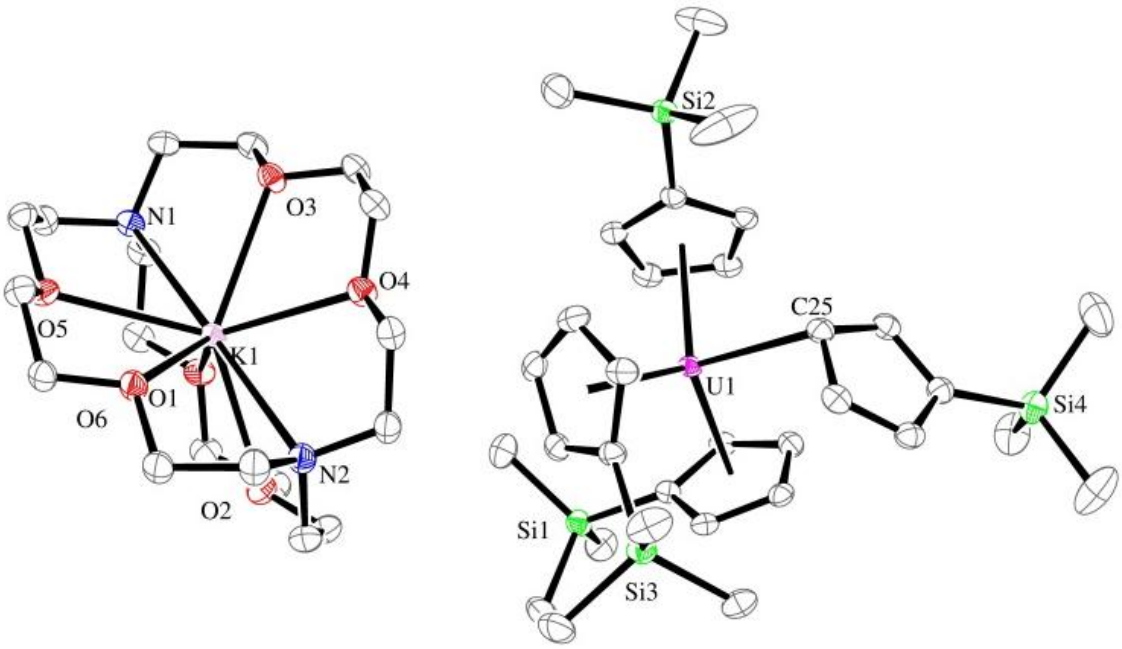

Figure 2.15. Thermal ellipsoid plot of [K(crypt)][Cp′$_4$U], **28-U**, drawn at the 50% probability level with hydrogen atoms and a co-crystallized diethyl ether molecule omitted for clarity.

The reaction of **23-U** with excess C_8H_8 also produces $(C_8H_8)_2U$ and the potassium salt of the cyclopentadienyl ligand, [K(18-crown-6)][Cp″]. However with this larger cyclopentadienyl ring, the neutral tris(cyclopentadienyl) U^{III} complex, **20-U**, was isolated, eq 2.7, instead of the tetrakis(cyclopentadienyl) product shown in eq 2.6. Reaction of either **21-U** or **22-U** with one equivalent of C_8H_8 produced the same products in reduced yield. Reaction of **20-U** with C_8H_8 gave no reaction at room temperature over 1 week.

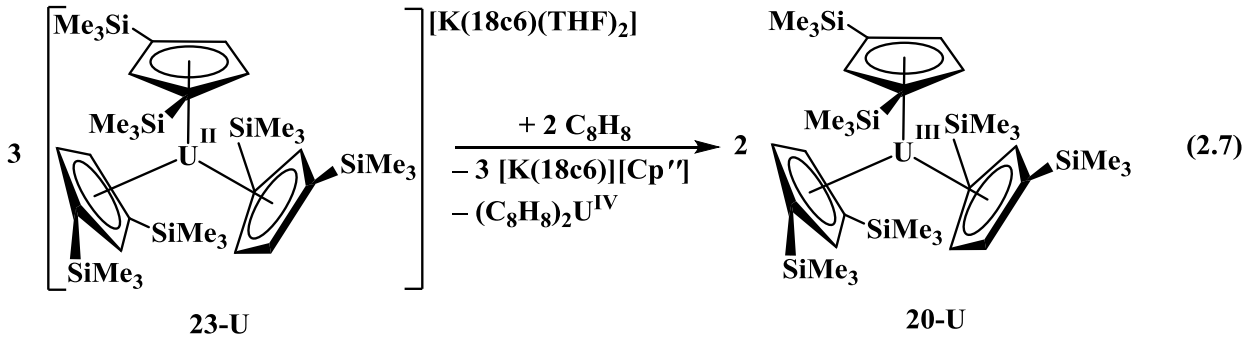

Complex **28-U** is the first crystallographically characterized example of a tetrakis(cyclopentadienyl) U^{III} complex, although several U^{IV} examples have been synthesized through direct synthesis or isolation as a side product: Cp_4U,[64-67] $(C_5H_4Me)_4U$,[68-70] $[C_5H_4CH(Me)CH_2C_5H_4]UCp_2$,[71] $(C_5H_4PPh_2)_4U$[72] and $(C_5H_4PPh_2)_2U(C_5H_4PPh_2)_2M(CO)_4$ (M = Cr, Mo).[72] The only crystallographically characterized tetrakis(cyclopentadienyl) U^{IV} complex is Cp_4U.[73-74]

An yttrium analog of **28-U** is known, namely [K(crypt)][Cp′$_4$Y], **28-Y**,[22] that is not isomorphous but has the same coordination environment containing three η^5-Cp′ rings and one η^1-Cp′ ligand. The ^{1}H NMR spectrum of **28-U** contains a single set of resonances from room temperature down to −90 °C, Figure 2.16, suggesting that all of the rings are η^5 -bound in solution. This contrasts with **28-Y** that shows two different $SiMe_3$ resonances in a 1:3 ratio at low temperature.[22] The 2.56(2) Å U–(η^5-Cp′ centroid) average distance and the 2.776(2) Å U–C25(η^1-Cp′) distance in **28-U** are numerically larger than those in the yttrium complex, 2.48(1) and 2.680(2) Å,[22] respectively, which is consistent with the larger ionic radius of U^{III} vs Y^{III} (1.025 Å vs. 0.900 Å, respectively, using the six coordinate Shannon radii).[75]

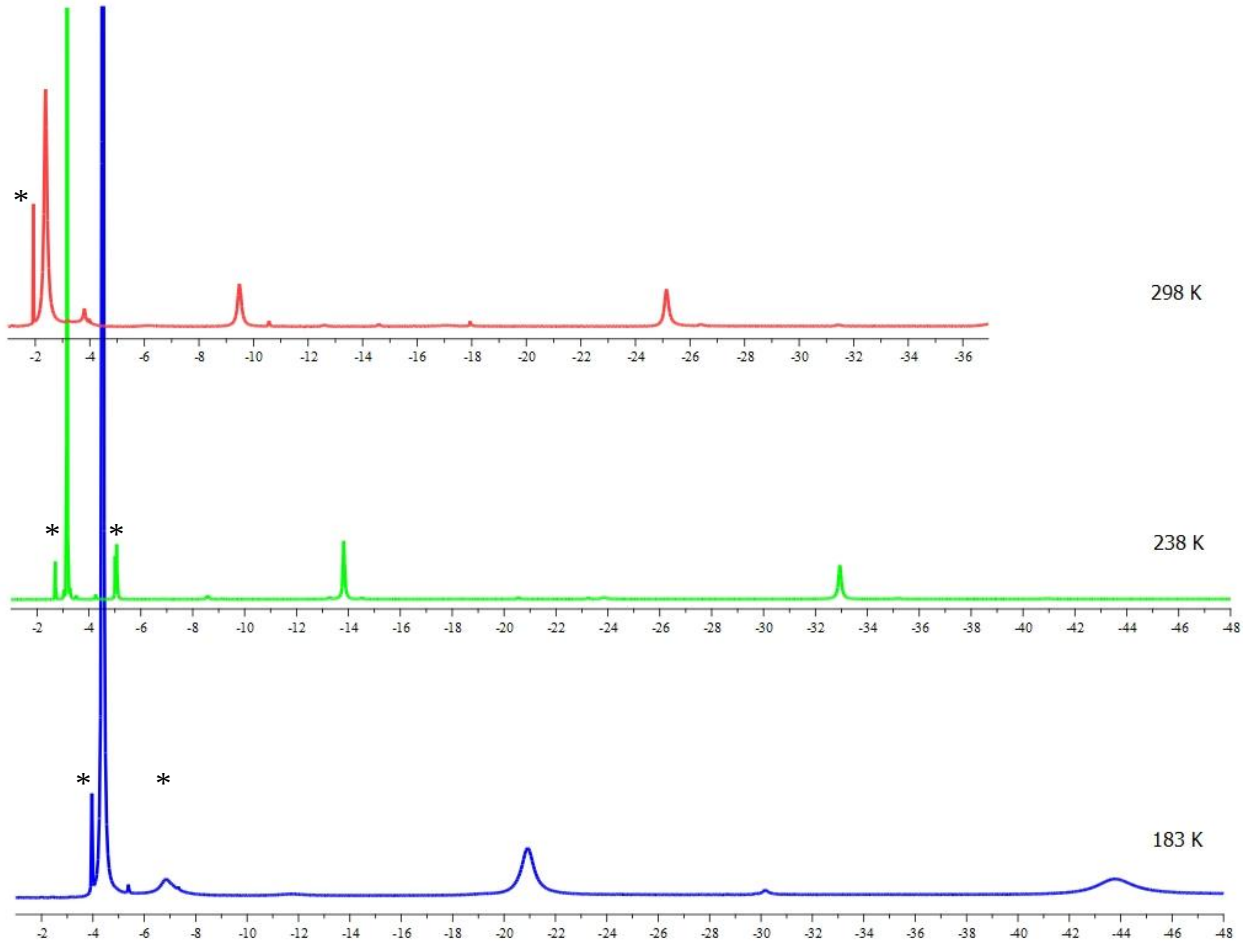

Figure 2.16. Variable temperature ^{1}H NMR spectra of [K(crypt)][Cp′$_4$U], **28-U**, in THF-d_8, at 298 K (top, red trace), 238 K (middle, green trace), and 183 K (blue, bottom trace), minor impurities denoted by *.

Independent Syntheses of [K(crypt)][Cp′$_4$U], 28-U. To obtain useful quantities of **28-U** in pure form for full characterization, direct syntheses were pursued. Complex **28-U** can be made in 85% yield from crypt, KCp′, and **8-U** in THF. It can also be obtained in 64% yield by reacting the U^{II} complex **21-U**, with Cp′$_2$Pb in THF, Figure 2.17.

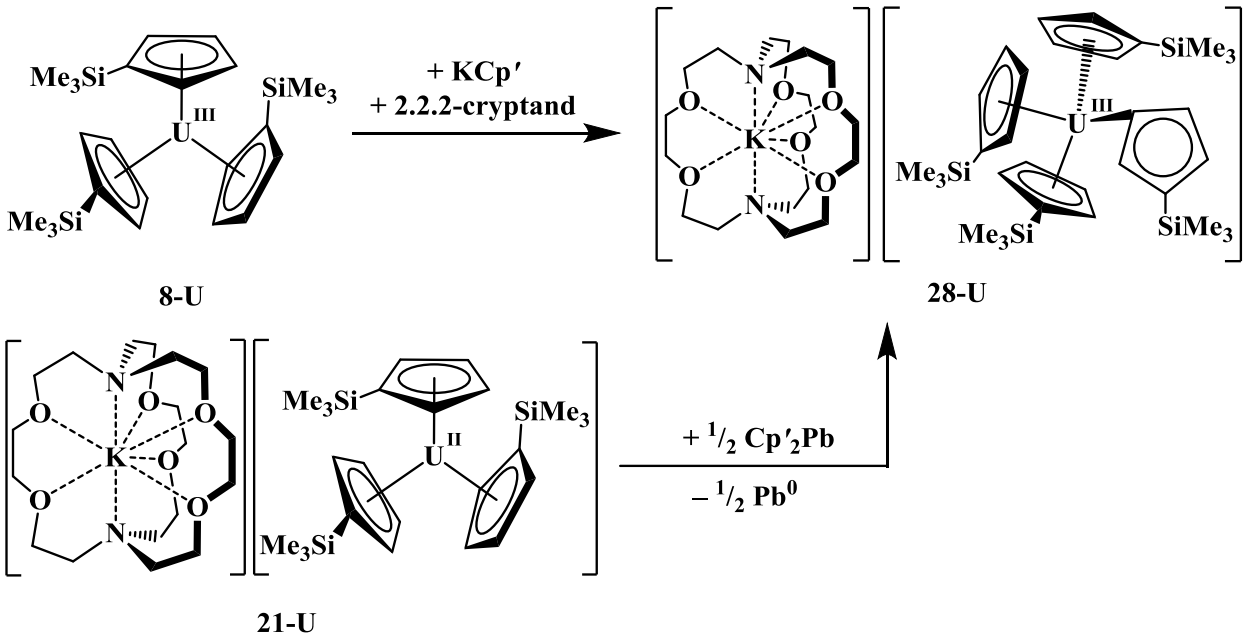

Figure 2.17. Multiple syntheses of [K(crypt)][Cp′$_4$U], **28-U**.

Synthesis and Characterization of Cp′$_2$Pb, 30. The Cp′$_2$Pb, **30**, used in Figure 2.17 was obtained by a modification of the previous reported synthesis from $PbCl_2$ and KCp′ with vacuum distillation and a 7% yield.[25] In this study, bright yellow **30** was obtained in 86% yield from PbI_2 and KCp′ in THF and extraction into hexane. **30** was characterized by ^{1}H, ^{13}C, ^{29}Si and ^{209}Pb NMR spectroscopies and show the expected number of signals and are similar to the analogous Cp″ compound, Cp″$_2$Pb.[76] X-ray crystallography and shows an infinite polymeric zigzag chain, which is similar to that of Cp_2Pb, Figure 2.18.[77-79] .

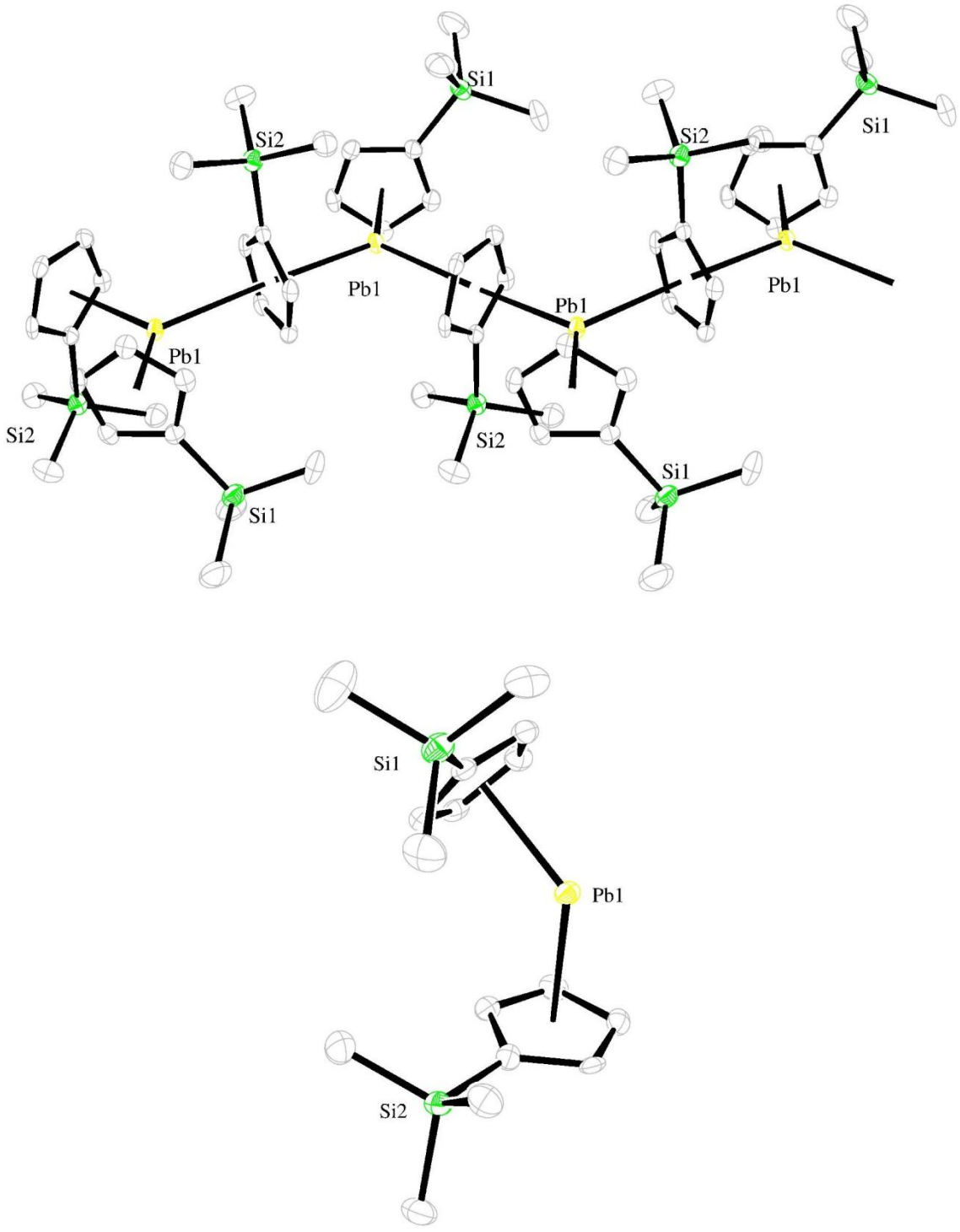

Figure 2.18. Thermal ellipsoid plot of Cp'_2Pb, **30**, tetramer (top) and **30** monomer (bottom), drawn at the 50% probability level with hydrogen atoms omitted for clarity.

The Pb–(terminal Cp′ ring centroid) distance is 2.468 Å, which is equivalent to Cp_2Pb at 2.47 Å.[77-79] The two bridging Cp′ rings in **30** show Pb–(bridging Cp′ cent) distances of 2.700 and 2.840 Å, again comparable to Cp_2Pb at 2.72 and 2.89 Å. These Pb–(Cp′ cent) distances are similar to other crystallographically characterized bis(cyclopentadienyl)lead compounds, although they are monomeric, Cp''_2Pb (2.459, 2.505 Å),[76] $(C_5Me_4H)_2Pb$ (2.420, 2.638 Å),[80] $(C_5Me_5)_2Pb$ (2.480, 2.623 Å),[81] $[C_5(CH_2Ph)_5]_2Pb$ (2.499, 2.607 Å),[82] $(C_5H_2{}^iPr_3)_2Pb$ (2.470 Å),[83] and $[C_5Me_4(SiMe_2{}^tBu)]_2Pb$ (2.460 Å).[84-85] The Cp'_t–Pb–Cp'_b (Cp'_t = terminal Cp′ ring, Cp'_b = bridging Cp′ ring) angle is 123.2°, while the Cp'_t–Pb–$Cp'_{b'}$ ($Cp'_{b'}$ = symmetry equivalent bridging Cp′ ring) angle is 126.4° and the Cp'_b–Pb–$Cp'_{b'}$ angle is 110.2°, similar to Cp_2Pb at 123°, all other $Cp^x{}_2Pb$ compounds have Cp^x–Pb–Cp^x angles that range from 139.7° for $(C_5Me_4H)_2Pb$[80] to 180° for $(C_5H_2{}^iPr_3)_2Pb$[83] and $[C_5Me_4(SiMe_2{}^tBu)]_2Pb$.[84-85]

Decomposition Studies of 21-U vs. 22-U. It was reported that **21-U** decomposes in THF at room temperature with first order kinetics and a $t_{½}$ of 1.5 h as measured in 3 mM solutions,[1] but the mechanism of the decomposition is not known. Decomposition studies were conducted on **22-U** and **23-U** to see how they compared with **21-U**. Visually, both Cp″ complexes display much greater thermal stability than **21-U** since they maintain their intense U^{II} colors at room temperature over several days. The complexes **22-U** and **23-U** complexes also differ from **21-U** in that they turn light yellow-brown rather than dark red upon decomposition (see below). Quantitative measurements were done by UV/vis spectroscopy monitoring the reduction of the absorption at λ = 470 nm. The data collected from scans taken every 15 min over 17 h using 1.5 mM solutions appear to be first order with respect to **22-U** and **23-U** with $t_{½}$ of 20(1) and 15(1) h respectively, Figure 2.19.

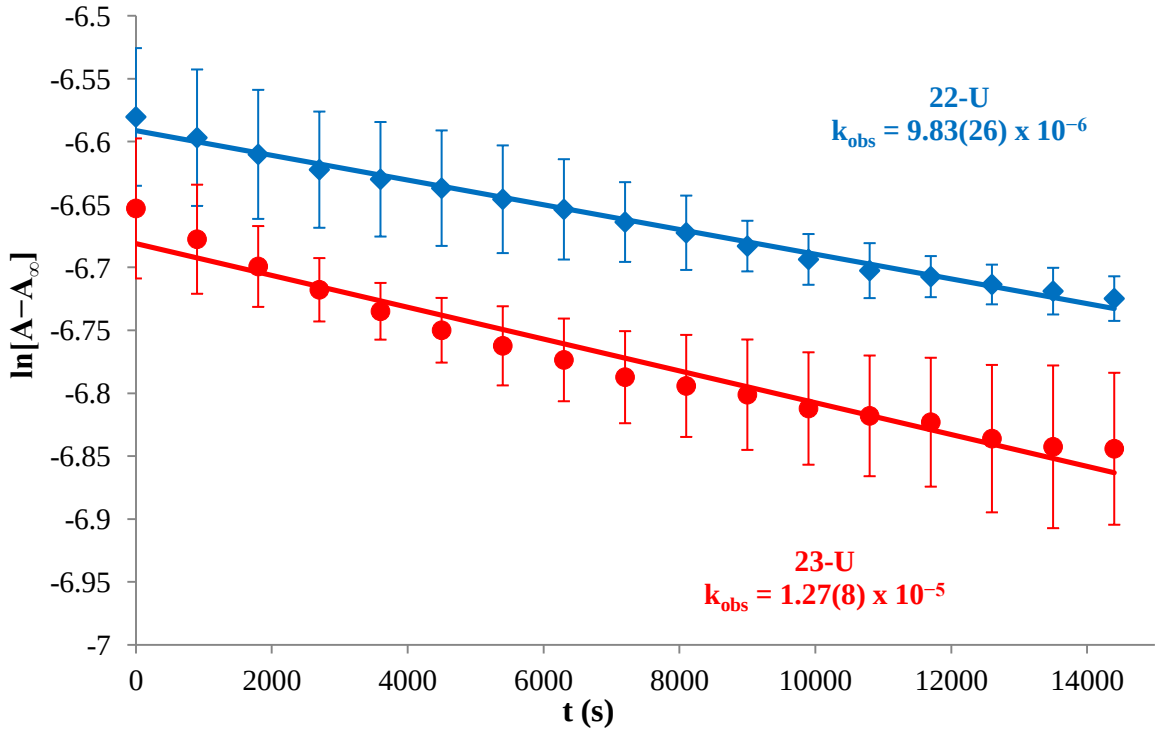

Figure 2.19. Decrease in absorbance at λ = 470 nm for **22-U** (blue diamonds) and **23-U** (red circles), recorded in THF at 298 K in 15 min intervals with error bars indicating 3σ range.

Decomposition of the sodium salts, **24-U** and **25-U**, was also examined by UV/vis spectroscopy, but these complexes appear to be more complicated since the data fit neither first nor second order models. These sodium salts also have higher thermal stability than **21-U**, as solutions of the sodium salts maintain their U^{II} color for days standing at room temperature.

In the course of studying the thermal stability of these complexes, a synthesis of the 18-crown-6 analog of **21-U**, namely "[K(18-crown-6)$(THF)_2$][Cp'_3U]," gave an isolable decomposition product. Potassium-graphite reduction of **8-U** gave a dark green color, consistent with the formation of "[Cp'_3U]$^-$" but the sample quickly turned dark red, consistent with the decomposition of **21-U**. The solution was placed in a −30 °C freezer and yielded a crystallographically–characterizable decomposition product identified as the bimetallic U^{III}

hydride [K(18-crown-6)(OEt_2)][($Cp'_3U)_2$(μ–H)], **29**, Figure 2.20, and 2.21 and Table 2.4. The origin of the hydride is unknown, but is likely the solvent.[76, 86] This complex is similar to the previously identified bridging hydrides, $(THF)_2Na(Cp_3U)_2$(μ–H)[87] and [Na(18-crown-6)$(THF)_2$][($Cp'_3U)_2$(μ–H)].[62] Complex **29** displays a linear U–H–U unit surrounded by staggered Cp′ rings. A similar arrangement was observed in [Na(18-crown-6)$(THF)_2$][($Cp'_3U)_2$(μ–H)],[62] although the hydride was not located. This type of staggered ring structure and linear core was also observed in Cp'_3U–O–UCp'_3.[88]

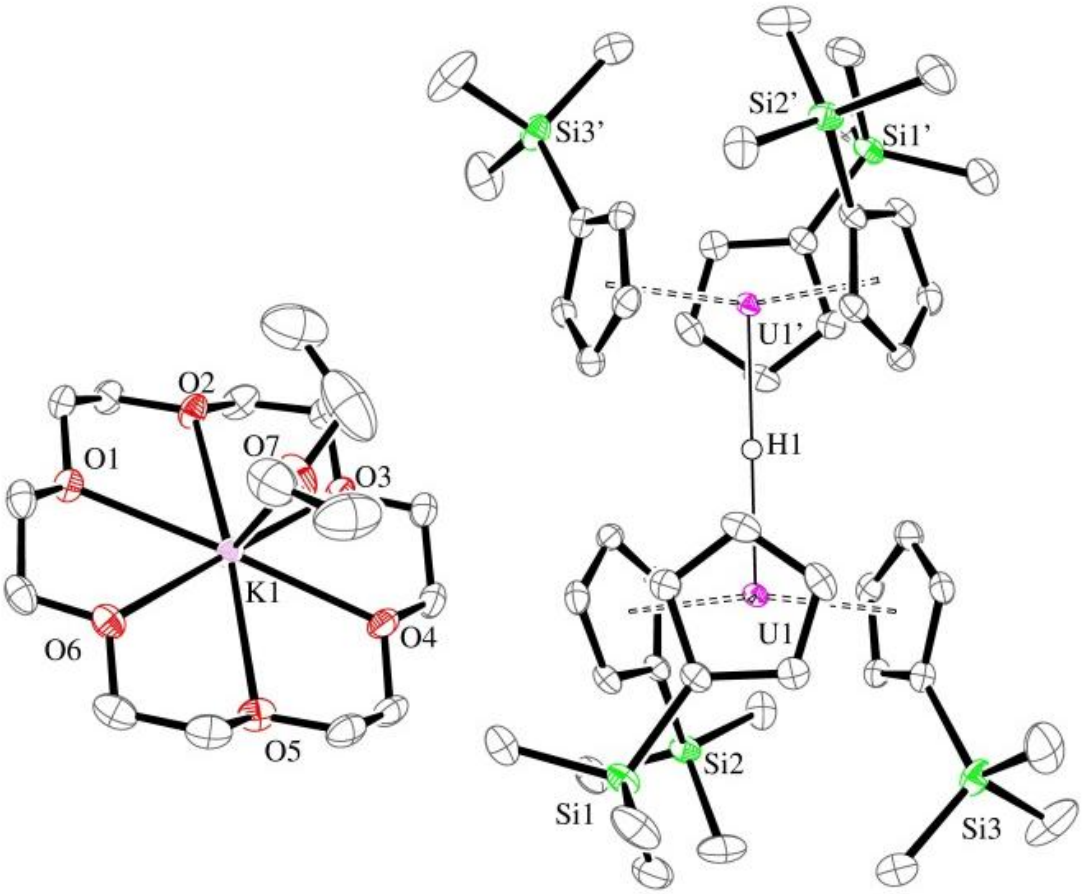

Figure 2.20. Thermal ellipsoid plot of [K(18-crown-6)(OEt_2)][($Cp'_3U)_2$(μ–H)], **29**, drawn at the 50% probability level with all hydrogen atoms, except H1, a co-crystallized diethyl ether molecule omitted for clarity. Only one of the two crystallographically independent units have been depicted.

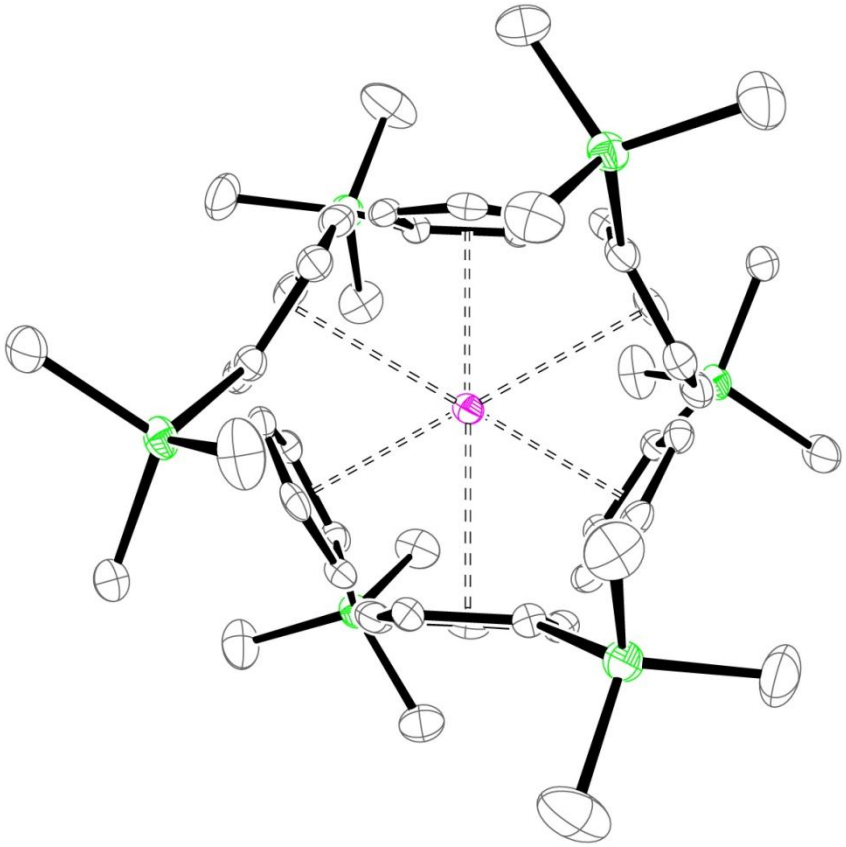

Figure 2.21. Thermal ellipsoid plot of anionic portion of $[(Cp'_3U)_2(\mu\text{–}H)]^-$, **29**, as viewed down the U–H–U axis, drawn at the 50% probability level with the $[K(18\text{-crown-6})(OEt_2)]^+$ cation, all hydrogen atoms, except H1, and a co-crystallized diethyl ether molecule omitted for clarity. Only one of the two crystallographically independent units have been depicted.

Table 2.4. Metrical Parameter Comparisons of [K(18-crown-6)(OEt_2)][$Cp'_3U–H–UCp'_3$], **29**,* With Other [$Cp^x_3U–H–UCp^x_3$]$^-$ Complexes. ***29** Has Two Crystallographically Independent Units.

	29	[Na(18c6)$(THF)_2$] [$(Cp'_3U)_2(\mu\text{-H})$][62]	$(THF)_2Na(Cp_3U)_2$ $(\mu\text{-H})$[87]
U-cent avg (Å)	2.560(8) 2.555(4)	2.56(9)	2.53(3)
U-H (Å)	2.24(1) 2.25(1)	-	2 2.4
U···U (Å)	4.4857(3) 4.4910(3)	4.4638(4)	4.403(2)
cent–U–cent avg (°)	119.1(6) 119.0(5)	119(1)	118(1)
U–H–U (°)	180 180	-	160

DISCUSSION

The synthesis and isolation of **22-U**, and **23-U**, by reduction of **20-U** demonstrates that the generation of cyclopentadienyl U^{II} complexes is not limited to the Cp′ ligand in **21-U**. The fact that **23-U**, and **24-U**, can be synthesized demonstrates that the reduction of U^{III} to U^{II} in molecular complexes can be accomplished with Na (−2.7 V vs SHE) as well as by K (−2.9 V vs SHE) and that the countercations for these anionic complexes can contain Na^+ as well as K^+ ions. These studies also show that alkali metal reduction of **20-U** to generate $(Cp''_3U)^-$ does not form reduced dinitrogen products. This is similar to the reduction of **20-La** to form **22-La** which can be done under N_2.[3, 5] Complexes **21-U**, **22-U** and **23-U** have the U^{II} center surrounded by three cyclopentadienyl rings, a coordination geometry that has been a common structural feature for

new M^{II} ions of the lanthanides and actinides, eq 2.1 and 2.3.[1, 3-8] The only other coordination environment observed for these ions is the arene tris(aryloxide) ligand system in [K(crypt)]{[(^{Ad,Me}ArO)$_3$mes]U}, eq 2.2.[2]

In general, the Cp″ complexes **22-U** to **25-U** are more thermally stable than the Cp′ complex **21-U** which makes both synthesis and characterization less difficult. In contrast to the synthesis of **21-U** that requires low temperatures from start to finish, the first order $t_{1/2}$ values of 20 h and 15 h for **22-U** and **23-U**, respectively, allow the syntheses to be done at room temperature. This enhanced stability also allows the ^{29}Si NMR spectra to be obtained at room temperature instead of at −103 °C as previously necessary for **21-U**, as described in Chapter 1.[17] The −322 ppm shift originally found for **21-U** at low temperature was the lowest shift ever observed in the ^{29}Si NMR spectrum of a uranium complex. The −329, −327, −329 and −330 ppm shifts observed for **22-U**, **23-U**, **24-U** and **25-U**, respectively, are consistent with this low value observed for **21-U** and fit with the observed trend for +4, +3, and +2 uranium complexes that the shifts become increasingly negative as the oxidation state decreases.[17]

Although the complexes **22-U** to **25-U** are more thermally stable than **21-U**, their spectroscopic and magnetic properties are similar. Both **21-U** and **22-U** to **25-U** have UV/vis spectra, Figures 2.5 and 2.6, with intensities much higher than those of the trivalent analogs, **20-U** and **8-U**/**8-U(THF)**, respectively. The NIR spectra of **21-U** and **22-U** to **25-U** also have a similar appearance, Figures 2.7 and 2.8.

The similarities extend to the magnetic susceptibility of **21-U** and **22-U**. Variable-temperature data collected at 0.1 T reveal room temperature $\chi_M T$ values of 0.98 and 0.64 emu·K/mol, respectively. Both values are lower than the value of 1.33 emu·K/mol found for the U^{III} precursor, **8-U** (theoretical value for a $5f^3$ ion, 1.64 emu·K/mol). The lower magnetic

susceptibilities of **21-U** and **22-U** are consistent with the presence of a different oxidation state from **8-U**.[54]

The magnetic data on **21-U** and **22-U** can be evaluated using the $5f^3\ 6d^1$ electron configuration for the U^{II} ion as postulated for **21-U** on the basis of DFT calculations and UV/visible spectroscopy, with the 6*d* orbital having primarily d_{z^2} character.[1] Using LS coupling as a first approximation and assuming a $5f^3\ 6d_{z^2}{}^1$ configuration, the theoretical room temperature $\chi_M T$ value is 0.9 emu·K/mol. The 0.98 emu·K/mol value measured for **21-U** is a good match. However, an LS coupling model predicts the same theoretical $\chi_M T$ value for a $5f^4$ configuration. Hence, no conclusions on electron configuration can be drawn from the magnetic data. Moreover, the room temperature value of $\chi_M T$ for **22-U** agrees well with the room temperature $\chi_M T$ value of 0.63 emu·K/mol (1 T) reported for the divalent uranium complex [K(crypt)]{[(^{Ad,Me}ArO)$_3$mes]U}, which is stated to have a $5f^4$ configuration.[2] The larger $\chi_M T$ value at 300 K for **21-U** compared to **22-U** and to [K(crypt)]{[(^{Ad,Me}ArO)$_3$mes]U} appears to arise from a temperature-independent paramagnetic contribution identified by field-dependent $\chi_M T$ data**,** Figure 2.10. The gradual decline in $\chi_M T$ for **21-U** and **22-U** with decreasing temperature and the 1.8 K values of $\chi_M T$, 0.12 emu·K/mol and 0.04 emu·K/mol, respectively, are similar to those of K(crypt)]{[(^{Ad,Me}ArO)$_3$mes]U}, which exhibited a $\chi_M T$ of 0.07 emu·K/mol at 2 K.[2]

It is challenging to conjecture on the electronic configuration using magnetic susceptibility data alone, since LS coupling affords an imperfect model for complexes wherein covalency might be a mitigating factor in metal-ligand interactions. In addition, this model predicts the same theoretical $\chi_M T$ value for a $5f^3\ 6d_{z^2}{}^1$ and a $5f^4$ configuration. However, in

conjunction with reported data on **21-U**,[1] and reported magnetic data for the series **21-Ln**,[89] these magnetic data are consistent with a $5f^3\ 6d^1$ electron configuration in the case of **21-U** and **22-U**.

Reactivity studies on **21-U** and **23-U** show that they each react with both H_2 and $PhSiH_3$ to make the U^{III} hydrides, **9** and **26**, respectively, while the respective trivalent compounds **8-U** and **20-U** do not react with H_2. The existence of **26** as a distinct complex from **23-U**, is evidence that the crystal structures of the $(Cp''_3U)^{1-}$ anions, **23-U** and **24-U**, contain U^{II} and not $(U^{III}–H)^{2+}$. The formation of the bridged U^{III} hydride, **29**, in the decomposition of an 18-crown-6 salt of $(Cp'_3U)^{1-}$ suggests there are other routes to make uranium hydrides from these U^{II} compounds. Lappert has found hydride products in attempts to make Y^{II}, La^{II} and Ce^{II} complexes.[76, 86]

Complexes **21-U** and **23-U** reduce 1,3,5,7-cyclooctatetraene to $(C_8H_8)^{2-}$ and form the extensively studied U^{IV} complex, uranocene $(C_8H_8)_2U$.[19, 21, 90-94] This U^{II} reactivity differs from that of the Th^{II} analog, **23-Th**, in which the $(C_8H_8)^{2-}$ reduction product retains cyclopentadienyl ligands, $Cp''_2Th(C_8H_8)$, eq 2.5.[4] It also differs from the reactivity of the U^{III} complexes, **8-U** and **20-U**. The former reacts with C_8H_8 to form $Cp'_2U(C_8H_8)$[63] and the latter does not react.

In the cyclooctatetraene reactions, both U^{II} and Th^{II} effect the two electron reduction of C_8H_8 to $(C_8H_8)^{2-}$ and the formation of U^{IV} products that are observed consistent with $An^{II} \rightarrow An^{IV} + 2\ e^-$ half-reactions (An = U, Th). However, the uranium reactions are more complicated since U^{III} complexes are formed as byproducts. In the case of U^{II} with Cp′, this byproduct is formed as the tetrakis(cyclopentadienyl) complex, **28-U**. An analogous tetrakis(cyclopentadienyl) complex apparently is not favored with the larger Cp″ ligand and the byproduct is the tris(cyclopentadienyl) complex **20-U**. In each of these cases, these U^{III} products indicate that some $U^{II} \rightarrow U^{III} + e^-$ processes are also occurring. Since U^{III} is more accessible than Th^{III}, it is possible that these one electron processes will be more facile with U^{II} than with

Th^{II} complexes. Another difference between Th and U is the larger size of Th^{IV} compared to U^{IV}, 1.21 vs. 1.17 Å, respectively, for 12-coordinate radii[75] $Cp''_2U(C_8H_8)$ would be more sterically crowded than $Cp''_2Th(C_8H_8)$ is.[95]

The origin of the greater stability of $(Cp''_3U)^{1-}$, vs **21-U**, is not clear. The larger $(Cp'')^{1-}$ ligand does provide more steric protection of the metal center. In addition, the di–silyl substituted ligand could reduce the electron density on the metal center if the $SiMe_3$ group is electron withdrawing with respect to H in this system.[86, 96-99] In any case, the observed greater reactivity of **21-U** vs **22-U** to **25-U** is consistent with data on U^{III} analogs where more reactivity has been reported for **8-U** than for **20-U**.[23, 60-63, 88, 100-108]

CONCLUSIONS

Crystallographically characterizable complexes of U^{II} are accessible not only using the mono-silyl Cp′ ligand as found previously with **21-U**, but also with the sterically bulkier di–silyl Cp″ ligand. The new examples of U^{II} complexes, **22-U**, **23-U**, **24-U,** and **25-U**, demonstrate that sodium metal can be used as a reductant and a variety of countercations will form isolable complexes. The complexes **22-U** to **25-U** also show that U^{II} compounds more thermally stable than **21-U** can be synthesized. The magnetic susceptibility data on **21-U** and **22-U** are similar as are the UV/vis/NIR and ^{29}Si NMR spectra and are consistent with the +2 oxidation state for uranium. Complexes **21-U** and **23-U** react with H_2 and $PhSiH_3$ to form U^{III} hydrides which establishes that the U^{II} complexes are not $(U^{III}–H)^{2+}$ compounds. Cyclooctatetraene is reduced to $(C_8H_8)^{2-}$ by **21-U** and **23-U**, a formal two electron redox process, but the presence of U^{III} byproducts, **28-U** and **20-U**, suggest that one electron pathways may also be traversed in these reactions. A difference in reactivity between **21-U** and **23-U** is that in the sterically bulkier Cp″

system, the tetrakis(cyclopentadienyl) byproduct does not form. The existence of the U^{II} anion, $(Cp''_3U)^{1-}$, demonstrates that, along with $(Cp'_3U)^{1-}$ and the Meyer complex, [K(crypt)]{[(^{Ad,Me}ArO)$_3$mes]U}, there are at least three coordination environments that can be used to investigate the chemistry of this new oxidation state of uranium.

REFERENCES

(1) MacDonald, M. R.; Fieser, M. E.; Bates, J. E.; Ziller, J. W.; Furche, F.; Evans, W. J., *J. Am. Chem. Soc.* **2013,** *135*, 13310-13313.

(2) La Pierre, H. S.; Scheurer, A.; Heinemann, F. W.; Hieringer, W.; Meyer, K., *Angew. Chem., Int, Ed.,* **2014,** *53*, 7158-7162.

(3) Hitchcock, P. B.; Lappert, M. F.; Maron, L.; Protchenko, A. V., *Angew. Chem., Int. Ed.,* **2008,** *47*, 1488-1491.

(4) Langeslay, R. R.; Fieser, M. E.; Ziller, J. W.; Furche, F.; Evans, W. J., *Chem. Sci*. **2015,** *6*, 517-521.

(5) MacDonald, M. R.; Ziller, J. W.; Evans, W. J., *J. Am. Chem. Soc.* **2011,** *133*, 15914-15917.

(6) MacDonald, M. R.; Bates, J. E.; Fieser, M. E.; Ziller, J. W.; Furche, F.; Evans, W. J., *J. Am. Chem. Soc.* **2012,** *134*, 8420-8423.

(7) MacDonald, M. R.; Bates, J. E.; Ziller, J. W.; Furche, F.; Evans, W. J., *J. Am. Chem. Soc.* **2013,** *135*, 9857-9868.

(8) Fieser, M. E.; MacDonald, M. R.; Krull, B. T.; Bates, J. E.; Ziller, J. W.; Furche, F.; Evans, W. J., *J. Am. Chem. Soc.* **2015,** *137*, 369-382.

(9) Windorff, C. J.; MacDonald, M. R.; Meihaus, K. R.; Ziller, J. W.; Long, J. R.; Evans William, J., *Chem. Eur. J.* **2016,** *22*, 772-782.

(10) Bain, G. A.; Berry, J. F., *J. Chem. Educ.* **2008,** *85*, 532.

(11) In lieu of a correction for newly discovered U(II), the uranium correction for **21-U** and **22-U** used was that of U(III).

(12) Evans, D. F., *J. Chem. Soc.* **1959**, 2003-2005.

(13) Evans, D. F.; Fazakerley, G. V.; Phillips, R. F., *J. Chem. Soc. A* **1971**, 1931-1934.

(14) Schubert, E. M., *J. Chem. Educ.* **1992,** *69*, 62.

(15) Peterson, J. K.; MacDonald, M. R.; Ziller, J. W.; Evans, W. J., *Organometallics* **2013,** *32*, 2625-2631.

(16) Carmichael, C. D.; Jones, N. A.; Arnold, P. L., *Inorg. Chem.* **2008,** *47*, 8577-8579.

(17) Windorff, C. J.; Evans, W. J., *Organometallics* **2014,** *33*, 3786-3791.

(18) Bergbreiter, D. E.; Killough, J. M., *J. Am. Chem. Soc.* **1978,** *100*, 2126-2134.

(19) Edelstein, N.; Lamar, G. N.; Mares, F.; Streitwieser Jr, A., *Chem. Phys. Lett.* **1971,** *8*, 399-402.

(20) Fischer, R. D., *Organometallics of the f-elements*. D. Reidel Pub. Co.: Boston, 1979.

(21) Zalkin, A.; Raymond, K. N., *J. Am. Chem. Soc.* **1969,** *91*, 5667-5668.

(22) Kotyk, C. M.; MacDonald, M. R.; Ziller, J. W.; Evans, W. J., *Organometallics* **2015,** *34*, 2287-2295.

(23) del Mar Conejo, M.; Parry, J. S.; Carmona, E.; Schultz, M.; Brennann, J. G.; Beshouri, S. M.; Andersen, R. A.; Rogers, R. D.; Coles, S.; Hursthouse, M. B., *Chem. Eur. J.* **1999,** *5*, 3000-3009.

(24) Berthet, J.-C.; Le Marechal, J.-F.; Lance, M.; Nierlich, M.; Vigner, J.; Ephritikhine, M., *Dalton Trans.* **1992**, 1573-1577.

(25) Jutzi, P.; Schlüter, E., *J. Organomet. Chem.* **1983,** *253*, 313-316.

(26) APEX2 Version 2013.10-0, Bruker AXS, Inc.; Madison, WI 2013.

(27) SAINT Version 8.34a, Bruker AXS, Inc.; Madison, WI 2013.

(28) Sheldrick, G. M. SADABS, Version 2014/5, Bruker AXS, Inc.; Madison, WI 2014.

(29) Sheldrick, G. M. SHELXTL, Version 2014/7, Bruker AXS, Inc.; Madison, WI 2014.

(30) International Tables for Crystallography 1992, Vol. C., Dordrecht: Kluwer Academic Publishers.

(31) Parsons, S., Flack, H. D., Wagner, T. *Acta Crystallogr.*, .B69, 249-259, 2013.

(32) APEX2 Version 2012.4-0, Bruker AXS, Inc.; Madison, WI 2012

(33) SAINT Version 7.68a, Bruker AXS, Inc.; Madison, WI 2009.

(34) Sheldrick, G. M. SADABS, Version 2008/1, Bruker AXS, Inc.; Madison, WI 2008.

(35) Sheldrick, G. M. SHELXTL, Version 2008/4, Bruker AXS, Inc.; Madison, WI 2008.

(36) Sheldrick, G. M. SHELXL 2013/3, 2013.

(37) International Tables for X-Ray Crystallography 1992, Vol. C., Dordrecht: Kluwer Academic Publishers.

(38) APEX2 Version 2014.11-0, Bruker AXS, Inc.; Madison, WI 2014.

(39) SAINT Version 8.34a, Bruker AXS, Inc.; Madison, WI 2013.

(40) Sheldrick, G. M. SADABS, Version 2014/5, Bruker AXS, Inc.; Madison, WI 2014.

(41) Sheldrick, G. M. SHELXTL, Version 2014/7, Bruker AXS, Inc.; Madison, WI 2014.

(42) International Tables for Crystallography 1992, Vol. C., Dordrecht: Kluwer Academic Publishers.

(43) APEX2 Version 2011.4-1, Bruker AXS, Inc.; Madison, WI 2011.

(44) SAINT Version 7.68a, Bruker AXS, Inc.; Madison, WI 2009.

(45) Sheldrick, G. M. SADABS, Version 2008/1, Bruker AXS, Inc.; Madison, WI 2008.

(46) Sheldrick, G. M. SHELXTL, Version 2014/7, Bruker AXS, Inc.; Madison, WI 2014.

(47) International Tables for Crystallography 1992, Vol. C., Dordrecht: Kluwer Academic Publishers.

(48) LeMaréchal, J. F.; Villiers, C.; Charpin, P.; Nierlich, M.; Lance, M.; Vigner, J.; Ephritikhine, M., *J. Organomet. Chem.* **1989,** *379*, 259-269.

(49) Berthet, J.-C.; Le Marechal, J.-F.; Ephritikhine, M., *J. Chem. Soc., Chem. Commun.* **1991**, 360-361.

(50) Newton, T. W. *Kinetics of the Oxidation-Reduction Reactions of Uranium, Neptunium, Plutonium, and Americium in Aqueous Solutions*; TID--26506 United States10.2172/4188896Tue Feb 05 16:23:52 EST 2008Dep. NTISTIC; NSA-32-022026English; Oak Ridge National Lab: Oak Ridge, TN, 1975; p Medium: P; Size: Pages: 140.

(51) Howes, K. R.; Bakac, A.; Espenson, J. H., *Inorg. Chem.* **1988,** *27*, 791-794.

(52) Privalov, T.; Macak, P.; Schimmelpfennig, B.; Fromager, E.; Grenthe, I.; Wahlgren, U., *J. Am. Chem. Soc.* **2004,** *126*, 9801-9808.

(53) Morris, D. E.; Da Re, R. E.; Jantunen, K. C.; Castro-Rodriguez, I.; Kiplinger, J. L., *Organometallics* **2004,** *23*, 5142-5153.

(54) Kindra, D. R.; Evans, W. J., *Chem. Rev.* **2014,** *114*, 8865-8882.

(55) Morss, L. R.; Edelstein, N. M.; Fuger, J., *The Chemistry of the Actinide and Transactinide Elements*. 4th ed.; Springer: Dordrecht, The Netherlands, 2010; Vol. 1-6.

(56) Lukens, W. W. Trivalent Metallocene Chemistry of Some Uranium, Titanium and Zirconium Complexes. University of California - Berkeley, Berkeley, California, USA, 1995.

(57) Lukens, W. W.; Speldrich, M.; Yang, P.; Duignan, T. J.; Autschbach, J.; Kogerler, P., *Dalton Trans.* **2016,** *45*, 11508-21.

(58) Wasserman, H. J.; Zozulin, A. J.; Moody, D. C.; Ryan, R. R.; Salazar, K. V., *J. Organomet. Chem.* **1983,** *254*, 305-311.

(59) Evans, W. J.; Kozimor, S. A.; Ziller, J. W., *J. Am. Chem. Soc.* **2003,** *125*, 14264-14265.

(60) Brennan, J. G.; Andersen, R. A.; Robbins, J. L., *J. Am. Chem. Soc.* **1986,** *108*, 335-336.

(61) Mehdoui, T.; Berthet, J.-C.; Thuery, P.; Ephritikhine, M., *Dalton Trans.* **2004**, 579-590.

(62) Berthet, J.-C.; Villiers, C.; Le Maréchal, J.-F.; Delavaux-Nicot, B.; Lance, M.; Nierlich, M.; Vigner, J.; Ephritikhine, M., *J. Organomet. Chem.* **1992,** *440*, 53-65.

(63) Boussie, T. R.; Moore, R. M.; Streitwieser, A.; Zalkin, A.; Brennan, J.; Smith, K. A., *Organometallics* **1990,** *9*, 2010-2016.

(64) Fischer, E. O.; Hristidu, Y., *Z. Naturforsch., B: Chem. Sci.* **1962,** *17b*, 275-276.

(65) Anderson, M. L.; Crisler, L. R., *J. Organomet. Chem.* **1969,** *17*, 345-348.

(66) Chang, C. C.; Sung-Yu, N. K.; Hseu, C. S.; Chang, C. T., *Inorg. Chem.* **1979,** *18*, 885-886.

(67) Ossola, F.; Rossetto, G.; Zanella, P.; Paolucci, G.; Fischer, R. D., *J. Organomet. Chem.* **1986,** *309*, 55-63.

(68) Bursten, B. E.; Casarin, M.; DiBella, S.; Fang, A.; Fragala, I. L., *Inorg. Chem.* **1985,** *24*, 2169-2173.

(69) Brennan, J. G.; Andersen, R. A.; Zalkin, A., *J. Am. Chem. Soc.* **1988,** *110*, 4554-4558.

(70) Weydert, M.; Brennan, J. G.; Andersen, R. A.; Bergman, R. G., *Organometallics* **1995,** *14*, 3942-3951.

(71) Dormond, A.; Duval-Huet, C.; Tirouflet, J., *J. Organomet. Chem.* **1981,** *209*, 341-354.

(72) Dormond, A.; Hepiégne, P.; Hafid, A.; Moise, C., *J. Organomet. Chem.* **1990,** *398*, C1-C5.

(73) Burns, J. H., *J. Am. Chem. Soc.* **1973,** *95*, 3815-3817.

(74) Burns, J. H., *J. Organomet. Chem.* **1974,** *69*, 225-233.

(75) Shannon, R., *Acta Crystallogr., Sect. A.* **1976,** *32*, 751-767.

(76) Coles, M. P.; Hitchcock, P. B.; Lappert, M. F.; Protchenko, A. V., *Organometallics* **2012,** *31*, 2682-2690.

(77) Bombieri, G.; Panattoni, C., *Acta Crystallogr., Sect. C.* **1966,** *20*, 595-595.

(78) Panattoni, C.; Bombieri, G.; Croatto, U., *Acta Crystallogr., Sect. C.* **1966,** *21*, 823-826.

(79) Overby, J. S.; Hanusa, T. P.; Young, V. G., *Inorg. Chem.* **1998,** *37*, 163-165.

(80) Evans, W. J.; Clark, R. D.; Forrestal, K. J.; Ziller, J. W., *Organometallics* **1999,** *18*, 2401-2402.

(81) Atwood, J. L.; Hunter, W. E.; Cowley, A. H.; Jones, R. A.; Stewart, C. A., *J. Chem. Soc., Chem. Commun.* **1981**, 925-927.

(82) Schumann, H.; Janiak, C.; Hahn, E.; Kolax, C.; Loebel, J.; Rausch, M. D.; Zuckerman, J. J.; Heeg, M. J., *Chem. Ber.* **1986,** *119*, 2656-2667.

(83) Burkey, D. J.; Hanusa, T. P.; Huffman, J. C., *Inorg. Chem.* **2000,** *39*, 153-155.

(84) Constantine, S. P.; Hitchcock, P. B.; Lawless, G. A., *Organometallics* **1996,** *15*, 3905-3906.

(85) Constantine, S. P.; Cox, H.; Hitchcock, P. B.; Lawless, G. A., *Organometallics* **2000,** *19*, 317-326.

(86) Gun'ko, Y. K.; Hitchcock, P. B.; Lappert, M. F., *Organometallics* **2000,** *19*, 2832-2834.

(87) Le Marechal, J. F.; Villiers, C.; Charpin, P.; Lance, M.; Nierlich, M.; Vigner, J.; Ephritikhine, M., *J. Chem. Soc., Chem. Commun.* **1989**, 308-310.

(88) Berthet, J.-C.; Le Maréchal, J.-F.; Nierlich, M.; Lance, M.; Vigner, J.; Ephritikhine, M., *J. Organomet. Chem.* **1991,** *408*, 335-341.

(89) Meihaus, K. R.; Fieser, M. E.; Corbey, J. F.; Evans, W. J.; Long, J. R., *J. Am. Chem. Soc.* **2015**.

(90) Streitwieser, A.; Mueller-Westerhoff, U., *J. Am. Chem. Soc.* **1968,** *90*, 7364-7364.

(91) Streitwieser, A.; Muller-Westerhoff, U.; Sonnichsen, G.; Mares, F.; Morrell, D. G.; Hodgson, K. O.; Harmon, C. A., *J. Am. Chem. Soc.* **1973,** *95*, 8644-8649.

(92) Streitwieser, A.; Dempf, D.; La Mar, G. N.; Karraker, D. G.; Edelstein, N., *J. Am. Chem. Soc.* **1971,** *93*, 7343-7344.

(93) Streitwieser, A.; Mueller-Westerhoff, U.; Mares, F.; Grant, C. B.; Morrell, D. G.; Marks, T. J.; Miller, S. S., *Inorg. Synth.* **1979,** *19*, 149-154.

(94) Seyferth, D., *Organometallics* **2004,** *23*, 3562-3583.

(95) Takase, M. K.; Ziller, J. W.; Evans, W. J., *Chem. Eur. J.* **2011,** *17*, 4871-4878.

(96) Gassman, P. G.; Deck, P. A.; Winter, C. H.; Dobbs, D. A.; Cao, D. H., *Organometallics* **1992,** *11*, 959-960.

(97) Hanusa, T. P., *Chem. Rev.* **1993,** *93*, 1023-1036.

(98) Cassani, M. C.; Duncalf, D. J.; Lappert, M. F., *J. Am. Chem. Soc.* **1998,** *120*, 12958-12959.

(99) Zachmanoglou, C. E.; Docrat, A.; Bridgewater, B. M.; Parkin, G.; Brandow, C. G.; Bercaw, J. E.; Jardine, C. N.; Lyall, M.; Green, J. C.; Keister, J. B., *J. Am. Chem. Soc.* **2002,** *124*, 9525-9546.

(100) Zalkin, A.; Brennan, J. G., *Acta Crystallogr., Sect. C.* **1985,** *41*, 1295-1297.

(101) Schock, L. E.; Seyam, A. M.; Sabat, M.; Marks, T. J., *Polyhedron* **1988,** *7*, 1517-1529.

(102) Berthet, J.-C.; Lance, M.; Nierlich, M.; Vigner, J.; Ephritikhine, M., *J. Organomet. Chem.* **1991,** *420*, C9-C11.

(103) Jemine, X.; Goffart, J.; Leverd, P. C.; Ephritikhine, M., *J. Organomet. Chem.* **1994,** *469*, 55-57.

(104) Leverd, P. C.; Ephritikhine, M.; Lance, M.; Vigner, J.; Nierlich, M., *J. Organomet. Chem.* **1996,** *507*, 229-237.

(105) Mehdoui, T.; Berthet, J.-C.; Thuéry, P.; Salmon, L.; Rivière, E.; Ephritikhine, M., *Chem. Eur. J.* **2005,** *11*, 6994-7006.

(106) Minasian, S. G.; Krinsky, J. L.; Williams, V. A.; Arnold, J., *J. Am. Chem. Soc.* **2008,** *130*, 10086-10087.

(107) Maron, L.; Eisenstein, O.; Andersen, R. A., *Organometallics* **2009,** *28*, 3629-3635.

(108) Minasian, S. G.; Krinsky, J. L.; Rinehart, J. D.; Copping, R.; Tyliszczak, T.; Janousch, M.; Shuh, D. K.; Arnold, J., *J. Am. Chem. Soc.* **2009,** *131*, 13767-13783.

CHAPTER 3

TRIMETHYLSILYLCYCLOPENTADIENYL (Cp′) URANIUM CHEMISTRY: MULTIPLE SYNTHESES OF Cp'_4U AND Cp'_3UMe/Cp'_3UCl MIXTURES THAT ARE MORE CRYSTALLINE THAN PURE Cp'_3UMe

INTRODUCTION†

The first well-characterized organometallic complex of an actinide was synthesized in 1956[1] by reacting NaCp (Cp = C_5H_5) with the common binary halide UCl_4 in analogy to the synthesis of Cp_2Fe from NaCp and $FeCl_2$. However, in the uranium case, not all chlorides were displaced and the heteroleptic product, Cp_3UCl, was obtained.[1] It was not until 1962 that the homoleptic Cp_4U was isolated.[2] Structural characterization of tetrakis(cyclopentadienyl)U^{IV} complexes has also lagged behind other classes of cyclopentadienyl uranium complexes: although the structure of (η^5–Cp)$_4$U was determined in 1973,[3-4] it was another 20 years until the thorium analog, Cp_4Th, was characterized by X-ray crystallography.[5] In 2017 the neptunium analog, Cp_4Np, was characterized by X-ray crystallography.[6] Numerous examples of tetrakis(cyclopentadienyl)U^{IV} complexes made by direct synthesis or as side products are in the literature such as $(C_5H_4Me)_4U$,[7-9] $[C_5H_4CH(Me)CH_2C_5H_4]UCp_2$,[10] $(C_5H_4PPh_2)_4U$,[11] and $(C_5H_4PPh_2)_2U(C_5H_4PPh_2)_2M(CO)_4$ (M = Cr, Mo),[11] but none of these had been crystallographically characterized.

As described in Chapter 2 crystallographic data on a tetrakis(cyclopentadienyl)U(III) complex were obtained from the reaction of the U^{II} complex, [K(crypt)][Cp′$_3$U], **21-U**[12] (crypt = 2.2.2-cryptand; Cp′ = $C_5H_4SiMe_3$), with 1,3,5,7-cyclooctatetraene. This reaction formed

†Portions of this chapter are prepared for submission to the *Journal of Organometallic Chemistry*. Windorff, C. J.; MacDonald, M. R.; Ziller, J. W.; Evans, W. J.

[K(crypt)][Cp′$_4$U], **28-U**,[13] as a byproduct according to eq 3.1. X-ray crystallography revealed that **28-U** contained three η^5–Cp′ rings and one η^1–Cp′ ligand, but this complex could only be compared with the corresponding yttrium analog, [K(crypt)][Cp′$_4$Y], **28-Y**,[14] and to one other structurally-characterized (tetracyclopentadienyl)uranium example, namely (η^5–Cp)$_4$U.

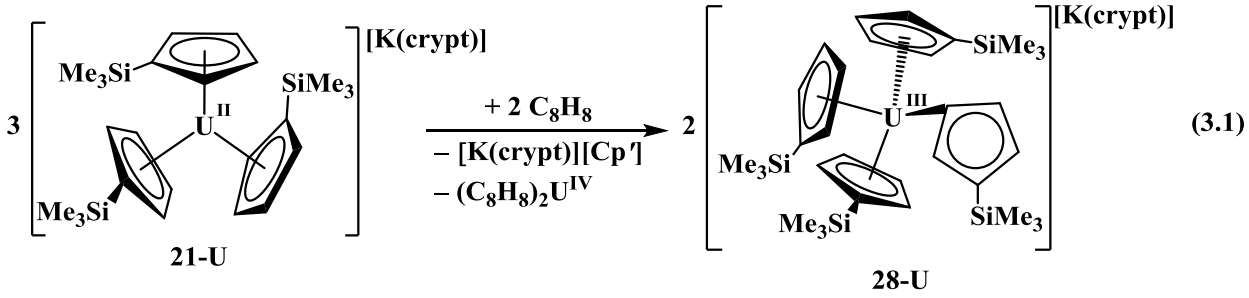

(3.1)

This Chapter describes efforts to synthesize and characterize the U^{IV} analog, namely Cp′$_4$U, **37-U**, to determine if all of the Cp′ rings will bond to the metal in an η^5 fashion as is the case of other Cp$_4$An (An = Th, U, Np) complexes, or if the steric hindrance of the Cp′ ring will cause variable coordination modes as was observed in the M^{III} analogs **28-U** and **28-Y**.

Attempts to synthesize **37-U** directly from KCp′ and UCl$_4$ or UI$_4$(OEt$_2$)$_2$ in C$_6$D$_6$ at 80 °C for over 2 weeks were unsuccessful: only Cp′$_3$UX (X = Cl, **33-U**; I, **34**)[15-16] was isolated in high yield. This is consistent with the earlier cyclopentadienyl uranium results.

An alternative route to homoleptic cyclopentadienyl *f*-element complexes, especially sterically crowded complexes, involves elimination of KBPh$_4$ as a byproduct in the reaction of a cyclopentadienyl potassium reagent with an *f*-element (BPh$_4$)$^{1-}$ salt.[17-26] Accordingly, the synthesis of **37-U** was pursued along these lines with the known intermediates Cp′$_3$UMe, **35**,[16] and [Cp′$_3$U(THF)][BPh$_4$], **36**,[24] Figure 3.1. A third route would be to oxidize a U^{III} complex such as Cp′$_3$U, **8-U**.

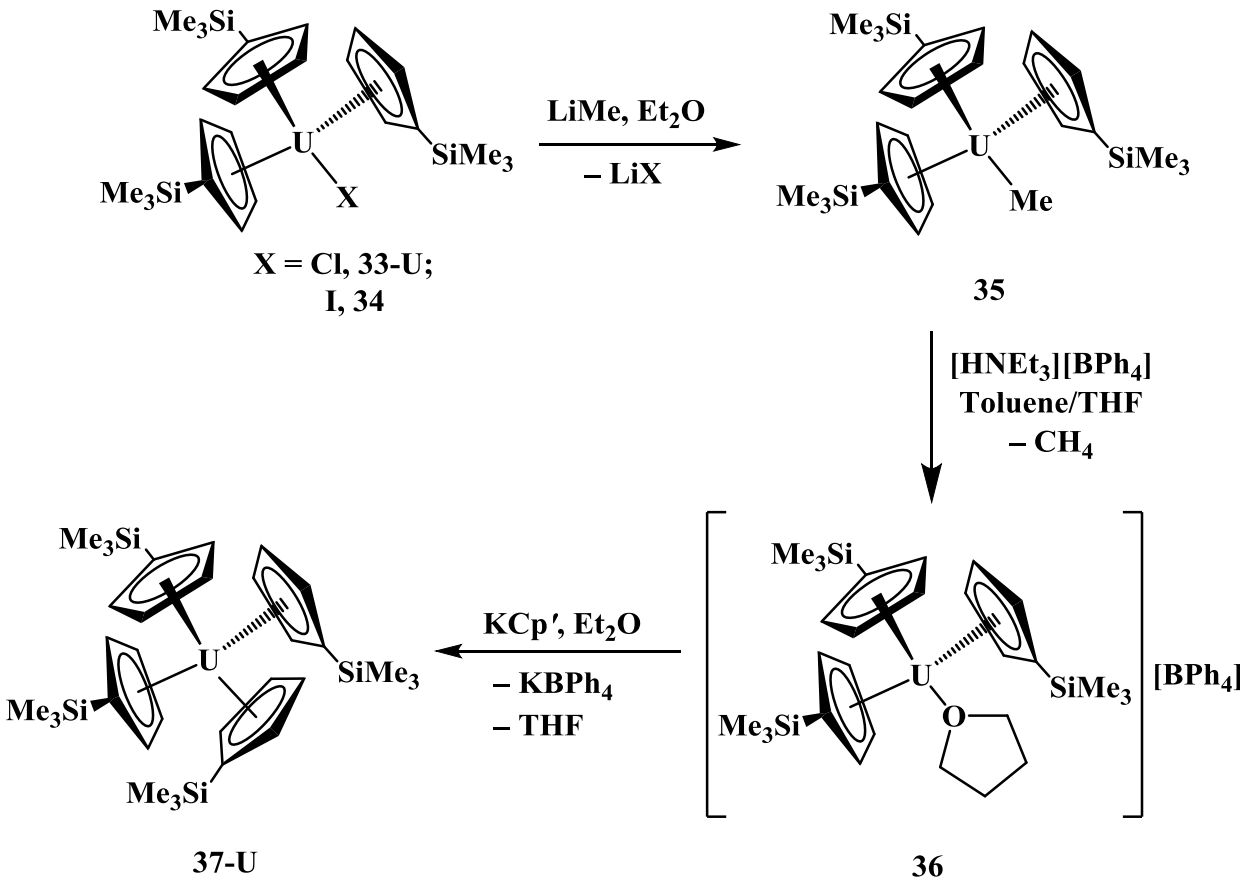

Figure 3.1. Synthetic scheme for the synthesis of Cp'_4U, **37-U**, using only tetravalent intermediates.

This Chapter will discuss the multiple synthetic pathways to **37-U** by addition of KCp′ to a cationic complex, $[Cp'_3U(THF)][BPh_4]$, **36**, and by the oxidation of **8-U** with ½ equiv Cp'_2Pb, **30** or by oxidation of $(Cp'_4U)^-$ with $AgBPh_4$, Here $(Cp'_4U)^-$ can be the $[K(crypt)]^+$ salt as isolated in **28-U** or a "$[K(THF)_x]^+$" salt generated in situ by addition of KCp′ to **8-U** in THF. These results are compared with the analogous thorium chemistry where Cp'_4Th, **37-Th** can be isolated from the reaction of $ThBr_4(THF)_4$ with excess KCp′ in a low yield.

EXPERIMENTAL

All manipulations and syntheses described below were conducted with the rigorous exclusion of air and water using standard Schlenk line and glovebox techniques under an argon or dinitrogen atmosphere. Solvents were sparged with UHP argon (Praxair) and dried by passage through columns containing Q-5 and molecular sieves prior to use. Deuterated NMR solvents (Cambridge Isotopes) were dried over sodium benzophenone ketyl or sodium/potassium alloy, degassed by three freeze-pump-thaw cycles, and vacuum transferred before use. ^{1}H, ^{13}C{^{1}H}, and ^{29}Si{^{1}H} NMR spectra were recorded on a Bruker GN500 or CRYO500 MHz spectrometer operating at 499.3, 125.6 and 99.2 MHz, respectively, at 298 K unless otherwise stated. ^{1}H and ^{13}C NMR spectra were referenced internally to solvent resonances. ^{29}Si NMR spectra were referenced externally to $SiMe_4$. IR spectra were recorded as KBr pellets on a Varian 1000 FT-IR spectrometer. Elemental analyses were performed on a Perkin-Elmer 2400 Series II CHNS elemental analyzer. UV/vis spectra were collected in THF at 298 K using a Varian Cary 50 Scan UV/vis spectrophotometer in a 1 mm cuvette. Near IR spectra were collected in THF at 298 K using a Perkin Elmer Lambda 900 UV/vis/NIR Spectrometer in a 1 cm cuvette. All optical spectra were recorded as 1.5 – 2 mM solutions. Solvent was removed from MeLi obtained as a 1.6 M solution in Et_2O and the reagent was used as a solid. The following compounds were prepared following literature procedures: UCl_4,[27] $UI_4(OEt_2)_2$,[28] Cp'_3U,[12] [K(crypt)][Cp'_4U],[13] $ThCl_4(DME)_2$,[29] $ThBr_4(THF)_4$,[30] Cp'_2Pb,[13] KCp′,[31] $AgBPh_4$[32] and $[HNEt_3][BPh_4]$.[24]

Cp'_3UCl, 33-U. This compound was prepared by a modification of the literature method.[15] In a glovebox, white KCp′ (1.00 g, 5.67 mmol) was added to a green slurry of UCl_4 (0.674 g, 1.77 mmol) in Et_2O (90 mL). The mixture quickly turned orange and was stirred

overnight. Volatiles were removed under reduced pressure and the solid was dissolved in hexane. The solution was centrifuged to remove white insolubles (presumably KCl and excess KCp′) and the volatiles were removed under reduced pressure to give light orange Cp′$_3$UCl (1.00 g, 82%) as confirmed by ^{1}H NMR spectroscopy.[15] Similar yields are obtained from the same reaction in toluene. ^{1}H NMR (C_6D_6): δ 16.53 (s, $C_5H_4SiMe_3$, 6H), −5.62 (s, $C_5H_4Si\mathit{Me}_3$, 27H), −17.16 (s, $C_5\mathit{H}_4SiMe_3$, 6H);[15] ^{29}Si NMR (C_6D_6): δ −62.9 ($C_5H_4\mathit{Si}Me_3$). Orange crystals suitable for X-ray diffraction were grown from Et_2O at −15 °C.

Cp′$_3$ThCl, 33-Th. In a glovebox, solid KCp′ (210 mg, 1.19 mmol) was added to a clear and colorless solution of $ThCl_4(DME)_2$ (210 mg, 0.385 mmol) in toluene (15 mL). White solids quickly precipitated from solution and the mixture was stirred overnight. The mixture was centrifuged to removed white insolubles (presumably KCl), filtered and dried under reduced pressure. The product was extracted into hexane and dried under reduced pressure to yield Cp′$_3$ThCl, **33-Th**, (200 mg, 76%) as a white solid. ^{1}H NMR (C_6D_6): δ 6.41 (s, $C_5\mathit{H}_4SiMe_3$, 12H) 0.39 (s, $C_5H_4Si\mathit{Me}_3$, 27H); ^{13}C{^{1}H} NMR (C_6D_6): δ 130.70 (i–$\mathit{C}_5H_4SiMe_3$), 127.45 ($\mathit{C}_5H_4SiMe_3$), 121.71 ($\mathit{C}_5H_4SiMe_3$), 0.56 ($C_5H_4Si\mathit{Me}_3$), all assignments were confirmed by HMQC.

Cp′$_3$ThBr, 38. In a glovebox, solid $ThBr_4(THF)_4$ (840 mg, 1.00 mmol) was added to a clear and colorless solution of KCp′ (530 mg, 3.02 mmol) in Et_2O (20 mL). White solids quickly precipitated from solution and the mixture was stirred overnight. The mixture was centrifuged to removed white insolubles (presumably KBr), filtered and dried under reduced pressure. The product was extracted into hexane and dried under reduced pressure to yield Cp′$_3$ThBr, **38**, (580 mg, 80%) as a white solid. ^{1}H NMR (C_6D_6): δ 6.52 (t, 2.5 Hz, $C_5\mathit{H}_4SiMe_3$, 6H) 6.40 (t, 2.5 Hz,

$C_5H_4SiMe_3$, 6H), 0.39 (s, $C_5H_4Si\mathit{Me}_3$, 27H). X-ray quality crystals were grown from a concentrated toluene solution at −30 °C.

Cp′$_3$UI, 34. This is a modification of the literature procedure.[16] In a glovebox, white KCp′ (103 mg, 0.585 mmol) was added to a red suspension of $UI_4(OEt_2)_2$ (152 mg, 0.170 mmol) in toluene (7 mL). The solution quickly turned orange and was stirred overnight. Volatiles were removed under reduced pressure, the remaining solid was dissolved in hexane, the mixture was centrifuged to remove gray insolubles (presumably KI and excess KCp′), and the volatiles were removed under reduced pressure to give a red solid confirmed to be Cp′$_3$UI (126 mg, 95%) by ^{1}H NMR spectroscopy in C_7D_8.[16] Similar yields are obtained from the synthesis in Et_2O. ^{1}H NMR (C_7D_8): δ 3.52 (s, $C_5\mathit{H}_4SiMe_3$, 6H), −3.82 (s, $C_5\mathit{H}_4SiMe_3$, 6H), −6.80 (s, $C_5H_4Si\mathit{Me}_3$, 27H); ^{1}H NMR (C_6D_6): δ 3.26 (s, $C_5\mathit{H}_4SiMe_3$, 6H), −3.82 (s, $C_5\mathit{H}_4SiMe_3$, 6H), −6.55 (s, $C_5H_4Si\mathit{Me}_3$, 27H); ^{13}C{^{1}H} NMR (C_6D_6): δ 322.7 ($\mathit{C}_5H_4SiMe_3$), 261.3 ($\mathit{C}_5H_4SiMe_3$), 246.9 ($\mathit{C}_5H_4SiMe_3$), −1.2 ($C_5H_4\mathit{Si}Me_3$); ^{29}Si NMR (C_6D_6): δ −77.8 ($C_5H_4\mathit{Si}Me_3$). Orange crystals suitable for X-ray crystallography were grown in Et_2O at −15 °C.

Cp′$_3$UMe, 35, from Cp′$_3$UCl. This was prepared by a modification of the literature method that used LiMe•LiBr in Et_2O.[16] In a glovebox, white MeLi (7 mg, 0.3 mmol) was added to a stirred orange solution of Cp′$_3$UCl, **33**, (88 mg, 0.13 mmol) in Et_2O (5 mL). The solution was stirred overnight and turned darker orange. The volatiles were removed under reduced pressure and the residual solid extracted into hexane. The mixture was centrifuged to remove white solids (presumably LiCl and excess MeLi). The volatiles were removed under reduced pressure to give an orange oil that was analyzed to be Cp′$_3$UMe, **35**, by ^{1}H NMR spectroscopy[16] (80 mg, 94 %). ^{1}H NMR (C_6D_6): δ 8.13 (s, $C_5\mathit{H}_4SiMe_3$, 6H), −5.56 (s, $C_5H_4Si\mathit{Me}_3$, 27H), −6.17 (s, $C_5\mathit{H}_4SiMe_3$, 6H), −195.35 (s, U-*Me*, 3H);[16] ^{29}Si NMR (C_6D_6): δ −73.5 ($C_5H_4\mathit{Si}Me_3$).

In some cases, ^{1}H NMR analysis of aliquots of the reaction mixture indicated that the reaction was not complete and some **33** remained. In these cases, a small amount of additional MeLi (0.5 – 1 eq) was added and this was repeated until there was no **33** present in the ^{1}H NMR spectrum.

Cp′$_3$UMe, 35, from Cp′$_3$UI. In a synthesis analogous to that above, solid MeLi (4 mg, 0.2 mmol) was added to a red stirred solution of Cp′$_3$UI, **34**, (75 mg, 0.097 mmol) in Et_2O (5 mL). The solution was stirred overnight and turned dark orange. The volatiles were removed under reduced pressure, extracted into hexane and centrifuged to remove white solids (presumably LiI and excess MeLi). The volatiles were removed under reduced pressure to give an orange oil that was determined to be Cp′$_3$UMe, **35**, by ^{1}H NMR spectroscopy[16] (60 mg, 94 %).

[Cp′$_3$U(THF)][BPh$_4$], 36. This complex was synthesized by a variation of the literature method which uses Cp′$_3$UH as the precursor.[24] In a glovebox, a solution of Cp′$_3$UMe**, 35**, (69 mg, 0.10 mmol) in toluene (5 mL) was added to a stirred slurry of [$HNEt_3$][BPh_4] (38 mg, 0.090 mmol) in toluene (5 mL) and THF (1 mL). After the mixture stirred overnight, the red-orange solution was filtered and hexane (20 mL) was added. After 2 h of stirring, the precipitate was collected via centrifugation and dried under vacuum to yield [Cp′$_3$U(THF)][BPh_4], **36**, as a pale tan powder (75 mg, 80%). ^{1}H NMR (THF-d_8): δ 6.56 (s, *o*-B*Ph*$_4$, 8H), 6.50 (s, *m/p*-B*Ph*$_4$, 12H), 3.53 (s, *THF*, 4H), 1.68 (s, THF, 4H), 0.67 (s, $C_5H_4SiMe_3$, 6H), −2.94 (br s, $C_5H_4SiMe_3$, 6H), −3.61 (s, C_5H_4Si*Me*$_3$, 27H).[53]

Cp′$_4$U, 37-U, from [Cp′$_3$U(THF)][BPh$_4$] and KCp′. In a glovebox, addition of KCp′ (11 mg, 0.062 mmol) in Et_2O (2 mL) to a stirred suspension of tan [Cp′$_3$U(THF)][BPh_4], **36**, (60 mg, 0.057 mmol) in Et_2O (5 mL) generated a dark red mixture within 2 min. After 1 h, hexane

(5 mL) was added and the colorless precipitate, presumably $KBPh_4$ and excess KCp′, were removed via centrifugation. Slow removal of volatiles under reduced pressure to yielded Cp'_4U, **37-U** (33 mg, 74%) as a dark red crystalline solid. ^{1}H NMR (C_6D_6, 298 K): δ −1.95 (s, $C_5H_4Si\mathit{Me}_3$, 36H), −10.71 (s, $C_5\mathit{H}_4SiMe_3$, 8H), −22.46 (s, $C_5\mathit{H}_4SiMe_3$, 8H); ^{1}H NMR (C_7D_8, 298 K): δ −1.85 (s, $C_5H_4Si\mathit{Me}_3$, 36H), −10.85 (s, $C_5\mathit{H}_4SiMe_3$, 8H), −22.14 (s, $C_5\mathit{H}_4SiMe_3$, 8H); ^{1}H NMR (C_7D_8, 193 K): δ −1.65 (br s, $\nu_{1/2}$ = 175 Hz, $C_5H_4Si\mathit{Me}_3$, 36H), −21.72 (br s, $\nu_{1/2}$ = 500 Hz, $C_5\mathit{H}_4SiMe_3$, 8H), −28.28 (br s, $\nu_{1/2}$ = 875 Hz, $C_5\mathit{H}_4SiMe_3$, 8H); ^{13}C NMR (C_7D_8, 298 K): δ 218.6 ($\mathit{C}_5H_4SiMe_3$), 185.2 ($\mathit{C}_5H_4SiMe_3$), 152.7 ($\mathit{C}_5H_4SiMe_3$), 1.7 ($C_5H_4Si\mathit{Me}_3$); ^{29}Si NMR (C_6D_6, 298 K): δ −63.9 ($C_5H_4\mathit{Si}Me_3$); ^{29}Si NMR (C_7D_8, 298 K): δ −62.8 ($C_5H_4\mathit{Si}Me_3$); ^{29}Si NMR (C_7D_8, 193 K): δ −78.3 ($C_5H_4\mathit{Si}Me_3$). Evans method (THF, 298 K): 2.41 μ_B. UV/vis/NIR (THF) λ_{max} nm (ε, $M^{-1}cm^{-1}$): 333 (5300), 506 (600), 544 (500), 591 (400) 666 (200), 704 (200), 932 (100), 1028 (100), 1055 (100), 1122 (100), 1200 (200), 1302 (100). IR: 3876m, 3090w, 2952m, 2895m, 2238w, 1558w, 1448m, 1402m, 1373w, 1247m, 1183m, 1111w, 1080m, 1040m, 901m, 832s, 771s, 750s, 685m, 636m, 621m, 569w cm^{-1}. Anal. Calcd for $C_{32}H_{52}Si_4U$: C, 48.83; H, 6.66. Found: C, 48.84; H, 6.64. Slow removal of solvent under reduced pressure yielded dark red crystals of Cp'_4U, **37-U**, suitable for X-ray crystallography

37-U from [K(crypt)][Cp′$_4$U], 28-U, and AgBPh$_4$. In a glovebox, $AgBPh_4$ (33 mg, 0.076 mmol) was added to a maroon solution of [K(crypt)][Cp′$_4$U], **28-U** (78 mg, 0.065 mmol), in THF (2 mL) and the solution quickly became darker maroon. After 10 min the volatiles were removed under reduced pressure, the solids were extracted into hexane, and the mixture was filtered to remove black and white insoluble material (presumably Ag and [K(crypt)][BPh_4], respectively). The solvent was removed under reduced pressure to yield **37-U** (43 mg, 84%) as identified by ^{1}H NMR spectroscopy.

37-U from Cp'_3U, KCp′, and $AgBPh_4$. In a glovebox Cp'_3U, **8-U**, (40 mg, 0.061 mmol) and KCp′ (11 mg, 0.061 mmol) were combined in a vial and stirred in Et_2O (2 mL) for 2 min. Then THF (0.5 mL) was added and the solution changed from green to red. After the mixture was stirred for 20 min, $AgBPh_4$ (29 mg, 0.068 mmol) was added. The solution turned maroon and was stirred for 15 min. The solvent was removed under reduced pressure, the solids were dissolved in hexane, the mixture was filtered to remove black and white insolubles (presumably Ag and $KBPh_4$, respectively), and the solvent was removed under reduced pressure to yield a dark maroon powder (42 mg, 88%), confirmed to be **37-U** by ^{1}H NMRspectroscopy.

37-U from Cp'_3U, 8-U, and Cp'_2Pb, 30. A yellow solution of Cp'_2Pb, **30**, (70 mg, 1.5 mmol) in Et_2O (5 mL) was added dropwise over 30 sec to a stirred solution of **8-U** (200 mg, 0.3 mmol) in Et_2O (5 mL). The mixture changed to dark red as it was stirred for 15 min. A grey solid, presumably Pb, was removed by filtration, and the solvent was removed from the filtrate under reduced pressure. The resulting dark red crystals were rinsed with cold pentane (1 mL, −35 °C) and dried under vacuum to yield **37-U** as a dark red crystalline solid (171 mg, 72%) identified by ^{1}H NMR spectroscopy.

Cp'_4Th, 37-Th. In a glovebox a colorless KCp′ (1.500 g, 8.519 mmol) solution in Et_2O (20 mL) was added to a white suspension of $ThBr_4(THF)_4$ (1.550 g, 1.842 mmol) in Et_2O (40 mL) in a Teflon sealable greaseless high vacuum flask, the flask was sealed and removed from the glovebox. The reaction was refluxed for 2 h, cooled and the volatiles removed under reduced pressure. The flask was brought into the glovebox and hexane (60 mL) was added, the flask was sealed and removed from the glovebox. The mixture was refluxed for 1 h, cooled to room temperature and stirred overnight. The mixture was filtered on a M frit and washed with toluene (20 mL) and the volatiles removed under reduced pressure to give a 4:1 mixture of

Cp'_3ThBr:Cp'_4Th as determined by ^1H NMR spectroscopy. ^1H NMR (C_6D_6): δ 7.08 (t, 2.5 Hz, $C_5H_4SiMe_3$, 8H), 6.34 (t, 2.5 Hz, $C_5H_4SiMe_3$, 8H), 0.42 (s, $C_5H_4SiMe_3$, 36H). X-ray quality crystals were grown from a concentrated toluene solution at –30 °C to give a mixture of the two compounds and were separated *a la Pasteur*.

Synthesis of [K(crypt)][Cp′$_4$U], 28-U, from [K(crypt)][Cp′$_3$U]•THF, 21•THF, and Cp′$_4$U, 37-U. In a glovebox, a solution of **37-U** (31 mg, 0.039 mmol) in THF (2 mL) was quickly added to a stirred cold solution of crystals of **21•THF** (45 mg, 0.040 mmol) in THF (5 mL, −35 °C). The color quickly changed from black/green to dark red. After stirring for 30 min while warming to room temperature, the solvent was removed under reduced pressure until the volume was ca. 0.5 mL. Et_2O (10 mL) was added to the dark red oil and the solution was stored at −35 °C for 6 h. The mother liquor was removed and the solids were rinsed with cold Et_2O (1 mL, −35 °C) and dried under vacuum to yield **28-U** (32 mg, 68%) as a dark red crystalline solid. The mother liquor and Et_2O rinses were combined, dried under reduced pressure, dissolved in hexane, and dried under reduced pressure, 3 × to give **8-U** (21 mg, 85%) both products were confirmed by ^1H NMR spectroscopy .[13]

Co-crystallization of Cp′$_3$UMe/Cp′$_3$UCl, 33/35. In a glovebox, a red-orange solution of Cp'_3UCl, **33-U**, (348 mg, 0.508 mmol) in Et_2O (10 mL) was added to a stirred slurry of LiMe (12 mg, 0.537 mmol) in Et_2O (5 mL). The mixture turned darker red-orange as it stirred over 24 h. The mixture was centrifuged to remove white solids, presumably LiCl, and the red-orange supernatant was filtered and the solvent removed. The dark red-orange oily residue was extracted with pentane (5 mL) and filtered to remove small amounts of white solids, and the solvent was removed under vacuum to yield a dark red oil (305 mg).[16] Dissolution of the oil in minimal pentane and storage at −35 °C afforded orange crystals of Cp'_3UMe, **35**, and Cp'_3UCl,

33-U, in a 4:1 ratio by X-ray crystallography. ^{1}H NMR analysis of the mother liquor revealed a 13:1 ratio of **35**, and **33**, respectively. Evidently, an inadequate amount of MeLi was used in the preparation of this sample.

In another case, pure **35** and pure **33-U** were combined in a 4:1 ratio (**35**, 50 mg, 0.075 mmol; **33-U**, 13 mg, 0.018 mmol), dissolved in minimal pentane, and placed in −30 °C freezer for 2 d. Orange crystals were collected by decanting the mother liquor, washing the crystals with 0.5 mL of cold pentane, and drying under reduced pressure (yield 25 mg). ^{1}H NMR spectroscopy of a solution of the crystals revealed a 6:5 ratio of the two compounds, respectively, by integration. ^{1}H NMR spectroscopy analysis of the mother liquor showed **35** with a trace amount of **33-U**. In another experiment, a sample was prepared with 5:1 **35**:**33** stoichiometry (**35**, 60 mg, 0.90 mmol; **33-U**, 12 mg, 0.017 mmol) and isolated by the same method (yield 20 mg). ^{1}H NMR spectroscopy of a solution of the crystals revealed an 8:5 ratio of the two compounds, respectively. ^{1}H NMR spectroscopy analysis of the mother liquor showed **35** with a small amount of **33-U**, in an approximate 30:1 ratio, respectively.

X-ray Crystallographic Data. Crystallographic details for complexes Cp′$_3$UCl, **33-U**, Cp′$_3$UI, **34**, Cp′$_3$UCl/Me, **33/35**, and Cp′$_3$ThBr, **38**, are given summarized in the text below and in Table 3.1.

X-ray Data Collection, Structure Solution and Refinement for Cp′$_3$UCl, 33-U. An orange crystal of approximate dimensions 0.023 x 0.124 x 0.200 mm was mounted in a cryoloop and transferred to a Bruker SMART APEX II diffractometer. The APEX2[33] program package was used to determine the unit-cell parameters and for data collection (30 sec/frame scan time for 1212 frames of diffraction data). The raw frame data was processed using SAINT[34] and

SADABS[35] to yield the reflection data file. The centrosymmetric space group $P\bar{3}$ was assigned and later determined to be correct.

The structure was solved by direct methods and refined on F^2 by full-matrix least-squares techniques.[36] The analytical scattering factors[37] for neutral atoms were used throughout the analysis. The molecule was located on a three-fold rotation axis. Hydrogen atoms were included using a riding model.

At convergence, wR2 = 0.0545 and Goof = 1.168 for 91 variables refined against 2294 data (0.84Å), R1 = 0.0201 for those 2165 data with $I > 2.0\sigma(I)$.

X-ray Data Collection, Structure Solution and Refinement for Cp′$_3$UI, 34. An orange crystal of approximate dimensions 0.060 x 0.197 x 0.362 mm was mounted in a cryoloop and transferred to a Bruker SMART APEX II diffractometer. The APEX2[38] program package was used to determine the unit-cell parameters and for data collection (20 sec/frame scan time for a sphere of diffraction data). The raw frame data was processed using SAINT[39] and SADABS[40] to yield the reflection data file. Subsequent calculations were carried out using the SHELXTL[41] program. The Laue symmetry was 2/*m* and the systematic absences were consistent with the monoclinic space group $P2_1/c$ which was assigned and later determined to be correct.

The structure was solved by direct methods and refined on F^2 by full-matrix least-squares techniques. The analytical scattering factors[42] for neutral atoms were used throughout the analysis. Hydrogen atoms were located from a difference-Fourier map and refined (x,y,z and U_{iso}). At convergence, wR2 = 0.0372 and Goof = 1.104 for 418 variables refined against 6811 data (0.74Å), R1 = 0.0167 for those 6525 data with $I > 2.0\sigma(I)$.

X-ray Data Collection, Structure Solution and Refinement for Cp′$_3$UMe/Cl, 33/35. An orange crystal of approximate dimensions 0.235 x 0.288 x 0.295 mm was mounted on a glass

fiber and transferred to a Bruker SMART APEX II diffractometer. The APEX2[43] program package was used to determine the unit-cell parameters and for data collection (20 sec/frame scan time for a sphere of diffraction data). The raw frame data was processed using SAINT[44] and SADABS[45] to yield the reflection data file. Subsequent calculations were carried out using the SHELXTL[46] program. The systematic absences were consistent with the trigonal space groups *P*3 and $P\bar{3}$. The centrosymmetric space group $P\bar{3}$ was assigned and later determined to be correct.

The structure was solved by direct methods and refined on F^2 by full-matrix least-squares techniques.[47] The analytical scattering factors[48] for neutral atoms were used throughout the analysis. Hydrogen atoms were either located from a difference-Fourier amp and refined (x,y,z and U_{iso}) or were included using a riding model. The molecule was located on a three-fold rotation axis. The molecule was disordered. The atom sites at the positions defined by Cl(1) and C(9) were composed of approximately 20% chloride and 80% methyl ligands. Those ligands were included with partial site-occupancy-factors consistent with the above compositions.
At convergence, wR2 = 0.0514 and Goof = 1.188 for 121 variables refined against 2281 data (0.75 Å), R1 = 0.0184 for those 2250 data with $I > 2.0\sigma(I)$.

X-ray Data Collection, Structure Solution and Refinement for Cp′$_3$ThBr, 38. A colorless crystal of approximate dimensions 0.290 x 0.207 x 0.097 mm was mounted on a glass fiber and transferred to a Bruker SMART APEX II diffractometer. The APEX2[49] program package was used to determine the unit-cell parameters and for data collection (40 sec/frame scan time for a sphere of diffraction data). The raw frame data was processed using SAINT[50] and SADABS[51] to yield the reflection data file. Subsequent calculations were carried out using the SHELXTL[52] program. Thee systematic absences were consistent with the hexagonal space

groups $P3$ and $P\bar{3}$. The centrosymmetric space group $P\bar{3}$ was assigned and later determined to be correct.

The structure was solved by direct methods and refined on F^2 by full-matrix least-squares techniques.[53] The analytical scattering factors[54] for neutral atoms were used throughout the analysis. Hydrogen atoms were included using a riding model. The molecule is located on a 3-fold rotation axis.

At convergence, wR2 = 0.0875 and Goof = 1.134 for 91 variables refined against 2333 data (0.75 Å), R1 = 0.0328 for those 2203 data with $I > 2.0\sigma(I)$.

Table 3.1. X-ray Data and Collection Parameters for Cp'_3UCl, **33-U**, Cp'_3UI, **34**, Cp'_3UMe/Cl, **35/33**, and Cp'_3ThBr, **38**.

Compound	**33-U**	**34**	**35/33**	**38**
Empirical Formula	$C_{24}H_{39}ClSi_3U$	$C_{24}H_{39}ISi_3U$	$C_{24.80}H_{41.40}Cl_{0.20}Si_3U$	$C_{24}H_{39}Si_3BrTh$
Crystal Color	Orange	Orange	Orange	Colorless
Temperature (K)	133(2)	133(2)	143(2)	143(2)
Crystal System	Trigonal	Monoclinic	Trigonal	Trigonal
Space Group	$P\bar{3}$	$P2_1/c$	$P\bar{3}$	$P\bar{3}$
***a* (Å)**	15.4712(15)	13.2794(7)	15.5581(9)	15.562(2)
***b* (Å)**	15.4712(15)	24.5727(14)	15.5581(9)	15.562(2)
***c* (Å)**	6.9062(7)	8.5470(5)	6.8277(4)	7.1019(9)
α (deg)	90	90	90	90
β (deg)	90	93.0996(7)	90	90
γ (deg)	120	90	120	120
Volume (Å^3)	1431.6(3)	2784.9(3)	1431.3(2)	1489.5(4)
Z	2	4	2	2
ρ_{calcd} (Mg/m^3)	1.590	1.853	1.552	1.614
μ (mm^{-1})	5.897	7.075	5.824	6.476
R1[a] ($I > 2.0\sigma(I)$)	0.0201	0.0167	0.0184	0.0328
wR2 (all data)	0.0555	0.0372	0.0514	0.0875

[a]Definitions: $R1 = \Sigma||F_o| - |F_c||/\Sigma|F_o|$, $wR2 = [\Sigma w(F_o^2 - F_c^2)^2/\Sigma w(F_o^2)^2]^{1/2}$.

Goof = $S = [\Sigma[w(F_o^2-F_c^2)^2] / (n-p)]^{1/2}$ where n is the number of reflections and p is the total number of parameters refined.

RESULTS

Co-Crystallized Cp'_3UMe/Cp'_3UCl Precursors. The known Cp'_3UMe, **35**,[16] intermediate in the synthesis plan in Figure 3.1 can be prepared in a variety of ways. Both Cp'_3UCl, **33-U**,[15] and Cp'_3UI, **34**,[16] can be used as precursors for reactions with MeLi in Et_2O. The Cp'_3UMe, **35**, formed in these reactions is isolated as an orange oil, which is consistent with the initial report that the compound melts below room temperature.[16] However, in one Cp'_3UCl/MeLi reaction, the product was isolated as crystals instead of an oil. X-ray crystallographic analysis of the single crystals revealed a 4:1 mixture of **35** and **33-U**, Figure 3.2, which was evidently obtained by incomplete reaction. ^{1}H NMR analysis of the mother liquor revealed a 13:1 mixture of the methyl and chloride compounds.

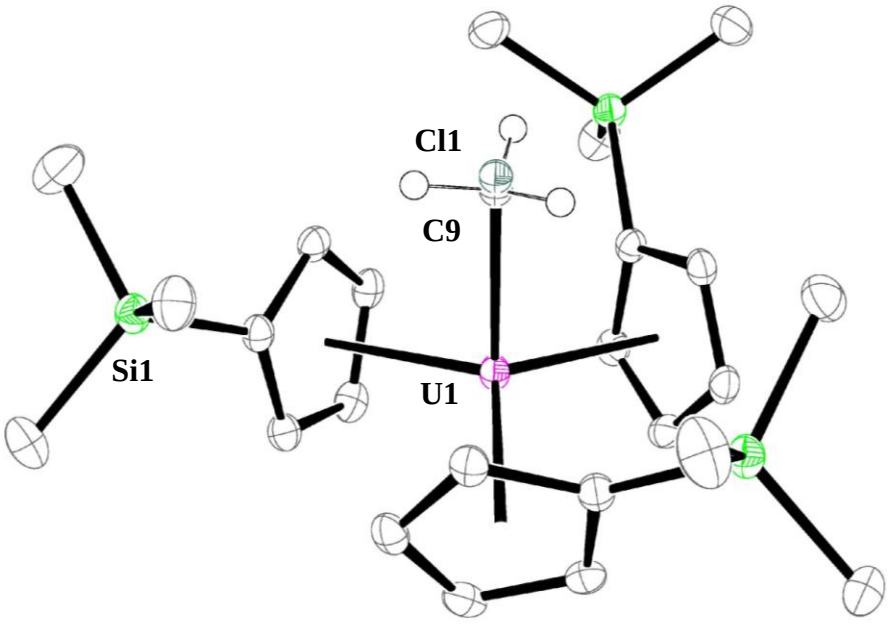

Figure 3.2. Thermal ellipsoid plot of Cp'_3UMe/Cl, **35/33**, 4:1 mixture, drawn at the 50% probability level with hydrogen atoms except the methyl hydrogens of C9, omitted for clarity.

The co-crystallized compounds crystallize with the Me or Cl ligand positioned on a three-fold rotation axis in the $P\bar{3}$ space group (Z = 2) with a U–CH_3 distance of 2.50(1) Å, a U–Cl distance of 2.66(1) Å, and a U–(ring centroid) distance of 2.487 Å, Tables 3.2 and 3.3. The (ring centroid)–U–Me and (ring centroid)–U–Cl angles are 98.9° and the (ring centroid)–U–(Cp′ ring centroid) angle is 117.7°.

In contrast to **35**, the halide complexes **33-U**[15] and **34**[16] are crystalline at room temperature and were crystallographically characterized for comparison. **33-U** crystallizes in the same $P\bar{3}$ space group, Figure 3.3, as the **35/33** mixture, but **34** crystallizes in the $P2_1/c$ space group, Figure 3.4. The metrical parameters of **33** are presented in Table 3.3 along with data on **33/35** and other tris(cyclopentadienyl)uranium chlorides, Cp''_3UCl,[55] [Cp′′ = $C_5H_3(SiMe_3)_2$–1,3] Cp_3UCl[56] (Cp = C_5H_5), $(C_5Me_4H)_3UCl$,[57] and Cp^*_3UCl[58] (Cp* = C_5Me_5). The metrical parameters of **35/33** are compared with the tris(cyclopentadienyl)uranium hydrocarbyl complexes Cp_3U^nBu,[59] $Cp'_3UCH{=}CH_2$,[16] $Cp_3U[\eta^1{-}CH_2C(Me){=}CH_2]$,[60] and Cp^*_3UMe,[61] in Table 3.2. Both Tables show that the metrical parameters in **35/33** and **33-U** are not unusual compared to other tris(cyclopentadienyl)U(IV) complexes when differences in ancillary ligand size are considered.

Table 3.2. Metrical Parameter Comparisons of Cp'_3UMe/Cl, **35/33**, With Other $(C_5R_5)_3UR'$ Complexes (cent = C_5R_5 Ring Centroid).

	U–C (Å)	U–(cent) (Å)	(cent)–U–C (°)	(cent)–U–(cent) (°)
Cp'_3UMe/Cl, **35/33**	2.50(1)	2.478	98.9	117.7
$Cp'_3UCH=CH_2$[16]	2.436(4)	2.48 2.48 2.49	95.1 100.0 100.2	116.4 117.2 120.0
Cp_3U^nBu[59]	2.43(2)	2.470 2.470 2.494	98.2 102.3 100.7	118.1 116.5 115.8
$Cp_3U[\eta^1–CH_2C(Me)=CH_2]$[60]	2.48(3)	2.44 2.44 2.47	102 99.5 97.5	119 115 118
Cp^*_3UMe[61]	2.66(2)	2.418	90	120

$Cp = (C_5H_5)^-$, $Cp^* = (C_5Me_5)^-$

Table 3.3. Metrical Parameter Comparisons of Cp'_3UCl, **33-U**, With Other $(C_5R_5)_3UCl$ Complexes (cent = C_5R_5 Ring Centroid).

	U–Cl (Å)	U–(cent) (Å)	(cent)–U–Cl (°)	(cent)–U–(cent) (°)
Cp'_3UCl, **33-U**	2.638(1)	2.437	100.0	117.0
Cp'_3UMe/Cl, **35/33**	2.66(1)	2.478	98.9	117.7
Cp''_3UCl[55]	2.614(2)	2.48 2.49 2.49	99.7 101.0 99.6	116.6 118.0 116.4
Cp_3UCl[56]	2.56(2)	2.43 2.48 2.47	101 100 101	115 120 115
$(C_5Me_4H)_3UCl$[57]	2.637	2.520	98.4	117.9
Cp^*_3UCl[58]	2.90(1)	2.551	90	120

$Cp'' = [C_5H_3(SiMe_3)_2–1,3]^-$, $Cp^* = (C_5Me_5)^-$

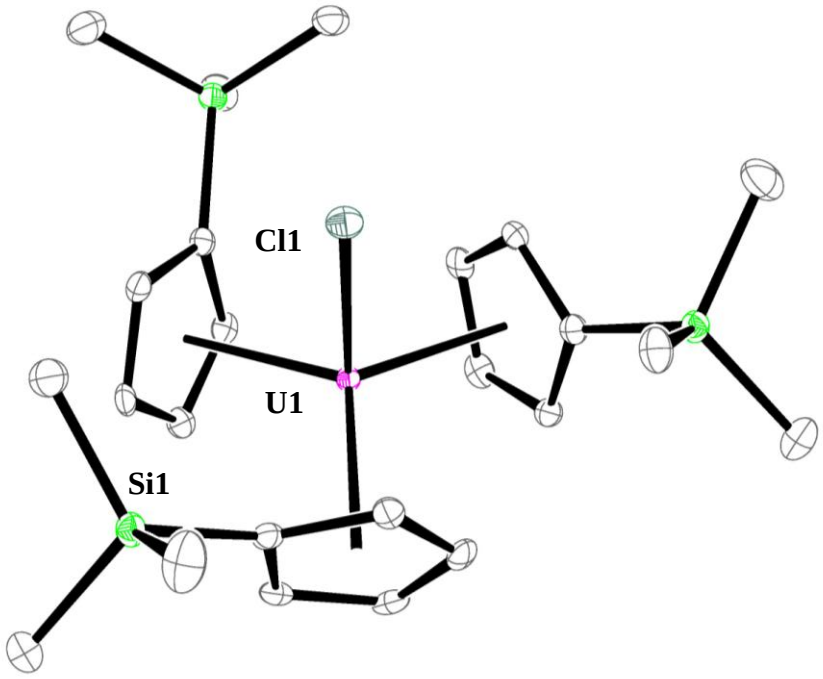

Figure 3.3. Thermal ellipsoid plot of Cp'_3UCl, **33-U**, drawn at the 50% probability level with hydrogen atoms omitted for clarity.

X-ray quality crystals of **34** were also obtained for comparison, Figure 3.4. This compound, prepared by salt metathesis of $UI_4(OEt_2)_2$[28] and KCp′ rather than the literature method of oxidation of Cp'_3U, **8-U**, by I_2,[16] and crystallizes from Et_2O at −15 °C in the $P2_1/c$ space group. The structure of **34** is similar to those in Figures 3.2 and 3.3, and the metrical parameters, compared with Cp_3UI[62] and $(C_5Me_4H)_3UI$[63] in Table 3.4, also show that there is nothing unusual in the structure.

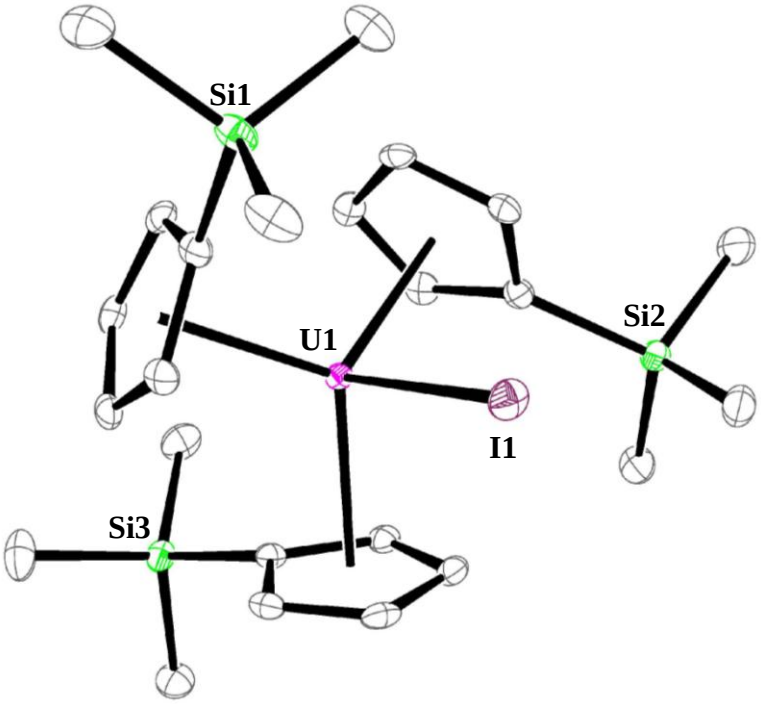

Figure 3.4. Thermal ellipsoid plot of Cp'_3UI, **34**, drawn at the 50% probability level with hydrogen atoms omitted for clarity.

Table 3.4. Metrical Parameter Comparisons of Cp'_3UI, **34**, With Other $(C_5R_5)_3UI$ Complexes (cent = C_5R_5 Ring Centroid).

	U–I (Å)	U–(cent) (Å)	(cent)–U–I (°)	(cent)–U–(cent) (°)
Cp'_3UI, **34**	3.0588(2)	2.480 2.475 2.478	101.2 101.6 97.9	116.1 116.4 118.3
Cp_3UI[62]	3.059(2)	2.467(3) 2.435(3) 2.449(3)	110.9(6) 101.3(6) 100.0(6)	114.5(7) 116.4(7) 119.0(8)
$(C_5Me_4H)_3UI$[63]	3.0338(5)	2.524	99.2	117.5

Independent Synthesis of Crystalline Cp'_3UMe/Cp'_3UCl, 35/33. A deliberately prepared mixture of **33-U** as a powder and **35** as an oil in a 1:4 ratio could be crystallized from a minimal amount of pentane at −30 °C to give orange crystalline solids. ^{1}H NMR spectroscopic analysis of the C_6D_6 solution of the crystalline product showed **33-U** and **35** in a ratio of 5:6. ^{1}H NMR analyses of the mother liquor revealed primarily **35**, with trace amounts of **33-U**. This is consistent with the initial metallocene ratio and the composition of the crystals. A similar reaction with a 1:5 starting ratio gave crystals that analyzed to have a 5:8 ratio of **33-U** and **35**. This shows that the composition of the crystals does not represent that of the starting mixture since the chloride evidently crystallizes more readily. These experiments also show that the composition of the crystals can be variable. Attempts to obtain single crystals from mixtures of the iodide analog, **34**, and **35** for X-ray analysis were unsuccessful.

Synthesis and Crystallographic Characterization of Cp'_3ThBr, 38. In the course of this study the thorium analogs, Cp'_3ThX (X = Cl, **33-Th**; Br, **38**), were made analogously to the uranium compounds Cp'_3UCl, **33-U** and Cp'_3UI, **34** from $ThCl_4(DME)_2$ and $ThBr_4(THF)_4$, respectively. X-ray quality crystals of Cp'_3ThCl, **33-Th**, were not obtained, but crystals of Cp'_3ThBr, **38**, were isolated and crystallographically characterized, Figure 3.5. Compound **38** is isomorphous with **33-U** and **35/33**, crystallizing in the same $P\bar{3}$ space group with a Th–Br distance of 2.8355(8) Å, and a Th-(ring centroid) distance of 2.535 Å. The (ring centroid)–Th–Br angle is 99.6° and the (ring centroid)–Th–(ring centroid) angle is 117.3. These distances are comparable to $(C_5Me_4H)_3ThBr$[64] with a Th–Br distance of 2.8372(8) Å and Th–(ring centroid) of 2.576 Å. The (ring centroid)–Th–Br angle is 99.8° and the (ring centroid)–Th–(ring centroid) angle is 117.7°.

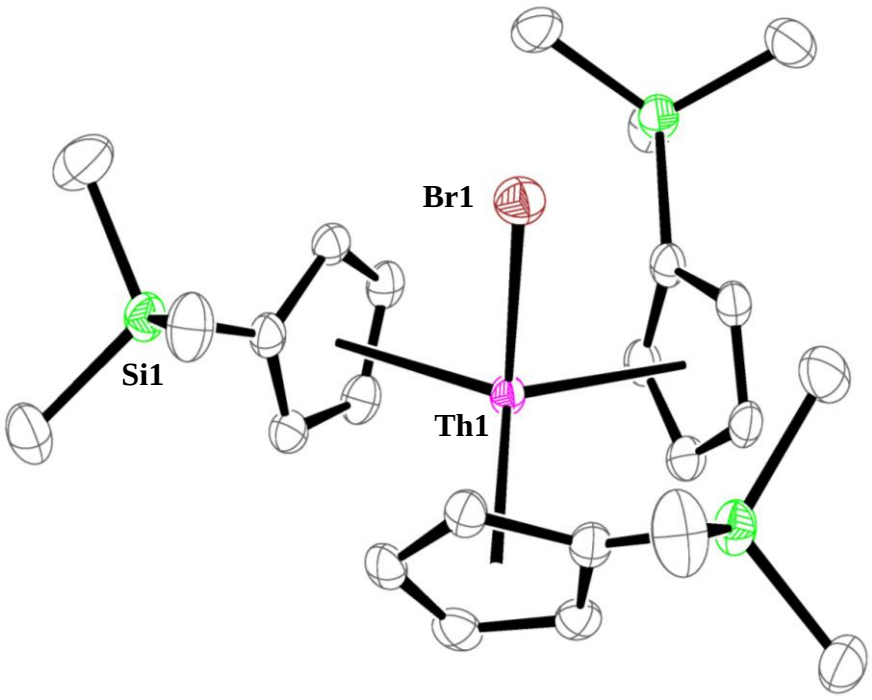

Figure 3.5. Thermal ellipsoid plot of Cp'_3ThBr, **38**, drawn at the 50% probability level with hydrogen atoms omitted for clarity.

Synthesis of Cp'_4U, 37-U. Following the synthetic route in Figure 3.1,[14-23] **35** was treated with $[HNEt_3][BPh_4]$ to form the U^{IV} cationic complex, $[Cp'_3U(THF)][BPh_4]$, **36**.[24] Addition of KCp′ to **36** provided Cp'_4U, **37-U**, in 74% yield.

Subsequently, an improved synthesis of **37-U** was found in which a bright yellow Et_2O solution of Cp'_2Pb, **30**, was added to a green/brown Et_2O solution of Cp'_3U, **8-U**. Cyclopentadienyl lead reagents have been used in the past to make *f* element cyclopentadienyl complexes.[13, 65-66] **37-U** was isolated after work up as a maroon powder in 72% yield, Figure 3.6. **37-U** could also be synthesized in yields of over 80% after work up by oxidation of **8-U** with $AgBPh_4$ in the presence on KCp′ or by $AgBPh_4$ oxidation of isolated $[K(crypt)][Cp'_4U]$, **28-U**,[13]

Figure 3.6. Oxidations with $AgBPh_4$ are commonly used to characterize reduced metal complexes,[12, 67-81] but they can also be useful synthetically.

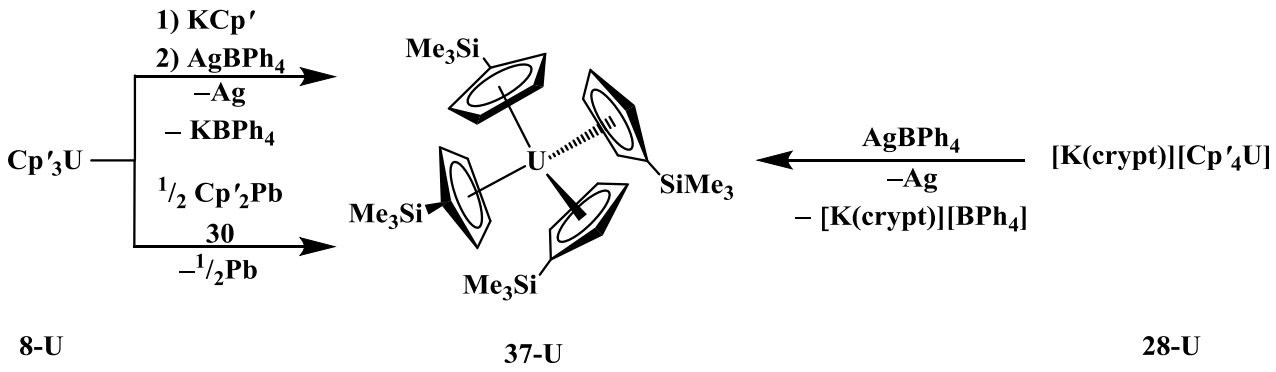

Figure 3.6. Synthetic scheme for the synthesis of Cp'_4U. **37-U**, through the oxidation of U^{III} precursors.

Structure of Cp'_4U, 37-U, and Cp'_4Th, 37-Th. Crystals of **37-U** were obtained by slow removal of hexane under reduced pressure. **37-U** was also crystallized from toluene, from Et_2O, and from a mixture of Et_2O and THF at −15 °C. The crystallographic data obtained established that each cyclopentadienyl ring was η^5–bound, i.e. the complex is $(\eta^5\text{–Cp}')_4U$, **37-U**. It has the same structural arrangement as $(\eta^5\text{–Cp})_4U$.[3-4] Unfortunately, although numerous well-shaped crystals of **37-U** were examined and gave strong diffraction patterns, detailed metrical information could not be obtained from the data. This was a result of disorder in all of the symmetry-equivalent Cp′ rings.

In the case of thorium, an excess of KCp′ reacted with $ThBr_4(THF)_4$ in warm Et_2O followed by removal of the ether and stirring in hot hexane from which a small amount of Cp'_4Th, **37-Th**, could be isolated as a 4:1 mixture of **38**:**37-Th**, by ^1H NMR spectroscopy. Crystallization from toluene at –30 °C provided crystals of both compounds from which block shaped crystals of **37-Th** could be separated *a la Pasteur*. The crystals of **37-Th** are

isomorphous with its uranium analog **37-U** and again show disorder due to the highly symmetric environment, establishing the same structural arrangement of four (η^5– Cp′) rings about the thorium center, Figure 3.7.

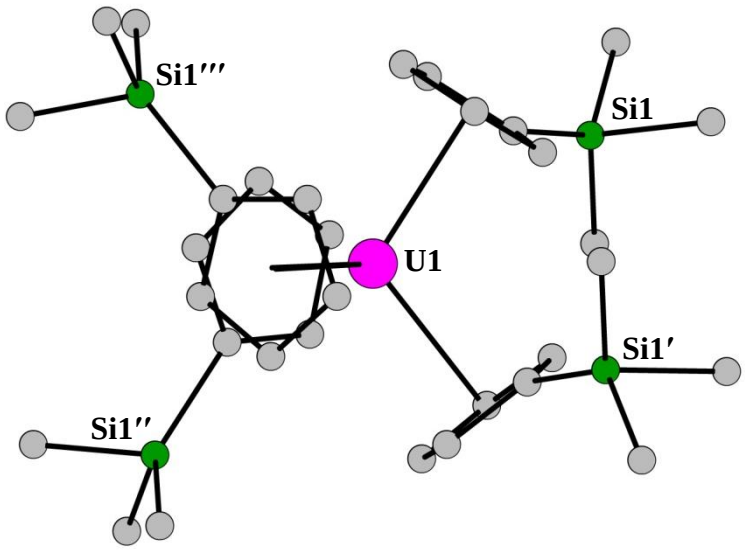

Figure 3.7. Ball and stick representation of Cp′$_4$U, **37-U**, with hydrogen atoms omitted for clarity, the analogous Cp′$_4$Th, **37-Th**, is isomorphous.

Spectroscopy of Cp′$_4$U, 37-U. The room temperature ^{1}H NMR spectrum of **37-U** contains a single set of Cp′ resonances (9:2:2) consistent with a single type of Cp′ environment with η^5–coordination. Variable temperature studies down to 193 K in C_7D_8 showed broadening and shifting of the resonances, but no splitting indicative of an η^5 to η^1 shift in coordination mode, Figure 3.8. Similarly, the ^{29}Si NMR spectrum contains a single signal both at room temperature (−62.8 ppm) and at 193 K (−78.3 ppm) in toluene-d_8. The resonance at −63.9 ppm in C_6D_6 displayed by Cp′$_4$U as well as the ^{29}Si NMR data on all of the U^{IV} compounds reported in this chapter are in the −60 to −80 ppm range previously observed for silicon-containing

complexes of U^{IV}, Chapter 1.[82] The room temperature UV/visible spectrum is similar to that of the U^{III} complex [K(crypt)][Cp′$_4$U], Chapter 2,[13] **28-U**, and the NIR spectrum shows sharp peaks similar to those of other Cp*$_2$UX$_2$ complexes (X = monoanion)[83] Figures 3.9 and 3.10

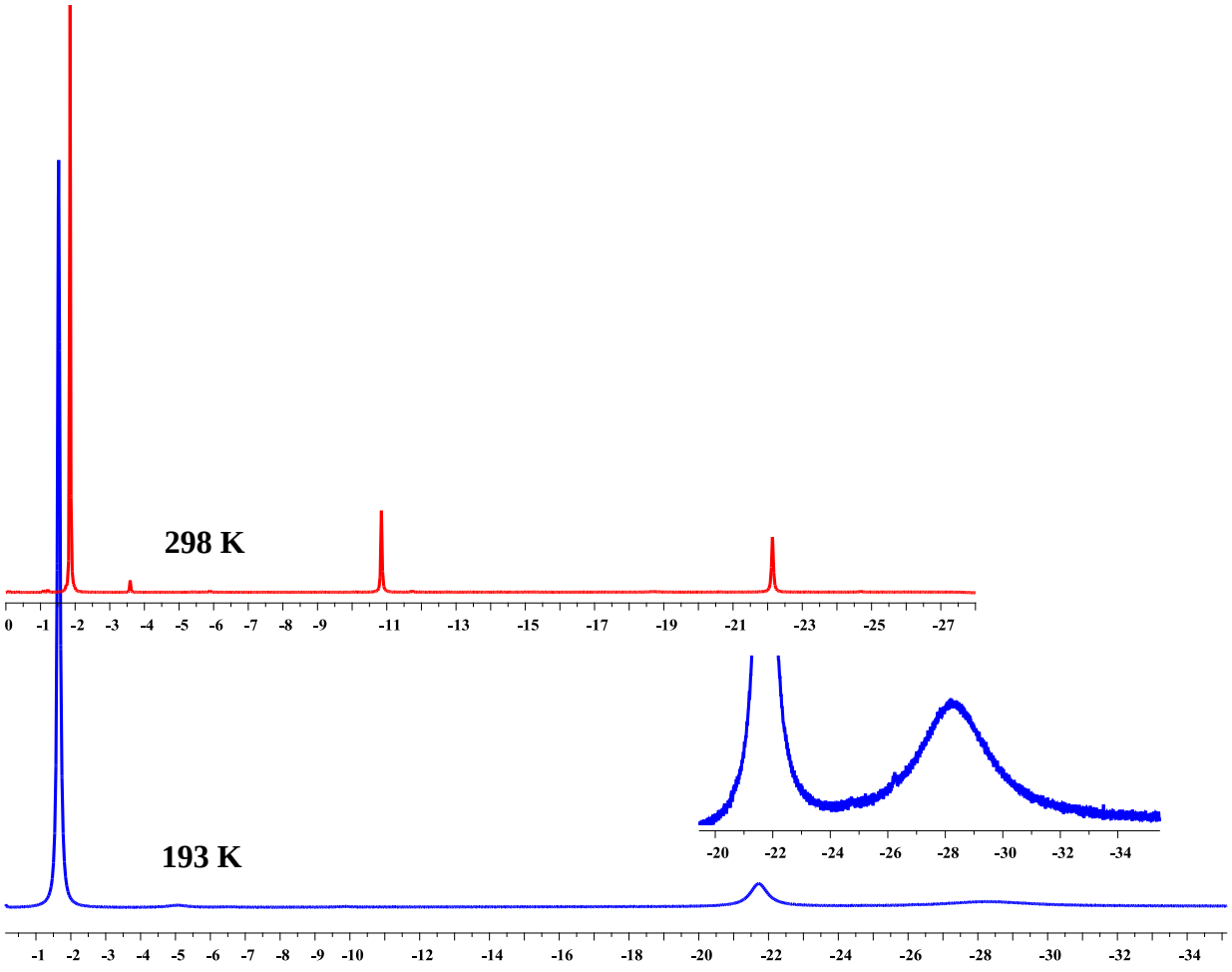

Figure 3.8. Variable Temperature ^{1}H NMR spectra of Cp′$_4$U, **37-U**, in toluene-d_8, at 298 K (top, red trace) and 193 K (bottom, blue trace).

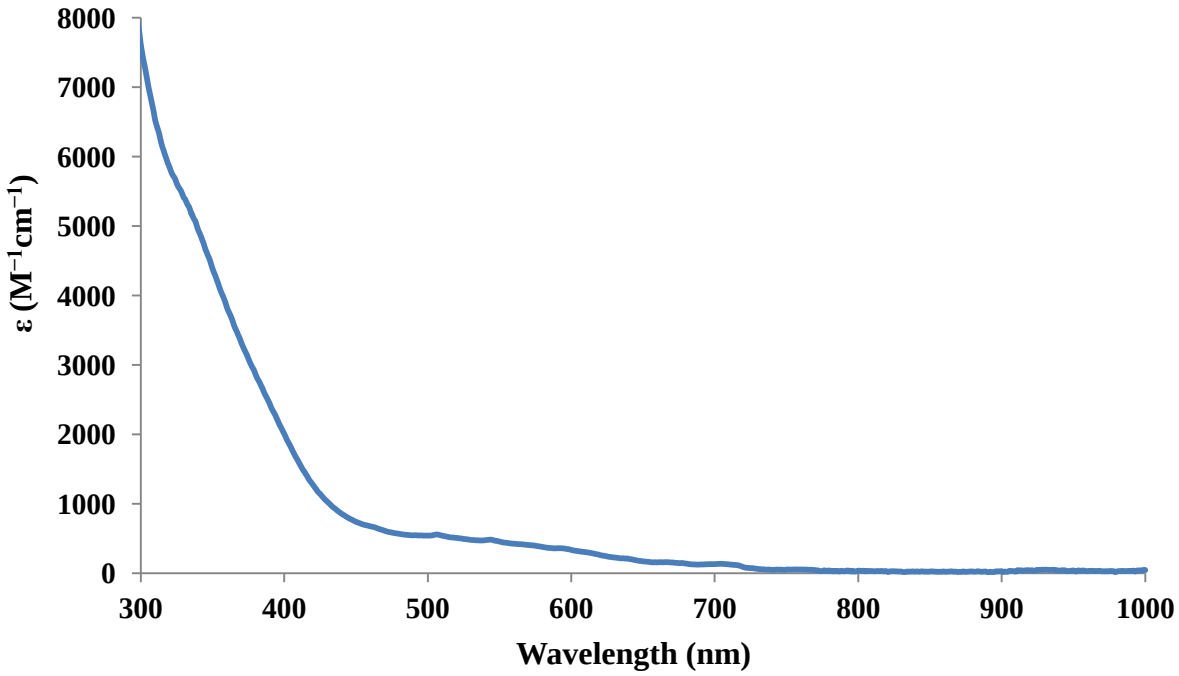

Figure 3.9. Experimental UV/vis spectrum of Cp′$_4$U, **27-U**, in THF at 298 K.

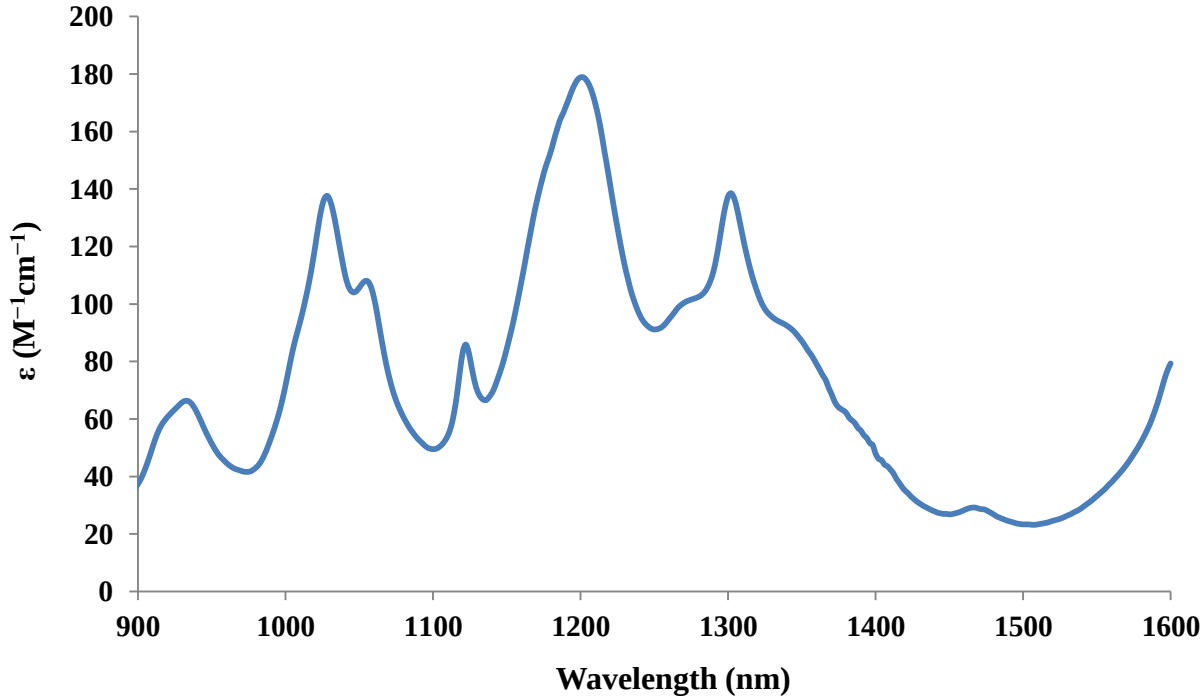

Figure 3.10. Experimental NIR spectrum of Cp′$_4$U, **37-U**, in THF at 298 K.

Synthesis of $(Cp'_4U)^{1-}$, 28-U, from Cp'_4U, 37-U, and $(Cp'_3U)^{1-}$, 21-U. An additional synthesis of the U^{III} complex **28-U**, was explored involving the comproportionation of the U^{IV} complex, Cp'_4U, **37-U**, and the U^{II} complex, [K(crypt)][Cp'_3U], **21-U**.[12] Addition of a THF solution of **37-U** to a stirred cold THF solution of **21-U** leads to a color change from black/green to red as the solution warmed to room temperature. One product, [K(crypt)][Cp'_4U], **28-U**, can be separated by crystallization at −35 °C and the other, in the mother liquor, was identified as **8-U** by ^{1}H NMR spectroscopy. Hence, the U^{IV} and U^{II} complexes react to form the U^{III} species according to eq 3.2.

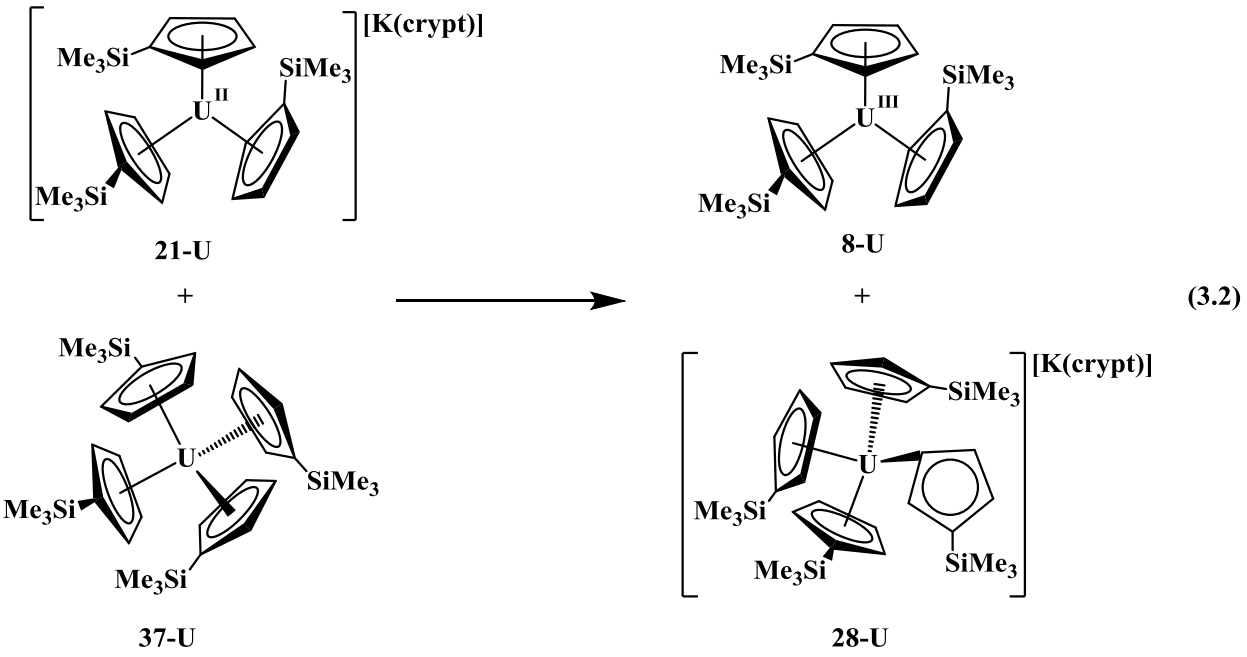

DISCUSSION

Although the Cp'_3AnX complexes (An = U; X = Cl,[15] I,[16] Me; [16] An = Th, X = Cl[9, 84-85]) have been known for over 25 years, no crystal structures of any of these compounds had been reported. Although these four organoactinide species are similar in composition, their

crystallization behavior is very different. Removal of solvent from Et_2O solutions of Cp'_3AnCl (An = U, **33-U**; Th, **33-Th**) forms a fluffy orange powder in the case of U and a fluffy white powder in the case of Th. Similar material precipitates from solutions of Et_2O at −30 °C for both **33-U** and **33-Th**. However, crystallization of **33-U** from Et_2O at −15 °C yields orange needles suitable for X-ray diffraction. Similarly, the Cp'_3UI complex, **34**, precipitates as an orange powder at −30 °C and forms X-ray quality needle-like crystals from solutions of Et_2O at −15 °C. The Cp'_3ThBr complex, **38**, is a white solid that can be crystallized from toluene at –30 °C, despite forming the same unit cell as **33-U**. In contrast, Cp'_3UMe, **35**, is an oil at room temperature and does not crystallize at either −15 °C or −30 °C.

However, a 1:4 mixture of **33-U** and **35** gives crystals suitable for X-ray diffraction and allows crystallographic data to be obtained on **35**. Historically, crystallography of mixtures of this type has been problematic since the mixture can be mistaken for a pure compound with strange bond distances as in the bond stretch isomerism case.[86] The co-crystallization is beneficial in this case since the mixture actually provides crystalline data that would otherwise be unobtainable from a pure sample. It is interesting to note that $(C_5Me_4H)_3U(CN)$ and $(C_5Me_4H)_3UCl$ also have been observed to co-crystallize with a 60/40 disorder of the CN^- and Cl^- ligands in a sample obtained from the reaction of $(C_5Me_4H)_3U$ with CN^tBu.[87]

In the case of tetrakis(cyclopentadienyl)An(IV) complexes, only a limited amount of structural data also has been in the literature. Although the Cp_4An data (An = Th, U, Np) have taken nearly 44 years to collect[3-6] and other related complexes were reported, no other structural data on this class had been obtained. Fortunately, Cp'_4U, **37-U**, the tetrakis(cyclopentadienyl) complex of interest for comparison with [K(crypt)][Cp'_4U], **28-U**, can be prepared in a number of ways in good yield although the traditional methods of ionic metathesis from uranium

tetrahalides fail. Surprisingly, the thorium analog Cp'_4Th, **37-Th**, could be isolated in low yield from the reaction of $ThBr_4(THF)_4$ and KCp'. This is likely due to the larger ionic radius of Th^{IV} (1.21 Å, 12 coordinate Shannon) compared to U^{IV} (1.17 Å).[88] Oxidative reactions using Cp'_2Pb, **30**, and $AgBPh_4$ with U^{III} precursors, Figure 3.6, proved to be the best synthetic routes to **37-U**. This demonstrates the value of considering U^{III} precursors for U^{IV} syntheses when the lower oxidation state precursors are available. The value of cyclopentadienyl lead reagents has previously been shown with Yb^{III} complexes by Lappert in the synthesis of Cp''_3Yb[66] and in the synthesis Cp^*_3Sm,[65] Cp^*_3U[19] and **28-U**.[13] Extensive precedent for use of silver salts for oxidation is also in the literature.[12, 67-81]

The fact that U^{IV} complex, **37-U**, has four η^5–Cp′ rings while the U^{III} analog, [K(crypt)][Cp'_4U], **28-U**, has three η^5–Cp′ rings and one η^1–Cp′ ring is unusual. Since the six-coordinate ionic radius of Shannon[41] for U^{III} is 0.135 Å larger than that for U^{IV}, it would be expected that the U^{III} ion could accommodate four η^5–Cp′ rings like the U^{IV} ion. Evidently the structural preferences do not depend solely on ionic radii in this case.

CONCLUSIONS

Although the trimethylsilylcyclopentadienyl complex, $(\eta^5$–$Cp')_4U$, **37-U**, is not readily synthesized by ionic metathesis from UCl_4, it can be generated from a cationic precursor, [$Cp'_3U(THF)$][BPh_4], **36**, and from the U^{III} complexes, Cp'_3U, **8-U**, and [K(crypt)][Cp'_4U], **28-U**, using Cp'_2Pb, **30**, and $AgBPh_4$, respectively. X-ray crystallography shows that this second structurally characterized tetra(cyclopentadienyl) uranium complex has four pentahapto rings which is like Cp_4U, but is different from the U^{III} complex, [K(cypt)][$(\eta^5$–$Cp')_3$](η^1–$Cp')_3U$], **28-U**. Synthesis of the precursors to **37-U** have revealed that a mixture of **35** and **33-U** is more

crystalline than **35** as a pure compound. This demonstrates an approach to obtaining crystal data on organoactinide complexes that do not readily crystallize, namely the addition of a closely related more crystalline complex.

REFERENCES

(1) Reynolds, L. T.; Wilkinson, G., *J. Inorg. Nucl. Chem.* **1956,** *2*, 246-253.

(2) Fischer, E. O.; Hristidu, Y., *Z. Naturforsch., B: Chem. Sci.* **1962,** *17b*, 275-276.

(3) Burns, J. H., *J. Am. Chem. Soc.* **1973,** *95*, 3815-3817.

(4) Burns, J. H., *J. Organomet. Chem.* **1974,** *69*, 225-233.

(5) Maier, R.; Kanellakopulos, B.; Apostolidis, C.; Meyer, D.; Rebizant, J., *J. Alloys Compd.* **1993,** *190*, 269-271.

(6) Dutkiewicz, M. S.; Apostolidis, C.; Walter, O.; Arnold, P. L., *Chem. Sci.* **2017,** *8*, 2553-2561.

(7) Bursten, B. E.; Casarin, M.; DiBella, S.; Fang, A.; Fragala, I. L., *Inorg. Chem.* **1985,** *24*, 2169-2173.

(8) Brennan, J. G.; Andersen, R. A.; Zalkin, A., *J. Am. Chem. Soc.* **1988,** *110*, 4554-4558.

(9) Weydert, M.; Brennan, J. G.; Andersen, R. A.; Bergman, R. G., *Organometallics* **1995,** *14*, 3942-3951.

(10) Dormond, A.; Duval-Huet, C.; Tirouflet, J., *J. Organomet. Chem.* **1981,** *209*, 341-354.

(11) Dormond, A.; Hepiégne, P.; Hafid, A.; Moise, C., *J. Organomet. Chem.* **1990,** *398*, C1-C5.

(12) MacDonald, M. R.; Fieser, M. E.; Bates, J. E.; Ziller, J. W.; Furche, F.; Evans, W. J., *J. Am. Chem. Soc.* **2013,** *135*, 13310-13313.

(13) Windorff, C. J.; MacDonald, M. R.; Meihaus, K. R.; Ziller, J. W.; Long, J. R.; Evans William, J., *Chem. Eur. J.* **2016,** *22*, 772-782.

(14) Kotyk, C. M.; MacDonald, M. R.; Ziller, J. W.; Evans, W. J., *Organometallics* **2015,** *34*, 2287-2295.

(15) Brennan, J. G.; Andersen, R. A.; Zalkin, A., *Inorg. Chem.* **1986,** *25*, 1756-1760.

(16) Schock, L. E.; Seyam, A. M.; Sabat, M.; Marks, T. J., *Polyhedron* **1988,** *7*, 1517-1529.

(17) Evans, W. J.; Seibel, C. A.; Ziller, J. W., *J. Am. Chem. Soc.* **1998,** *120*, 6745-6752.

(18) Evans, W. J.; Davis, B. L.; Ziller, J. W., *Inorg. Chem.* **2001,** *40*, 6341-6348.

(19) Evans, W. J.; Nyce, G. W.; Forrestal, K. J.; Ziller, J. W., *Organometallics* **2002,** *21*, 1050-1055.

(20) Evans, W. J.; Perotti, J. M.; Kozimor, S. A.; Champagne, T. M.; Davis, B. L.; Nyce, G. W.; Fujimoto, C. H.; Clark, R. D.; Johnston, M. A.; Ziller, J. W., *Organometallics* **2005,** *24*, 3916-3931.

(21) Berthet, J.-C.; Le Marechal, J.-F.; Ephritikhine, M., *J. Chem. Soc., Chem. Commun.* **1991**, 360-361.

(22) Berthet, J.-C.; Lance, M.; Nierlich, M.; Vigner, J.; Ephritikhine, M., *J. Organomet. Chem.* **1991,** *420*, C9-C11.

(23) Berthet, J.-C.; Villiers, C.; Le Maréchal, J.-F.; Delavaux-Nicot, B.; Lance, M.; Nierlich, M.; Vigner, J.; Ephritikhine, M., *J. Organomet. Chem.* **1992,** *440*, 53-65.

(24) Berthet, J.-C.; Le Marechal, J.-F.; Lance, M.; Nierlich, M.; Vigner, J.; Ephritikhine, M., *Dalton Trans.* **1992**, 1573-1577.

(25) Berthet, J.-C.; Ephritikhine, M.; Lance, M.; Nierlich, M.; Vigner, J., *J. Organomet. Chem.* **1993,** *460*, 47-53.

(26) Cendrowski-Guillaume, S. M.; Ephritikhine, M., *Dalton Trans.* **1996**, 1487-1491.

(27) Kiplinger, J. L.; Morris, D. E.; Scott, B. L.; Burns, C. J., *Organometallics* **2002,** *21*, 5978-5982.

(28) Carmichael, C. D.; Jones, N. A.; Arnold, P. L., *Inorg. Chem.* **2008,** *47*, 8577-8579.

(29) Cantat, T.; Scott, B. L.; Kiplinger, J. L., *Chem. Commun.* **2010,** *46*, 919-921.

(30) Clark, D. L.; Frankcom, T. M.; Miller, M. M.; Watkin, J. G., *Inorg. Chem.* **1992,** *31*, 1628-1633.

(31) Peterson, J. K.; MacDonald, M. R.; Ziller, J. W.; Evans, W. J., *Organometallics* **2013,** *32*, 2625-2631.

(32) Jordan, R. F.; Echols, S. F., *Inorg. Chem.* **1987,** *26*, 383-386.

(33) APEX2 Version 2014.11-0, Bruker AXS, Inc.; Madison, WI 2014.

(34) SAINT Version 8.34a, Bruker AXS, Inc.; Madison, WI 2013.

(35) Sheldrick, G. M. SADABS, Version 2014/5, Bruker AXS, Inc.; Madison, WI 2014.

(36) Sheldrick, G. M. SHELXTL, Version 2014/7, Bruker AXS, Inc.; Madison, WI 2014.

(37) International Tables for Crystallography 1992, Vol. C., Dordrecht: Kluwer Academic Publishers.

(38) APEX2 Version 2014.11-0, Bruker AXS, Inc.; Madison, WI 2014.

(39) SAINT Version 8.34a, Bruker AXS, Inc.; Madison, WI 2013.

(40) Sheldrick, G. M. SADABS, Version 2014/5, Bruker AXS, Inc.; Madison, WI 2014.

(41) Sheldrick, G. M. SHELXTL, Version 2014/7, Bruker AXS, Inc.; Madison, WI 2014.

(42) International Tables for Crystallography 1992, Vol. C., Dordrecht: Kluwer Academic Publishers.

(43) APEX2 Version 2011.4-1, Bruker AXS, Inc.; Madison, WI 2011.

(44) SAINT Version 7.68a, Bruker AXS, Inc.; Madison, WI 2009.

(45) Sheldrick, G. M. SADABS, Version 2008/1, Bruker AXS, Inc.; Madison, WI 2008.

(46) Sheldrick, G. M. SHELXTL, Version 2008/4, Bruker AXS, Inc.; Madison, WI 2008.

(47) Sheldrick, G. M. SHELXL-2013, 2013/3.

(48) International Tables for X-Ray Crystallography 1992, Vol. C., Dordrecht: Kluwer Academic Publishers.

(49) APEX2 Version 2011.4-1 Bruker AXS, Inc.; Madison, WI 2011.

(50) SAINT Version 7.68a, Bruker AXS, Inc.; Madison, WI 2009.

(51) Sheldrick, G. M. SADABS, Version 2008/1, Bruker AXS, Inc.; Madison, WI 2008.

(52) Sheldrick, G. M. SHELXTL, Version 2008/4, Bruker AXS, Inc.; Madison, WI 2008.

(53) Sheldrick, G. M. SHELXL-2013/3, 2013.

(54) International Tables for X-Ray Crystallography 1992, Vol. C., Dordrecht: Kluwer Academic Publishers.

(55) Blake, P. C.; Edelman, M. A.; Hitchcock, P. B.; Hu, J.; Lappert, M. F.; Tian, S.; Müller, G.; Atwood, J. L.; Zhang, H., *J. Organomet. Chem.* **1998,** *551*, 261-270.

(56) Wong, C.-H.; Yen, T.; Lee, T., *Acta Cryst.* **1965,** *18*, 340-345.

(57) Cloke, F. G. N.; Hawkes, S. A.; Hitchcock, P. B.; Scott, P., *Organometallics* **1994,** *13*, 2895-2897.

(58) Evans, W. J.; Nyce, G. W.; Johnston, M. A.; Ziller, J. W., *J. Am. Chem. Soc.* **2000,** *122*, 12019-12020.

(59) Perego, G.; Cesari, M.; Farina, F.; Lugli, G., *Acta Crystallogr., Sect. B.* **1976,** *32*, 3034-3039.

(60) Halstead, G. W.; Baker, E. C.; Raymond, K. N., *J. Am. Chem. Soc.* **1975,** *97*, 3049-3052.

(61) Evans, W. J.; Kozimor, S. A.; Ziller, J. W., *Organometallics* **2005,** *24*, 3407-3412.

(62) Rebizant, J.; Spirlet, M. R.; Apostolidis, C.; Kanellakopulos, B., *Acta Crystallogr., Sect. C.* **1991,** *47*, 854-856.

(63) Evans, W. J.; Kozimor, S. A.; Ziller, J. W.; Fagin, A. A.; Bochkarev, M. N., *Inorg. Chem.* **2005,** *44*, 3993-4000.

(64) Siladke, N. A.; Webster, C. L.; Walensky, J. R.; Takase, M. K.; Ziller, J. W.; Grant, D. J.; Gagliardi, L.; Evans, W. J., *Organometallics* **2013,** *32*, 6522-6531.

(65) Evans, W. J.; Forrestal, K. J.; Leman, J. T.; Ziller, J. W., *Organometallics* **1996,** *15*, 527-531.

(66) Coles, M. P.; Hitchcock, P. B.; Lappert, M. F.; Protchenko, A. V., *Organometallics* **2012,** *31*, 2682-2690.

(67) Windorff, C. J.; Chen, G. P.; Cross, J. N.; Evans, W. J.; Furche, F.; Gaunt, A. J.; Janicke, M. T.; Kozimor, S. A.; Scott, B. L., *J. Am. Chem. Soc.* **2017**.

(68) Burns, C. J.; Smith, W. H.; Huffman, J. C.; Sattelberger, A. P., *J. Am. Chem. Soc.* **1990,** *112*, 3237-3239.

(69) Boisson, C.; Berthet, J.-C.; Lance, M.; Nierlich, M.; Vigner, J.; Ephritikhine, M., *J. Chem. Soc., Chem. Commun.* **1995**, 543-544.

(70) Boisson, C.; Berthet, J. C.; Ephritikhine, M.; Lance, M.; Nierlich, M., *J. Organomet. Chem.* **1996,** *522*, 249-257.

(71) Arliguie, T.; Fourmigué, M.; Ephritikhine, M., *Organometallics* **2000,** *19*, 109-111.

(72) Enriquez, A. E.; Matonic, J. H.; Scott, B. L.; Neu, M. P., *Chem. Commun.* **2003**, 1892-1893.

(73) Evans, W. J.; Perotti, J. M.; Brady, J. C.; Ziller, J. W., *J. Am. Chem. Soc.* **2003,** *125*, 5204-5212.

(74) Carlson, C. N.; Kuehl, C. J.; Da Re, R. E.; Veauthier, J. M.; Schelter, E. J.; Milligan, A. E.; Scott, B. L.; Bauer, E. D.; Thompson, J. D.; Morris, D. E.; John, K. D., *J. Am. Chem. Soc.* **2006,** *128*, 7230-7241.

(75) Salmon, L.; Thuéry, P.; Ephritikhine, M., *Polyhedron* **2007,** *26*, 631-636.

(76) Evans, W. J.; Champagne, T. M.; Ziller, J. W., *Organometallics* **2007,** *26*, 1204-1211.

(77) Carlson, C. N.; Kuehl, C. J.; Ogallo, L.; Shultz, D. A.; Thompson, J. D.; Kirk, M. L.; Martin, R. L.; John, K. D.; Morris, D. E., *Organometallics* **2007,** *26*, 4234-4242.

(78) Fortier, S.; Wu, G.; Hayton, T. W., *Inorg. Chem.* **2009,** *48*, 3000-3011.

(79) Thomson, R. K.; Scott, B. L.; Morris, D. E.; Kiplinger, J. L., *C. R. Chimie* **2010,** *13*, 790-802.

(80) Gregson, M.; Lu, E.; McMaster, J.; Lewis, W.; Blake, A. J.; Liddle, S. T., *Angew. Chem., Int. Ed.,* **2013,** *52*, 13016-13019.

(81) Fieser, M. E.; MacDonald, M. R.; Krull, B. T.; Bates, J. E.; Ziller, J. W.; Furche, F.; Evans, W. J., *J. Am. Chem. Soc.* **2015,** *137*, 369-382.

(82) Windorff, C. J.; Evans, W. J., *Organometallics* **2014,** *33*, 3786-3791.

(83) Morris, D. E.; Da Re, R. E.; Jantunen, K. C.; Castro-Rodriguez, I.; Kiplinger, J. L., *Organometallics* **2004,** *23*, 5142-5153.

(84) Lin, Z.; Le Marechal, J. F.; Sabat, M.; Marks, T. J., *J. Am. Chem. Soc.* **1987,** *109*, 4127-4129.

(85) Jemine, X.; Goffart, J.; Ephritikhine, M.; Fuger, J., *J. Organomet. Chem.* **1993,** *448*, 95-98.

(86) Parkin, G., *Acc. Chem. Res.* **1992,** *25*, 455-460.

(87) del Mar Conejo, M.; Parry, J. S.; Carmona, E.; Schultz, M.; Brennann, J. G.; Beshouri, S. M.; Andersen, R. A.; Rogers, R. D.; Coles, S.; Hursthouse, M. B., *Chem. Eur. J.* **1999,** *5*, 3000-3009.

(88) Shannon, R., *Acta Crystallogr., Sect. A.* **1976,** *32*, 751-767.

CHAPTER 4

SMALL-SCALE METAL-BASED SYNTHESES OF LANTHANIDE IODIDE, AMIDE, AND CYCLOPENTADIENYL COMPLEXES AS SURROGATES FOR TRANSURANIC REACTIONS

INTRODUCTION[†]

This Chapter describes the exploration of synthetic details on small scale syntheses of lanthanide complexes that serve as models for transuranic chemistry. As described in the Introduction and Chapter 2, successful isolation and crystallographic characterization of Ln^{II} complexes [K(crypt)][Cp′$_3$Ln], **21-Ln** (Ln = La, Ce, Pr, Nd, Gd, Tb, Dy, Ho, Er, Y, and Lu; crypt = 2.2.2-cryptand, Cp′ = $C_5H_4SiMe_3$),[1-4] the corresponding U^{II} complex [K(crypt)][Cp′$_3$U], **21-U**,[5] as well as the La(II),[6] Th(II),[7] and U(II)[8] complexes [K(chelate)][Cp″$_3$M], **22-M** [Cp″ = $C_5H_3(SiMe_3)$–1,3; chelate = (18-crown-6)(THF)$_2$, 2.2.2-cryptand], has been possible. In light of these results, it was of interest to extend this chemistry to the heavier trans-uranium actinide elements neptunium, plutonium and americium. Indeed attempts to synthesize and isolate Np^{II} products have been made. However no definitive characterization was confirmed.[9-10]

The synthesis of complexes of plutonium is challenging due to the radioactivity of this element. Small scale reactions are preferred for safety reasons and it is desirable to conduct reactions with no more than 20 mg of metal content (0.084 mmol of ^{239}Pu). Since it is also desirable to minimize the number of reactions run and conserve the amount of plutonium used, optimization of reaction conditions is important. One method to determine optimum reaction

[†]Portions of this chapter are prepared for submission to *Inorganic Chemistry*: Windorff, C. J.; Dumas, M. T.; Ziller, J. W.; Kozimor, S. A.; Gaunt, A. G.; Evans, W. J.

conditions is to test analogous reactions with non-radioactive surrogates. Since the rare-earth metals are the closest analogs of the transuranic elements, their small-scale reactions can provide insight on how to best handle the chemistry of the radioactive actinides.

To aid in the synthesis of new transuranic complexes, small-scale reactions of several lanthanide complexes have been conducted starting from the metal, which is one convenient form in which transuranic elements are provided. The small-scale conversion of the lanthanide metals to iodides and the use of these small-scale iodide samples to generate typical *f*–element complexes, amides and cyclopentadienides, are reported here. Ce, and Nd were selected as representative surrogates for Pu and Am because they are similar in ionic radius (La^{III} = 1.03 Å, Np^{III} = 1.01 Å, Ce^{III} = 1.01 Å, Pu^{III} = 1 Å, Nd^{III} = 0.983 Å, Am^{III} = 0.975 Å for C.N. 6).[11] Some La samples were also examined to facilitate characterization by NMR spectroscopy since La^{III} is diamagnetic. The syntheses of $Ln[N(SiMe_3)_2]_3$, **15-Ln**, Cp'_3Ln, **8-Ln**, Cp''_3Ln, **20-Ln**, and $(C_5Me_4H)_3Ln$, **32-Ln**, are discussed since these are well established classes of *f*–element complexes and include precursors to complexes of new +2 ions.[1-8, 10, 12-15] Both the reactions and the complexes discussed are well precedented in the literature. The purpose of this study was to evaluate yield and purity available from these reactions *on a small scale* and the viability of these small-scale samples as starting materials. This research supported the isolation of the first molecular example of a Pu^{II} complex, Chapter 5,[13] and should be applicable to other transuranic studies.[16-27]

Metal iodide precursors are common in actinide chemistry[28-42] and UI_3L_x, UI_4L_x, and ThI_4L_x are most commonly synthesized from the elements.[28-33] Lanthanide triiodides are synthesized in many ways both in solution and in the solid state.[43] These include synthesis from the Ln_2O_3 oxides with NH_4I at elevated temperature,[44] from the oxides or metal with HI,

followed by dehydration with NH_4I,[45-48] from the metal and iodine,[49-50]diiodoethane, iodoform,[51-54] AlI_3, and HgI_2.[34, 43, 55-57] The lanthanide triiodides can be dissolved in THF to form the solvated species that crystallize in a variety of forms including $LnI_3(THF)_4$ (Ln = La, Pr, Ce),[49, 58-59] $[LnI_2(THF)_5][LnI_4(THF)_2]$ (Ln = Nd, Sm, Gd, Dy, Er, Tm, Yb, Y),[49, 60-64] $[LnI_2L_5][I]$, (L = THF,[62] py[50]) and, $[LnI_2(THF)_5][I_3]$ (Ln = La,[62] Yb[50]). A triiodide containing complex analogous to the latter compound has also been observed with plutonium: $[PuI_2(THF)_4(py)][I_3]$ (py = pyridine, NC_5H_5).[41] While numerous THF solvates of LnI_3 are characterized, there are fewer reports on pyridine and ether solvates,[50] and a study on the dissolution of LnI_3 in acetonitrile showed formation of $LnI_3(MeCN)_5$ (Ln = La, Ce) and $[Nd(MeCN)_9]_2[NdI_5(MeCN)][NdI_6][I]$.[65] LnI_3 is reported to dissolve in pyridine to form $LnI_3(py)_x$, but characterization of the complexes was not reported.[66-69] **15-Ln**, **8-Ln**, **20-Ln**, and **32-Ln** are typically synthesized from $LnCl_3(THF)_x$ and an alkali metal salt of the ligand, though some syntheses have utilized $Ln(O_3SCF_3)_3$ (Ln = La,[70] Ce[71]) or, in the case of cyclopentadienyl ligands, protonolysis from **15-Ln**.[72-73] Iodides have been used to synthesize $\{[C_5H_3(EMe_3)_2]_2LnI\}_2$ (Ln = La, Ce; E = C, Si)[74] and $Cp''_2LaI(THF)$.[74]

In this Chapter, the small scale synthesis of several classes of lanthanide complexes are described to demonstrate that these are viable routes for radioactive actinide analogs. The following classes of compounds are described: the LnI_3L_x solvates including $LnI_3(OEt_2)_x$, **39-Ln**, $LnI_3(py)_4$, **40-Ln**, the dissolution of **39-Ln** in THF to form $LnI_3(THF)_4$, **41-Ln**, and the use of $LnI_3(OEt_2)_x$, **39-Ln** to form common lanthanide amides, $Ln[N(SiMe_3)_2]_3$, **15-Ln**, and metallocenes, Cp'_3Ln, **8-Ln**, Cp''_3Ln, **20-Ln**, $(C_5Me_4H)_3Ln$, **32-Ln** (Ln = La, Ce, Nd), the reduction of **8-Ln** to **21-Ln•THF**, and the isolation of [K(crypt)][Cp''_3Nd], **22-Nd**.

EXPERIMENTAL

All manipulations and syntheses described below were conducted with the rigorous exclusion of air and water using standard Schlenk line and glovebox techniques under an argon or dinitrogen atmosphere. Solvents (THF, Et_2O, toluene, hexane, and pentane) were sparged with UHP argon (Praxair) and dried by passage through columns containing Q-5 and molecular sieves prior to use. Pyridine was dried over sodium, degassed, and distilled. All ethereal solvents and pyridine were stored over activated 4 Å molecular sieves. Deuterated NMR solvents (Cambridge Isotopes) were dried over sodium benzophenone ketyl, degassed by three freeze-pump-thaw cycles, and vacuum transferred before use. ^{1}H, $^{13}C\{^{1}H\}$ and $^{29}Si\{^{1}H\}$ NMR spectra were recorded on a Bruker GN500 MHz or Cryo500 spectrometer operating at 499.3 125, and 99.2 MHz, respectively, at 298 K unless otherwise stated. ^{1}H and $^{13}C\{^{1}H\}$ NMR spectra were referenced internally to solvent resonances, $^{29}Si\{^{1}H\}$ NMR spectra were referenced externally to $SiMe_4$. Elemental analyses were performed on a Perkin-Elmer 2400 Series II CHNS elemental analyzer. Lanthanum powder under oil (99.9% REO, Strem), was pumped into the glovebox overnight, decanted, washed with hexane several times and dried under vacuum. Ce, and Nd metal (99.5% REO, Stanford Materials Corporation) were pumped into the glovebox, filed to remove any oxide layer, and filed to form shavings. An $Nd_2Fe_{14}B$ magnet (United Nuclear) was passed over the filings to remove any iron particles that detached from the file. Iodine (99.8%, Acros) was sublimed before use. $KN(SiMe_3)_2$ (Aldrich) was dissolved in toluene, centrifuged, decanted, and dried under reduced pressure. Cp'_3Pr, **8-Pr**,[3] $UI_3(py)_4$, **40-U**,[29] and KC_5Me_4H[31] were prepared according to the literature. KCp″ was prepared according to the synthesis of KCp'_3.[75] $UI_3(py)_4$, **40-U**, was crystallized by diffusion of ether into a pyridine solution at ambient glovebox temperature.

$LaI_3(OEt_2)_x$, 39-La. Solid iodine (1.400 g 5.500 mmol) was added to a suspension of lanthanum powder (0.500 g, 3.60 mmol) in ether (40 mL) in a 100 mL round bottom flask and stirred for 4 days. During this time a gray powder precipitated, a pale orange color persisted in solution, and there was no evidence of remaining metal. The mixture was filtered on a 350 mL M frit and washed with ether (2 × 20 mL) and hexane (2 × 20 mL) until the filtrate was colorless. The gray solids were transferred to a tared scintillation vial and held under reduced pressure (10^{-3} torr) for 4h to yield a gray powder characterized as $LaI_3(OEt_2)_{1.6}$, (1.75 g, 76%, based on La) by elemental analysis. Anal. Calcd for $LaI_3(OEt_2)_{1.6}$: C, 12.45; H, 2.61. Found: C, 12.39; H, 2.46. A sample placed under 10^{-6} torr for 60 h analyzed as $LaI_3(OEt_2)_{0.75}$. Anal. Calcd for $LaI_3(OEt_2)_{0.75}$: C, 6.26; H, 1.31. Found: C, 7.24; H, 1.29

$CeI_3(OEt_2)_x$, 39-Ce. Following the procedure for **39-La**, iodine (1.240 g 4.886 mmol) was combined with Ce shavings (0.450 g, 3.22 mmol) to yield a gray powder characterized as $CeI_3(OEt_2)_{1.8}$, (1.82 g, 89%, based on Ce) by elemental analysis. Anal. Calcd for $CeI_3(OEt_2)_{1.8}$: C, 13.22; H, 2.77. Found: C, 13.93; H, 2.63. A sample placed under 10^{-6} torr for 60 h analyzed as $CeI_3(OEt_2)_{0.66}$. Anal. Calcd for $CeI_3(OEt_2)_{0.66}$: C, 5.62; H, 1.18. Found: C, 6.23; H, 1.05.

$NdI_3(OEt_2)_x$, 39-Nd. Following the procedure for **39-La**, iodine (0.752 g, 2.96 mmol), was combined with Nd shavings (0.284 g, 1.97 mmol) to yield a pale blue powder characterized as $NdI_3(OEt_2)_{1.5}$, (860 mg, 69%, based on Nd) as determined by elemental analysis. Anal. Calcd for $NdI_3(OEt_2)_{1.5}$: C, 11.33; H, 2.38. Found: C, 11.23; H, 2.04. A sample placed under 10^{-6} torr for 60 h analyzed as $NdI_3(OEt_2)_{0.66}$. Anal. Calcd for $NdI_3(OEt_2)_{0.66}$: C, 6.26; H, 1.31. Found: C, 7.24; H, 1.29.

$LaI_3(py)_4$, 40-La. When a solution of iodine (141 mg, 0.554 mmol) in pyridine (4 mL) was added to a pyridine (2 mL) suspension of lanthanum powder (51 mg 0.37 mmol), the

mixture quickly turned black and was stirred for 2 days. The mixture was centrifuged to remove a small amount of black material and the volatiles were removed under reduced pressure to yield a brown oil. The oil was triturated with ether, decanted, and dried under reduced pressure to yield $LaI_3(py)_4$, **40-La** (265 mg, 86%) as a brown solid. Colorless X-ray quality crystals were grown by diffusion of ether into a concentrated pyridine solution at −15 °C. ^{1}H NMR (C_6D_6): δ 9.06 (br s, *o-py*, 8H), 6.79 (t, J_H = 7.0 Hz, *p-py*, 4H), 6.51 (m, *m-py*, 8H); $^{13}C\{^1H\}$ (C_6D_6): δ 150.63 (*o-py*), 136.61 (*p-py*), 123.78 (*m-py*). Anal. Calcd for $LaI_3(py)_{3.5}$: C, 26.39; H, 2.21; N, 6.16. Found: C, 26.64; H, 2.41; N, 6.12.

$CeI_3(py)_4$, 40-Ce. Following the procedure for **40-La**, iodine (254 mg 1.08 mmol) was combined with Ce shavings (100 mg, 0.714 mmol) to yield $CeI_3(py)_4$, **40-Ce** (512 mg 57%) as a brown solid. ^{1}H NMR (C_6D_6): δ 9.49 (br s, *o-py*, 8H), 7.54 (br s, *p-py*, 4H), 7.39 (br s, *m-py*, 8H). Anal. Calcd for $C_{15}H_{15}N_3I_3Ce$: C, 23.76; H, 1.99; N, 5.54. Found: C, 24.07; H, 1.98; N, 5.22.

$NdI_3(py)_4$, 40-Nd. Following the procedure for **40-La**, iodine (135 mg 0.530 mmol) was combined with Nd shavings (49 mg 0.34 mmol) to yield $NdI_3(py)_4$, **40-Nd**, (259 mg 91%) as a brown solid. ^{1}H NMR (C_6D_6): δ 9.7 (br s, *p-py*, 4H) 7.7 (br s, *py*, 8H). Only two of the expected resonances were observed due to the paramagnetism of the Nd^{III} ion. Anal. Calcd for $C_{15}H_{15}N_3I_3Nd$: C, 23.64; H, 1.98; N, 5.51. Found: C, 23.71; H, 2.26; N, 5.16.

$LaI_3(THF)_4$, 41-La. As an alternative to the published procedures to **41-La**,[49, 53, 76-77] $LaI_3(OEt_2)_{1.6}$ (12 mg, 0.019 mmol) was dissolved in THF (3 mL) to give a colorless solution. This was filtered and the volatiles were removed under reduced pressure to give $LaI_3(THF)_4$ (15 mg, quantitative) as a white solid. Colorless X-ray quality crystals of **41-La** were grown over 2 weeks from a hot THF solution cooled to –30 °C which matched the unit cell of $LaI_3(THF)_4$.[59]

^{1}H NMR (C_6D_6): δ 3.77 (s, *THF*), 1.40 (s, *THF*); $^{13}C\{^{1}H\}$ NMR (C_6D_6): δ 69.50 (*THF*), 25.65 (*THF*). When **41-La** was crystallized from hot toluene cooled to ambient glovebox temperature, colorless crystals of $[LaI_2(THF)_5][LaI_4(THF)_2]$, **41-La′**, were isolated after 1 week and characterized by X-ray crystallography.

$CeI_3(THF)_4$, 41-Ce. As an alternative to the published procedures for **41-Ce**,[49, 57-58, 76-77] following the procedure for **41-La**, $CeI_3(OEt_2)_{0.66}$ (13 mg 0.023 mmol) was dissolved in THF (3 mL) to give $CeI_3(THF)_4$ (18 mg, 95%) as a white solid. Colorless X-ray quality crystals of **41-Ce** were grown over 2 weeks from a hot THF solution cooled to –30 °C which matched the unit cell of $CeI_3(THF)_4$.[58] ^{1}H NMR (C_6D_6): δ 3.75 (s, *THF*), 1.55 (s, *THF*); $^{13}C\{^{1}H\}$ NMR (C_6D_6): δ 68.23 (*THF*), 26.06 (*THF*).

$NdI_3(THF)_4$, 41-Nd. As an alternative to the published procedures for **41-Nd**[54, 78] following the procedure for **41-La**, $NdI_3(OEt_2)_{0.66}$ (13 mg, 0.023 mmol) was dissolved in THF (3 mL) to give $NdI_3(THF)_4$ (16 mg, quantitative) as a pale blue solid. Pale blue X-ray quality crystals of **41-Nd** were grown over 2 weeks from a hot THF solution cooled to –30 °C which matched the unit cell of $NdI_3(THF)_4$.[79] ^{1}H NMR (C_6D_6): δ 3.78 (s, br $\nu_{1/2}$ = 115 Hz, *THF*), 1.60 (s, br $\nu_{1/2}$ = 100 Hz, *THF*).

$La[N(SiMe_3)_2]_3$, 15-La. As an alternative to the published procedure,[80] a toluene (2 mL) solution of $KN(SiMe_3)_2$ (60 mg, 0.30 mmol) was added to a toluene (1 mL) suspension of $LaI_3(OEt_2)_{1.6}$ (48 mg 0.075 mmol). The solution was stirred overnight, volatiles were removed under reduced pressure and the product was extracted in pentane. Removal of the volatiles under reduced pressure yielded **15-La** as a white solid (44 mg, 95%) as confirmed by ^{1}H NMR analysis.[80] (C_6D_6): δ 0.28 (s, Si*Me*$_3$, 54H). $^{13}C\{^{1}H\}$ (C_6D_6): δ 3.67 (Si*Me*$_3$).

Isolation of {(THF)[(SiMe$_3$)$_2$N]$_2$La}$_2$(μ–O), 42. On one occasion, attempted crystallization of **15-La** from a concentrated Et_2O solution at –30 °C in the presence of adventitious oxygen and THF yielded colorless X-ray quality crystals of **42**.

Ce[N(SiMe$_3$)$_2$]$_3$, 15-Ce. As an alternative to the published procedure,[80] KN(SiMe$_3$)$_2$ (44 mg, 0.22 mmol) was added to a stirred slurry of $CeI_3(OEt_2)_{0.66}$ (40 mg, 0.071 mmol) in toluene (2 mL), which quickly turned bright yellow and was stirred overnight. Volatiles were removed under reduced pressure and the product was extracted into pentane and dried under reduced pressure to yield a yellow solid identified as **15-Ce** (30 mg, 70%) by ^{1}H NMR spectroscopy.[80] ^{1}H NMR (C_6D_6): δ −3.3 (s, Si*Me*$_3$, 54H).

Nd[N(SiMe$_3$)$_2$]$_3$, 15-Nd. As an alternative to the published procedure,[80] following the procedure for **15-Ce**, KN(SiMe$_3$)$_2$ (40 mg, 0.20 mmol) was combined with $NdI_3(OEt_2)_{0.66}$ (40 mg, 0.068 mmol) to give a blue solid identified as **15-Nd** (30 mg, 71%) as identified by ^{1}H NMR spectroscopy.[80] ^{1}H NMR (C_6D_6): δ −6.1 (s, Si*Me*$_3$, 54H).

Cp′$_3$Ce, 8-Ce. An ether (2 mL) solution of KCp′ (71 mg, 0.40 mmol) was added to a stirred slurry of $CeI_3(OEt_2)_{1.5}$ (70 mg, 0.134 mmol) in Et_2O (2 mL) . The solution quickly turned bright blue while forming white insoluble material. The blue mixture was stirred overnight and centrifuged to remove white insoluble material (presumably KI). The filtrate was dried under reduced pressure, extracted into pentane, filtered, and dried under reduced pressure to give a royal blue solid, identified as **8-Ce** (29 mg, 39 %) by ^{1}H NMR analysis.[72]

In situ Synthesis of 8-Ce. Solid iodine (30 mg, 0.12 mmol) was added to an ether (3 ml) suspension of cerium metal (11 mg, 0.082 mmol). After the mixture was stirred for 24 h, the solution was colorless and a pale white precipitate was present. The volume was reduced to 0.5 mL under reduced pressure and an ether (2 mL) solution of KCp′ (46 mg, 0.26 mmol) was added.

A blue solution quickly formed along with white insoluble material. The mixture was stirred overnight and centrifuged to remove the white insoluble material (presumably KI). The filtrate was dried under reduced pressure, extracted into pentane, filtered, and dried under reduced pressure to give a blue solid, identified as **8-Ce** (17 mg, 38% based on Ce metal) by ^{1}H NMR spectroscopy.[72]

Cp′$_3$Nd, 8-Nd. Solid iodine (36 mg, 0.14 mmol) was added to an ether (3 ml) suspension of neodymium metal (15 mg, 0.10 mmol). After the mixture was stirred for 24 h, the solution was colorless and a pale blue precipitate was present. The volume was reduced to 0.5 mL under reduced pressure and an ether (2 mL) solution of KCp′ (55 mg, 0.31 mmol) was added. A blue solution quickly formed which turned to mint green after approximately 3 h with the formation of white insoluble material. The mixture was stirred overnight and centrifuged to remove the white insoluble material (presumably KI). The filtrate was dried under reduced pressure, extracted into pentane, filtered, and dried under reduced pressure to give a mint green solid, identified as **8-Nd** (40 mg, 77% based on I_2) by ^{1}H NMR spectroscopy.[81]

Cp′′$_3$Ce, 20-Ce. As an alternative to the published procedure, [71-72, 82] solid iodine (30 mg, 0.12 mmol) was added to a stirred suspension of cerium shavings (11 mg, 0.082 mmol) in Et_2O (2 ml) and stirred 2 d during which time a colorless solid precipitated. Volatiles were removed under reduced pressure and washed with several portions of hexane and dried under reduced pressure. When an Et_2O (3 ml) solution of KCp′′ (65 mg, 0.26 mmol) was added, the solution quickly became green. Within 15 min the solution turned dark blue and a white solid precipitated (presumably KI). The mixture was stirred overnight and the volatiles were removed under reduced pressure. The product was extracted into hexane, filtered, and dried under

reduced pressure to give a royal blue solid identified as **20-Ce** (35 mg, 55%) by ^{1}H NMR spectroscopy.[72]

Cp′′$_3$Nd, 20-Nd. As an alternative to the published procedure,[73, 82-83] following the procedure for **20-Ce** solid iodine (41 mg 0.162 mmol) was combined with neodymium shavings (13 mg 0.090 mmol) and KCp′′ (70 mg 0.28 mmol) to give a green solid identified as **20-Nd** (55 mg, 80%) by ^{1}H NMR spectroscopy.[73, 82] ^{29}Si{^{1}H} NMR (C_6D_6): δ −61.3 (*Si*Me$_3$).

(C$_5$Me$_4$H)$_3$La, 32-La. As an alternative to the published procedure,[84] solid KC_5Me_4H (51 mg, 0.32 mmol) was added to a toluene (5 mL) suspension of $LaI_3(OEt_2)_{1.66}$ (49 mg 0.076 mmol), the mixture quickly turned yellow and was stirred overnight. The mixture centrifuged to remove white solids (presumable KI and excess KC_5Me_4H) and was dried under reduced pressure to give a yellow solid identified as **32-La** (36 mg 94%) by ^{1}H NMR spectroscopy.[84]

(C$_5$Me$_4$H)$_3$Ce, 32-Ce. As an alternative to the published procedure,[85] following the procedure for **32-La**, KC_5Me_4H (51 mg, 0.32 mmol) was combined with $CeI_3(OEt_2)_{1.5}$ (49 mg 0.078 mmol), to give a blue solid identified as **32-Ce** (30 mg, 76 %) by ^{1}H NMR spectroscopy.[86]

(C$_5$Me$_4$H)$_3$Nd, 32-Nd. As an alternative to the published procedure,[87] following the procedure for **32-La**, KC_5Me_4H (35 mg, 0.22 mmol) was combined with $NdI_3(OEt_2)_{0.66}$ (40 mg, 0.070 mmol) to give a green solid identified as **32-Nd** (25 mg, 71%) by ^{1}H NMR spectroscopy.[87] X-ray quality crystals were grown from a hot toluene solution cooled to −30 °C.

[K(crypt)][Cp′$_3$Ce]•THF, 21-Ce•THF. Similar to the published procedure[4] THF (0.5 mL) was added to a blue Et_2O (1.5 mL) solution of **8-Ce** (20 mg, 0.036 mmol) and crypt (16 mg, 0.042 mmol) causing an instant color change to yellow consistent with the formation of Cp′$_3$Ce(THF).[88] A pipette was packed with a glass fiber circle and KC_8 (40 mg, 30 mmol) to form a flash reduction column. The yellow solution, KC_8 reduction column, THF, Et_2O, an

empty 20 mL glass scintillation vial, and several glass pipettes were placed in a −30 °C freezer for 2 h. The solution was removed from the freezer and quickly passed through the reduction column into the new vial causing an instant color change to dark purple. The column was washed with cold THF until the effluent was colorless (1.5 mL) and the solution was returned to the freezer. After 2 h, the solution was carefully layered with cold Et_2O (4 mL) and returned to the freezer. Within 1 day dark purple/black X-ray quality crystals formed. A small sample was separated for unit cell analysis and the colorless mother liquor was decanted and washed with pentane (3 × 1 mL) and dried under reduced pressure. The purple crystals were identified as **21-Ce•THF** (24 mg, 65% crystalline yield) by unit cell analysis.[4]

[K(crypt)][Cp′$_3$Nd]•THF, 21-Nd•THF. Similar to the published procedures,[4] and following the procedure for **21-Ce•THF**, **8-Nd** (25 mg, 0.046 mmol) and crypt (18 mg, 0.048 mmol) were dissolved in Et_2O and THF added causing a color change from green to pale blue, and gave dark purple/black crystals identified as **21-Nd•THF** (35 mg, 73% crystalline yield) by unit cell analysis.[4]

[K(crypt)][Cp′$_3$Pr]•THF, 21-Pr•THF. Similar to the published procedures,[3] and following the procedure for **21-Ce•THF**, **8-Pr** (19 mg, 0.035 mmol) and crypt (13 mg, 0.036 mmol) were dissolved in Et_2O and THF added causing a color change from green to pale blue, and gave dark/black crystals identified as **21-Pr•THF** (24 mg, 65% crystalline yield) by unit cell analysis. [3]

[K(crypt)][Cp′′$_3$Nd], 22-Nd. KC_8 (25 mg, 0.18 mmol) was added to a green mixture of **20-Nd** (80 mg, 0.10 mmol) and crypt (40 mg, 0.11 mmol) in a 4:1 Et_2O:THF mixture (4 ml), at ambient temperature, causing an immediate change to dark purple. The mixture was stirred for 5 min, filtered to removed black insolubles (presumably graphite), washed with Et_2O (3 × 1 mL),

until the filtrate was colorless, and the volatiles were removed under reduced pressure to give a purple oil. The purple oil was triturated with hexane to give **22-Nd** as a dark purple powder (115 mg, 94%). Anal. Calcd. for $C_{57}H_{99}N_2O_6Si_6KNd$, C: 51.55, H: 8.40, N: 2.36; Found, C: 51.61, H: 8.62, N: 2.43. X-ray quality crystals were grown from a concentrated Et_2O solution layered with hexane at −30 °C.

X-ray Data Collection, Structure Determination, and Refinement. Crystallographic details for compounds $LaI_3(py)_4$, **40-La**, $UI_3(py)_4$, **40-U**, $[LaI_2(THF)_5][LaI_4(THF)_2]$, **41-La′**, $(C_5Me_4H)_3Nd$, **32-Nd** and [K(crypt)][Cp″$_3$Nd], **22-Nd**, are summarized in the text below and in Table 4.1.

X-ray Data Collection, Structure Solution and Refinement for $LaI_3(py)_4$, 40-La. A colorless crystal of approximate dimensions 0.280 x 0.257 x 0.244 mm was mounted on a glass fiber and transferred to a Bruker SMART APEX II diffractometer. The APEX2[89] program package and the CELL_NOW[90] were used to determine the unit-cell parameters. Data was collected using a 15 sec/frame scan time for a sphere of diffraction data. The raw frame data was processed using SAINT[91] and TWINABS[92] to yield the reflection data file (HKLF 5 format). [93] Subsequent calculations were carried out using the SHELXTL[94] program. The diffraction symmetry was 2/*m* and the systematic absences were consistent with the monoclinic space group $P2_1/n$ that was later determined to be correct.

The structure was solved by direct methods and refined on F^2 by full-matrix least-squares techniques. The analytical scattering factors[95] for neutral atoms were used throughout the analysis. Hydrogen atoms were located from a difference-Fourier map and refined (x,y,z and U_{iso}). Hydrogen atoms were included using a riding model.

At convergence, wR2 = 0.0705 and Goof = 1.163 for 254 variables refined against 6614 data (0.74Å), R1 = 0.192 for those 6158 with I > 2.0σ(I). The structure was refined as a two-component twin, BASF[96] = 0.44.

X-ray Data Collection, Structure Solution and Refinement for $UI_3(py)_4$, 40-U. A purple/green crystal of approximate dimensions 0.114 x 0.131 x 0.459 mm was mounted on a loop and transferred to a Bruker SMART APEX II diffractometer. The APEX2[97] program package was used to determine the unit-cell parameters and for data collection (15 sec/frame scan time for a sphere of diffraction data). The raw frame data was processed using SAINT[98] and SADABS[99] to yield the reflection data file. Subsequent calculations were carried out using the SHELXTL[100] program. The diffraction symmetry was 2/*m* and the systematic absences were consistent with the monoclinic space group $P2_1/n$ that was later determined to be correct.

The structure was solved by direct methods and refined on F^2 by full-matrix least-squares techniques. The analytical scattering factors[101] for neutral atoms were used throughout the analysis. Hydrogen atoms were located from a difference-Fourier map and refined (x,y,z and U_{iso}). Hydrogen atoms were included using a riding model.

At convergence, wR2 = 0.0498 and Goof = 1.102 for 253 variables refined against 6738 data (0.74 Å), R1 = 0.0221 for those 6295 data with I > 2.0σ(I).

X-ray Data Collection, Structure Solution and Refinement for $[LaI_2(THF)_5][LaI_4(THF)_2]$, 41-La′. A colorless crystal of approximate dimensions 0.118 x 0.202 x 0.269 mm was mounted in a loop and transferred to a Bruker SMART APEX II diffractometer. The APEX2[102] program package was used to determine the unit-cell parameters and for data collection (25 sec/frame scan time for a sphere of diffraction data). The raw frame data was processed using SAINT[103] and SADABS[104] to yield the reflection data file. Subsequent

calculations were carried out using the SHELXTL[105] program. The diffraction symmetry was 2/*m* and the systematic absences were consistent with the monoclinic space groups *Cc* and *C*2/*c*. It was later determined that space group *C*2/*c* was correct.

The structure was solved by dual space methods and refined on F^2 by full-matrix least-squares techniques. The analytical scattering factors[106] for neutral atoms were used throughout the analysis. Hydrogen atoms were located from a difference-Fourier map and refined (x,y,z and U_{iso}). Hydrogen atoms were included using a riding model.

At convergence, wR2 = 0.0528 and Goof = 1.007 for 197 variables refined against 4811 data (0.74Å), R1 = 0.0242 for those 4216 data with $I > 2.0\sigma(I)$. The absolute structure was assigned by refinement of the Flack parameter.[107]

X-ray Data Collection, Structure Solution and Refinement for $(C_5Me_4H)_3Nd$, 32-Nd. A green crystal of approximate dimensions 0.268 x 0.246 x 0.169 mm was mounted on a glass fiber and transferred to a Bruker SMART APEX II diffractometer. The APEX2[1] program package was used to determine the unit-cell parameters and for data collection (20 sec/frame scan time for a sphere of diffraction data). The raw frame data was processed using SAINT[2] and SADABS[3] to yield the reflection data file. Subsequent calculations were carried out using the SHELXTL[4] program. Three systematic absences were consistent with the hexagonal space groups R3 and $R\bar{3}$. The centrosymmetric space group $R\bar{3}$ was assigned and later determined to be correct.

The structure was solved by direct methods and refined on F^2 by full-matrix least-squares techniques. The analytical scattering factors[5] for neutral atoms were used throughout the analysis. Hydrogen atoms were included using a riding model.

At convergence, wR2 = 0.0317 and Goof = 1.134 for 90 variables refined against 1980 data (0.74 Å), R1 = 0.0135 for those 1904 data with I > 2.0σ(I). The structure refined as a merohedral twin.

X-ray Data Collection, Structure Solution and Refinement for [K(crypt)][Cp′′$_3$Nd], 22-Nd. A purple crystal of approximate dimensions 0.484 x 0.398 x 0.306 mm was mounted on a glass fiber and transferred to a Bruker SMART APEX II diffractometer. The APEX2[108] program package was used to determine the unit-cell parameters and for data collection (20 sec/frame scan time for a sphere of diffraction data). The raw frame data was processed using SAINT[109] and SADABS[110] to yield the reflection data file. Subsequent calculations were carried out using the SHELXTL[111] program. There were no systematic absences nor any diffraction symmetry other than the Friedel condition. The centrosymmetric triclinic space group $P\bar{1}$ was assigned and later determined to be correct.

The structure was solved by direct methods and refined on F^2 by full-matrix least-squares techniques. The analytical scattering factors[112] for neutral atoms were used throughout the analysis. Hydrogen atoms were included using a riding model.

At convergence, wR2 = 0.0600 and Goof = 1.061 for 622 variables refined against 15275 data (0.74 Å), R1 = 0.0239 for those 14376 data with I > 2.0σ(I). The structure was solved using the analogous thorium solution.[7]

Table 4.1. X-ray Data and Collection Parameters for $LaI_3(py)_4$, **40-La**; $UI_3(py)_4$, **40-U**, $[LaI_2(THF)_5][LaI_4(THF)_2]$, **41-La′**, $(C_5Me_4H)_3Nd$, **32-Nd**, and $[K(crypt)][Cp''_3Nd]$, **22-Nd**.

Compound	**40-La**	**40-U**	**41-La′**	**32-Nd**	**22-Nd**
Empirical Formula	$C_{20}H_{20}N_4I_3La$	$C_{20}H_{20}N_4I_3U$	$C_{28}H_{56}O_7I_6La_2$	$C_{27}H_{39}Nd$	$C_{51}H_{99}N_2O_6Si_6KNd$
Temperature (K)	173(2)	88(2)	88(2)	88(2)	133(2)
Crystal System	Monoclinic	Monoclinic	Monoclinic	Trigonal	Triclinic
Space Group	$P2_1/n$	$P2_1/n$	$C2/c$	$R\bar{3}$	$P\bar{1}$
***a* (Å)**	10.2000(5)	10.1516(16)	12.957(3)	15.6260(6)	12.2217(8)
***b* (Å)**	17.5694(9)	17.456(3)	12.152(3)	15.6260(6)	12.7389(8)
***c* (Å)**	15.3415(8)	15.227(2)	29.057(7)	16.4908(7)	22.2835(14)
α (deg)	90	90	90	90	100.9620(10)
β (deg)	99.9848(7)	100.086(2)	98.612(3)	90	104.5290(10)
γ (deg)	90	90	90	120	95.4640(10)
Volume (Å^3)	2707.7(2)	2656.6(7)	4524(2)	3487.1(3)	3259.6(4)
Z	4	4	4	6	2
ρ_{calcd} (Mg/m^3)	2.051	2.338	2.267	1.451	1.211
μ (mm^{-1})	5.010	9.608	5.992	2.243	1.012
R1[a] (*I* > 2.0σ(I))	0.0192	0.0221	0.0242	0.0135	0.0588
wR2 (all data)	0.0725	0.0498	0.0542	0.0322	0.0260

[a]Definitions: $R1 = \Sigma||F_o| - |F_c||/\Sigma|F_o|$, $wR2 = [\Sigma w(F_o^2 - F_c^2)^2/\Sigma w(F_o^2)^2]^{1/2}$.

Goof = $S = [\Sigma[w(F_o^2-F_c^2)^2] / (n-p)]^{1/2}$ where n is the number of reflections and p is the total number of parameters refined.

RESULTS AND DISCUSSION

Synthesis. $LnI_3(Et_2O)_x$, 39-Ln. Addition of iodine, either as a solid or in solution, to a suspension of lanthanide metal shavings in diethyl ether deposited solvated lanthanide triiodides, $LnI_3(Et_2O)_x$, **39-Ln**, (Ln = La, Ce = colorless; Nd = blue) as powders over the course of one to four days depending on the scale. Elemental analysis was used to quantify the average level of solvation in the powders: for La, x =1.6; for Ce x = 1.8; for Nd, x = 1.5. After these solids were exposed to high vacuum (10^{-6} torr), the solvation level was reduced to x = 0.75 (La) and 0.66 (Ce, Nd) as determined by elemental analysis. The complexes were isolated with good yields, 70 – 80%, and are easily isolable by centrifugation or can be used *in situ* (see below). A slight excess of iodine was used which can be removed by washing with hexane or pentane. Reactions could also be performed with a deficiency of iodine, in which case unreacted metal was present with lanthanide iodide product. The excess metal could be removed with a tweezers or later after reaction with a potassium amide or cyclopentadienyl reagent by the filtration that separated the KI.

$LnI_3(py)_4$, 40-Ln. When oxidations were performed in pyridine (NC_5H_5, py), the solutions quickly became brown. After the mixtures were stirred for two to four days and filtered or centrifuged, the products were isolated as brown oils that could be triturated with ether to yield $LnI_3(py)_4$, **40-Ln** (Ln = La, Ce, Nd), as brown powders. These materials were characterized by ^1H and ^{13}C NMR spectroscopy where possible, along with elemental analysis and X-ray crystallography. The ^1H and ^{13}C NMR resonances in **40-La** were shifted from their free pyridine values in C_6D_6[113] and in **40-Ce** and **40-Nd** the resonances were shifted and broadened by paramagnetism. As in the Et_2O reactions, a small excess of I_2 was used which was subsequently washed away with hexane. Excess iodine has the potential to form triiodide

products as observed for $[PuI_2(THF)_4(py)][I_3]$[11] and $[LnI_2(THF)_5][I_3]$ (Ln = La,[30] Yb[29]), but no evidence of such species was observed. The **40-Ln** complexes are slightly soluble in benzene and toluene. If the synthesis is conducted with a deficiency of iodine, the excess metal can be removed by filtration from **40-Ln**.

Diffusion of pentane into concentrated pyridine solutions allowed the isolation of single crystals of **40-La** suitable for X-ray crystallography. Crystals of the uranium analog, **40-U**,[29, 114] were also obtained similarly and structurally characterized, Figure 4.2, to confirm the method of crystallization since the structural report in the literature does not give synthetic experimental information.[114] These crystallizations were performed with less than 30 mg of material to better mimic the conditions of transuranic chemistry.

Complex **40-La** adopts a seven coordinate pentagonal bipyramidal geometry with two iodide ligands in the axial positions and the other equatorial. The pyridine ligands occupy the other equatorial positions, Figure 4.1. This is a typical structure for *f*–element trihalide tetrasolvates.[48-49, 58-59, 114-119] The La–I bond distances in **40-La** are similar to those in $LaI_3(THF)_4$, **41-La**,[59] while the 2.689(4) Å average La–N(py) distance is larger than the 2.54(1) Å average La–O(THF) distance in **41-La**, Table 4.2. The La–N(py) average distance in **40-La** is longer than the 2.605(8) Å analog in $LaCl_3(py)_4$[116] which is consistent with the larger size of iodide vs chloride, Table 4.2.

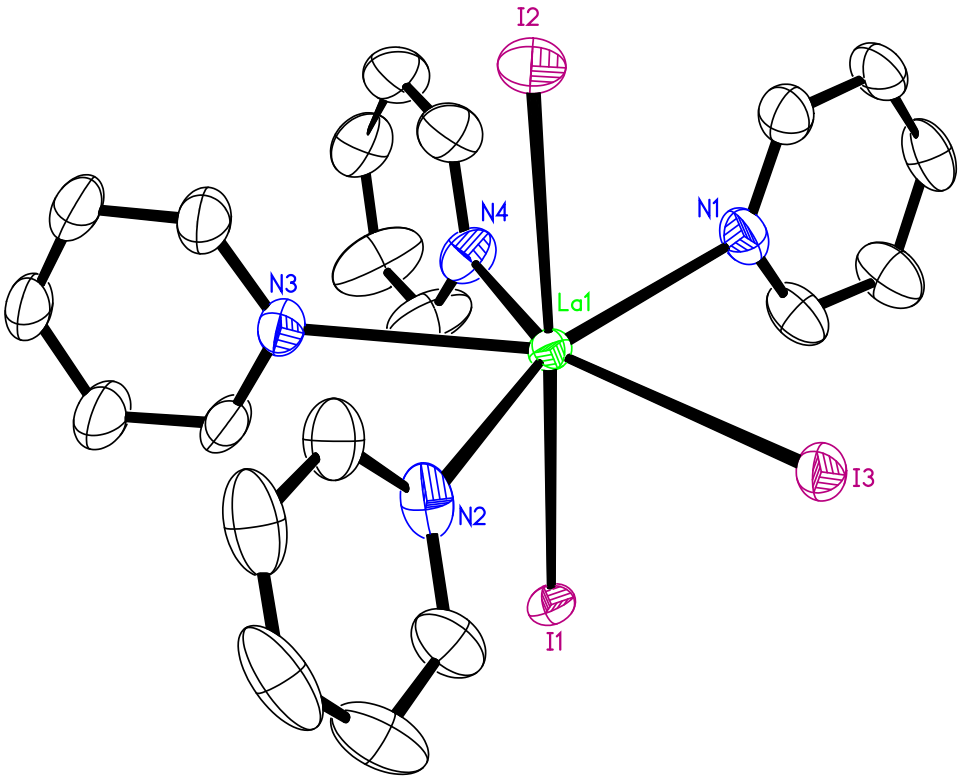

Figure 4.1. Thermal ellipsoid plot of $LaI_3(py)_4$, **40-La** , drawn at the 50% probability level with hydrogen atoms omitted for clarity.

Table 4.2. Metrical Parameter Comparisons for $LaI_3(py)_4$, **40-La**, With $LaI_3(THF)_4$, **41-La,**[59] and $LaCl_3(py)_4$ (ax = axial, equ = equatorial).[116]

	$LaI_3(THF)_4$, **41-La**[59]	$LaI_3(py)_4$, **40-La**	$LaCl_3(py)_4$[116]
La–X_{ax} (Å)	3.129(4) 3.142(4)	3.1543(3) 3.1522(3)	2.661(1) 2.652(1)
La–X_{equ} (Å)	3.190(4)	3.1943(3)	2.679(1)
La–L range (Å)	2.515(7)–2.576(8)	2.679(3)–2.699(3)	2.585(3)–2.619(4)
X_{ax}–La–X_{ax} (°)	171.4(1)	177.168(9)	173.42(4)
X_{ax}–La–X_{equ} (°)	94.9(1) 93.4(1)	86.938(8) 95.088(9)	91.11(4) 95.40(4)

The corresponding uranium complex, $UI_3(py)_4$, **40-U**, crystallized, in this study, in the $P2_1/n$ space group and is isomorphous with **40-La,** Figure 4.2. A *Pbca* structure of **40-U** was previously deposited in the Cambridge Structural Database[114] and has two independent molecules in the unit cell with metrical parameters similar to the $P2_1/n$ structure (Table 4.3). Comparison of **40-U** with $UI_3(THF)_4$, **41-U**,[29, 120] (Table 4.3) is similar to the comparison of **40-La** with **41-La**: the iodide distances are similar and the U–N(py) distances are longer than the U–O(THF) distances.

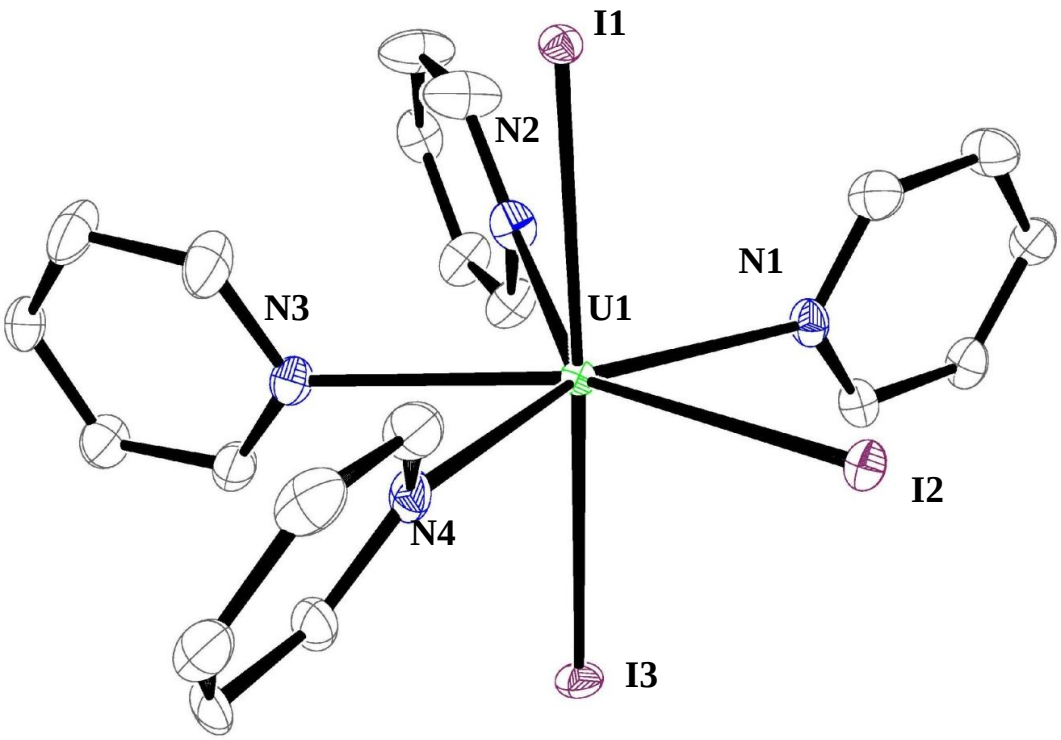

Figure 4.2. Thermal ellipsoid plot of $UI_3(py)_4$, **40-U** , drawn at the 50% probability level with hydrogen atoms omitted for clarity.

Table 4.3. Metrical Parameter Comparisons for $UI_3(py)_4$, **40-U** (Crystallized in $P2_1/n$) With $UI_3(THF)_4$, **41-U**,[29, 120] and $UI_3(py)_4$, **40-U‡*** (Crystallized in *Pbca*)[114] (ax = axial, equ = equatorial). ***40-U‡** Has Two Crystallographically Independent Units.

	$UI_3(THF)_4$, **41-U**[29, 120]	$UI_3(py)_4$[114]* (molecule 1)	$UI_3(py)_4$[114]* (molecule 2)	$UI_3(py)_4$ (this study)
U–I_{ax} (Å)	3.103(2) 3.119(2)	3.110 3.146	3.120 3.125	3.1311(5) 3.1317(5)
U–I_{equ} (Å)	3.167(2)	3.172	3.137	3.1718(4)
U–L range (Å)	2.48(1)–2.56(1)	2.607–2.682	2.638–2.685	2.644(3)–2.664(3)
I_{ax}–U–I_{ax} (°)	171.3(5)	175.4	177.1	177.313(8)
I_{ax}–U–I_{equ} (°)	95.90(5) 93.5(5)	96.1 89.0	94.0 88.9	94.57(1) 86.75(1)

$LnI_3(THF)_4$, 41-Ln. The etherate materials $LnI_3(OEt_2)_x$, **39-Ln**, could be converted to their THF adducts by dissolution in THF and removal of the volatiles under reduced pressure to give $LnI_3(THF)_4$, **41-Ln** (Ln = La, Ce, Nd), in high yield. This method produced materials with a consistent level of solvation. The compounds were identified by unit cell determination and comparison with the published structures.[58-59, 79, 121] Their ^1H and ^{13}C NMR spectra were recorded in C_6D_6 and displayed a single set of resonances shifted from the value for free THF in C_6D_6.[113] In the La case, crystallization of **41-La** from hot toluene instead of hot THF gave colorless crystals of $[LaI_2(THF)_5][LaI_4(THF)_2]$, **41-La′**, Figure 4.3. This salt is isomorphous with the Nd, Sm, Gd, Y and Yb analogs[49, 60-61, 64] and has structural parameters as expected based on the lanthanide contraction, Table 4.4). Formation of such salts is not uncommon for lanthanide trihalides depending on crystallization conditions.[49, 60-65, 122]

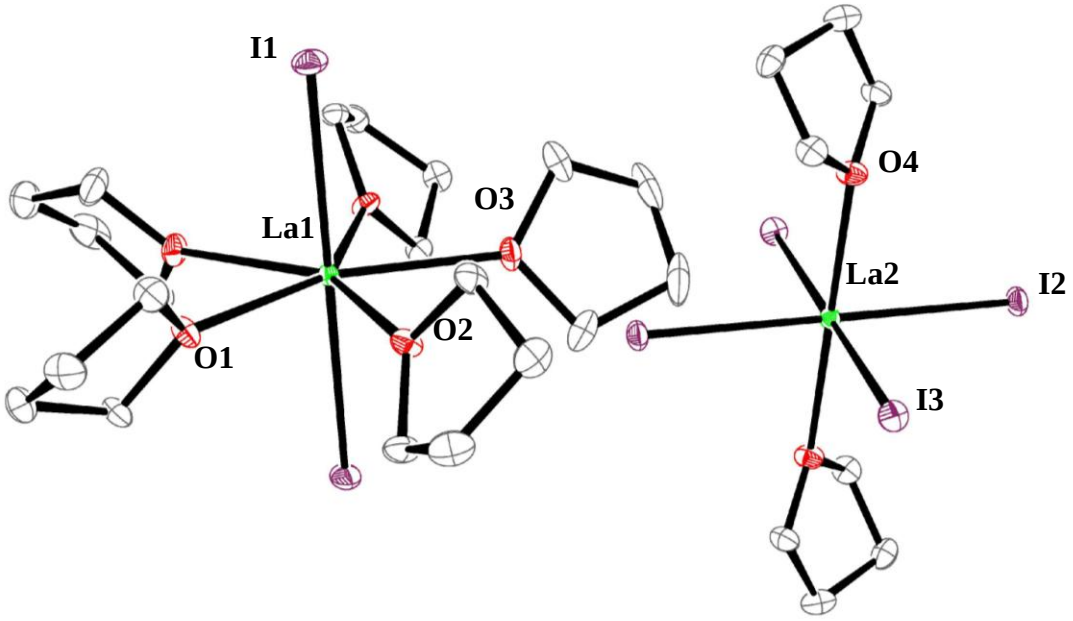

Figure 4.3. Thermal ellipsoid plot of $[LaI_2(THF)_5][LaI_4(THF)_2]$, **41-La′**, drawn at the 50% probability level with heteroatoms from the asymmetric unit labeled and hydrogen atoms omitted for clarity.

Table 4.4. Metrical Parameter Comparisons for $[LaI_2(THF)_5][LaI_4(THF)_2]$, **41-La′** With Other $[LnI_2(THF)_5][LnI_4(THF)_2]$, **41-Ln′**, Complexes.

	Ln–I (Å) Cation	Ln–O (Å) Cation	Ln–I (Å) Anion	Ln–O (Å) Anion	I–Ln–I (°) Cation	6 Coordinate Shannon Ionic Radius*[11]
41-La′	3.1121(7)	2.505(2) 2.505(3) 2.532(2)	3.1422(7) 3.1525(7)	2.462(2)	178.89(1)	1.032
41-Nd′[49]	3.0428(6)	2.458(7) 2.470(6) 2.467(9)	3.0843(6) 3.0718(7)	2.397(6)	179.04(4)	0.983
41-Sm′[60]	3.028(1)	2.441(4) 2.449(4) 2.455(4)	3.051(1) 3.071(1)	2.386(4)	179.0(1)	0.958
41-Gd′[49]	2.9952(4)	2.416(4) 2.425(4) 2.421(6)	3.0264(5) 3.0435(4)	2.347(4)	179.26(2)	0.938
41-Y′[49]	2.9685(6)	2.387(5) 2.391(5) 2.395(7)	3.0181(6) 2.9984(7)	2.299(6)	179.44(5)	0.9
41-Yb′[61]	2.9366 (9)	2.340 (6) 2.347 (8) 2.365 (6)	2.9641 (8) 2.9856 (9)	2.279 (6)	179.44(3)	0.868

$Ln[N(SiMe_3)_2]_3$, 15-Ln. Although many methods have been developed for the synthesis of tris(amide) lanthanide complexes, the syntheses most commonly use lanthanide trichloride starting materials.[80, 123-124] As described below, lanthanide triiodide powders, $LnI_3(OEt_2)_x$, **39-Ln**, prepared from the metal, are also viable starting materials for the synthesis of these compounds.

Addition of a toluene solution of $KN(SiMe_3)_2$ to a toluene suspension of **39-Ln** forms $Ln[N(SiMe_3)_2]_3$, **15-Ln**, in good yield after workup as confirmed by ^1H NMR spectroscopy.[80] Tris(amide) plutonium complexes have been prepared from the metal following this protocol[18] and could be examined for reduction to +2 complexes.[12]

In one case, an attempt to obtain X-ray quality crystals of **15-La**, a structure of $\{(THF)[(Me_3Si)_2N]_2La\}_2(\mu\text{–}O)$, **42**, was instead characterized, Figure 4.4. This is likely due to the presence of THF in the glovebox and adventitious water. The molecule is compared with the isomorphous samarium analog,[125] as well as $\{(Ph_3PO)[(Me_3Si)_2N]_2La\}_2(\mu\text{–}O)$,[126] Table 4.5.

Table 4.5. Metrical Parameter Comparisons for $\{(THF)[(Me_3Si)_2N]_2La\}_2(\mu\text{–}O)$, **42**, With Other $\{L[(Me_3Si)_2N]_2Ln\}_2(\mu\text{–}O)$ Complexes. *All Molecules Contain an Inversion Center.

	Ln–N (Å)	Ln–(μ–O) (Å)	Ln–O–Ln (°)
$\{(THF)[(Me_3Si)_2N]_2La\}_2(\mu\text{–}O)$, **42**	2.427 2.429	2.145	180
$\{(THF)[(Me_3Si)_2N]_2Sm\}_2(\mu\text{–}O)$[125]	2.322(3) 2.333(3)	2.0819(2)	180
$\{(Ph_3PO)[(Me_3Si)_2N]_2La\}_2(\mu\text{–}O)$[126]	2.488 2.366	2.328 2.335	138.6

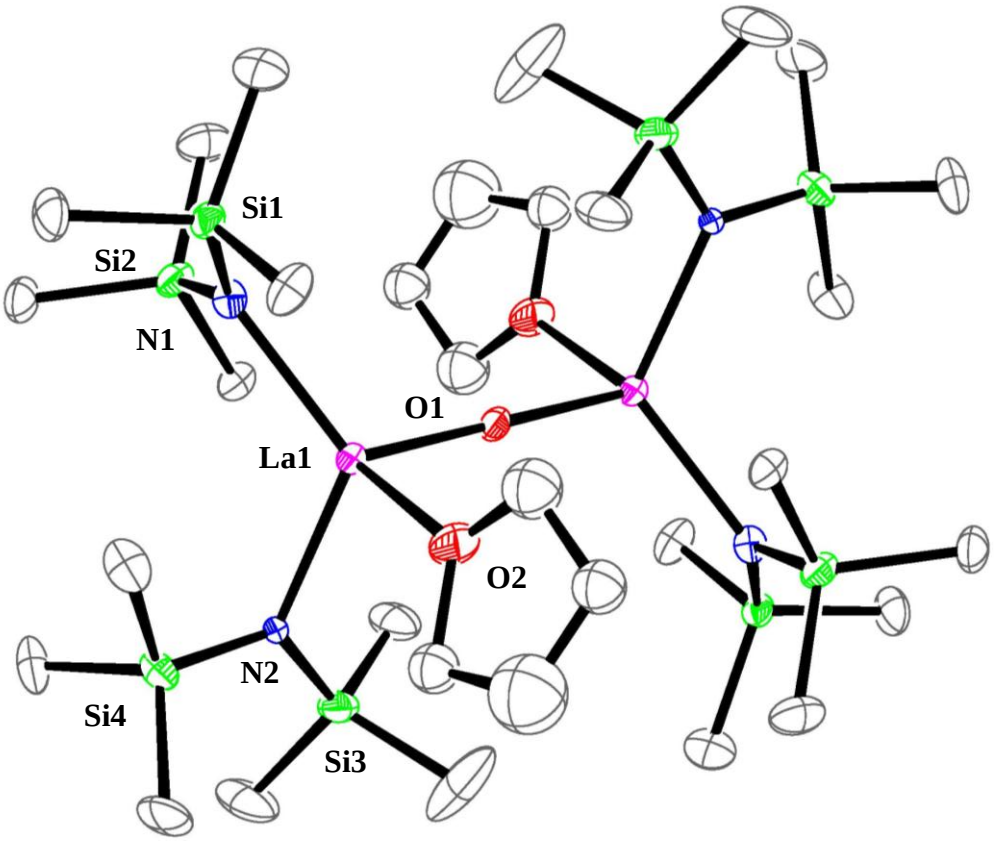

Figure 4.4. Preliminary thermal ellipsoid plot of {(THF)[$(Me_3Si)_2N$]$_2$La}$_2$(μ–O), **42**, drawn at the 50% probability level with heteroatoms in the asymmetric unit labeled and hydrogen atoms omitted for clarity.

Cp'_3Ln, 8-Ln. The Cp′ ligand was chosen as a representative ligand since its complexes recently led to the isolation of the lanthanides and uranium in the formal +2 oxidation state,[1-5, 127] The Cp'_3Ln complexes, **8-Ln**, are typically prepared from $LnCl_3$ with 3.1 equiv of KCp′.[1-4, 72, 75, 81, 128] A similar protocol with $LnI_3(OEt_2)_x$, **39-Ln**, in ether provides **8-Ln** in high yield. In addition, **8-Ln** can be prepared in high yield from **39-Ln** generated *in situ*, and single crystals of **8-Ln** could be obtained on small scale reactions done with 11–15 mg of metal. The samples of **8-Ln** prepared in this way could be reduced to form the Ln^{II} complexes [K(crypt)][Cp'_3Ln], **20-Ln**, as confirmed by unit cell analysis, in greater than a 60% yield [Ln = Ce, Pr, Nd].

Cp''_3Ln, 20-Ln. Since the Cp″ ligand was used to prepare Th(II)[7] and $(Cp''_3U)^{1-}$ is more stable than $(Cp''_3U)^{1-}$,[8] the preparation of Cp''_3Ln, **20-Ln**,[70-73, 82-83] on a small scale was also examined. This proved to be the protocol for preparing the starting material used to isolate Pu(II),[13] Chapter 5. Similar to the preparation of **8-Ln**, addition of 3.1 equiv of KCp″ to either isolated **39-Ln** or *in situ* generated **39-Ln**, gave Cp''_3Ln, **20-Ln**, in good yield [Ln = Ce, Nd].

With the successful isolation of M^{II} for [K(crypt)][Cp''_3M], **22-M**, M = La,[6] Ce,[129] Pr,[129] Th,[7] U,[8] and Pu,[13] the Nd analog was sought for comparison to the analogous plutonium and americium chemistry. In a manner similar to **22-U**, Chapter 2, addition of KC_8 to a green solution of **20-Nd** in a 4:1 Et_2O:THF solvent mixture immediately generated a dark purple solution with black insolubles (presumably graphite). Following work up dark purple crystals of [K(crypt)][Cp''_3Nd], **22-Nd**, Figure 4.5, were isolated and are isomorphous with **22-Th**, and **22-Pu**.

22-Nd shows a Nd–C range of Å, with average Nd–(centroid) distance of 2.54(1) Å and an average (centroid)–Nd–(centroid) angle of 120.0°. This compares well with the other M^{II} structures for M = La, Ce, Pr, Th and Pu based on decreasing radius as the series is traversed,

Table 4.6. The crystallographic data for **20-Nd**[83] are similar with an average Nd–C distance of 2.789(2) Å, and an average Nd–(centroid) distance of 2.53(3), again with a 120° average angle. The two $Nd^{II/III}$ compounds show indistinguishable bond metrics, similar to the case of [K(crypt)][Cp'_3, Nd], **21-Nd**.[4]

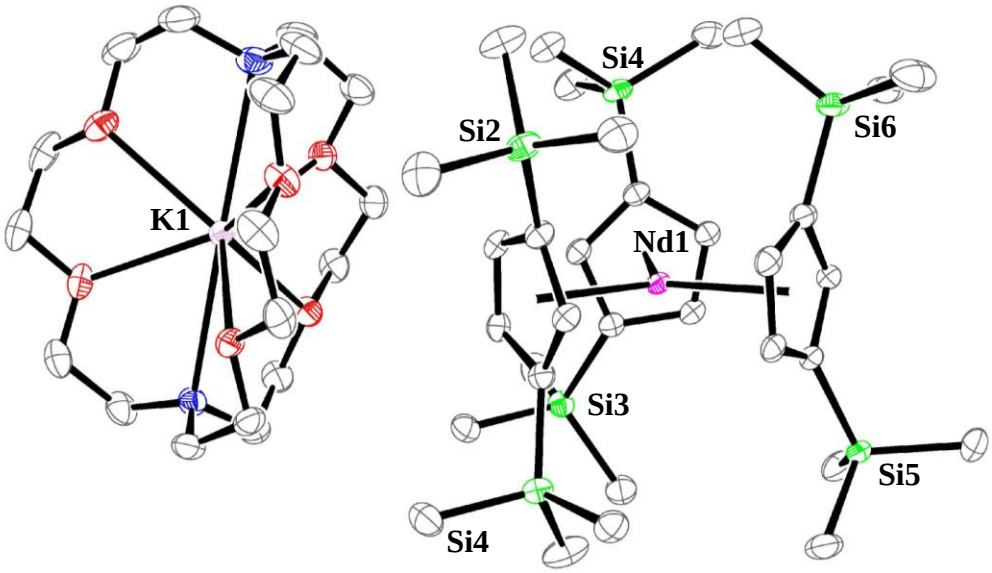

Figure 4.5. Thermal ellipsoid plot of [K(crypt)][Cp''_3Nd], **22-Nd**, drawn at the 50% probability level with hydrogen atoms omitted for clarity.

Table 4.6. Metrical Parameter Comparisons for [K(crypt)][Cp″$_3$Nd], **22-Nd** With Other [K(crypt)][Cp″$_3$M], **22-M**, Complexes, As Well As Cp″$_3$Nd, **20-Nd** (cent = Cp″ Ring Centroid).[83]

	M–C average (Å)	M–(centroid) (Å)	(centroid)–M–(centroid) (°)	M^{3+} 6 Coordinate Shannon Ionic Radius*[11]
22-La[6]	2.884(9)	2.612 2.606 2.642	117.2 123.3 119.4	1.032
22-Ce[129]	2.856(9)	2.579 2.574 2.609	117.4 119.4 123.1	1.01
22-Pu[13]	2.764(9)	2.509 2.536 2.522	122.7 119.8 117.5	1
22-Pr[129]	2.837(9)	2.558 2.552 2.588	121.9 117.5 119.4	0.99
22-Nd	2.817(9)	2.530 2.559 2.543	122.9 119.8 117.3	0.983
22-Th[7]	2.80(1)	2.512 2.533 2.519	122.6 119.8 119.6	*
20-Nd[83]	2.789(2)	2.468 2.548 2.558	121.8 120.3 117.8	0.983

*Six coordinate chosen since there is a Shannon radius for this coordination number for all the ions except Th^{III}.

$(C_5Me_4H)_3Ln$, 32-Ln. Preparation of tris(cyclopentadienyl) complexes of the larger ligand $(C_5Me_4H)^{1-}$ was also examined. The **32-Ln** series can be made from $LnI_3(OEt_2)_x$, **39-Ln**, in 70 – 90% yields again showing the viability of **39-Ln** generated from the elemental metal for organometallic synthesis. Despite its use in spectroscopy and reactivity,[130-136] the structure of $(C_5Me_4H)_3Nd$, **32-Nd**, has not been published. Cooling a hot toluene solution of **32-Nd** to −30 °C afforded green single crystals suitable for X-ray crystallography, Figure 4.6. **7-Nd** crystallizes in the $R\bar{3}$ space group and is isomorphous with the other members of the $(C_5Me_4H)_3M$ series (La,[87] Ce,[86] Pr,[86] Sm,[87] Tb,[84] Yb,[137] Lu,[138] Y,[139] Th,[140] U[141]), which crystallize in either the $R\bar{3}$ or $R\bar{3}r$ space groups, Table 4.7. The metrical parameters for **32-Nd** match those of the analogs based on the lanthanide contraction (Table 4.7) and are compared to other tris(cyclopentadienyl) neodymium complexes Table 4.8.

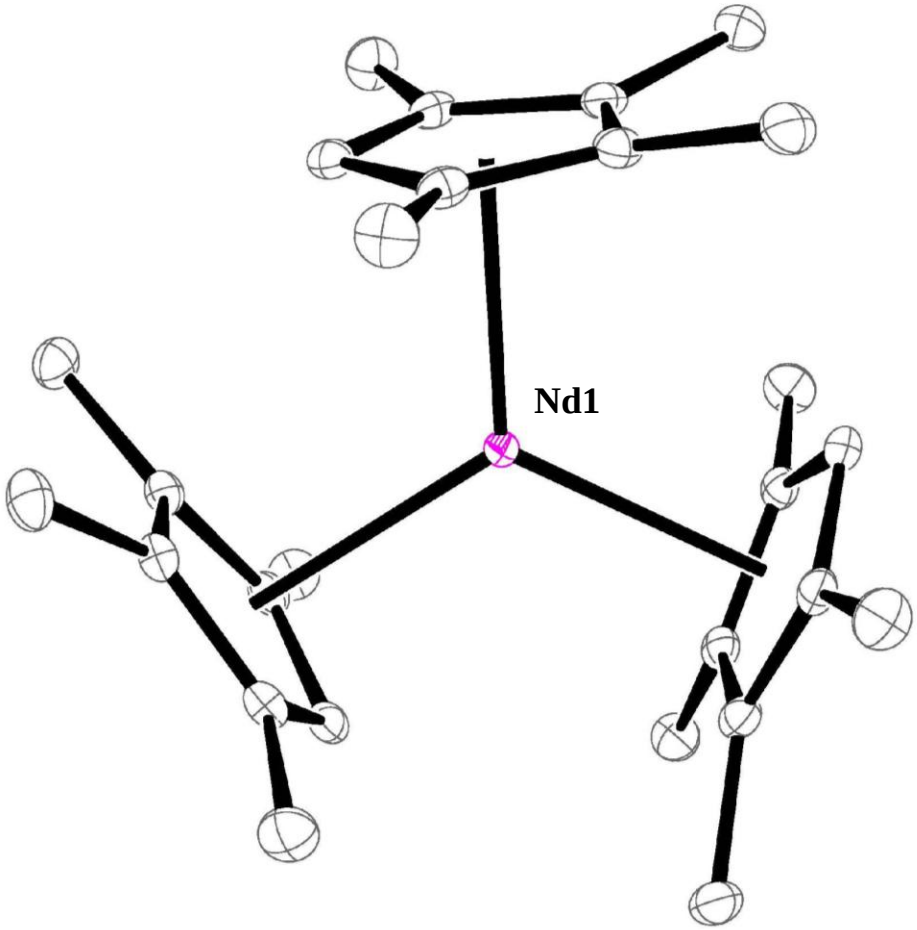

Figure 4.6. Thermal ellipsoid plot of $(C_5Me_4H)_3Nd$, **32-Nd**, drawn at the 50% probability level with hydrogen atoms omitted for clarity. Selected bond distances (Å) and angles (°): Nd–C(C_5Me_4H) range: 2.719(1)–2.852(2)Å; Nd–(centroid) 2.518; (centroid)–Nd–(centroid) 120°.

Table 4.7. Metrical Parameter Comparisons for $(C_5Me_4H)_3Nd$, **32-Nd**, With Other $(C_5Me_4H)_3M$, **32-M**, Complexes (cent = C_5Me_4H Ring Centroid). By Symmetry There is Only One Unique Ring Giving 120° Angles to All Rings.

M	Space Group	6 Coordinate Shannon Ionic Radius*[11]	M–(cent) (Å)
La[87]	$R\bar{3}r$	1.032	2.616
Ce[86]	$R\bar{3}$	1.01	2.552
Pr[86]	$R\bar{3}$	0.99	2.532
U[141]	$R\bar{3}$	1.025	2.523
Th[140]	$R\bar{3}$	*	2.518
Nd	$R\bar{3}$	0.983	2.516
Sm[87]	$R\bar{3}r$	0.958	2.489
Tb[84]	$R\bar{3}r$	0.923	2.445
Y[142]	$R\bar{3}$	0.9	2.441
Yb[137]	$R3$	0.868	2.41
Lu[138]	$R\bar{3}$	0.861	2.406

*Six coordinate chosen since there is a Shannon radius for this coordination number for all the ions except Th^{III}.

Table 4.8. Metrical Parameter Comparisons for $(C_5Me_4H)_3Nd$, **32-Nd**, With Other $(C_5R_5)_3Nd$ Complexes (cent = C_5R_5 Ring Centroid).

	Nd–(cent) (Å)	(cent)–Nd–(cent) (°)
$(C_5Me_4H)_3Nd$, **32-Nd**	2.516	120
$(C_5H_4{}^tBu)_3Nd$[143]	2.493 2.498 2.520	119.24 119.45 120.94
Cp'_3Nd, **8-Nd**[81]	2.4863(2) 2.4931(2) 2.4861(2)	120.535(8) 118.817(8) 120.065(8)
Cp''_3Nd, **20-Nd**[83]	2.468 2.548 2.558	121.8 117.8 120.3
$(C_5Me_5)_3Nd$[144]	2.582	120
$\{C_5H_4[CH(SiMe_3)_2]\}_3Nd$[145]	2.51 2.51 2.53	120.7 120.7 117.0

CONCLUSION

Small scale reactions of the elemental lanthanide metals, cerium and neodymium, of size similar to plutonium and americium have been found to provide viable routes to inorganic and organometallic complexes. These reactions provide protocols for developing transuranic chemistry starting from the elemental transuranic metals. Oxidation of the lanthanide metals with iodine in Et_2O provides the triiodides $[LnI_3(OEt_2)_x]$, **39-Ln**, that can be used directly as starting materials for $Ln[N(SiMe_3)_2]_3$, **15-Ln**, Cp'_3Ln, **8-Ln**, Cp''_3Ln, **20-Ln**, and $(C_5Me_4H)_3Ln$, **32-Ln**, or can be converted to the THF adducts, $LnI_3(THF)_4$, **41-Ln**. The syntheses were extended to isolate the Ln^{II} complexes [K(crypt)][Cp'_3Ln], **21-Ln**, and [K(crypt)][Cp''_3Nd], **22-**

Nd, on the small scale. Oxidation of the lanthanide metals with iodine in pyridine forms the tetra(pyridine) adducts, $LnI_3(py)_4$, **40-Ln**.

REFERENCES

(1) MacDonald, M. R.; Ziller, J. W.; Evans, W. J., *J. Am. Chem. Soc.* **2011,** *133*, 15914-15917.

(2) MacDonald, M. R.; Bates, J. E.; Fieser, M. E.; Ziller, J. W.; Furche, F.; Evans, W. J., *J. Am. Chem. Soc.* **2012,** *134*, 8420-8423.

(3) MacDonald, M. R.; Bates, J. E.; Ziller, J. W.; Furche, F.; Evans, W. J., *J. Am. Chem. Soc.* **2013,** *135*, 9857-9868.

(4) Fieser, M. E.; MacDonald, M. R.; Krull, B. T.; Bates, J. E.; Ziller, J. W.; Furche, F.; Evans, W. J., *J. Am. Chem. Soc.* **2015,** *137*, 369-382.

(5) MacDonald, M. R.; Fieser, M. E.; Bates, J. E.; Ziller, J. W.; Furche, F.; Evans, W. J., *J. Am. Chem. Soc.* **2013,** *135*, 13310-13313.

(6) Hitchcock, P. B.; Lappert, M. F.; Maron, L.; Protchenko, A. V., *Angew. Chem., Int. Ed.,* **2008,** *47*, 1488-1491.

(7) Langeslay, R. R.; Fieser, M. E.; Ziller, J. W.; Furche, F.; Evans, W. J., *Chem. Sci.* **2015,** *6*, 517-521.

(8) Windorff, C. J.; MacDonald, M. R.; Meihaus, K. R.; Ziller, J. W.; Long, J. R.; Evans William, J., *Chem. Eur. J.* **2016,** *22*, 772-782.

(9) Dutkiewicz, M. S.; Farnaby, J. H.; Apostolidis, C.; Colineau, E.; Walter, O.; Magnani, N.; Gardiner, M. G.; Love, J. B.; Kaltsoyannis, N.; Caciuffo, R.; Arnold, P. L., *Nat. Chem.* **2016,** *8*, 797-802.

(10) Dutkiewicz, M. S.; Apostolidis, C.; Walter, O.; Arnold, P. L., *Chem. Sci.* **2017,** *8*, 2553-2561.

(11) Shannon, R., *Acta Crystallogr., Sect. A.* **1976,** *32*, 751-767.

(12) Woen, D. H.; Chen, G. P.; Ziller, J. W.; Boyle, T. J.; Furche, F.; Evans, W. J., *Angew. Chem., Int. Ed.*, **2017,** *56*, 2050-2053.

(13) Windorff, C. J.; Chen, G. P.; Cross, J. N.; Evans, W. J.; Furche, F.; Gaunt, A. J.; Janicke, M. T.; Kozimor, S. A.; Scott, B. L., *J. Am. Chem. Soc.* **2017**.

(14) Evans, W. J., *Organometallics* **2016,** *35*, 3088-3100.

(15) Woen, D. H.; Evans, W. J., Expanding the + 2 Oxidation State of the Rare-Earth Metals, Uranium, and Thorium in Molecular Complexes. In *Handbook on the Physics and Chemistry of Rare Earths*, Jean-Claude, G. B.; Vitalij, K. P., Eds. Elsevier: 2016; Vol. Volume 50, pp 337-394.

(16) Gaunt, A. J.; Scott, B. L.; Neu, M. P., *Chem. Commun.* **2005**, 3215-3217.

(17) Sykora, R. E.; Assefa, Z.; Haire, R. G.; Albrecht-Schmitt, T. E., *Inorg. Chem.* **2006,** *45*, 475-477.

(18) Gaunt, A. J.; Enriquez, A. E.; Reilly, S. D.; Scott, B. L.; Neu, M. P., *Inorg. Chem.* **2008,** *47*, 26-28.

(19) Ingram, K. I. M.; Tassell, M. J.; Gaunt, A. J.; Kaltsoyannis, N., *Inorg. Chem.* **2008,** *47*, 7824-7833.

(20) Minasian, S. G.; Boland, K. S.; Feller, R. K.; Gaunt, A. J.; Kozimor, S. A.; May, I.; Reilly, S. D.; Scott, B. L.; Shuh, D. K., *Inorg. Chem.* **2012,** *51*, 5728-5736.

(21) Cross, J. N.; Villa, E. M.; Wang, S.; Diwu, J.; Polinski, M. J.; Albrecht-Schmitt, T. E., *Inorg. Chem.* **2012,** *51*, 8419-8424.

(22) Cary, S. K.; Silver, M. A.; Liu, G.; Wang, J. C.; Bogart, J. A.; Stritzinger, J. T.; Arico, A. A.; Hanson, K.; Schelter, E. J.; Albrecht-Schmitt, T. E., *Inorg. Chem.* **2015,** *54*, 11399-11404.

(23) Macor, J. A.; Brown, J. L.; Cross, J. N.; Daly, S. R.; Gaunt, A. J.; Girolami, G. S.; Janicke, M. T.; Kozimor, S. A.; Neu, M. P.; Olson, A. C.; Reilly, S. D.; Scott, B. L., *Dalton Trans.* **2015,** *44*, 18923-18936.

(24) Brown, J. L.; Batista, E. R.; Boncella, J. M.; Gaunt, A. J.; Reilly, S. D.; Scott, B. L.; Tomson, N. C., *J. Am. Chem. Soc.* **2015,** *137*, 9583-9586.

(25) Cary, S. K.; Ferrier, M. G.; Baumbach, R. E.; Silver, M. A.; Lezama Pacheco, J.; Kozimor, S. A.; La Pierre, H. S.; Stein, B. W.; Arico, A. A.; Gray, D. L.; Albrecht-Schmitt, T. E., *Inorg. Chem.* **2016,** *55*, 4373-4380.

(26) Silver, M. A.; Cary, S. K.; Stritzinger, J. T.; Parker, T. G.; Maron, L.; Albrecht-Schmitt, T. E., *Inorg. Chem.* **2016,** *55*, 5092-5094.

(27) Brown, J. L.; Gaunt, A. J.; King, D. M.; Liddle, S. T.; Reilly, S. D.; Scott, B. L.; Wooles, A. J., *Chem. Commun.* **2016,** *52*, 5428-5431.

(28) Clark, D. L.; Frankcom, T. M.; Miller, M. M.; Watkin, J. G., *Inorg. Chem.* **1992,** *31*, 1628-1633.

(29) Avens, L. R.; Bott, S. G.; Clark, D. L.; Sattelberger, A. P.; Watkin, J. G.; Zwick, B. D., *Inorg. Chem.* **1994,** *33*, 2248-2256.

(30) Clark, D. L.; Sattelberger, A. P.; Andersen, R. A., Lewis Base Adducts of Uranium Triiodide and Tris[Bis(Trimethylsilyl)Amido]Uranium. In *Inorg. Synth.*, John Wiley & Sons, Inc.: 1997; Vol. 31, pp 307-315.

(31) Evans, W. J.; Kozimor, S. A.; Ziller, J. W.; Fagin, A. A.; Bochkarev, M. N., *Inorg. Chem.* **2005,** *44*, 3993-4000.

(32) Carmichael, C. D.; Jones, N. A.; Arnold, P. L., *Inorg. Chem.* **2008,** *47*, 8577-8579.

(33) Monreal, M. J.; Thomson, R. K.; Cantat, T.; Travia, N. E.; Scott, B. L.; Kiplinger, J. L., *Organometallics* **2011,** *30*, 2031-2038.

(34) Asprey, L. B.; Keenan, T. K.; Kruse, F. H., *Inorg. Chem.* **1964,** *3*, 1137-1141.

(35) Bagnall, K. W.; Brown, D.; Jones, P. J.; Du Preez, J. G. H., *J. Chem. Soc.* **1965**, 350-353.

(36) Brown, D.; Edwards, J., *Dalton Trans.* **1972**, 1757-1762.

(37) Karraker, D. G., *Inorg. Chim. Acta* **1987,** *139*, 189-191.

(38) Cloke, F. G. N.; Hitchcock, P. B., *J. Am. Chem. Soc.* **2002,** *124*, 9352-9353.

(39) Berthet, J.-C.; Thuéry, P.; Ephritikhine, M., *Inorg. Chem.* **2005,** *44*, 1142-1146.

(40) Schnaars, D. D.; Wu, G.; Hayton, T. W., *Dalton Trans.* **2008**, 6121-6126.

(41) Gaunt, A. J.; Reilly, S. D.; Enriquez, A. E.; Hayton, T. W.; Boncella, J. M.; Scott, B. L.; Neu, M. P., *Inorg. Chem.* **2008,** *47*, 8412-8419.

(42) Reilly, S. D.; Brown, J. L.; Scott, B. L.; Gaunt, A. J., *Dalton Trans.* **2014,** *43*, 1498-1501.

(43) Meyer, G., *Synthesis of lanthanide and actinide compounds edited by G. Meyer and L.R. Morss*. Kluwer Academic: Dordrecht , The Netherlands, 1991.

(44) Young, R. C.; Hastings, J. L., *J. Am. Chem. Soc.* **1937,** *59*, 765-766.

(45) Hohmann, E.; Bommer, H., *Z. Anorg. Allg. Chemie* **1941,** *248*, 383-396.

(46) Taylor, M. D.; Carter, C. P., *J. Inorg. Nucl. Chem.* **1962,** *24*, 387-391.

(47) Kutscher, J.; Schneider, A., *Inorg. Nucl. Chem. Lett.* **1971,** *7*, 815-819.

(48) Boyle, T. J.; Ottley, L. A. M.; Alam, T. M.; Rodriguez, M. A.; Yang, P.; McIntyre, S. K., *Polyhedron* **2010,** *29*, 1784-1795.

(49) Izod, K.; Liddle, S. T.; Clegg, W., *Inorg. Chem.* **2004,** *43*, 214-218.

(50) Huebner, L.; Kornienko, A.; Emge, T. J.; Brennan, J. G., *Inorg. Chem.* **2004,** *43*, 5659-5664.

(51) Bruno, G.; Ciliberto, E.; Fischer, R. D.; Fragala, I.; Spiegl, A. W., *Organometallics* **1982,** *1*, 1060-1062.

(52) Kunze, M. R.; Steinborn, D.; Merzweiler, K.; Wagner, C.; Sieler, J.; Taube, R., *Z. Anorg. Allg. Chemie* **2007,** *633*, 1451-1463.

(53) Deacon, G. B.; Feng, T.; Junk, P. C.; Meyer, G.; Scott, N. M.; Skelton, B. W.; White, A. H., *Aust. J. Chem.* **2000,** *53*, 853 - 865.

(54) Lannou, M.-I.; Hélion, F.; Namy, J.-L., *Tetrahedron* **2003,** *59*, 10551-10565.

(55) Carter, F. L.; Murray, J. F., *Mat. Res. Bull.* **1972,** *7*, 519-523.

(56) Corbett, J. D.; Simon, A., *Inorg. Synth.* **1983,** *22*, 31-36.

(57) Voskoboynikov, A. Z.; Beletskaya, I. P., *Appl. Organometal. Chem.* **1995,** *9*, 479-482.

(58) Liddle, S. T.; Arnold, P. L., *Organometallics* **2005,** *24*, 2597-2605.

(59) Trifonov, A. A.; Weghe, P. V. d.; Collin, J.; Domingos, A.; Santos, I., *J. Organomet. Chem.* **1997,** *527*, 225-237.

(60) Xie, Z.; Chiu, K.-y.; Wu, B.; Mak, T. C. W., *Inorg. Chem.* **1996,** *35*, 5957-5958.

(61) Niemeyer, M., *Acta Crystallogr., Sect. E.* **2001,** *57*, m363-m364.

(62) Anfang, S.; Karl, M.; Faza, N.; Massa, W.; Dehnicke, K.; Magull, J., *Z. Anorg. Allg. Chemie* **1997,** *623*, 1425-1432.

(63) Evans, W. J.; Shreeve, J. L.; Ziller, J. W.; Doedens, R. J., *Inorg. Chem.* **1995,** *34*, 576-585.

(64) Yuan Fu-Gen, S. Q., Sun Jie, *Chin. J. Struct. Chem.* **2001,** *22*, 1501-1505.

(65) Brown, J. L.; Davis, B. L.; Scott, B. L.; Gaunt, A. J., *Inorg. Chem.* **2015,** *54*, 11958-11968.

(66) Wietzke, R.; Mazzanti, M.; Latour, J.-M.; Pecaut, J., *Dalton Trans.* **2000**, 4167-4173.

(67) Rivière, C.; Nierlich, M.; Ephritikhine, M.; Madic, C., *Inorg. Chem.* **2001,** *40*, 4428-4435.

(68) Berthet, J.-C.; Rivière, C.; Miquel, Y.; Nierlich, M.; Madic, C.; Ephritikhine, M., *Eur. J. Inorg. Chem.* **2002,** *2002*, 1439-1446.

(69) Berthet, J.-C.; Nierlich, M.; Ephritikhine, M., *Polyhedron* **2003,** *22*, 3475-3482.

(70) Cassani, M. C.; Gun'ko, Y. K.; Hitchcock, P. B.; Lappert, M. F.; Laschi, F., *Organometallics* **1999,** *18*, 5539-5547.

(71) Sofield, C. D.; Andersen, R. A., *J. Organomet. Chem.* **1995,** *501*, 271-276.

(72) Stults, S. D.; Andersen, R. A.; Zalkin, A., *Organometallics* **1990,** *9*, 115-122.

(73) Lukens, W. W.; Speldrich, M.; Yang, P.; Duignan, T. J.; Autschbach, J.; Kogerler, P., *Dalton Trans.* **2016,** *45*, 11508-21.

(74) Ortu, F.; Fowler, J. M.; Burton, M.; Formanuik, A.; Mills, D. P., *New J. Chem.* **2015,** *39*, 7633-7639.

(75) Peterson, J. K.; MacDonald, M. R.; Ziller, J. W.; Evans, W. J., *Organometallics* **2013,** *32*, 2625-2631.

(76) Rossmanith, K., *Monatsh. Chem.* **1995,** *126*, 897-900.

(77) Hazin, P. N.; Huffman, J. C.; Bruno, J. W., *Organometallics* **1987,** *6*, 23-27.

(78) Clark, D. L.; Gordon, J. C.; Scott, B. L.; Watkin, J. G., *Polyhedron* **1999,** *18*, 1389-1396.

(79) Balashova, T. V.; Kusyaev, D. M.; Kulikova, T. I.; Kuznetsova, O. N.; Edelmann, F. T.; Gießmann, S.; Blaurock, S.; Bochkarev, M. N., *Z. Anorg. Allg. Chemie* **2007,** *633*, 256-260.

(80) Bradley, D. C.; Ghotra, J. S.; Hart, F. A., *Dalton Trans.* **1973**, 1021-1023.

(81) Minasian, S. G.; Krinsky, J. L.; Rinehart, J. D.; Copping, R.; Tyliszczak, T.; Janousch, M.; Shuh, D. K.; Arnold, J., *J. Am. Chem. Soc.* **2009,** *131*, 13767-13783.

(82) Gun'ko, Y. K.; Hitchcock, P. B.; Lappert, M. F., *J. Organomet. Chem.* **1995,** *499*, 213-219.

(83) Xie, Z.; Chui, K.; Liu, Z.; Xue, F.; Zhang, Z.; Mak, T. C. W.; Sun, J., *J. Organomet. Chem.* **1997,** *549*, 239-244.

(84) Schumann, H.; Glanz, M.; Hemling, H., *J. Organomet. Chem.* **1993,** *445*, C1-C3.

(85) Evans, W. J.; Rego, D. B.; Ziller, J. W., *Inorg. Chem.* **2006,** *45*, 3437-3443.

(86) Evans, W. J.; Rego, D. B.; Ziller, J. W., *Inorg. Chem.* **2006,** *45*, 10790-10798.

(87) Schumann, H.; Glanz, M.; Hemling, H.; Ekkehard Hahn, F., *Z. Anorg. Allg. Chemie* **1995,** *621*, 341-345.

(88) Schneider, D.; Harmgarth, N.; Edelmann, F. T.; Anwander, R., *Chem. Eur. J.* **2017**.
(89) APEX2 Version 2014.9-0, Bruker AXS, Inc.; Madison, WI 2014
(90) Sheldrick, G. M. CELL_NOW, Version 2008/4, Bruker AXS, Inc.; Madison, WI 2008.
(91) SAINT Version 8.34a, Bruker AXS, Inc.; Madison, WI 2013.
(92) Sheldrick, G. M. TWINABS, Version 2012/1, Bruker AXS, Inc.; Madison, WI 2012.
(93) Sheldrick, G. M. TWINABS, Version 2012/1, Bruker AXS, Inc.; Madison, WI 2012.
(94) Sheldrick, G. M. SHELXTL, Version 2014/7, Bruker AXS, Inc.; Madison, WI 2014.
(95) International Tables for X-Ray Crystallography 1992, Vol. C., Dordrecht: Kluwer Academic Publishers.
(96) Sheldrick, G. M. SHELXTL, Version 2014/7, Bruker AXS, Inc.; Madison, WI 2014.
(97) APEX2 Version 2014.11-0, Bruker AXS, Inc.; Madison, WI 2014.
(98) SAINT Version 8.34a, Bruker AXS, Inc.; Madison, WI 2013.
(99) Sheldrick, G. M. SADABS, Version 2014/5, Bruker AXS, Inc.; Madison, WI 2014.
(100) Sheldrick, G. M. SHELXTL, Version 2014/7, Bruker AXS, Inc.; Madison, WI 2014.
(101) International Tables for Crystallography 1992, Vol. C., Dordrecht: Kluwer Academic Publishers.
(102) APEX2 Version 2014.11-0, Bruker AXS, Inc.; Madison, WI 2014.
(103) SAINT Version 8.34a, Bruker AXS, Inc.; Madison, WI 2013.
(104) Sheldrick, G. M. SADABS, Version 2014/5, Bruker AXS, Inc.; Madison, WI 2014.
(105) Sheldrick, G. M. SHELXTL, Version 2014/7, Bruker AXS, Inc.; Madison, WI 2014.
(106) International Tables for Crystallography 1992, Vol. C., Dordrecht: Kluwer Academic Publishers.
(107) Flack, H. D. Acta. Cryst., A39, 876-881, 1983. or Parsons, S., Flack, H. D., Wagner, T. *Acta Crystallogr*. B69, 249-259, 2013.
(108) APEX2 Version 2014.11-0, Bruker AXS, Inc.; Madison, WI 2014.
(109) SAINT Version 8.34a, Bruker AXS, Inc.; Madison, WI 2013.
(110) Sheldrick, G. M. SADABS, Version 2014/5, Bruker AXS, Inc.; Madison, WI 2014.
(111) Sheldrick, G. M. SHELXTL, Version 2014/7, Bruker AXS, Inc.; Madison, WI 2014.
(112) International Tables for Crystallography 1992, Vol. C., Dordrecht: Kluwer Academic Publishers.

(113) Fulmer, G. R.; Miller, A. J. M.; Sherden, N. H.; Gottlieb, H. E.; Nudelman, A.; Stoltz, B. M.; Bercaw, J. E.; Goldberg, K. I., *Organometallics* **2010,** *29*, 2176-2179.

(114) Berthet, J. C.; Thuery, P.; Ephritikhine, M. Private Communication to CSD, 2013, CCDC Deposit number 959293, Code XIMWEX

(115) Ninghai, H.; Yonghua, L.; Qi, S.; Yan, X.; Endong, S., *Acta Chim. Sinica* **1986,** *44*, 388-391.

(116) Li, J.-S.; Neumüller, B.; Dehnicke, K., *Z. Anorg. Allg. Chemie* **2002,** *628*, 45-50.

(117) Deacon, G. B.; Scott, N. M.; Skelton, B. W.; White, A. H., *Z. Anorg. Allg. Chemie* **2006,** *632*, 1945-1946.

(118) Vasudevan, K. V.; Smith, N. A.; Scott, B. L.; McKigney, E. A.; Blair, M. W.; Gordon, J. C.; Muenchausen, R. E., *Inorg. Chem.* **2011,** *50*, 4627-4631.

(119) Siffredi, G.; Berthet, J. C.; Thuery, P.; Ephritikhine, M. Private Communication to CSD, 2013, CCDC Deposit number 958358, Code ZIXTEH

(120) Clark, D. L.; Sattelberger, A. P.; Bott, S. G.; Vrtis, R. N., *Inorg. Chem.* **1989,** *28*, 1771-1773.

(121) Berthet, J. C.; Thuery, P.; Ephritikhine, M. Private Communication to CSD, 2013, CCDC Deposit number 959292, Code NARFUI01

(122) Evans, W. J.; Giarikos, D. G.; Ziller, J. W., *Organometallics* **2001,** *20*, 5751-5758.

(123) Goodwin, C. A. P.; Tuna, F.; McInnes, E. J. L.; Liddle, S. T.; McMaster, J.; Vitorica-Yrezabal, I. J.; Mills, D. P., *Chem. Eur. J.* **2014,** *20*, 14579-14583.

(124) Goodwin, C. A. P.; Joslin, K. C.; Lockyer, S. J.; Formanuik, A.; Morris, G. A.; Ortu, F.; Vitorica-Yrezabal, I. J.; Mills, D. P., *Organometallics* **2015,** *34*, 2314-2325.

(125) Brady, E. D.; Clark, D. L.; Keogh, D. W.; Scott, B. L.; Watkin, J. G., *J. Am. Chem. Soc.* **2002,** *124*, 7007-7015.

(126) Raithby, P. R.; Gohtra, J. S.; Bradley, D. C.; Hurthouse. M. B. Private Communication to CSD, 2012, CCDC Deposit number 893257, Code WEFNEC.

(127) Kotyk, C. M.; MacDonald, M. R.; Ziller, J. W.; Evans, W. J., *Organometallics* **2015,** *34*, 2287-2295.

(128) Krinsky, J. L.; Minasian, S. G.; Arnold, J., *Inorg. Chem.* **2011,** *50*, 345-357.

(129) Palumbo, C. T.; Ziller, J. W.; Evans, W. J., *Unpublished Results*.

(130) Reddmann, H.; Karbowiak, M.; Amberger, H.-D.; Drożdżyński, J., *Z. Anorg. Allg. Chemie* **2006,** *632*, 1953-1955.

(131) Amberger, H.-D.; Reddmann, H., *Z. Anorg. Allg. Chemie* **2007,** *633*, 443-452.

(132) Amberger, H.-D.; Reddmann, H., *Z. Anorg. Allg. Chemie* **2009,** *635*, 291-296.

(133) Amberger, H.-D.; Reddmann, H.; Mueller, T. J.; Evans, W. J., *J. Organomet. Chem.* **2011,** *696*, 2829-2836.

(134) Evans, W. J.; Lee, D. S.; Lie, C.; Ziller, J. W., *Angew. Chem., Int. Ed.*, **2004,** *43*, 5517-5519.

(135) Evans, W. J.; Rego, D. B.; Ziller, J. W.; DiPasquale, A. G.; Rheingold, A. L., *Organometallics* **2007,** *26*, 4737-4745.

(136) Ababei, R.; Massa, W.; Weinert, B.; Pollak, P.; Xie, X.; Clerac, R.; Weigend, F.; Dehnen, S., *Chem. Eur. J.* **2015,** *21*, 386-94.

(137) Shestakov, B. G.; Mahrova, T. V.; Larionova, J.; Long, J.; Cherkasov, A. V.; Fukin, G. K.; Lyssenko, K. A.; Scherer, W.; Hauf, C.; Magdesieva, T. V.; Levitskiy, O. A.; Trifonov, A. A., *Organometallics* **2015,** *34*, 1177-1185.

(138) Evans, W. J.; Lee, D. S.; Johnston, M. A.; Ziller, J. W., *Organometallics* **2005,** *24*, 6393-6397.

(139) Soller, B. S.; Sun, Q.; Salzinger, S.; Jandl, C.; Pöthig, A.; Rieger, B., *Macromolecules* **2016,** *49*, 1582-1589.

(140) Siladke, N. A.; Webster, C. L.; Walensky, J. R.; Takase, M. K.; Ziller, J. W.; Grant, D. J.; Gagliardi, L.; Evans, W. J., *Organometallics* **2013,** *32*, 6522-6531.

(141) del Mar Conejo, M.; Parry, J. S.; Carmona, E.; Schultz, M.; Brennann, J. G.; Beshouri, S. M.; Andersen, R. A.; Rogers, R. D.; Coles, S.; Hursthouse, M. B., *Chem. Eur. J.* **1999,** *5*, 3000-3009.

(142) Lorenz, S. E.; Schmiege, B. M.; Lee, D. S.; Ziller, J. W.; Evans, W. J., *Inorg. Chem.* **2010,** *49*, 6655-6663.

(143) Rodrigues, I.; Xue, T. Y.; Roussel, P.; Visseaux, M., *J. Organomet. Chem.* **2013,** *743*, 139-146.

(144) Evans, W. J.; Seibel, C. A.; Ziller, J. W., *J. Am. Chem. Soc.* **1998,** *120*, 6745-6752.

(145) Al-Juaid, S.; Gun'ko, Y. K.; Hitchcock, P. B.; Lappert, M. F.; Tian, S., *J. Organomet. Chem.* **1999,** *582*, 143-152.

CHAPTER 5

IDENTIFICATION OF THE FORMAL +2 OXIDATION STATE OF PLUTONIUM: SYNTHESIS AND CHARACTERIZATION OF THE $\{[C_5H_3(SiMe_3)]_3Pu^{II}\}^{1-}$ ANION

INTRODUCTION[†]

As described previously in the Introduction and Chapter 2, characterizing the chemical behavior of any element involves establishing its range of accessible oxidation states. Such understanding provides crucial information for predicting chemical behavior and physical properties. This is of particular interest for plutonium.

Based on Seaborg, McMillan, Kennedy, and Wahl's discovery of plutonium in 1940,[1-2] Pu has emerged as one of the most high profile elements in the periodic table. The recognition that plutonium chemistry is pivotal in a wide range of long-term global challenges has led to international efforts to provide fundamental understanding that underlies actinide processing and applications.[3-6] Unfortunately, advances in uncovering new properties for plutonium are slow compared to the 4*f* elements, uranium, and thorium.[7-9] The slower progress stems from the high specific-radioactivity and limited accessibility of plutonium isotopes. The most synthetically accessible isotope, ^{239}Pu, has a half-life ($t_{½}$) of 24,110(30) y and decays by emission of highly energetic alpha particles with energies of 4.1 to 5.2 MeV. Consequently, chemical research with plutonium needs to be conducted in specialized radiological facilities. Synthetic chemistry with

[†]Portions of this chapter have been published: Windorff, C. J.; Chen, G. P.; Cross, J. N.; Evans, W. J.; Furche, F.; Gaunt, A. J.; Janicke, M. T.; Kozimor, S. A.; Scott, B. L. *Journal of the American Chemical Society*, **2017**, *139*, 3970–3973. DOI: 10.1021/jacs.7b00706.

plutonium is performed on a small scale (~5-50 mg plutonium content) owing to the quantity limitations imposed for reasons of both safety and security.[4, 7] These constraints render synthetic work and characterization methods technically challenging, especially when targeting molecules that are reactive toward air/moisture. As an example, in 2016 there were 75 structures reported in the Cambridge Structural Database (CSD) containing air-reactive U–C bonds. In contrast the total number of CSD structural that contain anhydrous molecular plutonium compounds prepared under inert atmospheres was 25. None contained Pu–C bonds.[10]

As described previously, the +2 oxidation state is isolable for *f*-elements using the tris(silyl-cyclopentadienide) ligand environment, $(Cp'_3)^{3-}$ or $(Cp''_3)^{3-}$ [Cp′ = $C_5H_4SiMe_3$ and Cp″ = $C_5H_3(SiMe_3)_2$–1,3] and encapsulation of an alkali metal (Na, K) upon reduction using crown ethers (18-crown-6 or 12-crorwn-4) or 2.2.2-cryptand (crypt).[11-14] Among this series, eight elements (La, Ce, Pr, Gd, Tb, Ho, Er, and Lu) were reported to have unusual $4f^n5d^1$ ground state electronic configurations, as opposed to the typical $4f^{n+1}5d^0$.[12] It was proposed that the C_3–symmetric tris(cyclopentadienyl) environment stabilizes population of the 5*d*-orbitals (over the 4*f*-orbitals) in these unusual compounds.[12] These results were mirrored in the pursuit of U^{II} and Th^{II} which also contain the rare $5f^36d^1$ (U^{II}) and $5f^06d^2$ (Th^{II}) electron configurations.[11, 13-19]

Therefore, it was of interest to determine (1) whether a formal +2 oxidation state is stable and isolable for transuranic elements (specifically for Pu), and (2) whether the stable $5f^n6d^1$ (as opposed to $5f^{n+1}6d^0$) configurations would continue across the actinide series.[15-19] Previously, there were literature claims of plutonium in the formal +2 oxidation state, *e.g.* in PuH_2 and PuE (E = S, Se, Te), and in molten salts and the gas phase.[2, 22-26] However, the identities of these plutonium(II) compounds were not substantiated through single-crystal X-ray diffraction. This Chapter describes the successful synthesis, isolation, and characterization of a Pu^{II} containing

complex, namely [K(crypt)][Cp''_3Pu]. The first measurements of the Pu–C bond distance is also described. These results distinguish plutonium as being able to access more verified formal oxidation states than any other actinides.

EXPERIMENTAL SECTION

Caution! *^{238}Pu [$t_{1/2}$ = 87.7(1) y], ^{239}Pu [$t_{1/2}$ = 24,110(30) y], ^{240}Pu [$t_{1/2}$ = 6,561(7) y], ^{241}Pu [$t_{1/2}$ = 14.325(6) y], and ^{242}Pu [$t_{1/2}$ = 3.75(2) x 10^5 y] are serious health threats, due to their radioactive decay, as well as that of their daughters. Hence, all studies with plutonium were conducted with appropriate controls for the safe handling and manipulation of radioactive materials, i.e. in a radiation laboratory equipped with HEPA filtered hoods and continuous air monitors. All free-flowing solids that contained plutonium were handled in negative-pressure gloveboxes.*

The α-phase plutonium starting material was of weapons-grade composition and was obtained internally from Los Alamos National Laboratory. All manipulations and syntheses described below were conducted with the rigorous exclusion of air and water using an MBraun Labmaster 130 helium atmosphere drybox (for all of the plutonium chemistry) equipped with standalone Vacuum Atmospheres Genesis oxygen and moisture removal systems, in addition to with standard Schlenk techniques under an argon atmosphere for ligand and solvent preparation.

Diethyl ether, THF, pentane and n-hexane were dried using sodium benzophenone ketyl, exposed briefly to vacuum several times, vacuum transferred and stored on 4 Å molecular sieves prior to use. 2.2.2-cryptand (crypt, 4,7,13,16,21,24-hexaoxa-1,10-diazabicyclo[8.8.8]hexacosane, Aldrich) was placed under vacuum (10^{-3} Torr) for 12 h before use, $PhSiH_3$ (Aldrich) was dried over molecular sieves and degassed by three freeze-pump-thaw cycles, KH (Aldrich) was

obtained in oil and was washed with hexane several times. The following compounds were prepared following literature procedures: KC_8,[27] $AgBPh_4$,[28] KCp″ [Cp″ = $C_5H_3(SiMe_3)_2$–1,3] was made analogously to KCp′ (Cp′ = $C_5H_4SiMe_3$).[29] C_6D_6 and THF-d_8 (Cambridge Isotopes) were dried over sodium/potassium alloy, degassed by three freeze-pump-thaw cycles, and vacuum transferred before use. Celite® and glass fiber circles were dried in a vacuum oven before use.

^{1}H and ^{29}Si (INEPT) NMR spectra were recorded on a Bruker 400 MHz spectrometer operating at 400.1 and 79.5 MHz, respectively, at 298 K unless otherwise stated. ^{1}H NMR spectra were referenced internally to solvent resonances and ^{29}Si were referenced externally to $SiMe_4$. For radiological containment of transuranic solutions, NMR samples were placed inside 4 mm PTFE tube liners inside of 5 mm borosilicate glass NMR. However, samples of [K(crypt)][Cp″$_3$Pu], **22-Pu**, were loaded into a melting point capillary first and then placed in the PTFE tube liner (**22-Pu** cannot be placed directly into PTFE liner because it reacts with the liner material).

Solution phase electronic absorption spectra were collected in screw capped quartz cuvettes (loaded in a transuranic glovebox using parafilm during the loading procedure to wrap and protect the exterior surface of the cuvette and cap from radioactive contamination) at room temperature using a Varian Cary 6000i UV/vis/NIR spectrophotometer. The path length was 1 cm. Solid state UV/vis/NIR samples were recorded on crystals coated in Paratone-N oil, diluted in Cargile ultra low fluorescence oil for immersion microscopy and recorded on a CRAIC microphotospectrometer.

The IR spectra were recorded as a Nujol mull between two KBr plates, with tape wrapped around the interface of the two plates to protect the sample from air, and prevent loss of

radiological containment during transport from the glovebox to instrument (Nicolet 6700 FT-IR spectrometer). Extreme care had to be taken when loading the sample inside the glovebox to ensure the exterior surfaces of the salt plates did not become contaminated.

To ensure safe handling during diffraction studies, crystals of transuranic compounds were prepared for analyses with appropriate layers of containment prior to single crystal diffraction studies. Each transuranic crystal was coated in Paratone-N oil and mounted inside a 0.5 mm diameter quartz capillary, the ends were sealed with capillary wax, and the exterior of the capillary was coated with acrylic (Hard as Nails®) dissolved in ethyl acetate. The data were collected on a Bruker AXS SMART APEX II CCD detector, or a Bruker D8 diffractometer equipped with a CMOS detector.

Cp''_3Pu, **20-Pu**. In a 20 ml borosilicate-glass scintillation vial an ether solution (1.5 ml) of iodine (35 mg, 0.14 mmol) was added to plutonium metal (23 mg, 0.098 mmol) in ether (1.5 ml) and stirred for 2 d. A pale green powder deposited in the vial over the reaction time period and a small piece of unreacted plutonium metal (3 mg, 12%) was removed from the reaction. The volatiles were removed from the mixture and hexane (1.5 ml) was added to the mixture, briefly stirred, and the hexane solution pipetted away to remove the excess iodine. This procedure was repeated several times until the hexane was colorless and the product was dried under reduced pressure to yield a putative "$PuI_3(Et_2O)_x$," **39-Pu**, pale green powder. An ether solution (2.0 ml) of KCp″ (66 mg, 0.27 mmol) was added dropwise to **39-Pu** suspended in ether (1.5 ml). The color of the solution quickly progressed through shades of green before becoming blue over a period of ~10–20 min. Concomitantly, a white solid precipitated (presumably KI). The reaction mixture was stirred overnight. The dark blue mixture was dried under reduced pressure, taken up in hexane (3 ml) and filtered through a celite plug supported on a glass fiber

circle in a pipette to remove KI. The KI was washed with small portions of hexane (3 × 1 ml), until the filtrate was colorless. All volatiles were removed under reduced pressure to give a dark blue residue best described as a mixture of a sticky solid/oil and a powder. The product was taken up in ether (1.5 ml) and dried under reduced pressure 3 × to give a dark blue powder characterized as Cp''_3Pu, **20-Pu** (71 mg, 96% crude yield; 15 mg, 20% crystalline yield based on plutonium content). ^{1}H NMR (C_6D_6): δ 16.5 (br s, $\nu_{1/2}$ = 100 Hz, $C_5H_3(SiMe_3)_2$, 3H), 15.0 (br s, $\nu_{1/2}$ = 100 Hz, $C_5H_3(SiMe_3)_2$, 6H), −0.4 (s, $\nu_{1/2}$ = 6 Hz, $C_5H_3(SiMe_3)_2$, 54H); ^{29}Si NMR (C_6D_6): δ 8.4 ($\nu_{1/2}$ = 20 Hz, $C_5H_3(SiMe_3)_2$). UV/vis/NIR (0.0024 g dissolved in 2.2999 g of hexane, ε, $M^{-1}cm^{-1}$): 498 (250), 564 (530), 583 (610), 591 (580), 599 (590), 626 (530), 686 (270), 714 (260), 753 (100), 801 (30), 857 (20), 913 (100), 940 (115), 997 (40), 1059 (30), 1118 (120), 1224 (128), 1273 (60). X-ray quality crystals were grown from a concentrated pentane solution at −35 °C.

[K(crypt)][Cp''_3Pu], 22-Pu. *Method A.* In a 20 ml scintillation borosilicate-glass vial **20-Pu** (51 mg, 0.059 mmol) and crypt (24 mg, 0.065 mmol) were dissolved in ether (2 ml) with a glass coated magnetic stir bar and placed in the glovebox freezer at −35 °C. The following equipment and reagents were also cooled to −35 °C: (1) a separate vial with an excess of KC_8 (12 mg, 0.089 mmol), (2) several glass pipettes, (3) a pipette with an excess of KC_8 (ca. 30 mg) supported on a glass fiber circle, and (4) many empty vials. After 3 h all of the equipment and reagents were removed from the freezer. The KC_8 was added into the stirring solution **20-Pu** and crypt, which immediately resulted in a pronounced color change from blue to dark purple. Some black solid was observed (presumably graphite). After 2 min the mixture was passed through the KC_8 filter column and washed with ether until colorless. All volatiles were removed under reduced pressure to give a purple–black residue that was washed with pentane (2 × 5 ml)

to give a dark purple powder characterized as [K(crypt)][Cp′′$_3$Pu], **22-Pu** (71 mg, 94 % crude yield; 50 mg, 66 % crystalline yield). ^{1}H NMR (THF-d_8): δ 17.6 (br, s $\nu_{1/2}$ = 40 Hz, $C_5H_3(SiMe_3)_2$, 6H), 3.71 (s, OCH_2CH_2O, 12H), 3.65 (t, $^3J_{HH}$ = 4.5 Hz, NCH$_2$CH_2O, 12H), 2.62 (t, $^3J_{HH}$ = 4.5 Hz, NCH_2CH$_2$O, 12H), 1.6 (s, $\nu_{1/2}$ = 10 Hz, $C_5H_3(SiMe_3)_2$, 54H), −5.5 (br s, $\nu_{1/2}$ = 80 Hz, $C_5H_3(SiMe_3)_2$, 3H). UV/vis/NIR (single crystal): 500 nm (broad). UV/vis/NIR (single crystals of **22-Pu**, 0.0024 g dissolved in 2.4823 g THF, ε, M^{-1}cm^{-1}): 470 nm (broad, 2700). FTIR (cm^{-1}, nujol): 1296(m), 1260(sh), 1237(s), 1204(m), 1133(m), 1107(s), 1078(s), 952(s), 933(m), 920(s), 829 (vs), 798(sh), 746(s), 678(w), 632(w), 618(w). X–ray quality crystals were grown from an ether solution layered with hexane at –35 °C overnight

[K(crypt)][Cp′′$_3$Pu], 22-Pu. *Method B.* In a 20 ml borosilicate-glass scintillation vial solid crypt (33 mg, 0.89 mmol) was added to **20-Pu** (69 mg, 0.079 mmol), dissolved in ether (1.5 ml), forming a blue solution that was capped and placed in the glovebox freezer at −35 °C freezer. A glass pipette was packed with a glass fiber circle followed by KC_8 (ca. 55 mg, 0.41 mmol), placed in the −35 °C glovebox freezer along with two fresh pipettes, a vial containing ether and an empty vial. After 2 h all of the glassware was removed from the glovebox freezer and the blue solution was quickly passed through the KC_8 column with the effluent coming out dark purple-brown, into the empty vial. The column was washed 2 × with small amounts of cold ether until the effluent was colorless. The purple-brown solution was quickly evaporated and washed with pentane, to give **22-Pu** as a dark purple solid (68 mg, 66% crude; 38 mg, 37% crystalline yield), confirmed by UV/vis/NIR spectroscopy.

Oxidation of [K(crypt)][Cp′′$_3$Pu], 22-Pu, with AgBPh$_4$. $AgBPh_4$ (6 mg, 0.014 mmol) was added to a dark purple THF (1 ml) solution of **22-Pu** (15 mg, 0.012 mmol) in a 20 mL scintillation borosilicate vial with a glass coated magnetic stir bar. After 30 min the mixture was

filtered through a glass fiber circle in a glass pipette to remove black solids (presumably Ag^0). Volatiles were removed under reduced pressure. The blue solution was extracted into hexane and filtered through a plug of Celite supported on a glass fiber circle in a glass pipette to remove white precipitates (presumably [K(crypt)][BPh_4]). Volatiles were removed under reduced pressure to isolate **20-Pu** as a blue solid (9 mg, 86 % yield), as identified by ^{1}H NMR spectroscopy.

Reaction of Cp′′$_3$Pu, 20-Pu, with KH. 20-Pu (49 mg, 0.057 mmol) was dissolved in THF (1 ml) and transferred to a 20 mL scintillation borosilicate glass vial with crypt (24 mg, 0.063 mmol) which was transferred to a 20 mL scintillation borosilicate glass vial with KH (12 mg, 0.29 mmol), a glass coated magnetic stir bar, and THF (4 ml). After 4 h the mixture was filtered on a glass fiber circle in glass pipette and the volatiles were removed under reduced pressure to give a green oil. Trituration with hexane and extended drying under reduced pressure yielded a flocculent green powder (45 mg). UV/vis/NIR (0.028 g dissolved in 5.077 g THF, because the molecular weight is unknown the molar absorptivity values cannot be calculated, therefore only peaks are noted): 529, 605, 624, 747, 708, 819, 871, 902, 940, 1024, 1089, 1144, 1176, 1191, 1359. FTIR (nujol): 1299(s), 1260(s), 1238(s), 1135(m), 1106(s), 1079(s), 952(m), 925(m), 833(vs), 747(s), 722(sh), 688(w), 636(w).

Reaction of [K(Crypt)][Cp′′$_3$Pu], 22-Pu, with $PhSiH_3$. A THF solution (1.6 mL) of $PhSiH_3$ (1.7 mg, 0.016 mmol) was added to crystalline sample of **22-Pu** (9.6 mg, 0.0075 mmol) with agitation (no stir bar). No discernible immediate reaction took place and after 10 min an excess of neat $PhSiH_3$ was added (6.7 mg, 0.062 mmol), followed by agitation of the reaction solution intermittently over 25 min. The solution changed color to a forest-green and was filtered through a glass fiber plugged glass pipette and loaded into a quartz screw-cap cuvette

and analyzed by UV/vis/NIR spectroscopy to give a similar spectrum to the reaction of **20-Pu** + KH + crypt.

X-ray Crystallographic Data. Crystallographic details for complexes Cp''_3Pu, **20-Pu** and [K(crypt)][Cp''_3Pu], **22-Pu** are summarized in the text below and in Table 5.1.

X-ray Data Collection, Structure Solution and Refinement for Cp''_3Pu, 20-Pu. A blue crystal of approximate dimensions 0.10 x 0.10 x 0.70 mm was mounted in a quartz capillary, sealed, painted with hard as nails and transferred to a Bruker D8 diffractometer equipped with a CMOS detector. The APEX2[30] program package was used to determine the unit-cell parameters and for data collection. The raw frame data was processed using SAINT[31] and SADABS[32] to yield the reflection data file. Subsequent calculations were carried out using the SHELXTL[33] program. The diffraction symmetry was 2/*m* and the systematic absences were consistent with the monoclinic space groups *Cc* and *C*2/*c*. It was later determined that space group *C*2/*c* was correct.

The structure was solved by direct methods and refined on F^2 by full-matrix least-squares techniques. The analytical scattering factors[34] for neutral atoms were used throughout the analysis. Hydrogen atoms were located from a difference-Fourier map and refined (x,y,z and U_{iso}). Hydrogen atoms were included using a riding model. The absolute structure was assigned by refinement of the Flack parameter.[35]

X-ray Data Collection, Structure Solution and Refinement for [K(crypt)][Cp''_3Pu], 22-Pu. A very dark violet crystal of approximate dimensions 0.12 x 0.12 x 0.12 mm was mounted in a quartz capillary, sealed, painted with hard as nails and transferred to a Bruker AXS SMART APEX II CCD detector. The APEX2[36] program package was used to determine the unit-cell parameters and for data. The raw frame data was processed using SAINT[37] and

SADABS[38] to yield the reflection data file. Subsequent calculations were carried out using the SHELXTL[39] program. There were no systematic absences nor any diffraction symmetry other than the Friedel condition. The centrosymmetric triclinic space group $P\bar{1}$ was assigned and later determined to be correct.

The structure was solved by dual space methods and refined on F^2 by full-matrix least-squares techniques. The analytical scattering factors[40] for neutral atoms were used throughout the analysis. Hydrogen atoms were included using a riding model.

Table 5.1. X-ray Data and Collection Parameters for Cp''_3Pu, **20-Pu**, and [K(crypt)][Cp''_3Pu], **22-Pu**.

Compound	**20-Pu**	**22-Pu**
Empirical Formula	$C_{33}H_{63}Si_6Pu$	$C_{51}H_{99}N_2O_6Si_6KPu$
Temperature (K)	100(2) K	100(2) K
Crystal System	Monoclinic	Triclinic
Space Group	*C*2/*c*	$P\bar{1}$
***a* (Å)**	24.441(4)	12.2131(8)
***b* (Å)**	11.1218(19)	12.7370(8)
***c* (Å)**	17.219(3)	22.2524(14)
α (deg)	90°	100.8106(7)°
β (deg)	116.953(3)°	104.3697(6)°
γ (deg)	90°	95.5916(7)°
Volume (Å^3)	4172.3(12)	3255.8(4)
Z	4	2
ρ_{calcd} (Mg/m^3)	1.386	1.312
μ (mm^{-1})	1.772	1.228
R1[a] (*I* > 2.0σ(I))	0.0574	0.0235
wR2 (all data)	0.1333	0.0526

[a]Definitions: $R1 = \Sigma||F_o| - |F_c||/ \Sigma |F_o|$, $wR2 = [\Sigma w(F_o^2 - F_c^2)^2/ \Sigma w(F_o^2)^2]^{1/2}$.

Goof = $S = [\Sigma[w(F_o^2-F_c^2)^2] / (n-p)]^{1/2}$ where n is the number of reflections and p is the total number of parameters refined.

RESULTS AND DISCUSSION

Synthesis and Characterization of Cp″$_3$Pu, 20-Pu. To accomplish the plutonium chemistry described, experimental studies were performed with Dr. Andrew Gaunt and Dr. Stosh Kozimor at Los Alamos National Laboratory in laboratories dedicated to the study of actinide elements. To begin the synthetic studies of a molecular Pu^{II} complex it was first necessary to develop a synthetic route to the parent Cp″$_3$Pu, **20-Pu**, complex based on the available starting materials, namely Pu metal, which can be oxidized to PuX_3L_y[41] or an acidic stock solution which can be converted to $PuCl_4(DME)_2$.[42] While analogous chemistry is well established for lanthanides,[43-45] U,[46-47] and Th,[14, 48] only a handful of organoplutonium complexes have been reported in the literature.[4, 7] None were characterized by single-crystal X–ray diffraction studies. It was discovered that the established $PuI_3(py)_4$, **40-Pu**, precursor[49-50] did not cleanly yield the **20-Pu** target in a salt metathesis reaction with KCp″. This observation highlights the non-trivial nature of conducting organoplutonium chemistry. Instead, it was discovered that oxidation of Pu metal with iodine in diethyl ether to form a green $PuI_3(OEt_2)_x$, **39-Pu**, product,[51] followed by in situ treatment with three equivalents of KCp″, cleanly generates **20-Pu,** eq 1, by ^{1}H NMR analysis, as described for the lanthanides in Chapter 4. Crystallization of this compound from pentane at −35 °C generated single crystals in 20% yield that were confirmed by X–ray crystallography to be **20-Pu**, Figure 5.1. The bulk product of **20-Pu** was cleanly isolated in 96% yield as a blue powder.

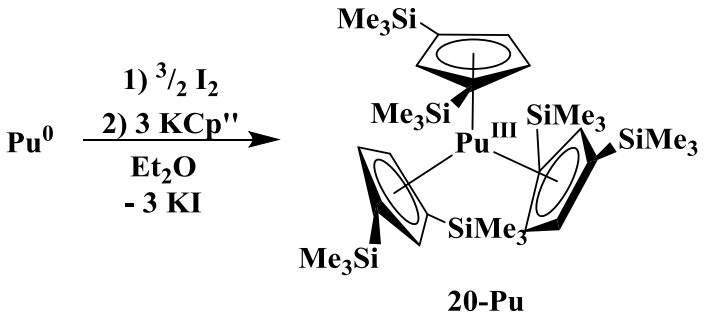

(5.1)

Complex **20-Pu** crystallizes in the *C*2/*c* space group with unit cell constants similar to the other Cp″$_3$M complexes, **20-M** (M = La, **20-La**, Ce, **20**-Ce, Nd, **20-Nd**, and U, **20-U**).[43, 45-46] However, it is not isomorphous with other early members of the **20-M** series (M = La, Ce, Nd, and U) although it displays similar bond metrics to the other **20-M** compounds with a Pu–C range of 2.633–2.931 Å, an average Pu–(centroid) length of 2.51 Å, and an average (centroid)–Pu–(centroid) angle of 120°, Table 5.2.

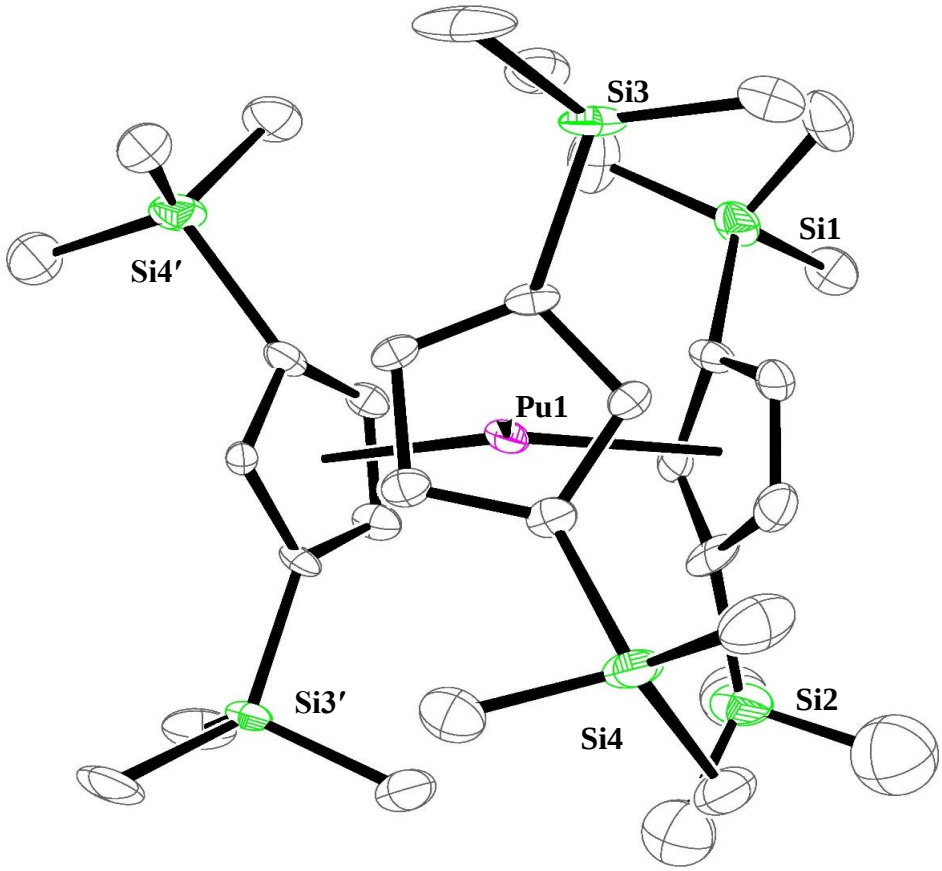

Figure 5.1. Thermal ellipsoid plot of Cp″$_3$Pu, **20-Pu**, drawn at the 50% probability level with disorder in the Cp″ ligands and hydrogen atoms omitted for clarity.

Table 5.2. X-ray Crystal and Metrical Parameter Comparisons for Cp''_3Pu, **20-Pu**, With Other Cp''_3M, **20-M**, Complexes (cent = Cp″ Ring Centroid).

	La[45]	U[46]	Ce[43]	Pu	Nd[45]	Th[14, 48]
6 Coordinate M^{3+} Radii (Å)*[52]	1.032	1.025	1.01	1	0.983	*
Space Group	*Cc*	*Ia*	*I*2/*c*	*C*2/*c*	*Cc*	$P2_1/c$
a (Å)	24.57	22.75	22.75	24.44	24.68	18.01
b (Å)	11.41	11.34	11.39	11.12	11.32	13.78
c (Å)	17.37	17.40	17.43	17.22	17.41	19.36
α (°)	90	90	90	90	90	90
β (°)	117.8	105.37	105.7	116.90	117.21	112.83
γ (°)	90	90	90	90	90	90
M–C avg. (Å)	2.852(8)	2.82(5)	2.83(4)	2.77(1)	2.789(2)	2.80(2)
M–(cent) (Å)	2.615 2.605 2.586	2.561 2.557 2.507	2.579 2.575 2.542	2.569 2.547 2.400	2.558 2.569 2.468	2.521 2.521 2.517
(cent)–M–(cent) (°)	120.5 119.9 199.6	120.8 119.8 119.2	120.4 119.9 119.6	122.8 121.9 115.1	121.8 120.3 117.8	120.1 120.1 119.8

*Six coordination chosen since there is a Shannon radius for this coordination number for all the ions except Th^{III}.

Complex **20-Pu** exhibits a paramagnetically-shifted ^{1}H NMR spectrum consistent with the solid state structure: −0.4 ppm, 54 H, $\nu_{1/2}$ = 6 Hz, Si(CH_3)$_3$; 16.5 ppm, 3 H, and 15.0 ppm, 6 H, $\nu_{1/2}$ = 100 Hz ppm, ring protons, Figure 5.2. The ^{29}Si NMR spectrum contained a single resonance at +8.4 ppm, which was distinct from the −14.59 ppm signal from KCp″,[47] Figure 5.2.

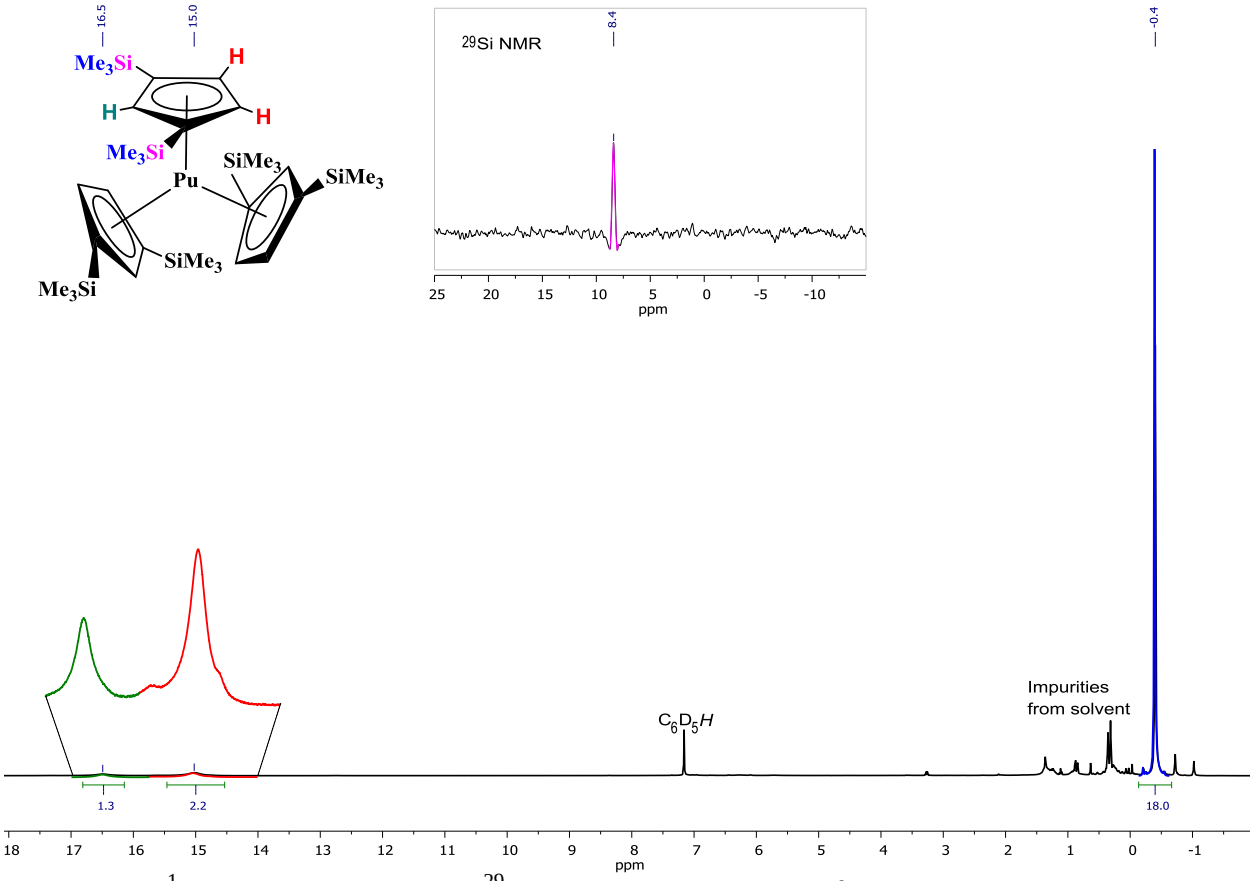

Figure 5.2. ^{1}H NMR spectrum with ^{29}Si NMR spectrum inset of Cp″$_3$Pu, **20-Pu**, in C_6D_6 at 298 K, with color labeling scheme for ligand in upper left corner.

Synthesis and Characterization of [K(crypt)][Cp′′$_3$Pu], 22-Pu. The bulk powdered form of **20-Pu** was used in the subsequent reaction step to form the Pu^{II} complex. Addition of potassium graphite, KC_8, to blue Et_2O solutions of **20-Pu** and crypt resulted in consumption of KC_8 and an immediate color change to dark purple. Following work up consisting of filtration to remove the solid graphite byproduct, evaporation of the solvent under reduced pressure, and washing the resulting residue with pentane to remove unreacted **20-Pu** and excess crypt, [K(crypt)][Cp′′$_3$Pu], **22-Pu**, was isolated as a very dark purple solid, eq. 2. Et_2O solutions of **22-Pu** layered with hexane and stored at −35 °C overnight generated very dark block-like green-violet single crystals in 65% crystalline yield that were suitable for X–ray diffraction studies.

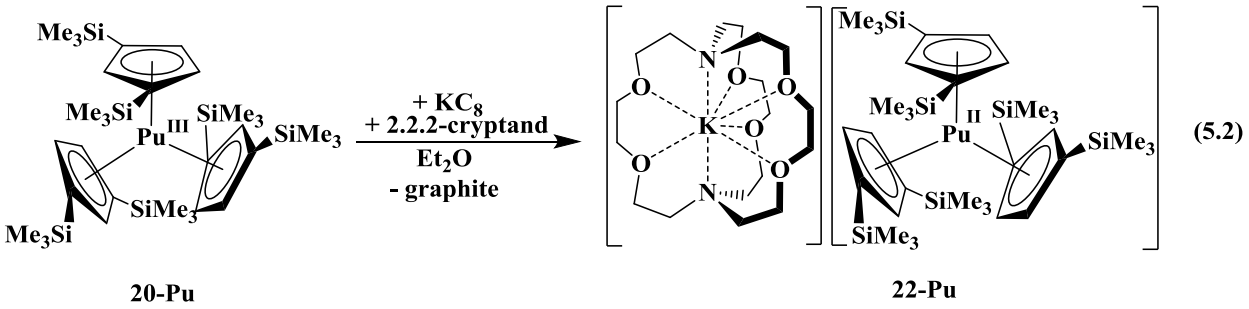

20-Pu **22-Pu** **(5.2)**

The structural determination of **22-Pu** confirms a molecular formula of [K(crypt)][Cp′′$_3$Pu] consistent with formally Pu^{II} based on charge balance, Figure 5.3. The salt crystallizes in the $P\bar{1}$ space group and is isomorphous with [K(crypt)][Cp′′$_3$Th], **22-Th**,[14] and [K(crypt)][Cp′′$_3$Nd], **22-Nd**, Chapter 4, but not [K(crypt)][Cp′′$_3$Ln], (Ln = La, Ce, Pr), which crystallizes with a different unit cell.[53, 54] The Pu–(centroid) average distance, 2.522 Å, in **22-Pu** is most closely comparable to **22-Th**, 2.521 Å, and both complexes feature an average (centroid)–M–(centroid) angle of 120°. A complete table with full comparisons to lanthanide metals can be found in Table 4.6

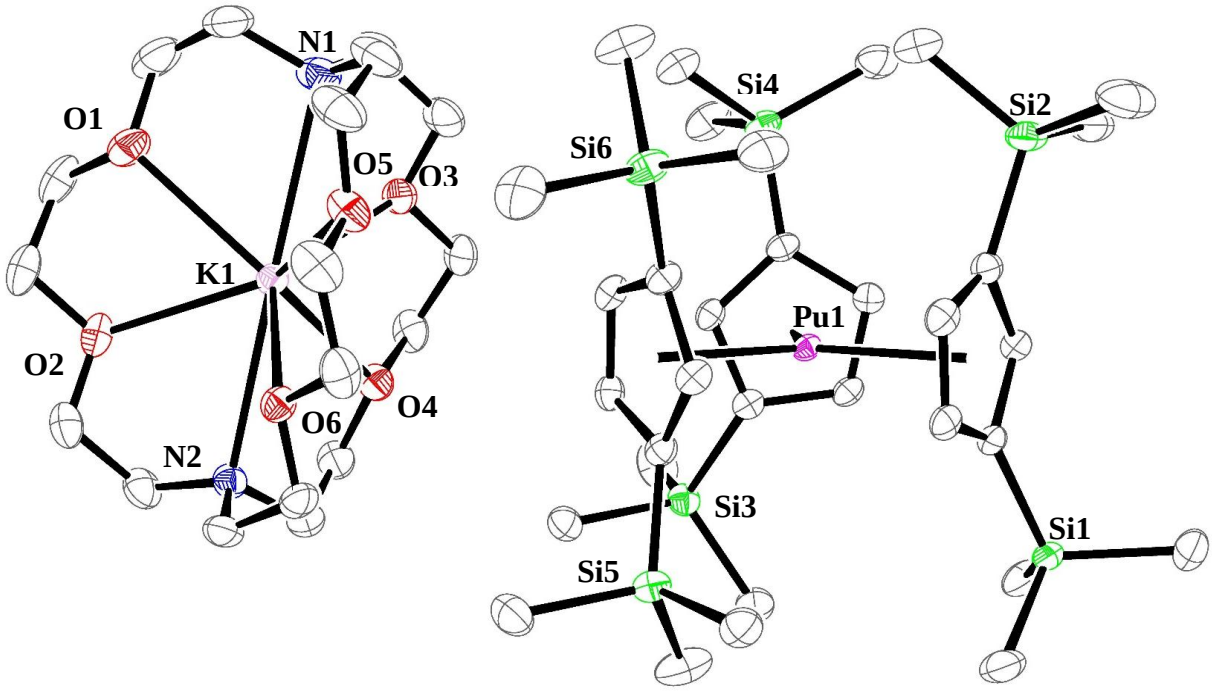

Figure 5.3. Thermal ellipsoid plot of [K(crypt)][Cp″$_3$Pu], **22-Pu**, drawn at the 50 % probability level with hydrogen atoms omitted for clarity.

The ^{1}H NMR spectrum of **22-Pu** in THF-d_8 is distinct from that observed for **20-Pu,** exhibiting paramagnetic signals for the $SiMe_3$ groups at 1.6 ppm (54 H, $\nu_{1/2}$ = 10 Hz) and ring protons tentatively assigned to broad features at −5.5 (3 H, $\nu_{1/2}$ = 80 Hz) and 17.5 (6 H, $\nu_{1/2}$ = 40 Hz) ppm, assigned based on relative integration, Figure 5.4. Resonances for the $[K(crypt)]^+$ cation are observed at 3.71, 3.65, and 2.62 ppm. As would be expected for a formal oxidation state of Pu^{II}, the complex is highly susceptible towards oxidation – solutions of **22-Pu** in PTFE NMR tubes decompose within minutes. Also, even when solutions of **22-Pu** were multiply contained, inside a glass capillary, nested within a doubly plugged PTFE NMR tube liner, and placed inside a glass NMR tube, the onset of decomposition was observed within 20 min of

removing the sample from the inert atmosphere glovebox. The rapid decomposition precluded characterizing **22-Pu** by ^{29}Si NMR spectroscopy. To further examine the spectroscopy of **22-Pu**, an infrared spectrum of **22-Pu** was recorded as a Nujol mull on KBr discs, for containment. The spectrum is compared with the uranium analog, **22-U**, in Figure 5.5. The similar spectra are consistent with the similar geometries of the two compounds.

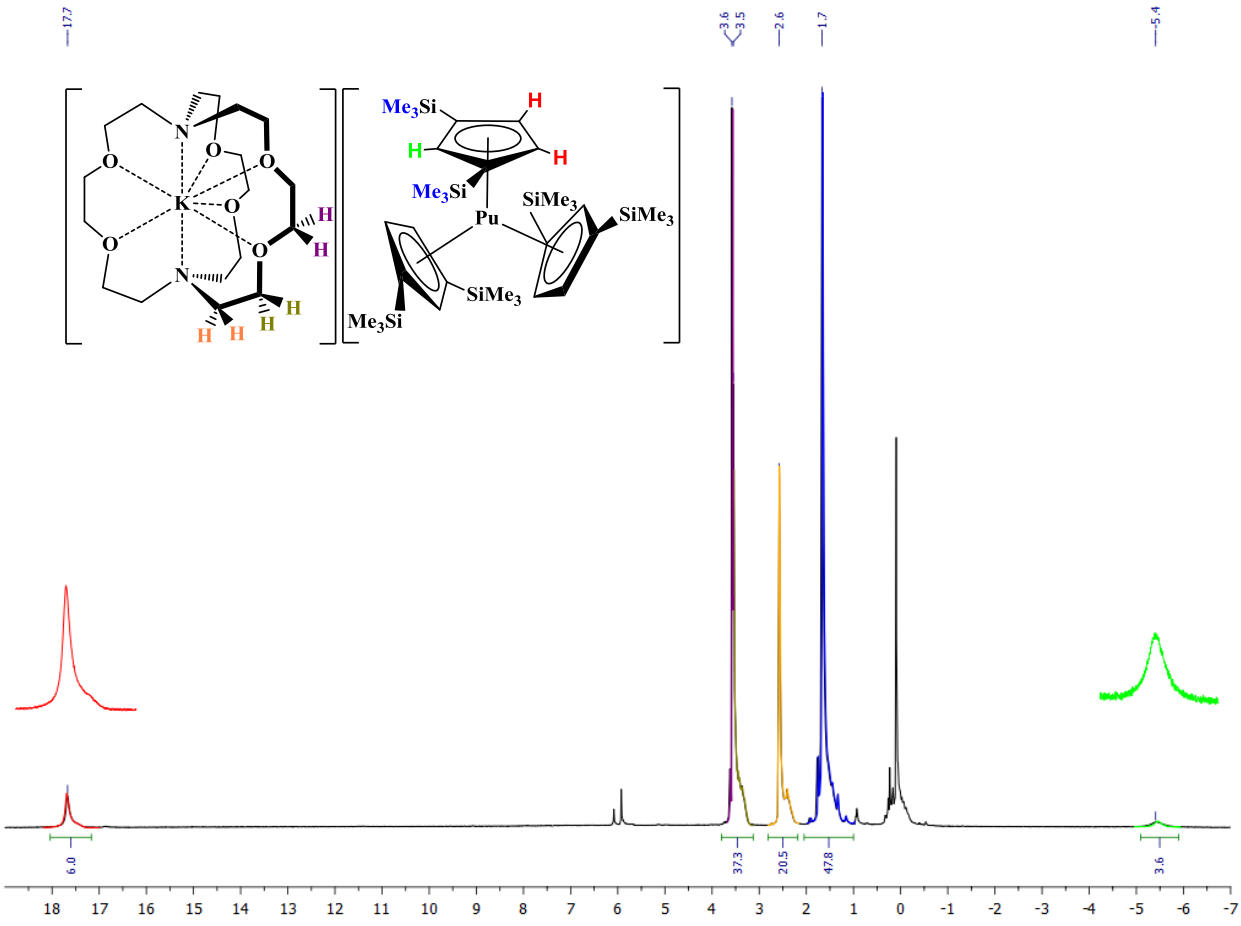

Figure 5.4: ^{1}H NMR spectrum of [K(crypt)][Cp″$_3$Pu], **22-Pu**, in THF-d_8 at 298 K, with color labeling scheme for ligand in upper left corner and resonances labeled with * corresponding to free [K(crypt)][Cp″].

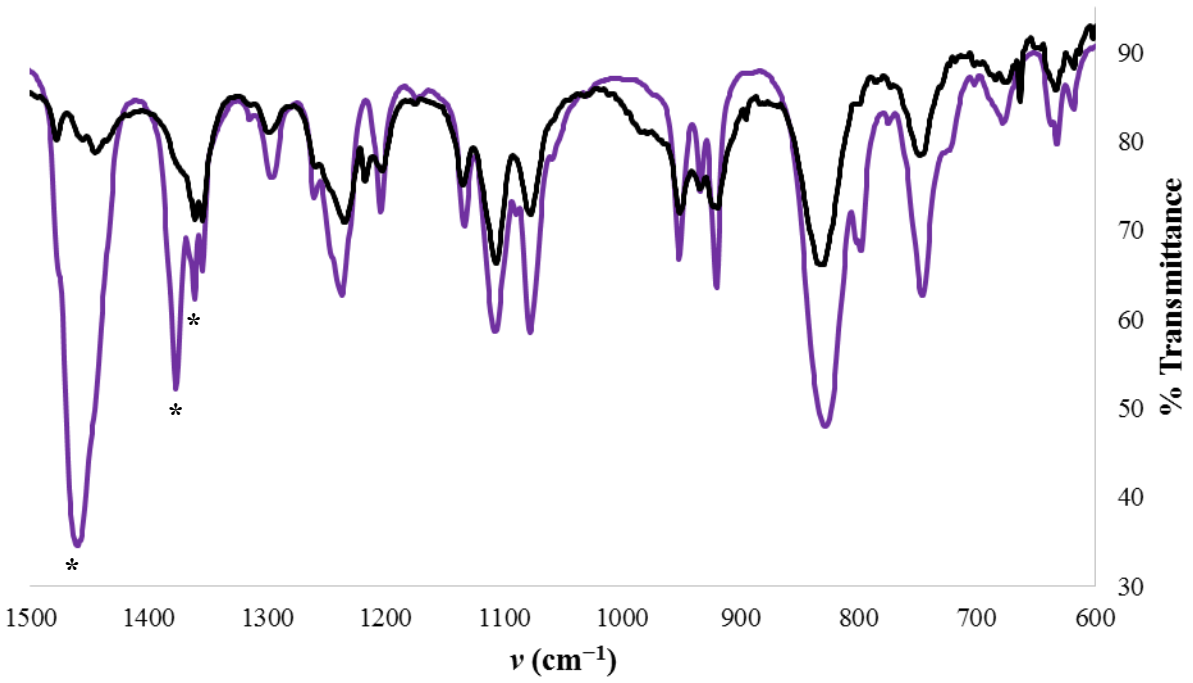

Figure 5.5. FTIR spectra of [K(crypt)][Cp″$_3$Pu], **22-Pu**, (purple trace, Nujol mull) compared with [K(crypt)][Cp″$_3$U], **22-U**, (black trace, KBr pellet) in fingerprint region with Nujol bands labeled by *.

Theoretical Calculations and Interpretations of Optical Spectra. Density functional theory (DFT) calculations were carried out at the University of California, Irvine by Guo Chen and Filipp Furche. Geometry optimizations using DFT predicted trigonal planar structures for both **20-Pu** and the $(Cp''_3Pu)^{1-}$ anion in **22-Pu**. The computation results are in good agreement with the crystallographic data, e.g. the calculated metal–(centroid) average distances of 2.48 Å for **20-Pu** and 2.53 Å for $(PuCp''_3)^{1-}$. The 0.05 Å difference in metal–(centroid) distance between **20-Pu** and **22-Pu** is larger than that observed between Cp″$_3$Th/Cp′$_3$U, and $(Cp''_3Th)^{1-}$/$(Cp'_3U)^{1-}$ (~0.02 Å) but less than the anticipated ~0.1 Å change in ionic radius from Pu^{III} to Pu^{II}. In comparison, the ionic radius increases by 0.12 from Pu^{V} to Pu^{IV} and by 0.14 Å

from Pu^{IV} to Pu^{III}. Mulliken population analysis suggests that the HOMO of $(Cp''_3Pu)^{1-}$, Figure 5.6, is predominantly a Pu–Cp″ non-bonding f_{z3} orbital. However, this HOMO also possesses appreciable (7%) d_{z2} character. The mixing of 5*f* and 6*d* orbitals is consistent with the slight $C_{3h} \rightarrow C_3$ pseudo-Jahn–Teller distortion on the complex due to the near degeneracy of the Pu^{II} $5f^{\ 5}6d^1$ and $5f^{\ 6}6d^0$ configurations. Thus, the calculations suggest that $(Cp''_3Pu)^{1-}$ is a borderline case between the traditional $4f^{n+1}5d^0$ lanthanide(II) molecules and the $4f^{\ n}5d^1$ lanthanide(II), U^{II}, and Th^{II} compounds. Calculations on $(Cp''_3An)^{1-}$ (An= Th–Cm) and other calculations on $(Cp'_3An)^{1-}$ (An = Th–Am)[19] also suggest that the $5f^{\ n}\ 6d^1$ to $5f^{\ n+1}\ 6d^0$ cross-over occurs around Pu.

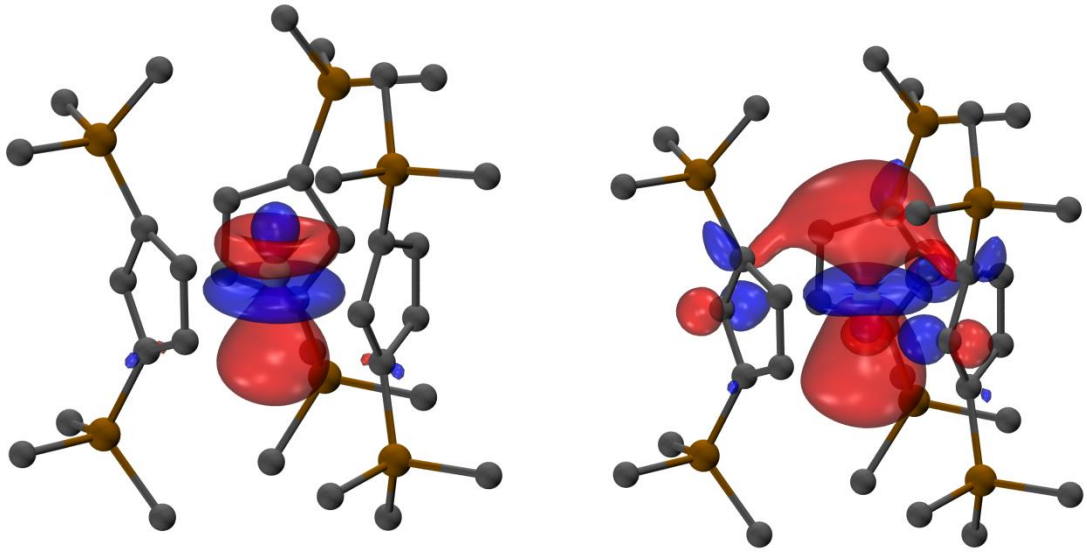

Figure 5.6. HOMO (left) and α-spin LUMO (right) of $(Cp''_3Pu)^1$.

The UV/vis/NIR absorption spectrum of **20-Pu** in hexane contains a broad and intense band near 580 nm (molar absorptivity = ~600 $M^{-1}cm^{-1}$), which is not typically observed in the spectra of complexes containing Pu^{III} ions, Figure 5.7.[2, 7, 50] Time-dependent DFT (TDDFT) calculations, suggest that this band predominantly originates from a $5f \rightarrow 6d$ transition. The

band is observable in the visible region because of the strong stabilization of the $6d_{z^2}$ orbital in the trigonal-planar ligand field. Numerous weak absorptions between 900 and 1400 nm are assigned to Laporte forbidden $5f \rightarrow 5f$ transitions characteristic of Pu^{III}.[2]

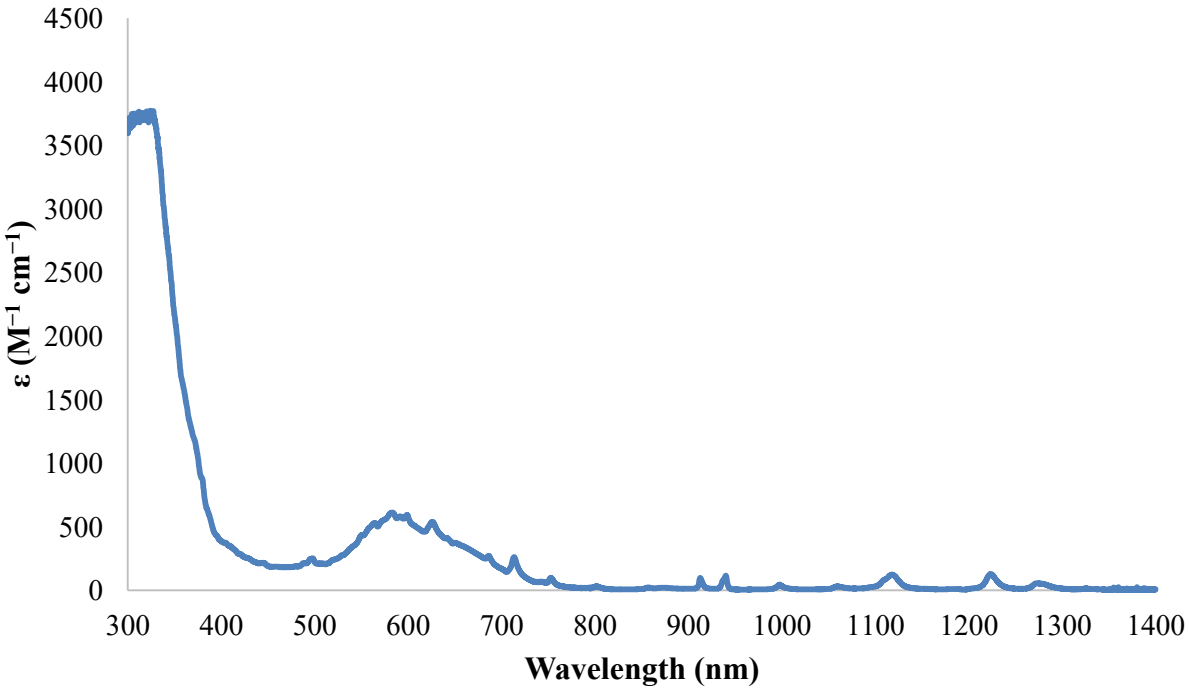

Figure 5.7. Experimental solution phase UV/vis/NIR spectrum of Cp''_3Pu, **20-U**, in hexane at 298 K.

Reduction of **20-Pu** to **22-Pu** imparts substantial changes in the UV/vis/NIR spectra. For example, the Pu^{III} $5f \rightarrow 5f$ transitions characteristic of **20-Pu** are detected as an impurity only in the solution phase UV/vis/NIR spectrum, Figure 5.8, and were not detected in solid-state UV/vis/NIR spectrum, Figure 5.9. Both the solution and solid state spectra of **22-Pu** are dominated by very broad bands with maxima at 470 nm that extended past 850 nm with an approximate molar absorptivity of 2700 M^{-1} cm^{-1}, this band is more intense than $5f \rightarrow 5f$

transitions typically observed in this region.

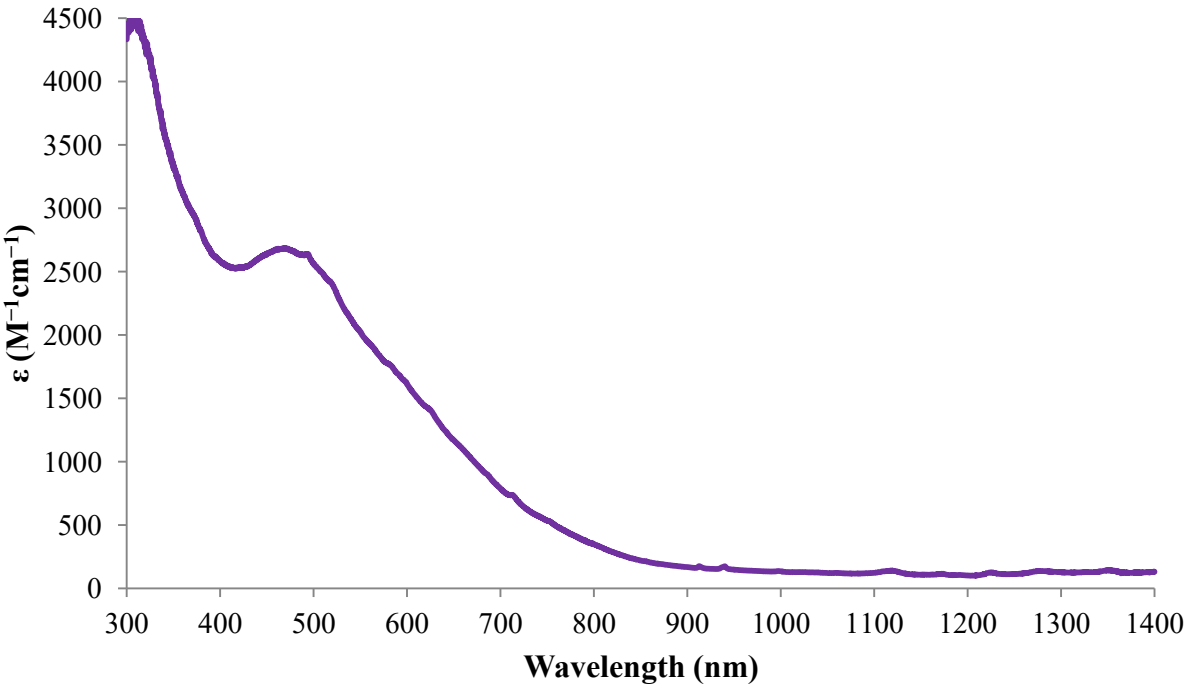

Figure 5.8. Experimental solution phase UV/vis/NIR spectrum of [K(crypt)][Cp″$_3$Pu], **22-Pu**, in THF at 298 K.

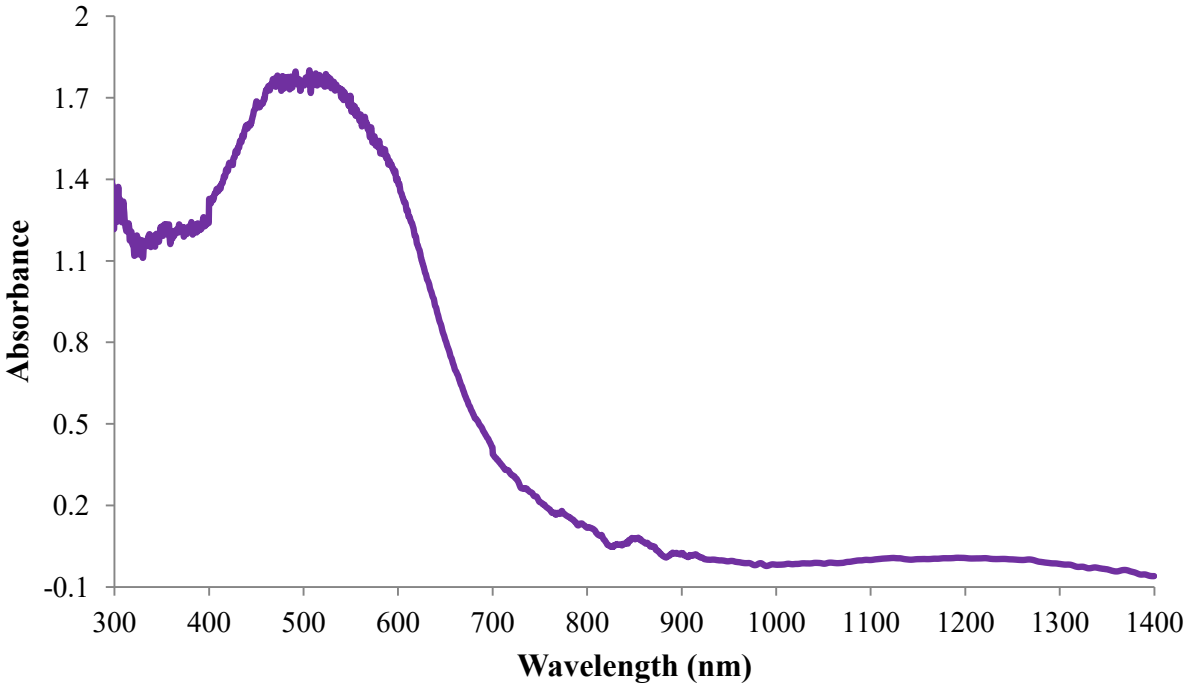

Figure 5.9. Experimental solid state UV/vis/NIR spectrum of [K(crypt)][Cp″$_3$Pu], **22-Pu**.

TDDFT calculations on $(Cp''_3Pu)^{1-}$ suggest that these intense absorptions arise primarily from metal-to-ligand charge transfer (MLCT) excitations originating from Pu 5*f* orbitals. Similar MLCT absorption bands were observed for $(Cp''_3Th)^{1-}$,[14] $(Cp''_3U)^{1-}$,[13] and $(Cp'_3U)^{1-}$[11] as well as the $4f^n5d^1$ $(Cp'_3Ln)^{1-}$ (Ln = Pr, Nd, Gd, Tb, Dy, Ho, Er, Lu) compounds,[55] but are absent in +2 lanthanide compounds with traditional $4f^n5d^0$ electronic configurations such as $(Cp'_3Sm)^{1-}$.[12] The unusually high intensity of these transitions compared with **20-Pu** may be rationalized by an increased electron repulsion in the $5f^6$ configuration of $(Cp''_3Pu)^{1-}$ compared with the $5f^5$ ground state configuration of the Pu^{III} ion

These factors red-shift the MLCT transitions into the visible region and lead to larger transition dipole moments involving coupling between 5*f* and ligand orbitals, ultimately providing a mechanism to increase the absorption intensities. In contrast, the 4*f* orbitals in

traditional Ln^{II} compounds with $4f^{n+1}5d^0$ configurations, such as $(Cp'_3Sm)^{1-}$, are considerably lower in energy and more contracted than the 5*f* orbitals in **22-Pu**. Hence, these compounds do not exhibit strong MLCT transitions in the visible spectrum.[53, 56] The calculations also suggest that the high energy of the 5*f* orbitals and stabilized $6d_{z^2}$ orbital results in low-energy $5f \rightarrow 6d$ transitions in $(Cp''_3Pu)^{1-}$. The calculated energy of this transition is near 3850 nm, outside the range of the conventional UV/vis/NIR spectrum provided in Figure 5.10. While some of the intensity of the visible transitions in **22-Pu** may be attributable to configuration mixing in the ground state and/or thermal population of the low-lying $5f^5 6d^1$ excited state, suggesting that $(Cp''_3Pu)^{1-}$ is somewhat of a hybrid, lying between traditional $5f^5 6d^1$ and $5f^6 6d^0$ configurations.

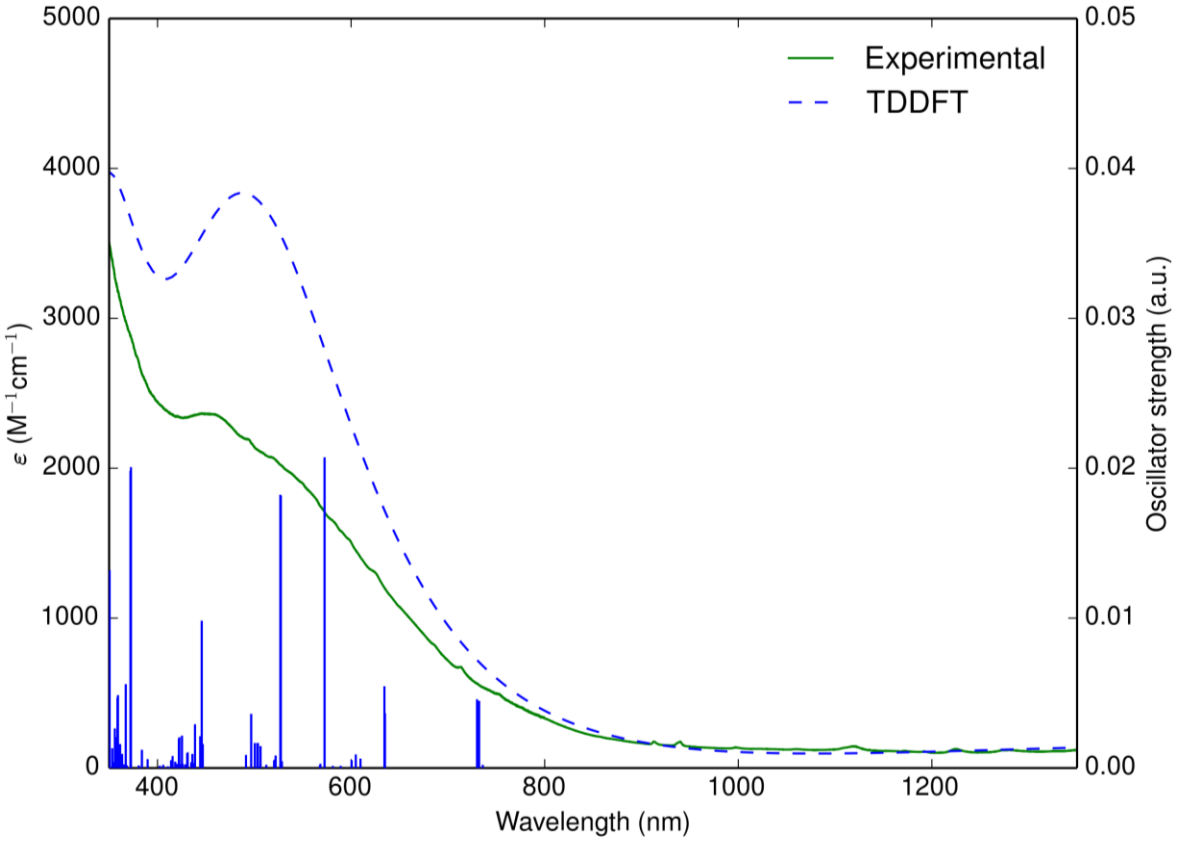

Figure 5.10. Experimental solution phase UV/vis/NIR spectrum of **22-Pu** (green trace) and TDDFT calculated UV/vis/NIR spectrum (blue dashed trace) with the blue bars representing the energy and oscillator strength of the excitations.

Reactivity studies on Pu^{II}/Pu^{III}. The initial discovery and characterization of a formally Pu^{II} molecule was a starting point for full understanding of the electronic structure and reactivity of this new formal oxidation state. However, a few preliminary reactivity studies were conducted to aid in demonstrating that **22-Pu** reacts as expected for a Pu^{II} complex. For example, treatment of **22-Pu** with an equivalent of the one-electron oxidant $AgBPh_4$ regenerates the parent trivalent **20-Pu**, in high yield. **20-Pu** was unambiguously identified by ^1H NMR spectroscopy, eq. 5.3. Analogous behavior has been observed in the oxidation of the related $(Cp'_3U)^{1-}/(Cp''_3U)^{1-}$ complexes to reform their trivalent parents Cp'_3U/Cp''_3U, respectively.[11, 13]

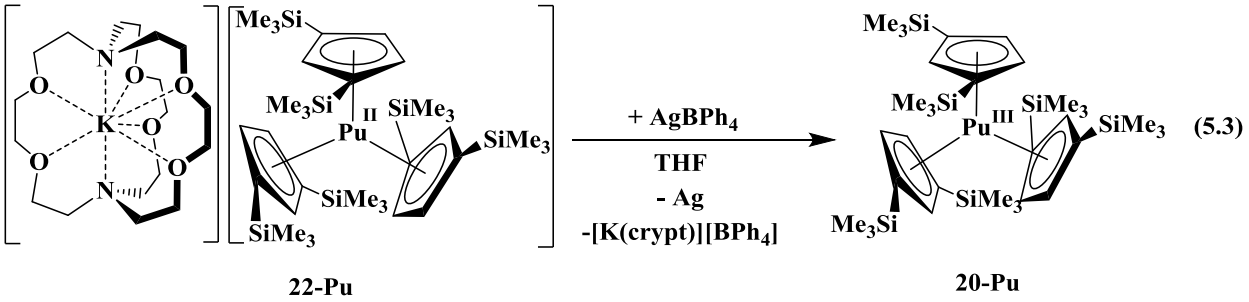

22-Pu **20-Pu** **(5.3)**

Experiments were also conducted to show that **22-Pu** is indeed a molecular Pu^{II} complex and not a $(Pu^{III}–H)^{2–}$ with a crystallographically undetected hydride through the attempted synthesis of the $(Pu^{III}–H)^{2–}$ compound, namely, [K(crypt)][Cp″$_3$PuH], **27-Pu**. This was performed in an analogous manner to the uranium reactions discussed in Chapter 2.[11, 13] Addition of KH and crypt to a blue THF solution of **20-Pu** gave a color change to green, from which a green flocculent solid could be isolated. Attempts to grow X-ray quality single crystals were not successful. Attempts to collect a ^{1}H NMR spectrum did not yield an assignable spectrum, as some or all of the signals may be NMR silent as was observed in the case of [K(18-crown-6)(THF)$_2$][Cp″$_3$UH], **26-U**, Chapter 2.[13] UV/vis/NIR spectroscopy showed a charge transfer band centered at ~600 nm with numerous weak $f \rightarrow f$ transitions, similar to **20-Pu** and consistent with a Pu^{III} ion,[2] Figure 5.11. To make a more direct comparison with the analogous uranium compound, [K(crypt)][Cp″$_3$UH], **27-U**, IR spectroscopy was examined, Figure 5.12. The spectra of the two compounds are nearly identical, as in the case of the divalent compounds **22-U** and **22-Pu**, Figure 5.5. The oxidation of **22-Pu** with excess $PhSiH_3$, analogous to the previously discussed uranium chemistry, Chapter 2,[11, 13] also gave a color change from dark purple to green. The UV/vis/NIR spectrum of this product is very similar to that of the product from the reaction of **20-Pu** with KH, Figure 5.10. The chemical and physical properties of this product are distinct from those of **22-Pu** in that it shows higher room temperature stability and it

does not react with Teflon as other M^{II} complexes do. While tempting to claim this product as "[K(crypt)][Cp″$_3$PuH], **27-Pu**," the evidence is not sufficient enough. It is, however, a chemically distinct species from **22-Pu**.

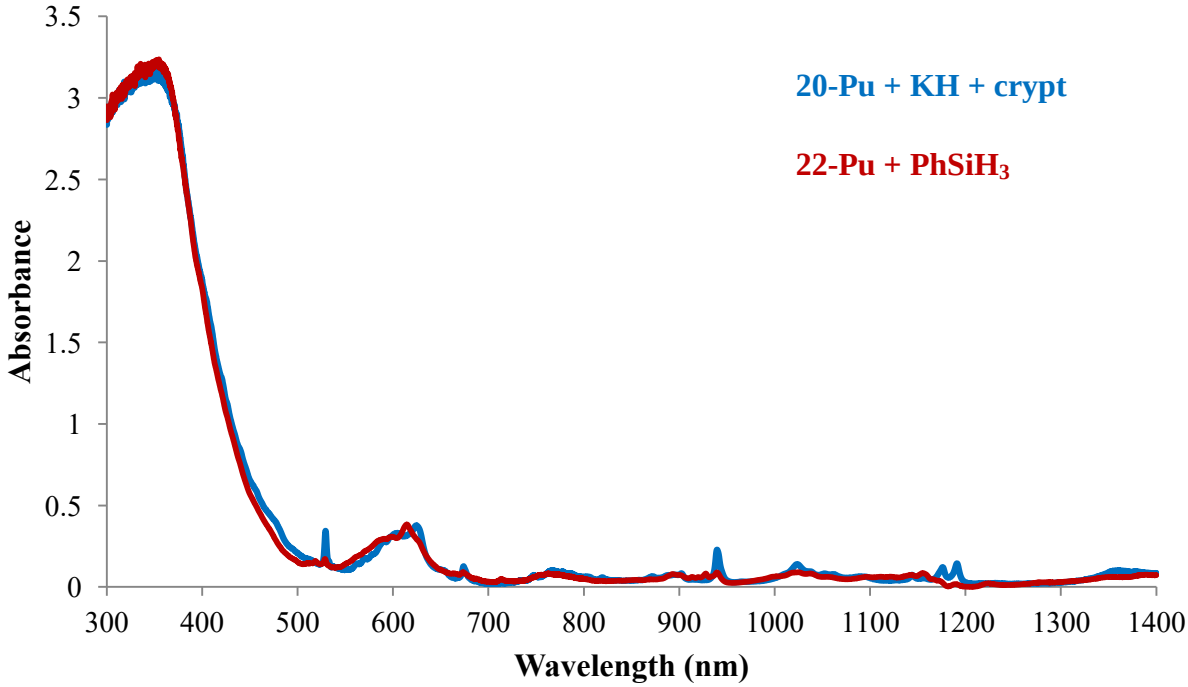

Figure 5.11. Experimental UV/vis/NIR spectra comparing reactivity of Cp″$_3$Pu, **20-Pu** with KH in the presence of crypt (blue trace) and the reactivity of [K(crypt)][Cp″$_3$Pu], **22-Pu** with an excess of $PhSiH_3$ (red trace) in THF at 298 K.

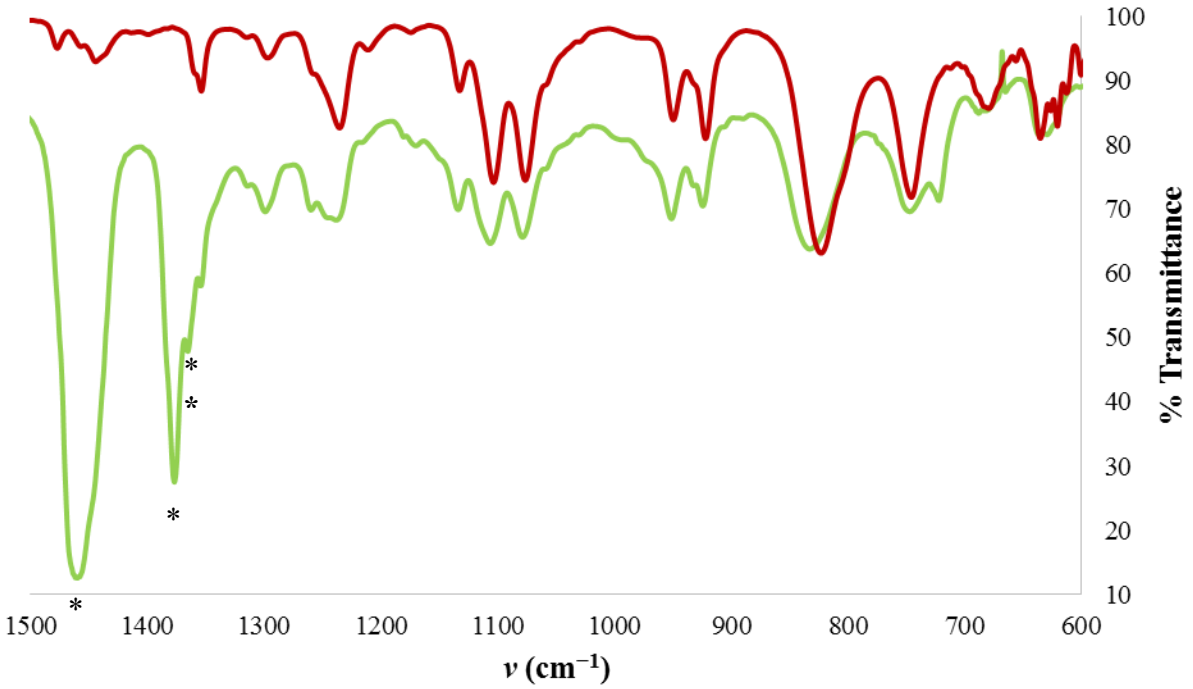

Figure 5.12. FTIR spectra of [K(crypt)][Cp″$_3$UH], **27-U**, (red trace, KBr pellet) and product of Cp″$_3$Pu, **20-Pu** + KH + crypt reaction (green trace, Nujol mull) in fingerprint region with Nujol bands labeled by *.

Decomposition of 22-Pu. To examine the thermal stability of **22-Pu**, a UV/vis/NIR sample was recorded over to time to examine the decomposition, Figure 5.13. These spectra demonstrate that the intense charge transfer band generated upon reduction from **20-Pu** to **22-Pu** is sensitive to purity. In another experiment, a stock solution of **22-Pu** was made, a sample was drawn for UV/vis/NIR analysis, the stock solution was kept inside the glovebox at ambient temperature overnight, and the UV/vis/NIR spectrum was again recorded. This revealed that even when stored under an inert atmosphere, **22-Pu** is relatively unstable in solution and decomposes after several hours at room temperature, Figure 5.14. The high sensitivity of **22-Pu** under an inert atmosphere has not been observed for any of the solutions of Pu(III)-organometallic complexes.[4, 7]

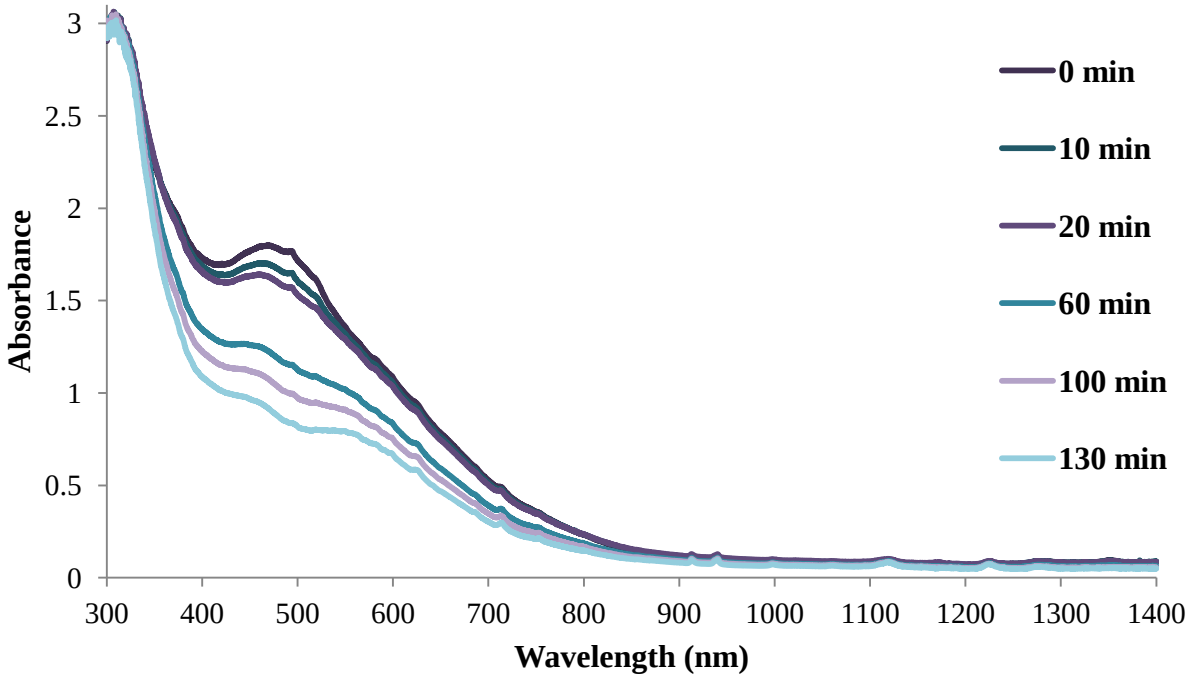

Figure 5.13. Experimental UV/vis/NIR spectra showing decomposition of [K(crypt)][Cp″$_3$Pu], **22-Pu**, in THF at 298 K with the experimental sample in a screw cap quartz cuvette stored outside of the glovebox.

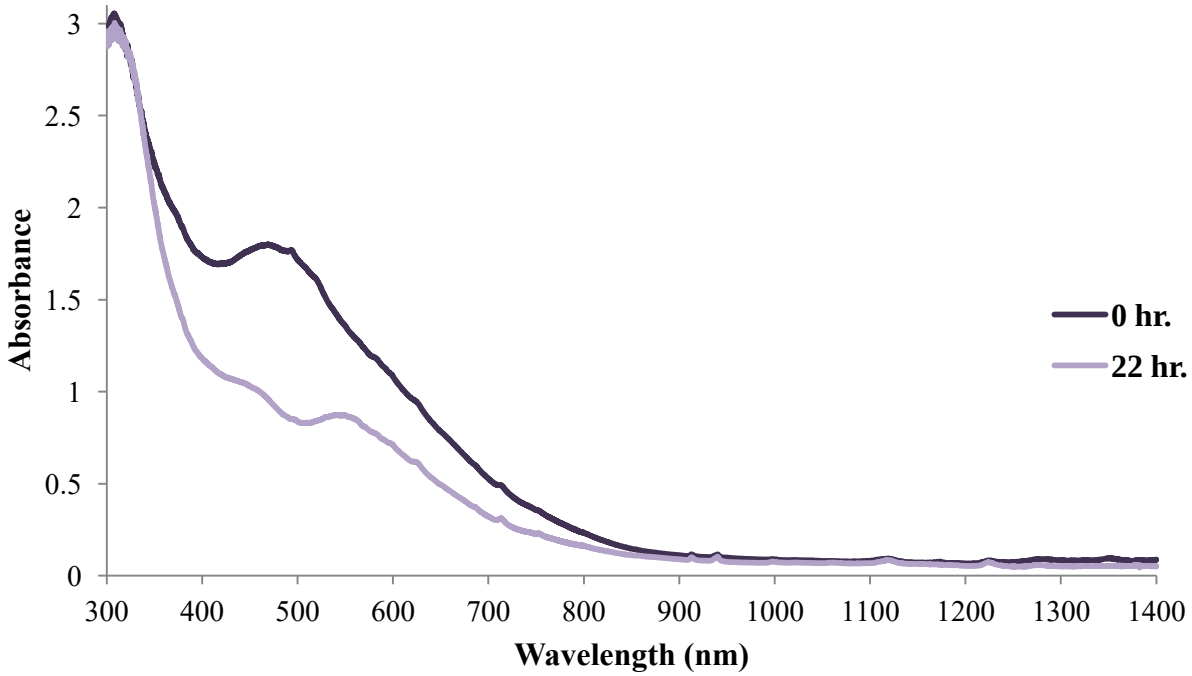

Figure 5.14. Experimental UV/vis/NIR spectra showing decomposition of [K(crypt)][Cp″$_3$Pu], **22-Pu**, in THF at 298 K with the experimental sample stored inside of a glovebox. A fresh sample of **22-Pu** was dissolved in a screw cap 4 mL borosilicate glass vial, an aliquot was drawn, and the UV/vis/NIR spectrum was recorded (dark purple trace). After 22 hour, another aliquot was drawn and the UV/vis/NIR spectrum was recorded (light purple trace).

CONCLUSION

In summary, crystallographically-characterizable organoplutonium complexes have been identified. The synthesis of Cp″$_3$Pu, **20-Pu**, demonstrates a previously unverified entry route into organometallic Pu chemistry. These experiments allowed the Pu–C bond distance to be measured by single crystal X-ray diffraction for the first time and allowed pursuit of analogues of Ln^{II}, Th^{II} and U^{II} molecules. Moreover, reduction of **20-Pu** to form [K(crypt)][Cp″$_3$Pu], **22-Pu**, is a significant finding for the 5*f* elements, namely that Pu^{II} complexes are accessible after over 70 years of chemical research. In contrast to the U^{II} and Th^{II} analogues, the analysis of **22-**

Pu is consistent with predominantly a $5f^6 6d^0$ ground state that has a low-lying $5f^5 6d^1$ state. The results open new frontiers for future research to probe the implications and further understanding of this electronic structure "break" in the actinide series.

REFERENCES

(1) Seaborg, G. T.; McMillan, E. M.; Kennedy, J. W.; Wahl, A. C., *Phys. Rev.* **1946,** *69*, 366-367.

(2) Morss, L. R.; Edelstein, N. M.; Fuger, J., *The Chemistry of the Actinide and Transactinide Elements*. 4th ed.; Springer: Dordrecht, The Netherlands, 2010; Vol. 1-6.

(3) Ephritikhine, M., *Dalton Trans.* **2006**, 2501-2516.

(4) Gaunt, A. J.; Neu, M. P., *C. R. Chimie* **2010,** *13*, 821-831.

(5) Hayton, T. W., *Chem. Commun.* **2013,** *49*, 2956-2973.

(6) Johnson, S. A.; Bart, S. C., *Dalton Transactions* **2015,** *44*, 7710-7726.

(7) Jones, M. B.; Gaunt, A. J., *Chem. Rev.* **2013,** *113*, 1137-1198.

(8) Ephritikhine, M., *Organometallics* **2013,** *32*, 2464-2488.

(9) Liddle, S. T., *Angew. Chem., Int. Ed.,* **2015,** *54*, 8604-41.

(10) Cambridge Structural Database, version November 2016.

(11) MacDonald, M. R.; Fieser, M. E.; Bates, J. E.; Ziller, J. W.; Furche, F.; Evans, W. J., *J. Am. Chem. Soc.* **2013,** *135*, 13310-13313.

(12) Fieser, M. E.; MacDonald, M. R.; Krull, B. T.; Bates, J. E.; Ziller, J. W.; Furche, F.; Evans, W. J., *J. Am. Chem. Soc.* **2015,** *137*, 369-382.

(13) Windorff, C. J.; MacDonald, M. R.; Meihaus, K. R.; Ziller, J. W.; Long, J. R.; Evans William, J., *Chem. Eur. J.* **2016,** *22*, 772-782.

(14) Langeslay, R. R.; Fieser, M. E.; Ziller, J. W.; Furche, F.; Evans, W. J., *Chem. Sci.* **2015,** *6*, 517-521.

(15) Bursten, B. E.; Rhodes, L. F.; Strittmatter, R. J., *J. Am. Chem. Soc.* **1989,** *111*, 2756-2758.

(16) Bursten, B. E.; Rhodes, L. F.; Strittmatter, R. J., *J. Less-Common Met.* **1989,** *149*, 207-211.

(17) Bursten, B. E.; Rhodes, L. F.; Strittmatter, R. J., *J. Am. Chem. Soc.* **1989,** *111*, 2758-2766.

(18) Strittmatter, R. J.; Bursten, B. E., *J. Am. Chem. Soc.* **1991,** *113*, 552-559.

(19) Wu, Q. Y.; Lan, J. H.; Wang, C. Z.; Cheng, Z. P.; Chai, Z. F.; Gibson, J. K.; Shi, W. Q., *Dalton Trans.* **2016,** *45*, 3102-3110.

(20) Dutkiewicz, M. S.; Farnaby, J. H.; Apostolidis, C.; Colineau, E.; Walter, O.; Magnani, N.; Gardiner, M. G.; Love, J. B.; Kaltsoyannis, N.; Caciuffo, R.; Arnold, P. L., *Nat. Chem.* **2016,** *8*, 797-802.

(21) Dutkiewicz, M. S.; Apostolidis, C.; Walter, O.; Arnold, P. L., *Chem. Sci.* **2017,** *8*, 2553-2561.

(22) Ward, J. W., *J. LessCommon Met.* **1983,** *93*, 279-292.

(23) Gibson, J. K.; Haire, R. G.; Santos, M.; Marçalo, J.; Pires de Matos, A., *J. Phys. Chem. A* **2005,** *109*, 2768-2781.

(24) Mikheev, N. B., *Inorg. Chim. Acta* **1987,** *140*, 177-180.

(25) Mikheev, N. B.; Kamenskaya, A. N., *Coord. Chem. Rev.* **1991,** *109*, 1-59.

(26) Mikheev, N. B.; Auerman, L. N.; Igor, A. R.; Alla, N. K.; Kazakevich, M. Z., *Russ. Chem. Rev.* **1992,** *61*, 990-998.

(27) Bergbreiter, D. E.; Killough, J. M., *J. Am. Chem. Soc.* **1978,** *100*, 2126-2134.

(28) Jordan, R. F.; Echols, S. F., *Inorg. Chem.* **1987,** *26*, 383-386.

(29) Peterson, J. K.; MacDonald, M. R.; Ziller, J. W.; Evans, W. J., *Organometallics* **2013,** *32*, 2625-2631.

(30) APEX2 Version 2014.11-0, Bruker AXS, Inc.; Madison, WI 2014.

(31) SAINT Version 8.34a, Bruker AXS, Inc.; Madison, WI 2013.

(32) Sheldrick, G. M. SADABS, Version 2014/5, Bruker AXS, Inc.; Madison, WI 2014.

(33) Sheldrick, G. M. SHELXTL, Version 2014/7, Bruker AXS, Inc.; Madison, WI 2014.

(34) International Tables for Crystallography 1992, Vol. C., Dordrecht: Kluwer Academic Publishers.

(35) Flack, H. D. Acta. Crystallogr., Sect A. 1983, 39, 876–881. or Parsons, S., Flack, H. D., Wagner, T. Acta Crystallogr., Sect B. 2013, 69, 249-259, 2013.

(36) APEX2 Version 2014.11-0, Bruker AXS, Inc.; Madison, WI 2014.

(37) SAINT Version 8.34a, Bruker AXS, Inc.; Madison, WI 2013.

(38) Sheldrick, G. M. SADABS, Version 2014/5, Bruker AXS, Inc.; Madison, WI 2014.

(39) Sheldrick, G. M. SHELXTL, Version 2014/7, Bruker AXS, Inc.; Madison, WI 2014.

(40) International Tables for Crystallography 1992, Vol. C., Dordrecht: Kluwer Academic Publishers.

(41) Gaunt, A. J.; Reilly, S. D.; Enriquez, A. E.; Hayton, T. W.; Boncella, J. M.; Scott, B. L.; Neu, M. P., *Inorg. Chem.* **2008,** *47*, 8412-8419.

(42) Reilly, S. D.; Brown, J. L.; Scott, B. L.; Gaunt, A. J., *Dalton Trans.* **2014,** *43*, 1498-1501.

(43) Stults, S. D.; Andersen, R. A.; Zalkin, A., *Organometallics* **1990,** *9*, 115-122.

(44) Gun'ko, Y. K.; Hitchcock, P. B.; Lappert, M. F., *J. Organomet. Chem.* **1995,** *499*, 213-219.

(45) Xie, Z.; Chui, K.; Liu, Z.; Xue, F.; Zhang, Z.; Mak, T. C. W.; Sun, J., *J. Organomet. Chem.* **1997,** *549*, 239-244.

(46) del Mar Conejo, M.; Parry, J. S.; Carmona, E.; Schultz, M.; Brennann, J. G.; Beshouri, S. M.; Andersen, R. A.; Rogers, R. D.; Coles, S.; Hursthouse, M. B., *Chem. Eur. J.* **1999,** *5*, 3000-3009.

(47) Windorff, C. J.; Evans, W. J., *Organometallics* **2014,** *33*, 3786-3791.

(48) Blake, P. C.; Lappert, M. F.; Atwood, J. L.; Zhang, H., *J. Chem. Soc., Chem. Commun.* **1986**, 1148-1149.

(49) Zwick, B. D.; Sattelberger, A. P.; Avens, L. R., *Transuranium Organometallic Elements: The Next Generation*. American Chemical Society: Washington D. C., 1992.

(50) Avens, L. R.; Bott, S. G.; Clark, D. L.; Sattelberger, A. P.; Watkin, J. G.; Zwick, B. D., *Inorg. Chem.* **1994,** *33*, 2248-2256.

(51) Gaunt, A. J.; Enriquez, A. E.; Reilly, S. D.; Scott, B. L.; Neu, M. P., *Inorg. Chem.* **2008,** *47*, 26-28.

(52) Shannon, R., *Acta Crystallogr., Sect. A.* **1976,** *32*, 751-767.

(53) Hitchcock, P. B.; Lappert, M. F.; Maron, L.; Protchenko, A. V., *Angew. Chem., Int. Ed.*, **2008,** *47*, 1488-1491.

(54) Palumbo, C. T.; Ziller, J. W.; Evans, W. J. *Unpublished results.*

(55) MacDonald, M. R.; Bates, J. E.; Ziller, J. W.; Furche, F.; Evans, W. J., *J. Am. Chem. Soc.* **2013,** *135*, 9857-9868.

(56) Evans, W. J., *Organometallics* **2016,** *35*, 3088-3100.

Postscript

"It's only work and it should make you feel terrible."

– Stosh Kozimor